

AD-A275 955



2

AD _____

3

CONTRACT NO: DAMD17-91-C-1071

TITLE: MECHANISMS AND TREATMENT OF OP-INDUCED SEIZURES AND NEUROPATHOLOGY

PRINCIPAL INVESTIGATOR: Michael T. Shipley, Ph.D.

SDTIC
ELECTE
FEB 24 1994
C D

CONTRACTING ORGANIZATION: University of Cincinnati
College of Medicine
231 Bethesda Avenue
Cincinnati, Ohio 45267-0521

REPORT DATE: August 18, 1993

TYPE OF REPORT: Midterm Report

PREPARED FOR: U.S. Army Medical Research and
Development Command, Fort Detrick
Frederick, Maryland 21702-5012

DISTRIBUTION STATEMENT: Approved for public release;
distribution unlimited

The views, opinions and/or findings contained in this report are those of the author(s) and should not be construed as an official Department of the Army position, policy or decision unless so designated by other documentation.

94-05958



DTIC SOURCE INFORMATION 3

94 2 23 237

REPORT DOCUMENTATION PAGE

Form Approved
OMB No. 0704-0188

Public reporting burden for this collection of information is estimated to average 1 hour per response, including the time for reviewing instructions, searching existing data sources, gathering and maintaining the data needed, and completing and reviewing the collection of information. Send comments regarding this burden estimate or any other aspect of this collection of information, including suggestions for reducing this burden, to Washington Headquarters Services, Directorate for Information Operations and Reports, 1215 Jefferson Davis Highway, Suite 1204, Arlington, Va. 22202-4302, and to the Office of Management and Budget, Paperwork Reduction Project (0704-0188), Washington, DC 20503.

1. AGENCY USE ONLY (Leave blank)		2. REPORT DATE August, 1993		3. REPORT TYPE AND DATES COVERED Midterm, 6/30/91-6/29/93	
4. TITLE AND SUBTITLE Mechanisms and treatment of OP-induced seizures and neuropathology				5. FUNDING NUMBERS DAMD 17-91-C-1071	
6. AUTHOR(S) M.T. Shipley, M. Ennis, M. El-Etri, L. Zimmer and M. Jiang					
7. PERFORMING ORGANIZATION NAME(S) AND ADDRESS(ES) University of Cincinnati College of Medicine 231 Bethesda Ave. Cincinnati, OH 45267-0521				8. PERFORMING ORGANIZATION REPORT NUMBER	
9. SPONSORING/MONITORING AGENCY NAME(S) AND ADDRESS(ES) U.S. Army Medical Research and Development Command Fort Detrick Frederick, MD 21702-5012				10. SPONSORING/MONITORING AGENCY REPORT NUMBER	
11. SUPPLEMENTARY NOTES					
12a. DISTRIBUTION/AVAILABILITY STATEMENT Approved for public release, distribution unlimited.				12b. DISTRIBUTION CODE	
13. ABSTRACT (Maximum 200 words) This report summarizes studies on the mechanisms and treatment of soman-induced seizures and neuropathology. Major goals of this work are to identify the first sites exhibiting soman-induced hyperactivity and neuropathology, and to determine if neurotransmitters other than acetylcholine (ACh) are altered by soman. Markers for <i>c-fos</i> and reactive astrocytes pinpointed sites of seizures and neuropathology, and neurochemistry quantified neurotransmitter levels. Piriform cortex (PC) and the noradrenergic (NE) nucleus locus coeruleus (LC) first exhibited <i>c-fos</i> and reactive astrocytes after soman. Seizures, <i>c-fos</i> and reactive astrocytes in PC were also produced by stimulation of endogenous ACh inputs to PC. Soman caused increased LC neuronal activity, producing sustained NE release leading to depletion in convulsive but not nonconvulsive rats. As NE is proconvulsant in several seizure models, we hypothesize that soman-induced NE release plays a critical role in seizure induction and/or maintenance. This work indicates that increased ACh and NE play important roles in soman-induced seizures, and suggests new therapeutic approaches involving NE antagonists. Since many NE antagonists are used clinically, their combination with ACh antagonists could provide an improved, rapidly deployed postexposure protective regimen.					
14. SUBJECT TERMS Soman, acetylcholine, acetylcholinesterase, Piriform Cortex, norepinephrine, locus coeruleus, seizures, convulsions				15. NUMBER OF PAGES 153	
				16. PRICE CODE	
17. SECURITY CLASSIFICATION OF REPORT Unclassified		18. SECURITY CLASSIFICATION OF THIS PAGE Unclassified		19. SECURITY CLASSIFICATION OF ABSTRACT Unclassified	
				20. LIMITATION OF ABSTRACT UL	

FOREWORD

In conducting the research described in this report, the investigators adhered to the "Guide for the Care and Use of Laboratory Animals," prepared by the Committee on Care and Use of Laboratory Animals of the Institute of Laboratory Animal Resources (DHHS Publication No. (NIH) 86-23, Revised 1985).

Citations of commercial organizations and trade names in this report do not constitute an official Department of the Army endorsement or approval of the products or services of these organizations.

Accession For	
NTIS CRA&I	<input checked="" type="checkbox"/>
DTIC TAB	<input type="checkbox"/>
Unannounced	<input type="checkbox"/>
Justification	
By	
Distribution /	
Availability Codes	
Dist	Avail and/or Special
A-1	

ACKNOWLEDGMENTS

We are grateful for the support and interest of our Contracting Officer's Representative, Dr. Michael Adler. We thank Lydia Hu and Ming-xin Song for expert technical assistance. The data presented in Chapters 5,6 and 7 were published in *Experimental Neurology* (^{47, 49, 58}, respectively).

TABLE OF CONTENTS

Foreword.....	1
Acknowledgments.....	2
List of Figures.....	4
List of Tables.....	7
Chapter 1. Introduction.....	8
Chapter 2. Soman-induced seizures and protooncogene expression.....	14
Chapter 3. Glial cells and soman neuropathology.....	24
Chapter 4. Stimulation of endogenous cholinergic inputs to PC produces seizures, increased <i>FOS</i> expression and up-regulation of astrocytes.....	28
Chapter 5. Brain norepinephrine reductions in soman-intoxicated rats: association with convulsions and AChE inhibition, time course, and relation to other monoamines.....	36
Chapter 6. Tonic activation of locus coeruleus neurons by systemic or intracoerulear microinjection of an irreversible acetylcholinesterase inhibitor: increased discharge rate and induction of <i>c-fos</i>	51
Chapter 7. Pilocarpine-induced convulsions in rats: evidence for muscarinic receptor-mediated activation of locus coeruleus and norepinephrine release in cholinolytic seizure development.....	71
Chapter 8. Determination of extracellular norepinephrine levels in the olfactory bulb using <i>in vivo</i> microdialysis.....	94
Chapter 9. <i>In vitro</i> whole cell patch clamp recording of rat olfactory bulb mitral cells: biophysical and synaptic properties.....	109
Chapter 10 Conclusion: A two-stage mechanism for soman-induced seizures.....	134
References.....	138

LIST OF FIGURES

Figure 1. Rapid, selective induction of <i>c-fos</i> and glial fibrillary acidic protein (GFAP) in piriform cortex (PC) by a single convulsive dose of soman.....	17
Figure 2. NHDB stimulation experimental paradigm.....	30
Figure 3. NHDB stimulation evokes cortical seizure activity.....	31
Figure 4. NHDB stimulation induces rapid <i>FOS</i> expression in PC: blockade by muscarinic receptor antagonism.....	32
Figure 5. Effect of soman on NE levels in olfactory bulb and forebrain in convulsive and nonconvulsive animals.....	41
Figure 6. Correlation between changes in forebrain and olfactory bulb NE levels in convulsive and nonconvulsive animals.....	41
Figure 7. Correlation between AChE activity and NE levels in convulsive and nonconvulsive animals.....	41
Figure 8. Effect of soman on DA, DOPAC and HVA.....	45
Figure 9. Effect of soman on 5-HT and 5-HIAA.....	45
Figure 10. Systemic soman increases LC discharge and desynchronizes cortical EEG.....	56
Figure 11. Effect of systemic soman on LC discharge rate.....	56
Figure 12. Systemic injection of soman induces <i>c-fos</i> expression in LC neurons.....	57
Figure 13. Systemic soman inhibits AChE in LC.....	58
Figure 14. Microinjection of soman directly into LC tonically activates LC neurons via muscarinic cholinergic receptor activation.....	61
Figure 15. Analysis of the effects of intracoerulear soman on LC neuronal activity.....	61
Figure 16. Dose-dependent activation LC neurons by intracoerulear soman.....	61
Figure 17. Induction of <i>c-fos</i> expression in LC neurons by intracoerulear microinjection of soman.....	63
Figure 18. Intracoerulear microinjection of soman focally inhibits AChE in LC.....	64

Figure 19. Effect of pilocarpine on NE levels in olfactory bulb and forebrain of convulsive and nonconvulsive animals.....	78
Figure 20. Effect of pilocarpine on DA and metabolites DOPAC and HVA levels.....	80
Figure 21. Effect of pilocarpine on 5-HT and metabolite 5-HIAA levels.....	80
Figure 22. Robust activation of LC neurons by systemic or intracoerulear microinjection of pilocarpine	83
Figure 23. Systemic administration of pilocarpine causes a long lasting activation of LC neurons.....	83
Figure 24. Activation of LC neurons by systemic or intracoerulear microinjection of pilocarpine induces expression of <i>c-fos</i> in LC neurons	84
Figure 25. Elevated extracellular potassium increases synaptic release of NE	98
Figure 26. Local infusion of the NE uptake blocker desipramine (DMI) increases NE recovery.....	99
Figure 27. Local infusion of acetylcholine (ACh) potently increases extracellular NE levels.....	102
Figure 28. Local infusion of the muscarinic receptor agonist pilocarpine reduces NE levels.....	103
Figure 29. Local infusion of soman increases NE recovery	104
Figure 30. Selective, confirmed activation of locus coeruleus (LC) increases synaptic release of olfactory bulb NE.....	105
Figure 31. Biocytin filled mitral cells in olfactory bulb slices	115
Figure 32. Mitral cell membrane properties	116
Figure 33. Mitral cell membrane currents measured under voltage clamp.....	117
Figure 34. Spontaneous excitatory potentials in mitral cells.....	119
Figure 35. Extracellularly recorded responses of cells in the mitral cell layer to stimulation of the olfactory nerve layer (ONL)	120
Figure 36. EPSP responses to olfactory nerve layer stimulation	121
Figure 37. Spike generation in the mitral cell apical dendrite.....	124

Figure 38. Voltage clamp record of mitral cell response to olfactory nerve layer stimulation125

Figure 39. Voltage division between axial resistance of the apical dendrite and the membrane resistance of the mitral cell.....126

LIST OF TABLES

Table 1. Time course of changes in forebrain levels of NE, DA, 5-HT, and major metabolites following a single dose of soman (78 $\mu\text{g}/\text{kg}$).....	42
Table 2. Time course of changes in olfactory bulb levels of NE, DA, 5-HT, and major metabolites following a single dose of soman (78 $\mu\text{g}/\text{kg}$).....	42
Table 3. Forebrain NE and AChE levels in convulsive and nonconvulsive rats 1 hr following a single dose of soman (78 $\mu\text{g}/\text{kg}$).....	43
Table 4. Time course of changes in forebrain level of NE, DA, 5-HT, and metabolites following a single dose of pilocarpine (300 mg/kg, ip).....	79
Table 5. Time course of changes in olfactory bulb level of NE, DA, 5-HT, and metabolites following a single dose of pilocarpine (300 mg/kg, ip)	79

1. INTRODUCTION

This report documents progress in an ongoing study of the central effects of organophosphate (OP) poisoning. In our previous contract, we described the anatomy and physiology of a model central cholinergic system, the projection from the horizontal limb of the diagonal band (NHDB) to the main olfactory bulb. These basic studies have led to experiments described in the present report, which focus more directly on the central mechanisms and treatment of OP-induced seizures.

There are several major roadblocks to the understanding and treatment of OP-induced seizures. One of the chief problems is the lack of information about the temporal sequence and spatial pattern of seizure initiation and spread throughout the brain after soman intoxication. For example, it is not known if unhydrolyzed acetylcholine (ACh) exerts a global stimulation of brain neurons and if this general increase in excitability causes seizures or, alternatively, whether hyperactivity in one or a few discrete subpopulation(s) of neurons triggers seizures which then spread to other parts of the brain. There is evidence that the latter alternative is likely, as several specific areas of the brain are selectively vulnerable to neuropathology after OP intoxication. Specifically, the cerebral cortex and hippocampus frequently show the first signs of cell damage and necrosis after OP poisoning and in other seizure models. We hypothesize that areas exhibiting the first signs of pathology may be the first sites in the brain to undergo excessive levels of hyperactivity after OP intoxication, and thus, may be key sites of seizure initiation. We believe that additional information about OP actions on the circuit connections, intrinsic neurotransmitters and receptors, and the neurophysiology of such trigger sites is critical to the development of specific antidotes directed at blocking the initial induction of seizures.

A second major problem is that little is known about the underlying neurochemical basis of OP-induced seizures. This problem is underscored by the fact that current drugs used to treat the peripheral symptoms of OP intoxication do not prevent centrally generated seizures which can cause permanent brain damage (^{103, 126}). Although a primary cause of cholinergic seizures is excess ACh, centrally acting muscarinic blockers alleviate convulsions only if administered a short time after soman exposure (¹²¹). Moreover, there is only a weak relationship between acetylcholinesterase (AChE) inhibition and the incidence of convulsions (^{47, 89}). Similarly, there is little systematic relationship between ACh and GABA, a neurotransmitter prominently implicated in seizure generation, with the incidence of soman-induced convulsions. On the basis of such findings, we hypothesize that excess release of unhydrolyzed ACh may lead to activation of other neurotransmitter-specific cell groups that contribute to the generation and/or maintenance of OP-induced seizures.

Two major goals of our current contract are thus to: (1) identify the first brain sites to exhibit signs of neuronal hyperactivity and neuropathology after administration of the OP soman, and (2) to

determine whether the levels of other neurotransmitters are selectively altered after soman administration. To address the first question, we used staining for the protooncogene, *c-fos* (*FOS*) to pinpoint the initial location to seizures. Increased expression of *FOS*, and other immediate early genes, has recently been shown in response to neural hyperactivity, cellular stress and neuronal injury. To identify other neurotransmitters that may be involved in OP-induced seizures, neurochemical techniques were used to examine regional changes in neurotransmitter levels after soman administration.

In a comprehensive set of experiments described in Chapter 2, the distribution of *FOS* staining was mapped after rats were given a single sublethal dose of the OP soman that straddled the threshold for seizure generation. In rats exhibiting behavioral convulsions, but not in nonconvulsive rats, markedly increased *FOS* expression was present in layers II-III of the piriform cortex (PC) as early as 30-45 min after injection of soman. Since PC is typically the first structure exhibiting damage after soman intoxication, this finding suggests that *FOS* expression is a reliable marker for the early stages of neural damage, and further suggests that seizures begin in PC and spread to other brain structures. Unexpectedly, there was also strong *FOS* expression by 35-45 min in a brainstem area, the nucleus locus coeruleus (LC), the largest noradrenergic cell group in the brain. At longer survival times, there was a progressive spread or wave of *FOS* expression in other cortical areas and the hippocampus.

In these same experiments, we also determined if soman administration produced changes in the activity of astrocytes (Chapter 3). Astrocytes have long been known to be involved in the response to injury of the central nervous system (CNS). The importance of these cells in the response to injury has been recently emphasized by the discovery of a marker specific to astrocytes, glial fibrillary acidic protein (GFAP). We found that there was a robust increase in GFAP staining in layers II-III of PC that was nearly simultaneous (60-120 min) with the increase in *FOS* in these same layers. These results indicate that there is a rapid activation of astrocytes in the same layers of PC exhibiting neuronal hyperactivity (i.e., *FOS* expression) and destined for neuropathology.

These findings lead us to hypothesize that sustained release of ACh in PC from the terminals of cholinergic neurons after soman administration triggers expression of *FOS* and up-regulation of astrocytes in neurons of layers II-III in PC. We refer to this as the "*cholinergic trigger hypothesis*". The cholinergic trigger hypothesis predicts that sustained release of ACh in PC from the terminals of cholinergic neurons, originating in the nucleus of the diagonal band (NHDB), should cause seizures and the selective expression of *FOS* in neurons of layers II-III in PC as is observed following soman. Chapter 4 summarizes experiments conducted to test this hypothesis. Microwire electrodes were chronically implanted to directly stimulate cholinergic neurons in NHDB on one side of the brain in awake unrestrained animals. Shortly after the onset of NHDB stimulation, the rats exhibited behavioral signs similar to some of those observed following soman administration. In addition, NHDB stimulation

desynchronized the electroencephalograph (EEG) and, in some cases, produced bursts of spindle activity. The animals were sacrificed after 10-40 min of intermittent train stimulation of NHDB, and then brains were processed for detection of *FOS*. Consistent with our hypothesis, *FOS* was selectively expressed by the majority of layer II-III PC neurons ipsilateral to the stimulated NHDB. Ten minutes of NHDB stimulation was sufficient to produce light to moderate *FOS* expression in some animals. There was little or no expression in control (implanted but not stimulated) animals. NHDB stimulation for 20 or 40 min evoked a progressive increase in *FOS* expression in layers II and III of PC, hippocampus and in entorhinal cortex. In addition, activation of NHDB for 1 hr substantially increased GFAP staining in PC compared to implanted control animals.

As we hypothesize that NHDB-evoked *FOS* expression in PC is due to cholinergic stimulation produced by release of endogenous acetylcholine from NHDB terminals onto PC neurons, we predicted that cholinergic receptor antagonists should block NHDB-evoked *FOS* expression in PC. Consistent with this hypothesis, systemic administration of the muscarinic receptor antagonist scopolamine consistently blocked NHDB-evoked *FOS* expression, EEG effects and behaviors. In contrast, systemic administration of the nicotinic receptor antagonist, mecamylamine, did not block the effects of NHDB stimulation.

Chapter 5 summarizes our neurochemical survey of changes in the levels of central neurotransmitters produced by soman poisoning. As several lines of evidence suggest that the modulatory monoaminergic neurotransmitters may be involved in seizures, our neurochemical studies focused on changes in NE, dopamine (DA), and serotonin (5-HT). Similar to experiments in Chapter 2, animals were administered a periconvulsive dose of soman and allowed to survive for various times after injection. The forebrain and olfactory bulb were isolated and monoamine levels were determined by HPLC with electrochemical detection (⁴⁷). We found that there was a rapid, selective reduction of NE in convulsive, but not in nonconvulsive rats; forebrain NE levels were decreased by 50% at 1 hr and 70% at 2 hr following soman injection. Recovery of NE began at 8 hr and was complete by 96 hr following soman administration. Although nonconvulsive rats showed other signs of intoxication, NE levels in these rats were unchanged. DA and 5-HT levels were not significantly affected in either convulsive or nonconvulsive rats. However, 5-hydroxyindoleacetic acid (5-HIAA), the major metabolite of 5-HT, and homovanillic acid (HVA) and 3,4-dihydroxyphenylacetic acid (DOPAC), the two major metabolites of DA, were increased significantly in the forebrain of convulsive, but not nonconvulsive rats, indicating an increase in 5-HT and DA turnover. However, in contrast to the abrupt decline in NE, these increases in DA and 5-HT metabolites were slow and progressive. Taken together, these suggest that rapid, sustained, NE release could play a role in the induction and/or maintenance of soman-induced convulsions, whereas increased release of 5-HT and DA may be a consequence of seizures (El-

Etri et al., 1992).

Chapter 6 describes studies examining the effects of soman on LC neurons. As noted above, LC is the largest NE cell group and projects throughout the entire CNS. LC was one of the first sites to exhibit elevated *FOS* after soman, and our neurochemical studies found that NE levels were rapidly depleted in convulsing animals after soman administration. Based on these results, we hypothesized that soman causes a sustained increase in the activity of LC neurons, leading to massive release of NE (^{47, 58}). Thus, we examined whether LC neuronal activity, *FOS* expression, and AChE staining are altered after peripheral (systemic) or direct intracerebral injection of soman in anesthetized rats. Both modes of soman administration rapidly and potently increased the discharge of LC neurons (⁵⁸). These results demonstrate that soman potently and tonically activates LC neurons. This effect appears to be mediated by direct inhibition of AChE in LC leading to a rapid accumulation of ACh. Unhydrolyzed ACh tonically activates LC neurons via muscarinic receptors. Soman-induced activation of LC neurons does not require seizures. We conclude that depletion of forebrain and olfactory bulb NE after systemic administration of soman results from tonic hypercholinergic stimulation of LC. These new results are of considerable significance as NE is proconvulsant in a number of seizure models. Thus, we hypothesize that soman-induced NE release may play a critical role in the induction and/or maintenance of soman-induced seizures. We refer to this as the "*noradrenergic trigger hypothesis*."

The preceding results indicate that the rapid release of NE by cholinolytic agents may play an important role in the initiation and/or maintenance of convulsions. In Chapter 7, we tested the hypothesis that NE release in soman-intoxicated rats is due to muscarinic activation of LC. Specifically, we have investigated the effects of the muscarinic receptor agonist and potent seizurogenic agent, pilocarpine, on NE release and LC discharge. As in our soman studies, NE levels declined rapidly and substantially only in convulsive rats. The time course and magnitude of these changes were similar to those observed following soman administration. Similarly, neither DA nor 5-HT levels were changed in either convulsive or nonconvulsive rats. Systemic administration of pilocarpine caused a sustained, five-fold increase in mean LC neurons firing rate (⁴⁹). Microinjections of pilocarpine directly into LC caused a similar increase in the firing rate of LC neurons (⁴⁹). Thus, increases in LC discharge rate produced by pilocarpine were nearly identical to those produced by soman. The effects of systemically and intracerebrally administered pilocarpine on LC discharge were reversed by the muscarinic receptor antagonist scopolamine. Furthermore, both modes of pilocarpine administration induced robust *FOS* expression in LC (⁴⁹).

The aforementioned neurochemical studies demonstrated profound reductions of NE only in convulsing animals following soman or pilocarpine administration. However, the finding that both of these agents cause rapid increases in LC neuronal activity led us to hypothesize that these agents cause

an initial period of excessive NE release leading rapidly to a depletion of forebrain NE levels. Whole tissue neurochemical studies are limited by the drawback that they can only detect decreases in the level of neurochemicals. To mitigate this problem, as described in Chapter 8, we implemented *in vivo* microdialysis techniques to measure the extracellular levels of transmitters, a technique that allows detection of steady state levels and increases or decreases in transmitter. Using this technique, we found that confirmed, selective activation of LC neurons results in a marked release of forebrain NE levels.

The application of *in vivo* microdialysis allows assessment of presynaptic influences on neurotransmitter release. We were interested in this subject as there is an extensive literature of presynaptic cholinergic control of NE release in the peripheral nervous system. Chapter 8 summarizes our recent experiments examining the influence of cholinergic receptor agents on NE levels in the olfactory bulb. We found that local infusion of ACh or soman through the dialysis probe increases NE release, suggesting that there may be significant local cholinergic control of terminal NE release. In contrast, local infusion of the selective muscarinic agonist pilocarpine decreased NE release, suggesting that soman- and ACh-induced NE release is mediated by a nicotinic receptor. In agreement with this possibility, nicotine infusion through the dialysis probe potently increased NE release in preliminary studies. These findings are in excellent agreement with studies in the autonomic nervous system and *in vitro* brain slices demonstrating that muscarinic receptors inhibit, and nicotinic receptors stimulate, terminal NE release. Taken together, these results indicate that NE release caused by systemic administration of soman is mediated by: (1) A direct excitatory action on LC cell bodies mediated by muscarinic receptor stimulation, and (2) A presynaptic, nicotinic receptor-mediated facilitation of NE release. The finding that nicotinic receptor activation increases NE release is important because recent hypotheses about the central actions of soman poisoning have focused almost exclusively on muscarinic receptors. Our new findings indicate that CNS nicotinic receptors may also play a key role in soman's central actions.

Chapter 9, the final chapter of this report, describes the application of newly developed patch clamping and conventional sharp electrode intracellular techniques in our laboratory. A goal of our contract is to determine the cellular/membrane actions of soman, cholinergic agonists and NE on PC neurons. A proposed set of experiments will utilize patch clamp and conventional intracellular techniques in *in vitro* PC slice preparations to accomplish this goal.

These overall findings led us to the following hypothesis for the generation of seizures by OP intoxication. AChE inhibition by OPs results in excess unhydrolyzed ACh in both the PC and LC. The ACh excess in LC causes rapid firing of LC neurons, with resulting excess NE in PC. The combination of excess ACh and NE produces a "dual trigger," resulting in extreme excitability and increased activity of PC neurons. PC neurons receive, and are extensively interconnected by, excitatory amino acid (EAA)

synapses. We predict that heightened sensitivity will cause increased responsiveness to EAAs, in turn, leading to increased feedforward and feedback release of EAAs. These primary events represent the *initiation stage* of seizure generation. In effect, increased excitability caused by excess ACh and NE produces a self-sustaining, cascading EAA circuit. We speculate that this circuit represents a maintenance stage of seizures, as synaptic connections may be sufficiently strengthened to maintain hyperactivity even if the initial ACh and NE triggers are no longer active. This intense, but focal seizure activity in PC then rapidly spreads to other parts of the brain.

Our studies indicate that increased levels of both ACh and NE play an important role in soman-induced seizures. The involvement of NE in the generation of soman-induced seizures could provide an important new therapeutic approach involving pharmacological agents directed at NE receptors. Since many such agents are already in clinical use for treatment of cardiovascular symptoms and migraine headache, effective agents could be rapidly applied clinically without extensive testing and FDA approval. In this regard, it is noteworthy that previous studies (^{10, 28-30}) have shown that an α_2 -adrenergic agonist, clonidine, provides some protection against the convulsive, but not the lethal, actions of soman. Clonidine's protective action was synergistic with the protective actions of atropine. The studies presented here provide a possible mechanistic explanation for this protective effect: clonidine directly inhibits LC neuronal activity, decreases terminal release of NE, and reduces excitatory responses of LC neurons to ACh. The net effect of clonidine's actions is to protect target cortical structures from exposure to excess NE. Since a variety of NE agonists and antagonists are already in clinical use, further studies of these agents in combination with cholinergic antagonists could yield an improved postexposure therapeutic regimen which could be rapidly deployed to military personnel.

2. SOMAN-INDUCED SEIZURES AND PROTOONCOGENE EXPRESSION

INTRODUCTION

A wealth of recent evidence has demonstrated that depolarization and/or second-messenger activation in brain neurons leads to the rapid induction of protooncogenes, the DNA transcriptional regulatory proteins *c-fos* (*FOS*) and *c-jun*. After sustained depolarizing and/or second-messenger activation, a series of intracellular messengers cause the rapid transcription of a set of regulatory genes--protooncogenes or "early immediate" genes--leading to the rapid synthesis of protooncogene protein products. These proteins act on the genome to promote the transcription of additional genes encoding proteins required to maintain the metabolic or physiologic activities of the cell (17, 35, 76, 86, 90, 130, 156, 170). Thus, induction of protooncogenes such as *c-fos* indicates that the cell is adaptively responding to external stimuli by the production of proteins necessary to the continued function of the cell. In addition, under extreme stress protooncogenes may also promote the transcription of genes encoding proteins critical to cell survival. Protooncogene induction, thus, is the earliest known macromolecular signal of physiological activation of neurons. If *FOS* expression could be detected *in situ* after soman poisoning, then it might be possible to determine the earliest neurons activated by this OP. Thus, we tested whether soman-induced seizures increased *FOS* expression.

METHODS

Soman Administration. Adult male Sprague-Dawley rats (270-295g; Harlan Laboratories, Indianapolis, IN) were housed in pairs with free access to food and water for at least 1 week prior to use. A single dose (78 µg/kg, im) of soman (pinacolyl methylphosphonofluoridate) in saline was administered into the left hind leg. This dose was sufficient to cause convulsions in about one-half of the injected animals and nearly complete inhibition of acetylcholinesterase (AChE) in the rat forebrain. Rats survived for 30-45 min, 1 hr, 2 hr, 8 hr, and 24 hr after injection. For each selected period, control animals were injected with proportional volumes of saline (0.9%). A minimum of five animals were included in each group.

Scoring of Convulsive versus vs. Nonconvulsive Rats. Soman-injected animals were observed every 5 min for the first 45 min and then every hour for the predetermined time periods. For each rat, the presence or absence of convulsions was noted. Soman-intoxicated rats fell into two distinct groups, either convulsive or nonconvulsive. Absence of convulsions disqualified animals for

immunocytochemical analysis. Rats which developed convulsions did so within 20 min of injection and maintained convulsions for several hours.

Perfusion and Histology. At the end of the specified survival times, animals were anesthetized with pentobarbital (80 mg/kg; ip) and perfused transcardially with 100-200 ml of 0.9% saline for 1 min followed by 900-1000 ml of 4% paraformaldehyde in 0.1 M phosphate buffer (PB) (pH 7.4, 4° C) for 20 min. The brains were rapidly removed from the skull and postfixed in the same solution (4° C) for 1.5 hr and then placed in 30% sucrose in 0.1 M PB for 24 hr. Serial, 30-40- μ m-thick frozen sections were cut in the coronal plane and alternately placed in separate trays containing 0.1 M PB for immunocytochemical visualization of *FOS*. For *FOS* immunocytochemistry, free-floating sections were: (i) rinsed (30 min) in 0.1 phosphate buffered saline (PBS); (ii) placed in 2% normal rabbit serum (NRS) in PBS containing 2% Triton X-100 (TX) overnight; (iii) incubated in anti-sheep primary antibody overnight (Cambridge Biochemicals) at 1:5000 in 2% PBS-TX and 2% NRS for 24-48 hr at 4° C with gentle agitation; (iv) rinsed in PBS-TX (1 hr) and then incubated in biotinylated rabbit anti-sheep IgG in PBS-TX (1.5 hr, room temperature); (v) rinsed in PBS-TX (1 hr) and incubated for 1 hr in avidin-biotin-peroxidase complex in 0.1 M PBS-TX and then rinsed in PBS-TX (30 min); (vi) incubated in 0.05% diaminobenzidine (DAB) with 0.1% hydrogen peroxide in PBS-TX for 10 min and rinsed in PB (30 min); and (vii) sections were mounted on subbed slides, air-dried, dehydrated in graded alcohol and xylene, and coverslipped with DPX mountant.

RESULTS

Characteristics of Soman-Induced Seizures. All rats injected with soman showed signs of intoxication. Rats were classified as *convulsive* according to the following criteria: (i) "red tears" (lacrimation); (ii) tonic shaking movements of the head and body; (iii) excess salivation; (iv) defecation; and (v) labored breathing. The onset of soman-induced intoxication occurred 10-15 min following administration and convulsions rapidly increased in intensity over the next 30 min. Convulsive activity was intense between 1 and 4 hr and declined thereafter. By 8 hr after soman administration (n=9), rats no longer exhibited convulsions. Nonconvulsive rats exhibited other signs of soman intoxication including a decrease in motor activity, muscle fasciculations at the injection site, and reduced responsiveness to external stimuli during the first few hours of intoxication. Only rats exhibiting well-characterized physical signs of soman-induced convulsions (68%) were used for immunocytochemical analysis.

Time Dependence of *FOS* Expression. Of the control animals (n=10), a few had low levels of

positive *FOS* reactivity. A few *FOS* positive cells were in piriform cortex (PC), entorhinal (Ent) cortices. Only the supraoptic nucleus (SO) had intense levels of *FOS* under control conditions.

Thirty to Forty-five Minutes. Animals sacrificed between 30-45 min had *FOS* expression above controls in restricted areas of the brain. A heavy band of *FOS* positive cells was present throughout the entire rostral-caudal extent of PC layer II. Entorhinal cortex (Ent) also displayed *FOS* immunoreactive cells. A few *FOS* positive cells were also present in endopiriform nucleus (En) and olfactory tubercle (Tu). The pontine nucleus locus coeruleus (LC) contained a large number of *FOS* positive cells. In the olfactory bulb, neurons in the mitral cell layer (Mi), internal plexiform layer (IPI), and the internal granular layer (IGr) were lightly stained, but the intensity of *FOS* in the bulb was similar to several control animals. In the basal forebrain, a small number of *FOS*-positive cells were present in the lateral septal nuclei (LSN). The thalamic reticular nucleus (Rtn) displayed strong increases of *FOS* over controls while other thalamic structures were devoid of *FOS*.

One Hour. At 1 hr after soman administration, there was a progressive increase in the intensity of *FOS* staining and in the number of *FOS* positive cells in the same structures exhibiting intense *FOS* expression at 30-45 min. PC layer II, LC, Ent, En, Tu and Rtn had much more intense *FOS* expression than in the 30-45 min cases. *FOS* expression was also evident in layer III of PC and anterior olfactory nuclei (AON). Mi, IPI, and IGr of the olfactory bulb had increased levels of *FOS* staining over controls. Anterior cingulate cortex (Cg) had low levels of *FOS* positive cells. The LSN had higher levels of *FOS* expression. Low levels of *FOS* staining appeared in the septofimbrial (SFi) and septohypothalamic (SHy) nuclei. As in the 30-45 minute animals, the thalamus, except for the Rtn, was devoid of *FOS* expression.

Two Hours. At 2 hr following soman injection, *FOS* staining in PC layers II and III, LC, and Rtn was similar to that in the 1 hr cases. Tu and En showed increased *FOS* expression. The septal region had similar *FOS* expression as in the 1 hr cases. AON and regions in the olfactory bulb had maintained expression of *FOS* as in the 1 hr cases. In addition to PC and Cg, a number of other cortical areas now exhibited elevated *FOS* expression including insular, parietal, temporal, frontal, retrosplenial, perirhinal, entorhinal and occipital cortices. In addition to the Rtn, low levels of *FOS* staining was now present in anteroventral (AV), paraventricular (Pa), and anterodorsal (AD) thalamic nuclei. *FOS* expression was also evident after 2 hours in the caudate putamen (CPu), dentate gyrus (DG) of the hippocampus, medial preoptic (MPO), and medial habenular (MHb) nuclei.

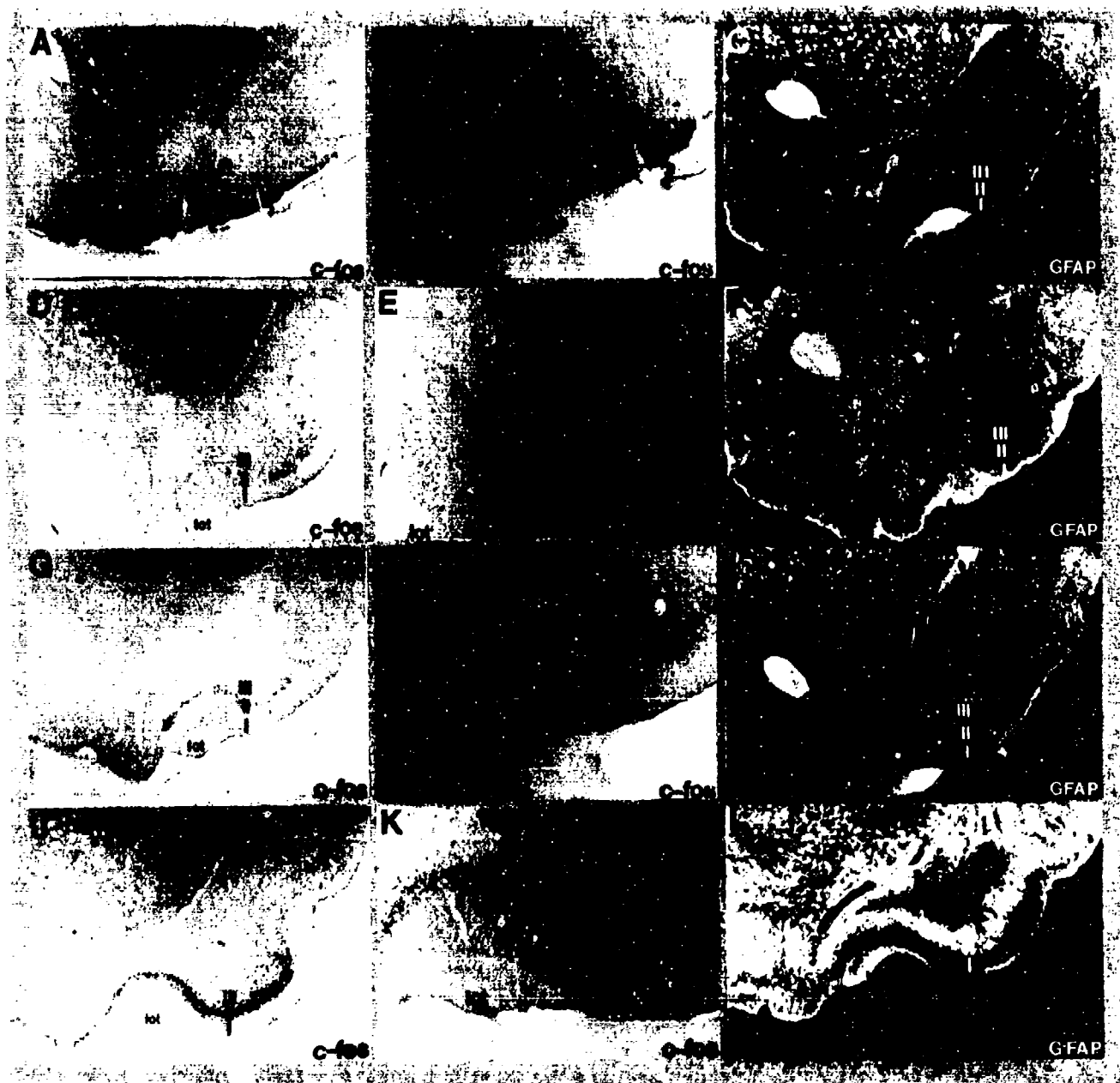


Figure 1. Rapid, selective induction of *c-fos* and glial fibrillary acidic protein (GFAP) in piriform cortex (PC) by a single convulsive dose of soman. Convulsing animals were sacrificed at different time intervals from 0 to 120 min (times indicated in middle row) and sections from all animals were processed simultaneously for immunohistochemical staining of *c-fos* (first two columns A, B, D, E, G, H, J, K) or GFAP to stain for reactive astrocytes (third column; C, F, I, L). *c-fos* and GFAP stained sections are serially adjacent. For the *c-fos* stained sections, low- (first column) and high- (middle column) power micrographs demonstrate localization of *c-fos* staining in layers II and III of PC. Both the number of cells and the intensity of staining increase progressively between 0 (A,B) and 120 (J,K) min. GFAP staining (right column) is visible at 1 hr and is strongly expressed at 2 hr following intoxication. GFAP is located in the same layers as *c-fos*. LO: lateral olfactory tract.

Four Hours. Animals allowed to survive for 4 hr after injection had continued, intense levels of *FOS* staining in the same regions as in the 2 hr cases. In the hippocampus the DG had even more robust *FOS* staining, and the CA1, CA2, and CA3 fields of hippocampus now expressed strong levels of *FOS*.

Eight Hours. By 8 hr after soman treatment, *FOS* expression substantially declined in regions of the olfactory bulb, CPu and cortical areas mentioned above. Robust *FOS* was persistent in PC layers II and III while En and Tu were notably devoid of *FOS*. LC still had hardy *FOS* expression after 8 hr. Curiously, Rtn was devoid of *FOS*. Hippocampal structures mentioned above maintained strong levels of *FOS* staining as in the 4 hr cases.

Twenty-four Hours. By 24 hr after soman administration *FOS* staining in most areas had declined to control levels. Only layers II and III of PC, Mi of the bulb, and hippocampus had maintained *FOS* expression. A striking feature of animals sacrificed 24 hr after-soman was severe necrosis in layer II of caudal PC. Animals allowed to survive beyond 24 hours (data not shown) had severe neuropathology throughout the entire rostral-caudal extent of PC.

DISCUSSION

The major results of this study are: (1) Systemic administration of the anticholinesterase soman produces profound convulsions and robust expression of the immediate early gene protein product *FOS* in a restricted number of brain regions; (2) The spatial distribution of neurons expressing *FOS* and the intensity of *FOS* staining exhibited a temporal gradient. At 30-45 min after soman administration, the earliest time intervals examined, robust *FOS* expression was consistently observed in only three brain regions, LC, PC, and Rtn. After 2 hr, *FOS* expression was seen throughout several cortical regions, hippocampus, and CPu. By 24 hr, after-soman, there was marked neuropathology in PC, the site of the earliest and most intense *FOS* expression in the brain, and a demonstrative decrease in *FOS* throughout the CNS. These results suggest that a restricted set of brain structures are involved in the earliest manifestation of cholinolytic seizures. These structures, as described below, thus, may, be involved in the generation and dissemination of soman -nduced seizures.

***FOS*: Use and Limitations**

Numerous studies have shown that activation of secondary messenger signaling pathways or depolarization of neurons leads to the induction of the proto-oncogene *FOS*. While several previous reports have shown that seizures induce *FOS* expression in several neocortical areas and the hippocampus, the temporal pattern of *FOS* expression was not examined. The goal of the present study

was to map the regional and time-dependent expression of *FOS* in order to pinpoint the first brain regions that undergo elevated neural activity following soman administration. There are several potential limitations and pitfalls of this approach, however, that require consideration.

(1) All neurons activated by soman may not express the *FOS* protein. Cells are known to express different protooncogenes in response to increased activity and/or brain damage (*Jun e*, *Jun b* and *d*, *Crox*, etc.). However, in several experiments we stained for several proto oncogenes (*jun d*, *jun b*, and *zif*) and found that their temporal and spatial distribution was essentially identical to *FOS*.

(2) The level of transcription of the *FOS* gene product in some cells may vary and *FOS* protein might not be detected at the dilutions of *FOS* antibody used in this experiment. In intact control animals, constitutive or basal expression of *FOS* from animal to animal or brain region to brain region may vary dramatically. High levels of constitutive expression may prevent or mask detection of stimulation-induced increases in *FOS* expression. To mitigate this potential problem, we screened a number of dilutions to identify a concentration at which there was little or no constitutive expression of *FOS* in most brain areas. Thus, the antibody concentration used in this study was biased toward detecting increased *FOS* expression following soman administration. A potential problem with this approach is that our antibody concentration may have been too dilute to detect increases in some neuronal populations; However, the present finding of robust *FOS* protein expression in several brain regions within 30 min of soman-induced convulsions, a time substantially shorter than reported in several other seizure studies, indicates that the sensitivity of our procedure was sufficient to detect very rapid increases in *FOS* expression.

(3) *FOS* gene transcription and translation may take longer in some cells than others; thus the temporal pattern could reflect different rates of transcription/translation rather than spread of neural activity. For example, expression of *FOS* may be triggered early in some neurons by direct cholinergic stimulation, while delayed expression in other cells occurs only after seizure development. We recognize these possibilities; however, the main goal of this study was to pinpoint the earliest neurons activated after soman administration, irrespective of whether *FOS* is triggered by ACh or seizures. Moreover, we hypothesize that the first wave of *FOS* expression is caused by ACh stimulation rather than seizures. Both LC and PC neurons are cholinceptive, and ACh is known to increase excitability of both groups of neurons. In addition, we have previously reported that LC neurons begin to increase their activity following soman administration at a time preceding the onset of seizures (⁵⁸). Finally, studies by others indicate that *c-fos* is the most rapidly expressed proto oncogene after seizures and elevated neuronal activity. Thus, we are confident that the temporal sequence of expression closely reflects the times that different populations of neurons undergo elevated activity, rather than representing delayed rates of transcription/translation.

(4) *FOS* staining may not reveal neurons that are inhibited following soman. This is an important consideration since soman-induced inhibition of specific neural populations may play an important role in seizure generation. For example, inhibition of GABAergic interneurons could lead to increased activity and/or excitability, promoting seizure generation. We recognize that neuronal inhibition may play an important role in seizures; however, at some point, the initiation and propagation of seizures requires elevated levels of neuronal activity. As *FOS* staining is a sensitive marker of neuronal hyperactivity, we believe the results of the present study accurately reveal subsets of neurons undergoing heightened activity prior to and/or during soman-induced seizures.

Piriform Cortex

The demonstration that piriform cortex (PC) was invariably the first structure in the brain to express *FOS* after soman-induced convulsions was a pivotal observation. It has long been known that PC has a preferentially low threshold for soman-induced seizures. Of equal importance, it is also well established that the PC is the most vulnerable site in the brain to soman-induced neuropathology. The demonstration that *FOS* is rapidly induced, specifically in PC neurons, therefore indicates that the expression of this molecule selectively pinpoints the earliest neurons known to be affected by soman. Further, a subset of PC neurons express *FOS*: the neurons of layers II and III of PC. This selectivity of neuronal subpopulations further reinforced the idea that *FOS* is pinpointing the neurons affected by soman. Evidence from this and many other laboratories shows that soman-induced cell death is highly preferential for these same layer II and III PC neurons (189, 199). Thus, after soman, the first neurons in the brain to express *FOS* are the same neurons that show the highest frequency of cell death in soman-induced neuropathology. *FOS*, therefore, selectively and sensitively identifies the first brain neurons affected by soman. Animals subjected to the same doses of soman, but allowed to survive for progressively longer times before staining for *FOS*, showed progressive induction of *FOS* in other brain regions.

PC receives a massive cholinergic innervation from basal forebrain cholinergic neurons in the nucleus of the diagonal band (NHDB). We have labeled cholinergic fibers in the PC with antibodies to choline acetyltransferase (ChAT), the synthetic enzyme for ACh; ChAT immunocytochemical staining is diagnostic of cholinergic innervation. The results demonstrate that the cholinergic innervation of PC is heavier than the corresponding cholinergic innervation of hippocampus and neocortex. The cholinergic innervation is particularly dense in layers I, II, and III; these same cortical layers exhibit dense AChE staining. Cholinergic inputs to PC arise in the basal forebrain from the nucleus of the diagonal band (NHDB). Following systemic injections of convulsive doses of soman, rapid (30-45 min) *FOS* expression is restricted to neurons whose cell bodies and dendrites occupy layers I, II, and III. Therefore, the first neurons in the brain to express *FOS* after soman administration are neurons that

receive the heaviest cholinergic projection of any cortical structure.

Considerable evidence, particularly in the last five years, has spotlighted PC as the site in the cerebral cortex most selectively vulnerable to the seizurogenic actions of a number of neuroactive compounds. Of even greater significance from the perspective of soman's seizurogenic action is that several recent studies have demonstrated that PC is not only selectively seizure-prone, but that seizures initiated in PC spread to the rest of the cerebral cortex. A recent study has even suggested that a rostral subcomponent of PC is especially epileptogenic (¹⁵⁹). Cholinergic agonists microinjected into PC cause seizures which spread to the rest of the brain. Microinjections of the GABA agonist muscimol into this restricted part of rostral PC can effectively block the initiation of seizure, and if given after the initiation of seizures, can prevent the spread of seizures to the rest of the cortex. Meldrum and colleagues (¹²⁸) more recently reported that microinjections of EAA agonists at any rostrocaudal site of PC initiates seizures that spread throughout the cortex. In addition, they have demonstrated that femptomolar concentrations of EAA agonists injected into PC can trigger seizures in animals given subconvulsive doses of the cholinergic muscarinic agonist pilocarpine. Meldrum and co-workers have also shown that focal injection of 250 fmol-10 nmol of an N-methyl-D-aspartate (NMDA) receptor antagonist 2-amino-7-phosphonoheptanoate (APH) in PC prevents seizures normally caused by convulsive doses of pilocarpine. These findings, taken together with the known pathological vulnerability of PC to soman and our new results showing that PC is the first brain structure to express *FOS* after soman intoxication, strongly support the hypothesis that soman-induced seizures are initiated in PC and that PC serves as a focus for the propagation of seizures to other cortical areas via EAA-mediated corticocortical association pathways.

PC is composed of three distinct layers. Layer I is composed of afferent axon terminals from olfactory bulb and association axons forming cortico-cortical connections throughout the length of PC. These association axons originate in layers II and III of PC and send collaterals throughout PC, hippocampus, olfactory bulb and other neocortical areas. The finding that *FOS* is preferentially expressed in layers II and III of PC is thus significant as these layers contain the neurons which give rise to the majority of the cortico-cortical association fibers that anatomically link rostral and caudal PC with each other and with other areas of the cortex. Studies in Haberly's ⁷⁹ lab (1985) indicate that these circuits primarily use EAAs as their primary transmitter. A critical role for EAAs in soman-induced seizures has been demonstrated by Sparenborg et al. (¹⁸⁴) who found that injections of the NMDA antagonist MK-801 block the induction of seizures in soman-treated animals.

Both nicotinic (N) and muscarinic (M) receptors are present in PC. Thus hypercholinergic stimulation of PC by soman could activate M-, and/or N-receptors. The available evidence on central N-receptors to date indicates they are rapidly activating and rapidly desensitizing receptors. M-receptors,

however, have several properties which make their role in cholinergic seizures attractive. *In vitro* cellular neurophysiological studies of hippocampal neurons indicate that agonists to the M-receptors dramatically increase the level and duration of pyramidal neurons responsiveness to coactivation of EAA inputs. ACh, acting via an M-receptor-mediated, second-messenger system, potently blocks a Ca^{2+} -modulated, K^+ -mediated, voltage-dependent after hyperpolarization. (AHP) (18, 27, 37, 40, 41, 81, 113, 144, 207). It has been proposed that hyperpolarization protects cortical neurons from being overexcited by EAAs.

Based on the preceding observations, we hypothesize that cholinergic overstimulation of PC triggers a mechanism which involves the release of EAAs. The initial consequence of soman administration is an immediate and irreversible inhibition of AChE, causing a continuous accumulation of unhydrolyzed ACh from cholinergic terminals. We further hypothesize that the primary consequence of cholinergic hyperstimulation and the blockade of the M-receptor AHP is to dramatically increase the responsiveness of these neurons to EAAs that are being tonically released by the majority of synapses impinging on them. Because these cortical neurons are progressively excited by EAA inputs, they release more EAAs at their own synaptic terminals on other cortical neurons, thus further feeding an EAA "chain reaction."

Locus Coeruleus

The finding of *FOS* expression in LC by 30-45 min after soman was surprising as there is very little evidence for a role of norepinephrine (NE) in soman-induced seizures. However, in view of neurochemical findings and other recent results by others, the finding of soman-induced *FOS* induction in LC is of considerable potential significance. All LC neurons synthesize and release NE, and LC is the largest NE cell group in the brain. In addition, the entire cerebral cortex including PC and hippocampus is innervated by axons originating in LC (65). Thus, LC's anatomical projections place it in a position to exert a global influence on neuronal excitability, and thus seizure initiation or maintenance. The finding that *FOS* is rapidly and strongly induced in LC neurons suggests that there may be a massive increase in NE release soon after soman administration. This possibility was confirmed by experiments described in Chapters 5, 6 and 8.

The idea that NE release in forebrain may contribute to seizures has precedent in the literature. *In vitro* cellular electrophysiological studies demonstrate that NE acting at a β -receptor blocks the afterhyperpolarization potential (AHP) in hippocampal pyramidal neurons. As a result of blocking the AHP, these cortical neurons become hyperexcitable to activation of afferent EAA synapses and to exogenously applied EAA agonists. Thus, NE activation of β -receptors has a seizure-promoting action very similar to that produced by ACh acting at muscarinic receptors. In this regard, it is significant that

pharmacological experiments have demonstrated that β -receptors are densely concentrated in layers II-III of PC and layers II-III of the neocortex (23, 94, 95, 155). These are the same layers where we found *FOS* induction in neurons after soman-induced seizures. Other evidence also points to the possible involvement of NE in soman-induced seizures. ¹⁰⁵ and Noebels (1981) reported that in a single gene, seizure-prone mutant mouse, there is a 50% increase in the number of neurons in LC and corresponding increases of NE cortex fibers or terminals in the forebrain. *In vitro* studies of PC slices have demonstrated that physiological concentrations of exogenous NE dramatically increase excitatory transmission and neural activity in PC; this action is blocked by nonselective α - and β -blockers (38, 61, 73, 75, 78, 114, 115, 142). Moreover, NE was also found to significantly increase potassium-evoked release of endogenous EAAs (glutamate, aspartate) from PC slices. These findings support the idea that soman-induced, sustained release of NE in PC could initiate or facilitate seizures by increasing the responsiveness of cortical neurons to EAA and by facilitating EAA release.

If, as suggested by the *FOS* results, LC neurons are driven to hyperactivity by soman, causing increased release of NE, then the AHP should be significantly reduced or blocked, thus rendering cortical neurons hyperresponsive to EAAs. In this case, NE and ACh hyperstimulation may act cooperatively, or even synergistically, to potentiate cortical neurons' hyperresponsiveness to EAAs because both NE and ACh block the K^+ -mediated AHP ((18, 27, 37, 40, 41, 81, 113, 144, 207). Thus, if soman causes sustained hyperactivity of LC with sustained release of NE, then cortical neurons will be confronted with a "double whammy," hypercholinergic and hypernoradrenergic stimulation blocking the AHP, thus making cortical neurons hyperactive to EAA synaptic inputs.

Another neurotransmitter contained in many LC neurons which may play a role in soman-induced seizures is neuropeptide Y (NPY). Evidence in the peripheral nervous system suggests that during high-frequency activation of NE-containing neurons, NPY is co-released with NE. NPY through its actions at a non-NE receptor has been shown to potentiate the actions of NE by more than tenfold. Although the present data on neuropeptides are limited, it has been suggested that NPY may also potentiate the actions of NE in the CNS. Recent data have shown that NPY is released in high quantities in the brain during electroconvulsive shocks which produce seizures. Furthermore, NPY receptors are highly concentrated in layers II and III of PC. Since soman causes the sustained activation of LC neurons, it may be postulated that NPY potentiates the response of PC and other cortical neurons to NE, thus causing cortical neurons to become even more hyperresponsive to EAAs.

3. GLIAL CELLS AND SOMAN NEUROPATHOLOGY

INTRODUCTION

It has long been known that many traumatic events culminating in neuropathology are accompanied by dramatic changes in astrocytes. These changes range from the classical observation that glial cells increase in number and density in sites of brain injury (gliosis) to the more recent finding that astrocytes change their morphology by increasing the number and thickness of their processes following injury and deafferentation (52, 161). A watershed discovery was the isolation and characterization of a molecule unique to the cytoskeleton of astrocytes. Antibodies to this molecule (glial fibrillary acidic protein; GFAP) made it possible to selectively label and thus identify astrocytes in histological sections and tissue cultures (52). More important still, was the observation that following injury there was a dramatic increase in the amount of GFAP in astrocytes, doubtless corresponding to an increased production of cytoskeletal protein necessary for the increased number and thickness of astrocyte processes induced by trauma (8, 51, 161). It was shown that GFAP expression was not due to direct injury to the astrocytes. An injury in one part of the brain causing degenerative loss of axons and terminals in a far distant site in the brain caused GFAP expression in astrocytes associated with the degenerating axon terminals. This and many other studies have led to the conclusion that astrocytes "react," i.e., change shape and increase GFAP, in response to signals in neighboring cellular elements (8, 51, 161). The nature of these signals is an area of intense current research.

METHODS

Animals, soman injection and survival periods, and histological procedures are identical to those described in the preceding chapter. Antibodies to three proteins were used: (1) Glial fibrillary acidic protein (GFAP) - GFAP is a cytoskeletal filament specific to astrocytes. Our antibodies (rabbit) to GFAP were supplied by DAKO Corp. (2) OX-41 and OX-42 - These two-cell membrane proteins are used to recognize microglia (OX-42) and macrophages (OX-41, OX-42). Our antibodies were supplied by Sera Lab (mouse). Secondary antibodies directed against the species that produced the primary antibody are purchased from several sources according to their affinity and price.

RESULTS

There has been much confusion about the temporal relation between the onset of neuro-traumatic events and the first detectable changes in GFAP. As recently as 3 years ago, it was reported that 12 hr after the induction of seizures by metrazol, increased GFAP could be detected in the hippocampus (60). The significance of this observation was that previous studies had reported increased GFAP-increased only after 1-2 days. We decided to examine PC in animals in which soman had caused rapid (30-45 min) induction of *FOS* in PC neurons. We quickly realized however, that there was a problem with this kind of analysis that was also present in all other previously published studies of the time course of GFAP expression. In normal brain tissue, including PC, there is always some steady-state level of GFAP expression. The presence of GFAP in normal material is an impediment to detecting increased GFAP expression. The problem is a simple signal-to-noise issue; if there is appreciable resident GFAP expression (noise), detection of small, increases (signal) in GFAP is difficult. We solved this problem by performing a series of experiments in which we progressively diluted the concentration of primary antibodies used to detect GFAP to a level (threshold) at which little or no GFAP was detected in sections through PC of normal animals. Using this threshold-dilution method, we analyzed PC sections at various time intervals following soman; we compared animals in which soman had induced *FOS* in PC neurons with animals that did not convulse and in which *FOS* expression was low or not present. The results were very striking. In animals with neurons expressing *FOS* in layer III of PC, astrocytes confined to layer II consistently expressed elevated GFAP as early as 45 min after administration of soman (figure 1; 178).

These results warrant two conclusions: (1) Previous studies significantly overestimated the time from the onset of seizures to the first detectable increase in GFAP. The finding that GFAP is increased at 45 min and that the increase is coincident with the expression of *FOS* in adjacent hyperactive (stressed) neurons indicates that changes in astrocytes that are known to be strongly associated with pathology and cell death are remarkably rapid and parallel the earliest molecular signals of stress in adjacent neurons. (2) The observation that increased GFAP is restricted to layer II in astrocytes forming the immediate microenvironment of the neurons destined to die, taken with the temporally coordinate expression of *FOS* in those neurons, leads to the hypothesis that glial changes associated with neuron stress may be causally related to neuron death. The dramatic temporal and spatial coordinate expression of *FOS* in PC neurons and GFAP in nearby astrocytes is the earliest known neuropathological event in soman toxicity. By examining animals sacrificed at progressively longer time intervals after soman, we have found that the association of *FOS* expression in neurons and increased GFAP in adjacent astrocytes is a correlation that holds invariably across all brain regions examined.

Microglia and Macrophages. Macrophages are key cells in tissue pathology; they remove injury-induced cellular debris by phagocytosis. Macrophages are not present in normal brain tissue. It is

thought that injury recruits macrophages from circulation and possibly induces the transformation of resident microglia into macrophages (97). A recent study of hippocampal lesions suggested that an initial event in neuropathology involves microglia secretion of interferon which leads several hours later to the induction of GFAP in reactive astrocytes (71, 145). However, our results reported above indicate that GFAP expression is already dramatically increased at 1-2 hr. Thus, we have examined the reactions of microglia following soman using antibodies (OX-41, OX-42; ¹⁶²) that recognize microglia and macrophages.

Our results show that 4-6 hr after seizures, microglia convert to macrophages in PC. This indicates that microglial to macrophage transformation occurs significantly later than the neuronal expression of *FOS* and astrocyte expression of GFAP/quinolinic acid (QUIN). Taken together, these results suggest that neurons and/or astrocytes may provide the signals for microglial/macrophage reactions to pathology and not vice versa. A critical point, however, is that by 4-6 hr, macrophages are already present in PC. Since macrophages function primarily to phagocytose injury-related cellular debris, it appears, once again, that pathophysiological events are exceedingly rapid in soman-induced seizures. Thus, management of soman-induced seizures, by inactivating the triggers that initiate the seizures, may provide the best protection against brain damage.

CONCLUSIONS

Could Astrocytes Contribute to Neuropathology?

While early expression of GFAP in astrocytes associated with seizing neurons is indicative of "reactive gliosis," GFAP itself is not likely to be a molecule that figures directly in pathogenesis because GFAP is a structural protein. Increased GFAP expression is, rather, a sensitive signal indicating that the astrocytes are mobilizing other factors which contribute to toxicity. One molecule that may be particularly important in this regard is a tryptophan metabolite, quinolinic acid, which, in the brain, is produced exclusively by astrocytes (¹⁶⁸). Quinolinic acid (QUIN) first surfaced in relation to the brain, when based on its structural properties, it was suggested that QUIN might be a neurotoxin. It is now established that QUIN is a potent neurotoxin (¹⁶⁸). QUIN is a preferential NMDA receptor agonist (Schwarcz *et al.*, 1989). The synthetic (3-hydroxyanthranilic oxidase; 3-HAO) and degradative (quinolinic acid ribosyltransferase; QRST) enzymes for quinolinic acid are expressed in the brain exclusively by astrocytes (Kohler *et al.*, 1988). Thus, astrocytes both synthesize and degrade a molecule, which is both an NMDA agonist and at slightly higher concentrations, a potent neurotoxin. There is endogenous QUIN in brain homogenates, and the question arises as to the normal function of

this neurotoxic molecule and the regulatory controls that normally maintain its expression below toxic levels. Currently, little is known about the normal function of QUIN. It has been suggested that since QUIN is an effective agonist for the NMDA receptor, and since NMDA receptor activation has been strongly implicated in prolonging synaptically mediated events, the local secretion of QUIN by astrocytes, adjacent to active synapses, might provide a "local amplificatory" signal complementing neurally released EAAs to prolong the occupancy or increase the number of occupied NMDA receptors (¹⁶⁸). Consistent with this, Schwartz (personal communication) has shown that in hippocampal slices incubated in the presence of labeled precursors to QUIN, there is a dramatic increase in labeled QUIN following long-term potentiation (LTP). LTP requires the sustained activation of EAA synapses, and this appears to cause an increase in QUIN synthesis and release. Our hypothesis for the mechanism of soman-induced seizures is that combined cholinergic-noradrenergic hyperstimulation causes cortical neurons to become hyperactive to EAAs released by synapses on the cortical neurons. By increasing their excitability to EAAs, the neurons discharge more vigorously for the same amount of EAAs released upon them. As a consequence, since these same neurons release EAAs at their own synaptic terminals on other cortical neurons, some of which feed back on the original neurons, cortical circuits are further driven toward an EAA hyperexcitability "chain reaction" to seizures. If QUIN release, as suggested by Schwartz's study, is increased by astrocytes in the vicinity of neurons receiving increased EAA inputs, then the QUIN, by activating NMDA receptors, would further push the EAA chain reaction. Since the neurotoxic potency of QUIN is very great, it is conceivable, therefore, that the sustained hyperactivity produced by soman causes astrocytes associated with seizing neurons to secrete high levels of QUIN. Thus, QUIN would both feed the EAA chain reaction and, at the same time, have a neurotoxic action. In this event, the release of QUIN under conditions of soman-induced hyperexcitability would function synergistically with EAAs to accelerate the propagation of seizures and cell death.

4. STIMULATION OF ENDOGENOUS CHOLINERGIC INPUTS TO PC PRODUCES SEIZURES, INCREASED *FOS* EXPRESSION AND UP-REGULATION OF ASTROCYTES

INTRODUCTION

The preceding studies demonstrated that systemic administration of soman produces rapid induction of *FOS* and GFAP expression in layers II-III of piriform cortex (PC). These findings led us to hypothesize that sustained release of ACh in PC from the terminals of cholinergic neurons after soman administration triggers neuronal expression of *FOS* and up-regulation of astrocytes in PC. We refer to this as the "*cholinergic trigger hypothesis*". The cholinergic trigger hypothesis predicts that sustained release of ACh in PC from the terminals of cholinergic neurons, originating in the nucleus of the diagonal band (NHDB), should cause seizures and the selective expression of *FOS* in neurons of layers II-III in PC as is observed following soman. The following studies were designed to directly test this hypothesis.

METHODS

Electrode Implantation and NHDB Stimulation. Adult male Sprague-Dawley rats (270-295 g; Harlan Laboratories, Indianapolis, IN) were anesthetized with chloral hydrate (400 mg/kg, ip) and placed in a stereotaxic device with the skull flat. A hole was drilled in the skull at the coordinates for NHDB (0.0 mm bregma, 1.9 mm lateral to midline). A bipolar stimulation electrode, consisting of twisted stainless steel microwires (0.125 μ m diameter, factory-insulated except for bluntly cut tips) was advanced into NHDB (8.3 mm ventral to brain surface). A second electrode, consisting of a pair of 250 μ m diameter stainless steel wires (insulated except for bluntly cut tips) was implanted into the cortex (5.0 mm caudal to bregma, 1.0 mm lateral to the midline) to monitor the electroencephalogram (EEG). The tips were separated dorsoventrally by 500-1000 μ m and the electrode was implanted so that the superficial tip was approximately 200 μ m ventral to the brain surface (Fig. 2). The NHDB and EEG electrodes were and secured to skull screws with dental acrylic. One week following surgery, animals were placed in a clear plexiglas observation chamber and leads were attached to the two electrodes. There were three experimental conditions: (1) NHDB stimulation; NHDB was electrically stimulated with intermittent trains (12 Hz, 5 sec on/3 sec off, 400-500 μ A) for periods of 10, 20, 45 or 60 min. Stimuli were isolated constant current square wave pulses, 0.5 msec in duration and 400-500 μ A in intensity. (2) NHDB stimulation + drug; animals were treated as above, and also received injections of a cholinergic receptor antagonist. Animals received injections of the muscarinic receptor antagonist scopolamine

hydrochloride (2.0 mg/kg) or the nicotinic receptor antagonist mecamylamine hydrochloride (1.0 mg/kg, ip) 20 min prior to, and at the onset of, NHDB stimulation. (3) Controls; animals were implanted with NHDB and EEG electrodes and injected with proportional volumes of physiological saline, but received no stimulation. After the termination of NHDB stimulation, animals were deeply anesthetized and perfused with fixatives, and processed for immunohistochemical visualization of *FOS* or GFAP as described in Chapters 2 and 3. Tissue sections from the three experimental groups were simultaneously processed in the same reaction solutions to control for variability in staining intensity.

RESULTS

NHDB Stimulation. Within 5 min after the onset of NHDB stimulation, rats exhibited marked behavioral signs nearly of seizure activity that were nearly identical to those observed following soman administration. These included intense gnawing, salivation, sniffing, ipsilateral eye-blinking, rearing, and forepaw reaching. These stimulation-induced behaviors continued throughout the period of stimulation and frequently persisted for 5-10 min after the termination of stimulation. As illustrated in Figure 3, NHDB stimulation caused large amplitude EEG spike and wave activity, resembling seizure activity produced by soman administration; this seizure-like EEG activity persisted 20-40 min after the termination of NHDB stimulation in some cases.

As shown in Figure 4, electrical activation of NHDB neurons led to rapid elevation of *FOS* in PC neurons. *FOS* was selectively and robustly expressed by the majority of layer II-III neurons along the entire rostrocaudal extent PC ipsilateral to the stimulated site. NHDB-induced expression of *FOS* expression was very rapid. Elevated *FOS* staining compared to control animals was observed after 10 min of NHDB stimulation (n=1). Longer epochs of NHDB stimulation led to progressive increases in the number, and the intensity of *FOS*-positive neurons in PC. Following 20 min of NHDB stimulation (n=4), *FOS* was selectively and heavily expressed in a large population of layers II and III PC neurons. A few neurons in contralateral PC also expressed *FOS*; we attributed this staining to spread of excitation from the ipsilateral to the contralateral PC via the anterior commissure, a fiber tract which massively interconnects PC on the two sides of the brain. Future experiments will assess this possibility by stimulating NHDB in animals after transection of the anterior commissure.

After 45 min of NHDB stimulation (n=4), there was heavy *FOS* expression throughout layers II-III of PC and the appearance of *FOS* expression in several other cortical sites. There was strong *FOS* staining in the hippocampal dentate gyrus, and to a lesser extent, in the CA1, CA2, and CA3 fields. There was also elevated *FOS* expression in entorhinal cortex.

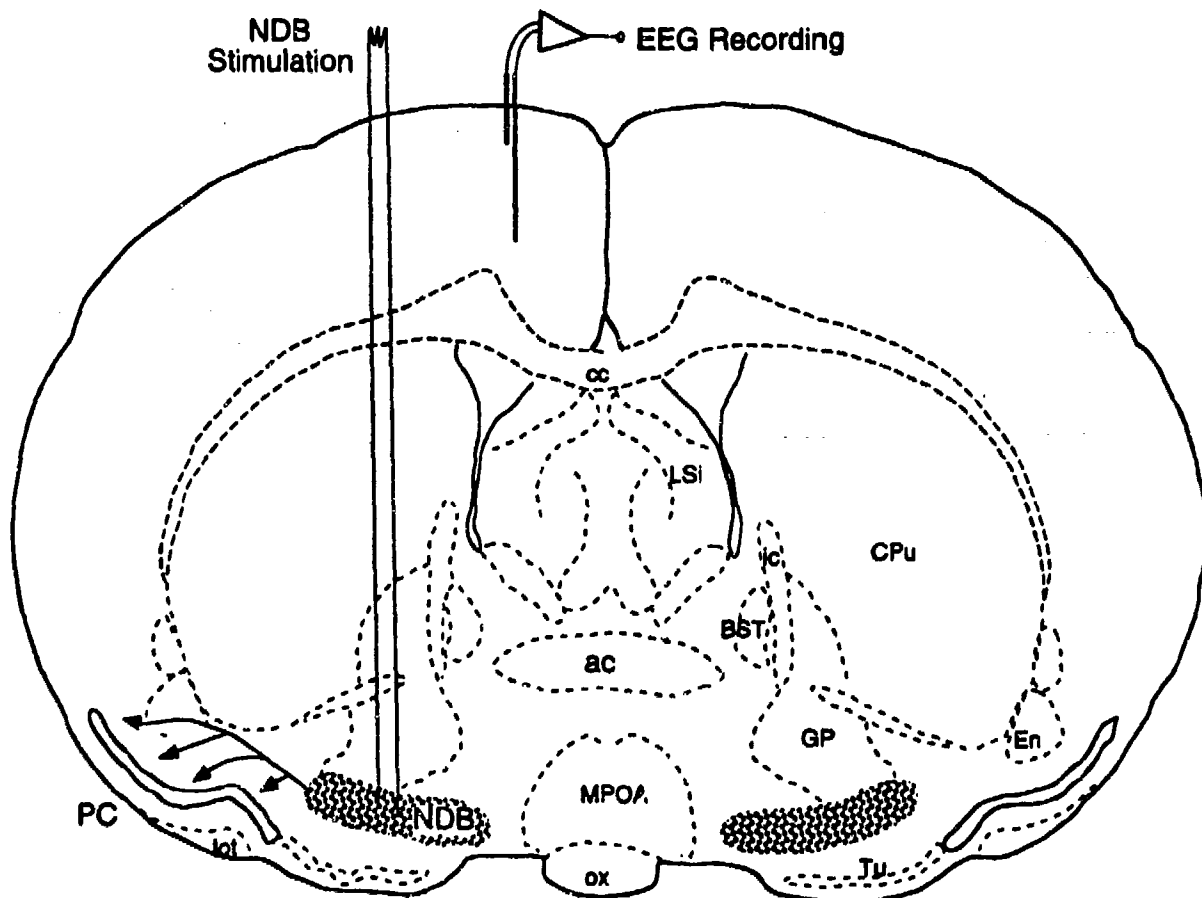


Figure 2. Schematic diagram of a coronal section through the forebrain illustrating the experimental paradigm. Animals were anesthetized and a bipolar stimulation electrode (paired 125 μ m stainless steel wires, insulated except for bluntly cut tips) was stereotaxically implanted in NDB, and a transcortical electrode was implanted to monitor the EEG. Seven to ten days later, awake, unrestrained animals were placed in an observation chamber and leads were attached to the electrodes. There were 3 experimental conditions:

- **NDB Stimulation** - NDB was electrically stimulated (400-500 μ A) with intermittent trains (5 sec on/3 sec) of 12 Hz stimulation for 20-60 min.
- **NDB Stimulation + Drug** - Identical to NDB Stimulation except that animals received two injections (ip) of the muscarinic receptor antagonist scopolamine or the nicotinic receptor antagonist mecamylamine; the first injection was given 20 min before and the second 5 min before the onset of NDB stimulation.
- **Control** - implanted animals that were not stimulated.

Ten to 40 min after the termination of stimulation, animals were anesthetized, perfused, and brains were removed and processed for immunohistochemical visualization of Fos. Brains from animals in the 3 experimental groups were simultaneously processed in the same antibody solutions to control for staining variability.

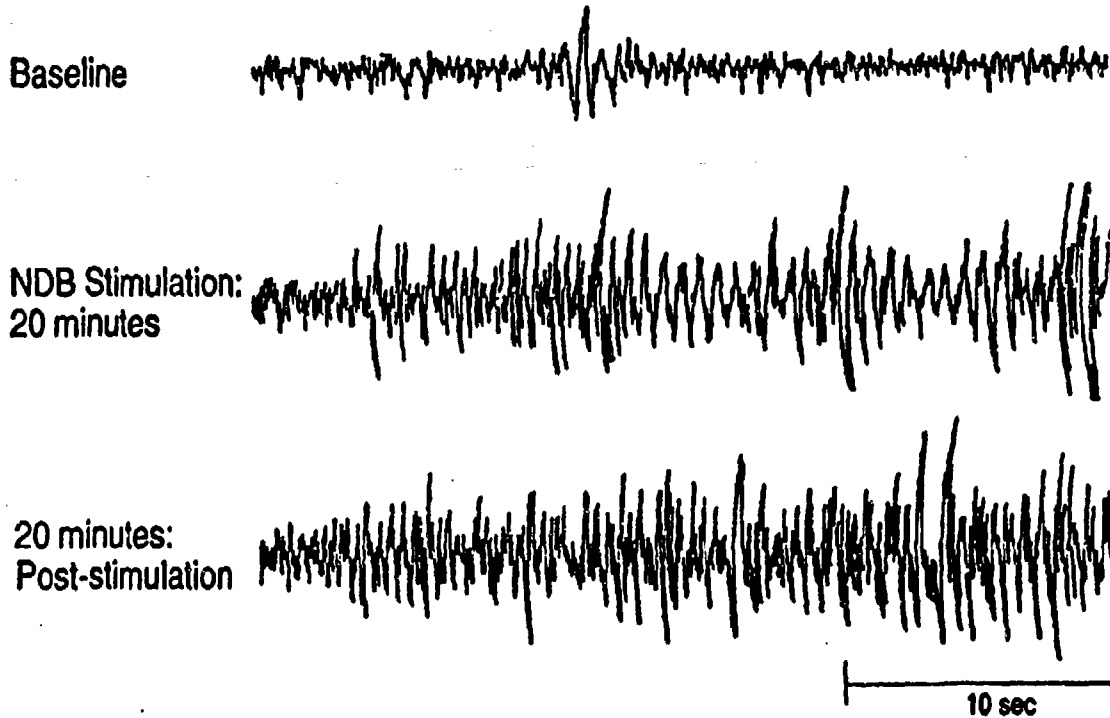


Figure 3. NDB stimulation evokes cortical seizure-like activity. Cortical EEG recordings before (Baseline, upper panel), during NDB stimulation (middle panel) and 20 min after the termination of NDB stimulation (lower panel). Note that NDB stimulation increases EEG spike and wave activity resembling cortical seizures produced by soman administration. This activity persists as long as 20-40 min after NDB stimulation, the time animals were anesthetized for perfusion.



Figure 4. NDB stimulation induces rapid Fos expression in PC; blockade by muscarinic receptor antagonism. Photomicrographs of Fos staining in PC and hippocampus in **NDB Stimulation** (upper row), **NDB Stimulation + Scopopolamine** (middle row) and **Control** (lower row) groups.

NDB Stimulation:

- PC - Low power (left) and high power (middle) photomicrographs of coronal sections through PC. Twenty min of NDB stimulation produced robust, selective Fos staining of layer II-III PC neurons. Note stimulation electrode tract to the right of the section.
- hippocampus (right column) - NDB stimulation also induced robust Fos expression in the dentate gyrus of the hippocampus.

NDB Stimulation + Scopopolamine: NDB stimulation after injection scopolamine did not produce Fos staining in PC or the hippocampus above control levels.

Control: There is very little constitutive Fos expression in implanted control animals.

Activation of the NHDB—PC pathway for 10-45 min did not produce detectable increases in the level of GFAP staining in PC or other cortical areas although there was focal, intense GFAP expression along the stimulation electrode tract and at the electrode tips in both control and NHDB stimulation cases. The "glial scar" formed by reactive astrocytes is attributed to neuronal damage that occurred during electrode implantation. After 60 min of NHDB stimulation, however, there was a marked increase in GFAP expression in PC (n=3). Similar to the distribution of *FOS*, GFAP expression was preferentially dense in layer II and the superficial part of layer III.

NHDB Stimulation + Drug. The preceding finding that activation of endogenous cholinergic inputs to PC produces cortical seizure activity and *FOS* expression in PC neurons essentially identical to that caused by soman strongly supports the cholinergic trigger hypothesis for soman's seizurogenic actions. This hypothesis also predicts that administration of cholinergic receptor antagonists should block the behavioral (convulsive) consequences of NHDB stimulation, and further, should prevent the expression of NHDB-evoked seizures and *FOS*. Both of these predictions were confirmed. Pretreatment with the muscarinic receptor antagonist scopolamine (2 mg/kg, ip): (1) Completely blocked or markedly attenuated the NHDB-evoked behaviors and seizure activity in seven of eight animals tested. Although animals exhibited increased motor activity, there was no evidence of any of the other convulsive behaviors; and (2) blocked or reduced the expression of *FOS* in PC and the hippocampus (7/8 animals). In contrast, administration of the nicotinic receptor antagonist mecamylamine was uniformly ineffective in reducing NHDB-evoked behaviors, cortical seizures or *FOS* expression.

In preliminary studies, we examined whether scopolamine pretreatment would block GFAP expression produced by 60 min of NHDB stimulation. In two cases tested, systemic administration of scopolamine, at doses shown above to block NHDB-evoked seizure activity and *FOS* expression, did not attenuate increased GFAP expression in PC.

Controls. In implanted control animals (n=8), there was very little or no *FOS* expression in PC and other cortical structures. Occasionally, there was a focal band of *FOS*-positive neurons at the site of the stimulation electrode. In addition, injection of scopolamine or mecamylamine did not influence the level of *FOS* expression in PC or other brain areas.

CONCLUSIONS

The results of this study demonstrate that activation of the source of endogenous cholinergic inputs to PC from NHDB produces a spectrum of motor behaviors and central effects that are essentially identical to those observed after soman intoxication. Specifically, electrical stimulation of NHDB: (1)

elicits several specific motor patterns (e.g., sniffing, twitching, rearing) that resemble convulsive activity produced by soman; (2) evoked large amplitude spike activity in the cortical EEG indicative of seizures; and (3) Produced rapid and robust elevation of *FOS* and GFAP expression layers II and III of PC as does systemic soman.

The temporal and spatial pattern of *FOS* expression following NHDB stimulation was remarkably similar to that observed after soman administration. As discussed in Chapter 2, the first detectable increase in *FOS* expression begins approximately 30-45 min after soman injection selectively in layers II and III of PC. In the present study, elevated *FOS* expression was observed 10-20 min after the onset of NHDB stimulation in the same layers of PC. The 10-15 min time lag for soman-induced *FOS* expression may reflect the time required for AChE inhibition and the buildup of unhydrolyzed ACh to produce sufficient cholinergic stimulation of PC neurons to induce elevated neuronal activity, and hence, *FOS* expression.

Similarly, the onset of elevated GFAP staining in the NHDB stimulation (60 min) and soman experiments (45-60 min, Chapter 3) are comparable. Moreover, in both sets of experiments, elevated GFAP expression was restricted to layers II and III of PC. The finding that elevated GFAP expression in astrocytes is temporally and spatially coincident with the expression of *FOS* in adjacent hyperactive (stressed) neurons indicates that changes in astrocytes, known to be strongly associated with pathology and cell death, are remarkably rapid and parallel the earliest molecular signals of hyperactivity and/or stress in adjacent neurons. The observation that increased GFAP is restricted to layer II-III astrocytes forming the immediate microenvironment of the neurons destined to die following soman poisoning, taken with the temporally coordinate expression of *FOS* in those neurons, leads to the hypothesis that glial changes associated with neuron stress may be causally related to neuron death. The dramatic temporal and spatial coordinate expression of *FOS* in PC neurons and GFAP in nearby astrocytes is the earliest known neuropathological event in soman toxicity. In this regard, it would be of interest to determine if layer II-III PC neurons undergo cell death in animals allowed to survive for longer periods of time after NHDB stimulation.

The striking similarity of the temporal and spatial spectrum of responses produced by NHDB stimulation to that produced by soman provides strong support to the cholinergic trigger hypothesis for soman's seizurogenic actions in the brain. NHDB provides the sole source of cholinergic input to PC. Although NHDB neurons, possibly some of those that project to PC, contain other neurotransmitters (e.g., GABA), our pharmacological finding that the effects of NHDB stimulation were dramatically attenuated or completely blocked by the muscarinic receptor antagonist scopolamine indicates that they were mediated by ACh acting at a muscarinic receptor. The failure of mecamylamine to block these responses indicates that there is not a substantial ganglionic nicotinic receptor component involved in

this pathway. However, as the drugs used in this study were administered systemically, we cannot conclude that scopolamine's actions were mediated by antagonism of ACh actions on cholinergic synapses in PC. Future studies utilizing microinjection of cholinergic antagonists into PC will resolve this issue.

Intriguingly, preliminary studies suggest that NHDB-evoked GFAP expression in PC was not attenuated by pretreatment with scopolamine. This finding suggests that ACh actions at the muscarinic receptor may not mediate increased astrocytic expression of GFAP. Thus, there may be a dissociation between the neurochemical mechanism(s) mediating *FOS* and GFAP expression.

In summary, these results demonstrate that activation of NHDB, the source of ACh input to PC, produces cortical seizure activity and patterns of *FOS* and GFAP expression comparable to soman. The ability of scopolamine to block NHDB evoked behaviors and *FOS* expression indicates that these effects are mediated by muscarinic receptor stimulation of PC neurons. Future studies will test this hypothesis at the cellular and membrane levels. Additional confirmation of this hypothesis will strengthen the proposal that the initiation of soman-induced seizures may be attenuated by blocking the cholinergic trigger through the use of selective muscarinic antagonists or other pharmacological compounds that block molecules in the muscarinic second messenger cascade.

5. BRAIN NOREPINEPHRINE REDUCTIONS IN SOMAN-INTOXICATED RATS: ASSOCIATION WITH CONVULSIONS AND AChE INHIBITION, TIME COURSE, AND RELATION TO OTHER MONOAMINES

INTRODUCTION

At sufficient doses, organophosphate (OP) toxins, including the chemical nerve agent soman, cause convulsions, neuropathology, and, ultimately, death (^{98, 103, 126}). A major problem in treating OP intoxication is that peripherally acting pharmacological agents which prevent death do not prevent seizures. Soman-induced seizures are especially prominent in cortical structures and can lead to irreversible brain damage (^{103, 126}). Although a primary cause of these symptoms is the excess of acetylcholine (ACh) which follows acetylcholinesterase (AChE) inhibition, centrally acting muscarinic blockers, such as atropine, alleviate but do not block the convulsive actions of OP nerve agents (¹²¹). Moreover, there is a relatively weak relationship between reductions of AChE and the incidence of convulsions (⁸⁹; present study). Likewise, there is little systematic relation between ACh and γ -aminobutyric acid (GABA) levels in the rat brain and soman-induced convulsions (¹¹⁰). These results suggest that OP-induced convulsions may not be due solely to changes in ACh or GABA.

It has been speculated that excess ACh-induced effects on other modulatory neurotransmitters, norepinephrine (NE), dopamine (DA), and serotonin (5-HT), may be involved in OP toxic actions, including the induction and/or maintenance of convulsions (⁸⁹). Of these three neurotransmitters, NE may be particularly important. Noradrenergic neurons in the locus coeruleus (LC) send fibers to all parts of the forebrain and are the sole source of NE to the cortex (Foote et al, 1983) and the olfactory bulb (^{62, 80, 125, 176}); thus, LC exerts a global influence on neuronal excitability. Several lines of evidence suggest that excess ACh produced by soman may increase NE release from LC neurons: (i) LC neurons contain high levels of AChE (³) and cholinergic agonists strongly increase the firing rates of LC neurons (^{2, 44, 45, 53}). (ii) Activation of LC results in increased release of NE (¹⁰²). (iii) We have shown that systemic injection of soman causes a sustained increase in the mean firing rate of LC neurons to five times the spontaneous rate (^{46, 48}; Chapter 6, this report). Furthermore, microinjection of soman into LC causes a comparable sustained increase in the firing rate of LC neurons (^{46, 48}; Chapter 6, this report). Taken together, these findings suggest that there could be rapid, sustained release of NE in soman-intoxicated rats as the result of increased firing of LC neurons.

Other studies also suggest that NE release may have important effects on the generation of OP-induced seizures. Brain NE level declines rapidly in guinea pigs receiving a convulsive dose of soman (⁶⁶) and in rabbits intoxicated with another irreversible AChE inhibitor, diisopropylfluorophosphate (DFP) (⁷²). The α_2 -noradrenergic receptor agonist, clonidine, provides the same degree of partial protection as atropine against soman-induced convulsions (but not death) and is synergistic with atropine in preventing seizures (^{10, 28-30}). Clonidine reduces release of ACh from cholinergic terminals (^{28, 30}). However, clonidine also inhibits LC neurons (^{2, 118}) and reduces release of NE from noradrenergic terminals. Thus, the protective action of clonidine could also be due to its direct actions on the LC-NE system.

In view of the relatively loose association between AChE, ACh or GABA levels and OP-induced convulsions (^{89, 110}) and in light of the suspected involvement of brain monoamines in this phenomenon (^{89, 110}), it was of interest to investigate the relationship between the changes in these amines and the incidence of convulsions. To do this, we determined the effects of a single dose (78 $\mu\text{g}/\text{kg}$) of soman on forebrain monoamine levels at six time intervals in the first 4 days following intoxication. At this dose, 68% of the rats developed convulsive seizures.

METHODS

Chemicals. Soman (pinacolyl methylphosphonofluoridate) was supplied by the U.S. Army Medical Research Institute of Chemical Defense (Aberdeen Proving Ground, Maryland). Monochloroacetic acid, octyl sodium sulfate, all biogenic amines and the internal standard 3,4-dihydroxybenzylamine hydrobromide (DHBA) were obtained from Sigma Chemical Co. Fisher Scientific was the source of L-cysteine, Na_2EDTA , perchloric acid and HPLC grade acetonitrile.

Soman Administration. Adult male Sprague-Dawley rats (290-340 g) were obtained from Harlan Laboratories (Indianapolis, IN). The rats were housed in pairs with free access to food and water at least 1 week before use. A single dose of soman (78 $\mu\text{g}/\text{kg}$) in saline was injected (im) into the left rear leg. This dose is approximately 65% of the median effective dose (ED_{50}) for convulsions in rats (^{89, 110}). For each survival period a control group of rats were injected with a proportional volume of vehicle.

Scoring of Convulsive versus Nonconvulsive Rats. Soman-injected rats were observed every 5 min in the first 30 min after injection and at longer intervals during the designated survival period. For each injected rat, the presence or absence of convulsions was noted during this observation period. Soman-intoxicated rats fell into clearly distinguishable groups - convulsive and nonconvulsive. Rats which

developed convulsions did so within 30 min after soman administration and continued to be convulsive for several hr (see Results).

Animal Procedure and Tissue Dissection. Rats were sacrificed by decapitation at 1, 2, 4, 8, 24 and 96 hr following soman administration. The brains were rapidly removed and the olfactory bulbs were separated from the remainder of the brain by cutting the olfactory peduncle. The cerebellum and underlying brainstem were removed and the forebrain was divided at the midline, followed by the removal of the remaining brainstem including the thalamus and hypothalamus. Forebrain samples (400-600 mg) and two olfactory bulbs (50-80 mg) were immediately frozen on dry ice, and stored at -70°C until assay.

Forebrain samples were homogenized using an ultrasonic tissue disrupter (Branson Sonic Power, Danbury, CT) at 0°C for 2 min in 1.0 ml of 0.10 M perchloric acid containing 0.1% cysteine as antioxidant and 10 ng of the internal standard (DHBA). About 200 μl of individual homogenates was transferred to an Eppendorf polypropylene tube and centrifuged at 1360 g for 7 min at 4°C . One hundred microliters of the supernatant was diluted with 200 μl of the homogenization solvent. The olfactory bulbs were treated identically except that the bulbs were homogenized for 1 min in 200 μl of solvent. For either tissue, 15 μl of the final solution was injected into the HPLC.

Chromatographic Methods and Assay of Monoamines. Monoamine concentrations including NE; DA and metabolites HVA and DOPAC; 5-HT and metabolite 5-HIAA were determined using a Bioanalytical Systems (West Lafayette, IN) Model 200 Liquid Chromatograph, equipped with a Model LC-4B Electrochemical Detector (Bioanalytical Systems). The glassy carbon working electrode was kept at 0.67 V against an Ag/AgCl reference electrode and the sensitivity of detection was kept at 10 nA (full scale). Chromatographic separations were effected with a 100 x 3.2 mm Biophase ODS 3- μm (C18) column (Bioanalytical Systems). The mobile phase consisted of 0.06 M monochloroacetic acid, 1.20 mM octyl sodium sulfate and 0.1 mM Na_2EDTA in the aqueous phase (pH 2.75) and 4.2% acetonitrile at a flow rate of 0.9 ml/min. In cases where the solvent front interferes with the early eluting peaks, the mobile phase was modified by lowering the pH to 2.75 and the acetonitrile content to 1.5%. The column and the electrochemical cell were held at 40 and 41 $^{\circ}\text{C}$, respectively. In forebrain monoamine assays, five standard solutions (15 μl each) were injected daily between the runs containing 0.3-1.5 ng of NE, HVA, DOPAC, 5-HT; 0.15-0.75 ng of 5-HIAA and 0.75-3.75 ng of DA and a constant amount (0.3 ng) of the internal standard DHBA. In olfactory bulb monoamines assay, five standard solutions (15 μl) were also similarly injected into HPLC but containing 0.3-1.5 ng of NE and 5-HT; 0.15-0.75 ng of DA, HVA, DOPAC, 5-HIAA and a constant amount (0.3 ng) of DHBA.

Determination of AChE. In a second experiment, the relation between residual AChE and NE depletion

was measured. Rats (n=17) were injected with the same dose of soman used in the first experiment. A set of control rats (n =11) was injected with a proportional volume of saline and processed in an identical manner. The rats were sacrificed by decapitation 1 hr following administration. Individual rat forebrains were dissected as described earlier and were divided sagittally at the midline. One hemisphere was assayed for monoamines and the second was assayed for AChE activity. To determine AChE activity the brains were homogenized in a Polytron homogenizer containing the following buffer (10 ml/g tissue): 1.0 M NaCl; 0.2 mM EDTA; 50.0 mM Tris-HCl (pH 7.4) and 1% Triton X-100. The homogenates were ultracentrifuged at 100,000 g for 30 min and the supernatants were removed for acetylcholinesterase (AChE) activity (in duplicate) with 0.45 mM acetylthiocholine iodide using the reported procedures (182). All assay tubes contained 50 μ M iso-OMPA (tetraisopropylpyrophosphoramide) to inhibit pseudochoolinesterase.

Statistical Analysis. Statistical analysis of the data was performed using unpaired, two-tailed Student's t-test.

RESULTS

Incidence and Signs of Soman-Induced Convulsions. All rats injected with soman exhibited behavioral signs of intoxication. Convulsive rats exhibited "red tears" (lacrimation), tonic shaking movements of the head and body, sometimes associated with excess salivation, defecation and labored breathing. Nonconvulsive rats exhibited other signs of soman intoxication, including a decrease in motor activities and reduced responsiveness to external stimuli during the first few hours of intoxication.

Convulsions were observed in 68% of injected rats. This incidence of convulsions in rats is slightly higher than that of 58% established for a similar dose of 81 μ g/kg soman (197). The onset of soman-induced convulsions was at 15-20 min after administration and this behavior gradually increased in intensity. All rats which developed convulsions during the post-soman survival period had done so by 30 min following injection; no additional rats developed convulsions after this period. Convulsive activity was intense between 1 and 4 hr and declined thereafter. In the 8 hr survival group, two of seven convulsive rats recovered from convulsions; convulsive activity in the remaining five rats was reduced in intensity at the time of sacrifice. In the 24 and 96 hr groups, all rats had recovered from convulsions. In the 96 hr group, surviving convulsive rats had lost on the average 30% of body weight; nonconvulsive rats in this group maintained their body weight. Mortality was insignificant in the 1 to 8 hr groups (3 of 71); however, there was significant mortality in the 24 hr (20 of 36 rats; 55%) and 96 hr (24 of 36

rats; 67%) groups. This mortality rate in rats is comparable to that of 46% reported for the larger dose of 120 $\mu\text{g}/\text{kg}$ (¹⁷³). All the rats which died prior to sacrifice had exhibited convulsions.

Relation Between NE Levels and Behavioral Convulsions. NE levels in the rat forebrain and olfactory bulbs of convulsive rats declined rapidly and dramatically following soman intoxication (Figure 5, Tables 1 and 2). One hour following soman administration, forebrain NE level decreased to 50% of control value. The decrease in NE was maximal at 2 hr, when forebrain NE was only one third (32%) of the control level. The maximum decrease of NE level in the olfactory bulb of convulsive rats was slightly less than in forebrain, but still large (43% of control level). NE levels remained severely depressed 4 hr after intoxication. NE recovered over the next 4 days; at 96 hr after intoxication, NE levels were very near control levels. The decreased NE levels in the convulsive rats at each survival time except 96 hr were highly significant ($p = 0.0001$). In contrast, NE levels in nonconvulsive rats remained very near control levels at all time points examined. There was no difference between NE levels in nonconvulsive, soman-treated animals and controls.

The correlation between convulsive activity and NE levels is illustrated in Figure 6, in which the bulb and forebrain and olfactory bulbs NE concentrations (ng/g tissue) are plotted for individual rats in the 2 and 4 hr survival groups. NE levels of convulsive and nonconvulsive rats clearly fall into two distinct, non-overlapping, groups. In all convulsive rats NE levels were drastically reduced, while in all nonconvulsive rats forebrain NE levels were near control levels. In addition, there is a strong correlation ($r^2 = 0.83$) between NE levels in bulb and forebrain of individual convulsive rats, indicating that the reduction of NE level is relatively uniform throughout the forebrain.

Correlation AChE Inhibition, NE Depletion and Convulsions. One possible explanation for the observation that NE levels fall into distinct groups corresponding to convulsive and nonconvulsive rats is that the degree of brain AChE inhibition after soman intoxication also falls into distinct groups. This might occur, for example, as the result of variability in the location of the injected drug relative to adipose tissue or major vessels in the injected muscle. Alternatively, inhibition of AChE could be approximately constant in all injected rats, but the development of convulsions might depend on other factors. To assess these possibilities, we conducted a second study in which we measured both forebrain NE level and residual AChE activity in a population of rats injected (im) with a single dose of 78 $\mu\text{g}/\text{kg}$ soman.

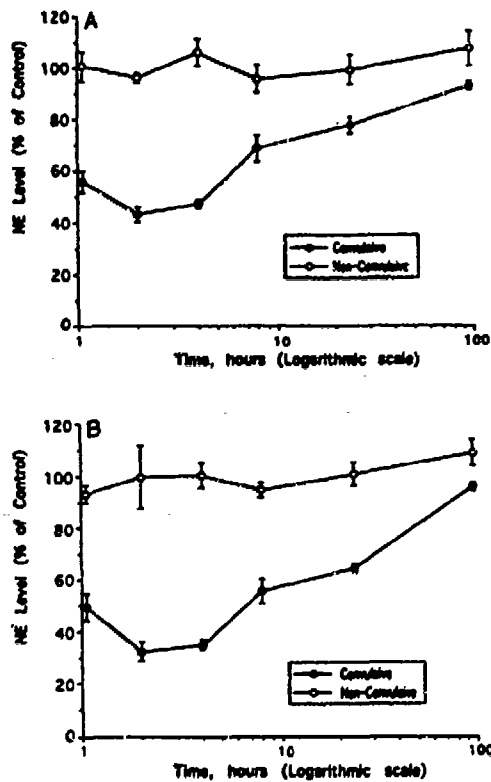


FIG. 5. Effect of soman on NE levels in olfactory bulb and forebrain in convulsive and nonconvulsive animals. NE levels in olfactory bulb (A) and forebrain (B) of convulsive and nonconvulsive rats following a single dose of 78 $\mu\text{g}/\text{kg}$ soman.

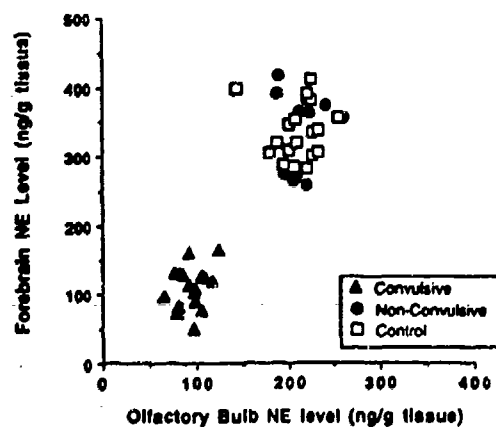


FIG. 6. Correlation between changes in forebrain and olfactory bulb NE levels in convulsive and nonconvulsive animals. Scatterplot of NE levels (ng/g tissue) in olfactory bulb and forebrain of convulsive and nonconvulsive rats following a single dose of 78 $\mu\text{g}/\text{kg}$ soman (pooled data for 2- and 4-h survival times.) NE levels for convulsive versus nonconvulsive and control rats fall into two nonoverlapping groups.

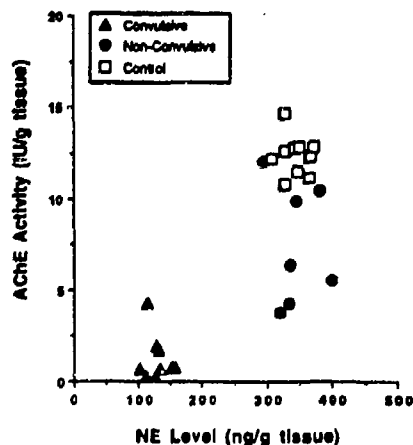


FIG. 7. Correlation between AChE activity and NE levels in convulsive and nonconvulsive animals. Scatterplot showing the relation between forebrain AChE activity, NE levels, and incidence of convulsions 1 h following a single dose of 78 $\mu\text{g}/\text{kg}$ soman.

TABLE 1
Time Course of Changes of Forebrain Levels of NE, DA, 5-HT, and Major Metabolites
Following a Single Dose of Soman (78 µg/kg)

Amine	Group	1 h	2 h	4 h	8 h	24 h	96 h
NE	C	349.1 ± 8.2	307.3 ± 8.1	362.9 ± 12.1	399.1 ± 12.1	379.0 ± 6.9	321.0 ± 9.2
	CV	178.4 ± 18.3*	99.0 ± 11.9*	123.1 ± 6.2*	222.1 ± 19.2*	244.0 ± 6.3*	306.4 ± 7.5
	NCV	325.8 ± 11.7	306.9 ± 37.0	354.5 ± 16.7	378.4 ± 11.6	381.9 ± 16.3	346.9 ± 16.0
DA	C	833.9 ± 78.9	831.5 ± 63.0	1020.6 ± 42.7	1206.9 ± 66.8	1006.3 ± 27.1	993.5 ± 31.2
	CV	1119.5 ± 87.3	820.8 ± 149.5	961.1 ± 71.8	1135.9 ± 101.7	1070.6 ± 64.8	1056.9 ± 84.6
	NCV	1084.7 ± 70.2	878.0 ± 200.5	962.3 ± 36.0	1099.3 ± 30.3	1012.8 ± 61.1	1028.9 ± 66.0
DOPAC	C	126.1 ± 9.8	87.7 ± 7.40	86.8 ± 4.8	88.1 ± 4.4	74.4 ± 2.4	81.0 ± 2.6
	CV	218.5 ± 22.8*	302.9 ± 29.4**	201.0 ± 21.0*	370.9 ± 67.9**	147.3 ± 18.7*	101.7 ± 9.9**
	NCV	156.6 ± 19.8	117.5 ± 23.9	85.3 ± 4.7	87.3 ± 3.8	78.9 ± 6.1	77.0 ± 7.6
HVA	C	107.8 ± 8.7	118.8 ± 7.7	88.0 ± 4.1	92.8 ± 4.0	71.4 ± 2.4	78.0 ± 2.8
	CV	154.6 ± 12.4**	244.3 ± 40.0**	326.7 ± 61.4**	381.6 ± 126.5**	136.3 ± 17.0*	90.4 ± 11.0**
	NCV	142.1 ± 8.6**	170.6 ± 8.7**	107.1 ± 9.0	104.4 ± 5.5	78.2 ± 9.8	66.9 ± 6.1
5-HT	C	286.0 ± 10.3	246.0 ± 15.7	298.6 ± 21.1	297.1 ± 17.4	348.2 ± 11.9	270.0 ± 9.0
	CV	207.4 ± 14.2	249.3 ± 14.2	235.6 ± 21.1	318.0 ± 16.2	378.9 ± 13.4	322.4 ± 9.4**
	NCV	301.9 ± 15.7	253.4 ± 12.1	279.4 ± 20.8	299.4 ± 13.7	375.9 ± 22.8	301.5 ± 24.3
5-HIAA	C	142.4 ± 7.0	129.1 ± 10.8	120.3 ± 8.5	146.6 ± 9.8	113.8 ± 4.7	108.9 ± 7.1
	CV	231.9 ± 19.6*	351.7 ± 37.9*	524.3 ± 36.6*	447.6 ± 31.0*	283.8 ± 18.8*	248.8 ± 8.2*
	NCV	169.4 ± 7.7	182.1 ± 20.8	182.6 ± 18.0	146.1 ± 7.8	140.8 ± 16.9**	114.5 ± 9.4
	C	n = 16	n = 9	n = 10	n = 9	n = 14	n = 9
	CV	12	9	8	6	11	5
	NCV	16	4	7	7	4	6

Note. Data expressed as means (ng/g tissue) ± SEM. C, control; CV, convulsive; NCV, nonconvulsive rats, and n, number of rats in each group.

* $P < 0.0006$.

** $P < 0.05$. Difference from control means determined using unpaired, two-tailed Student's *t* test.

TABLE 2
Time Course of Changes of Olfactory Bulb Levels of NE, DA, 5-HT, and Major Metabolites
Following a Single Dose of Soman (78 µg/kg)

Amine	Group	1 h	2 h	4 h	8 h	24 h	96 h
NE	C	197.1 ± 9.5	206.8 ± 4.8	211.4 ± 9.9	226.6 ± 18.4	205.7 ± 6.8	207.5 ± 6.6
	CV	110.0 ± 8.3*	90.2 ± 5.9*	99.9 ± 3.7*	155.7 ± 11.2**	169.7 ± 6.9*	192.8 ± 3.6
	NCV	196.4 ± 11.6	200.8 ± 4.5	223.6 ± 8.5	216.9 ± 12.3	204.6 ± 11.9	223.0 ± 14.2
DA	C	78.8 ± 3.8	81.9 ± 3.7	68.4 ± 1.7	72.5 ± 2.9	73.3 ± 2.9	73.4 ± 1.9
	CV	83.9 ± 7.1*	88.5 ± 6.3	89.4 ± 4.5*	77.3 ± 5.4	63.9 ± 3.1*	76.8 ± 2.6
	NCV	78.9 ± 3.6	77.5 ± 5.4	69.0 ± 1.0	69.6 ± 2.0	64.3 ± 3.1	73.8 ± 2.3
DOPAC	C	33.9 ± 2.9	38.4 ± 2.0	37.0 ± 1.9	32.3 ± 2.7	25.8 ± 2.0	24.9 ± 1.4
	CV	53.9 ± 3.8*	51.9 ± 3.2**	44.4 ± 2.9*	27.5 ± 1.6	12.4 ± 0.8*	22.9 ± 1.6
	NCV	37.5 ± 3.8	33.4 ± 0.5	24.7 ± 1.0	22.4 ± 1.1	15.4 ± 2.0	20.9 ± 2.0
HVA	C	72.8 ± 3.6	77.5 ± 5.9	62.4 ± 2.4	63.5 ± 5.6	69.0 ± 1.6	64.0 ± 2.6
	CV	96.9 ± 5.0**	92.9 ± 5.4	100.5 ± 3.9*	90.8 ± 4.6**	60.7 ± 3.0**	46.8 ± 2.4**
	NCV	82.6 ± 5.7	64.8 ± 1.7	56.3 ± 2.5	60.8 ± 3.5	48.1 ± 4.0**	57.9 ± 4.9
5-HT	C	136.3 ± 5.6	137.3 ± 6.1	124.4 ± 6.2	167.9 ± 5.3	182.0 ± 4.2	188.0 ± 5.6
	CV	152.6 ± 6.6**	180.0 ± 9.7	169.1 ± 10.0**	180.3 ± 8.7	182.9 ± 4.7	169.8 ± 12.1
	NCV	128.5 ± 5.7	126.2 ± 10.4	140.7 ± 4.9	161.4 ± 8.3	187.9 ± 6.4	140.7 ± 5.8
5-HIAA	C	99.0 ± 3.9	94.4 ± 7.8	78.7 ± 3.9	123.6 ± 8.5	71.8 ± 2.3	83.8 ± 4.4
	CV	119.0 ± 7.7**	165.0 ± 12.1**	148.4 ± 9.3*	138.7 ± 6.2	89.9 ± 4.6**	106.3 ± 6.3**
	NCV	100.4 ± 6.0	96.8 ± 2.8	79.2 ± 4.0	108.0 ± 3.9	74.4 ± 5.4	82.2 ± 7.1
	C	n = 16	n = 9	n = 10	n = 9	n = 14	n = 9
	CV	12	9	8	6	11	5
	NCV	16	4	7	7	4	6

Note. Data expressed as means (ng/g tissue) ± SEM. C, control; CV, convulsive; NCV, nonconvulsive rats, and n, number of rats in each group.

* $P < 0.0006$.

** $P < 0.05$. Difference from control means determined using unpaired, two-tailed Student's *t* test.

TABLE 3

Forebrain NE and AChE Levels in Convulsive and Non-convulsive Rats 1 h Following a Single Dose of Soman (78 $\mu\text{g}/\text{kg}$)

	Control	Convulsive	Nonconvulsive
NE Level (ng/g tissue)	345.8 \pm 6.2 (n = 11)	129.8 \pm 5.4° (n = 10)	344.9 \pm 13.3 (n = 7)
AChE Activity (IU/g tissue)	12.4 \pm .31 (n = 11)	1.32 \pm .38° (n = 10)	7.5 \pm 1.24° (n = 7)

Note. Data expressed as means \pm SEM. IU, enzyme activity sufficient to hydrolyze 1 μM of substrate per minute and *n*, number of rats.

° $P < 0.0005$. Difference from control means determined using unpaired, two-tailed Student's *t* test.

The relation between NE depletion or residual AChE activity and soman-induced convulsions in individual rat forebrain at 1 hr after soman administration is shown in Figure 7. The means of forebrain NE and AChE levels in convulsive and nonconvulsive rats as compared to those of control animals are presented in Table 3. As in the first experiment, NE levels fell into two distinct groups: As indicated in Table 1, NE level in convulsive rats was always less than 50% of control (mean, 38% of control level, $p = 0.0001$), but NE levels were unchanged in nonconvulsive rats (mean, 100% of control value). Convulsive rats also had a severely depressed AChE activity (mean, 10.6% of control level, $p = 0.0001$) and nonconvulsive rats had a less depressed level of AChE activity (mean, 60.5% of control level, $p = 0.0003$). Unlike NE levels, there is some overlap between the AChE levels of convulsive and nonconvulsive rats (Fig. 7). For example, two rats with AChE reduced to 30.5 and 34.4% of control levels were nonconvulsive, while another rat having 34.8% of control AChE level was convulsive. These findings are consistent with an earlier study indicating a lack of a close association between soman-induced convulsions and the degree of striatal AChE inhibition (⁸⁹). Thus, significant NE depletion is at least as good, if not a better, predictor than AChE inhibition of soman-induced convulsions.

Time-Course Effect of Soman on the Levels of DA, DOPAC and HVA. Mean values of DA, 5-HT, and their metabolites, in the forebrain and olfactory bulb of soman-intoxicated versus control rats are given in Tables 1 and 2, respectively. In both olfactory bulb and forebrain there is a slow and progressive increase in the metabolites with little or no changes in the levels of DA or 5-HT. This is taken as evidence for increased turnover of both DA and 5-HT but with a slower time course than for the reduction of NE levels.

Because of the very high levels of DA contained in the striatum, a significant part of DA and the metabolites HVA and DOPAC, in our forebrain measurements may result from remnants of striatum in the forebrain samples. Therefore, the substantial increase in forebrain DA and 5-HT turnover in soman-intoxicated rats may reflect, to a large extent, changes in the striatum but similar changes in cortex cannot be ruled out by the present results. It is also conceivable that increased DOPAC and HVA are due, in part, to metabolism of released NE. The concentration of DA metabolites in the olfactory bulbs of control rats is relatively high, indicating that there is normally rapid turnover of DA in this structure (^{15, 82}). Notwithstanding, there were still increased levels of DOPAC and HVA in the olfactory bulbs of convulsive animals.

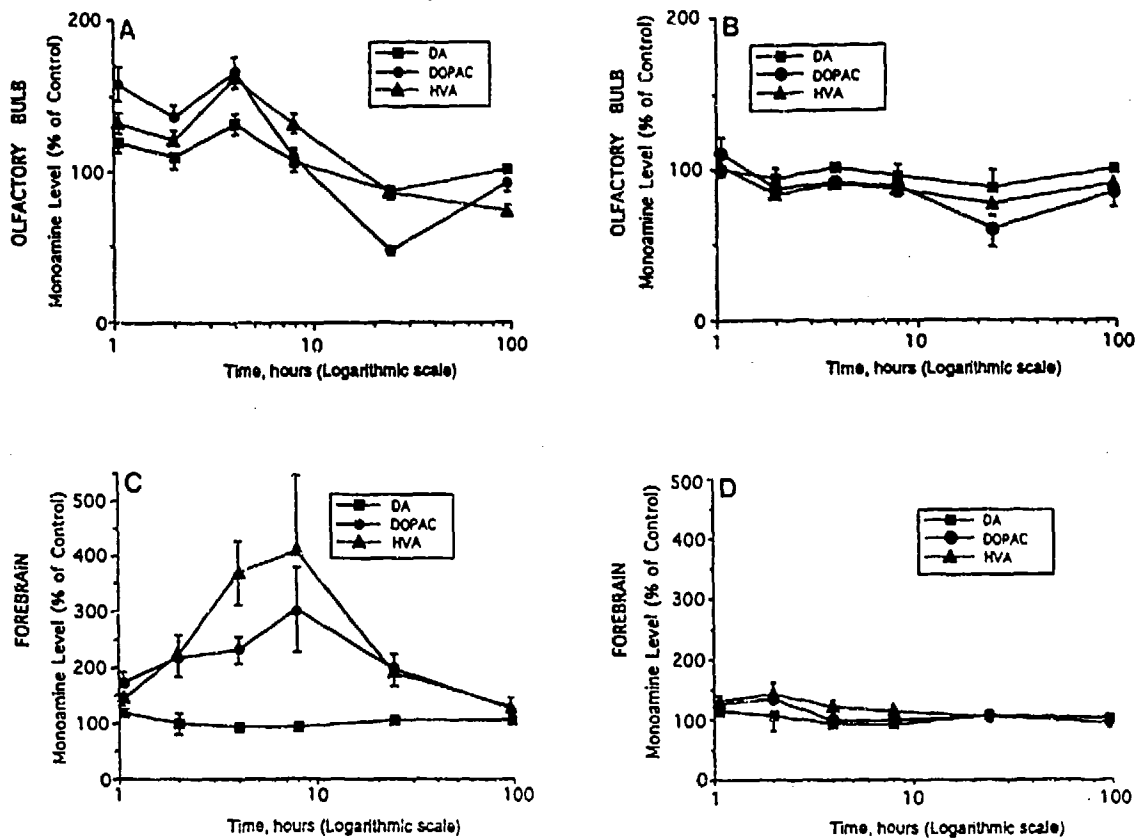


FIG. 8. Effect of soman on DA, DOPAC, and HVA. Time course of changes in the levels of DA, HVA, and DOPAC following a single dose of 78 $\mu\text{g}/\text{kg}$ soman: (A) olfactory bulbs of convulsive rats, (B) olfactory bulbs of nonconvulsive rats, (C) forebrains of convulsive rats, and (D) forebrains of nonconvulsive rats.

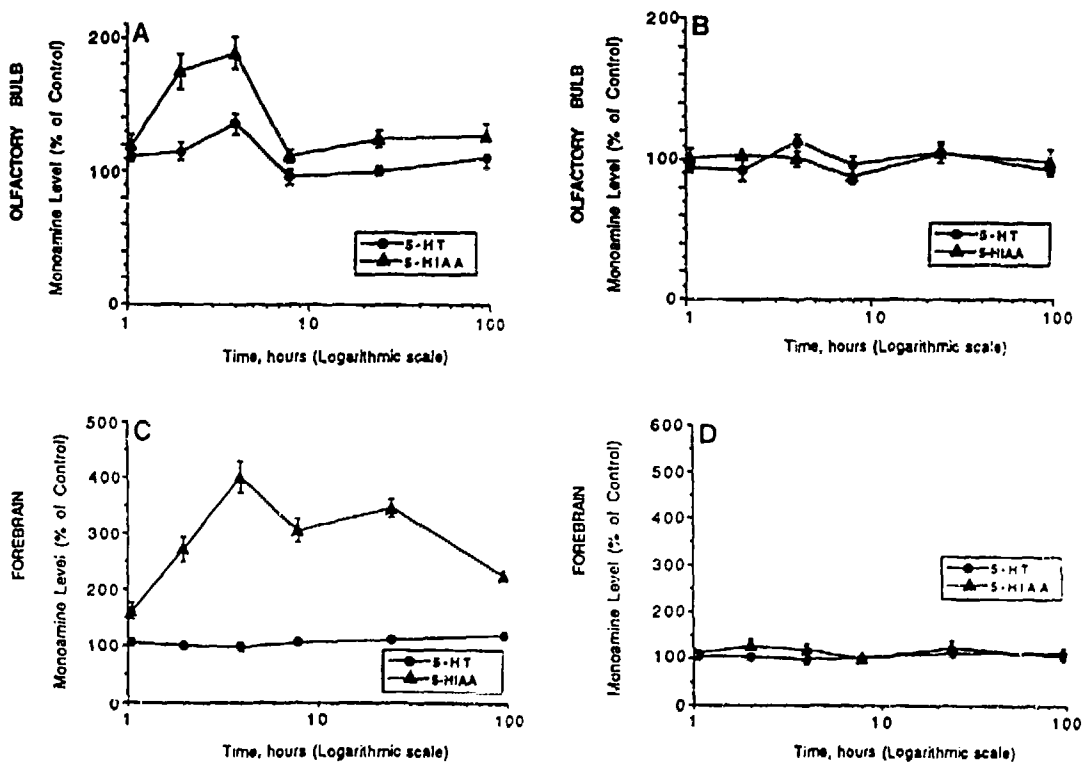


FIG. 9. Effect of soman on 5-HT and 5-HIAA. Time course of changes in the levels of 5-HT and major metabolite 5-HIAA following a single dose of 78 $\mu\text{g}/\text{kg}$ soman: (A) olfactory bulbs of convulsive rats, (B) olfactory bulbs of nonconvulsive rats, (C) forebrains of convulsive rats, and (D) forebrains of nonconvulsive rats.

The time-courses of soman effects on the levels of DA and major metabolites (HVA and DOPAC) in the forebrain and olfactory bulbs of convulsive and nonconvulsive rats are plotted in Figure 8. In each structure the mean level of DA in convulsive rats is relatively unchanged after soman administration; however, the levels of HVA and DOPAC were substantially increased. In the forebrains of convulsive rats, there was a progressive increase in the DA metabolites HVA and DOPAC reaching 300-400% of control levels 8 hr following soman intoxication. At 96 hr following soman administration, the concentrations of the two metabolites returned to approximately control values. These findings clearly indicate that there is a gradual increase in DA release in the forebrain during the first 24 hr after soman intoxication. In nonconvulsive rats, increases in HVA and DOPAC were relatively small.

Olfactory bulb DA metabolites, HVA and DOPAC, which derive entirely from intrinsic (i.e., juxtaglomerular) dopaminergic neurons, exhibit much smaller increases in convulsive rats than those observed in forebrain DA. These monoamines were little affected in nonconvulsive animals.

Time-Course Effect of Soman on the Levels of 5-HT and 5-HIAA. Both the rat forebrain and the olfactory bulb receive serotonergic projections from the raphe nuclei in the brainstem. In neither the forebrain nor the olfactory bulb of convulsive or nonconvulsive animals does soman cause a significant change in levels of 5-HT as compared to control means (Figure 9). In the forebrains of convulsive but not nonconvulsive rats, there is a delayed increase in 5-HIAA which reaches a maximum level of 400% of control at 4 hr, and then declines to 300% at 8 hr following soman administration. Increased 5-HIAA level in convulsive rats remained significantly high afterward reaching 346% of control level at 24 hr and only 226% of control level at 96 hr following intoxication. In the olfactory bulb, there is also an increase in 5-HIAA levels in convulsive rats, although the increase is much smaller than in the forebrain. The concentration of 5-HIAA in the olfactory bulb of convulsive rats had returned to approximately control levels by 8 hr after intoxication.

DISCUSSION

The present study demonstrates that: (i) there is a rapid, profound NE depletion only in animals with soman-induced convulsions, (ii) depleted forebrain NE in convulsive rats recovers by 4 days, (iii) NE depletion is as good as, or better, an indicator of the incidence of convulsions than the degree of AChE inhibition, and (iv) there is no change in DA or 5-HT levels after soman intoxication, but there is a delayed, progressive increase in forebrain DA and 5-HT turnover rates in convulsing animals.

Despite the presence of other signs of soman intoxication, NE levels in nonconvulsive rats remained near control levels at all intervals tested. In contrast, the decrease in NE levels in convulsive

rats was rapid and profound, with nearly 70% depletion from control levels in the forebrain at 2 and 4 hr after intoxication.

The strength of the correlation between convulsions and NE depletion is well documented in Figure 6, which shows data for individual rats. All convulsive rats had severely depressed levels of NE, whereas NE levels in nonconvulsive rats clustered tightly around control levels. Further, the close correlation between forebrain and olfactory bulb NE depletion suggests a global and not a localized depletion of NE.

Previous studies (^{66, 72}) did not examine the correlation between NE decreases and the incidence of OP-induced convulsions because, at the dose used in those studies, all rats had convulsions. Moreover, in these earlier experiments, NE levels were only measured during the first 4 hr following OP intoxication. Thus, the duration of the soman-induced depletion of NE was not determined. In the present study, the dose of soman (78 $\mu\text{g}/\text{kg}$) caused seizures in 68% of intoxicated rats which is slightly greater than the 58% reported for a single dose of 81 $\mu\text{g}/\text{kg}$ soman in a previous study (¹⁹⁷). Thus, we were able to examine forebrain NE and AChE levels in relation to the presence or absence of convulsions. In addition, we monitored NE changes for 4 days following soman treatment in order to determine if and when NE levels recovered.

In agreement with previous studies (^{66, 72}), NE levels in convulsive rats decreased to 50% of control level at 1 hr of soman intoxication. Decreases in NE levels were maximal (70%) at 2 and 4 hr following intoxication. NE levels in convulsive rats began to recover very slowly after 8 hr. The beginning of this recovery coincided roughly with the termination of convulsions. By 96 hr, NE levels of convulsive rats did not differ significantly from control values.

The dose of soman used produced widely differing degrees of AChE inhibition (Figure 7). Presumably, variables such as the exact placement of the injection, the quantity of peripheral cholinesterase present in individual animals, or access to the brain, underlie these differences in brain AChE inhibition. However, as shown in Figure 7, residual forebrain AChE levels did not fall into distinct, nonoverlapping groups associated with convulsions, as was the case for NE levels. Thus, the present results demonstrate a much stronger association of soman-induced convulsions with NE depletion, than with AChE inhibition. These results, taken with recent studies of the pharmacology of LC neurons and the postsynaptic actions of NE, (discussed below) suggest that NE may play an important role in OP-induced convulsions.

Changes in DA and 5-HT and Their Major Metabolites. In contrast to NE, both DA and 5-HT remained relatively constant in both groups of rats following soman intoxication. The metabolites of DA

(HVA and DOPAC) and 5-HT (5-HIAA), however, increased to four times control values in the forebrain. These increases in metabolites presumably result from increased release of DA and 5-HT from nerve terminals. Thus, it is possible that the release of all three of these modulatory neurotransmitters is increased following soman intoxication, but that NE release exceeds either the storage or synthetic capacity of LC terminals, thus resulting in significant reductions in the levels of this neurotransmitter. As with the NE decrease, increases in forebrain DA and 5-HT turnover occurred only in convulsive rats. However, the peak changes in these monoamines lag substantially behind the rapid decrease in NE levels.

Based on these findings it is conceivable, therefore, that NE, DA and 5-HT all contribute to the initiation of seizures as there was evidence for increased release of all three monoamines in convulsive animals 60 min following soman administration, the shortest survival time used in the present study. However, in a recent report where supraconvulsive doses of soman were used, NE was significantly decreased at 15 minutes following soman administration while at this short survival time there were no significant changes in either DA or 5-HT or their metabolites in cortex or hippocampus (FOSbraey et al., 1990). Taken with the results of our companion report (Chapter 6, this report) demonstrating a direct, immediate activation of LC neurons by either systemic or intracoeular soman, it seems reasonable to suggest that the rapid, sustained release of NE correlates better with the onset of convulsions (15-30 min) than the delayed increases in DA and/or 5-HT turnover. Direct confirmation of this hypothesis could be established by *in vivo* dialysis measurements; studies of this kind are planned.

For both DA and 5-HT, the increase in turnover was smaller in the olfactory bulb than in the forebrain. The dopaminergic innervation of the forebrain and olfactory bulb derives from separate populations of DA neurons. The DA in the olfactory bulb is associated with the intrinsic population of dopaminergic neurons in the glomerular layer. It is probable that the regulation of these different populations of DA neurons is independent. Less is known about the contributions of different brainstem 5-HT nuclei to the innervation of the olfactory bulb and forebrain. Thus, the significance of the difference between olfactory bulb and forebrain 5-HT metabolism is unclear.

Cholinergic Activation of NE Release. The present data thus are compatible with a unique role of NE in the early stages of OP-induced seizures. It is probable that the rapid decline in forebrain NE in convulsive rats is due to rapid synaptic release of NE from noradrenergic terminals. This possibility is consistent with recent electrophysiological results. *In vivo* extracellular and *in vitro* intracellular recording studies have demonstrated that LC neurons are strongly excited by cholinergic agonists (2, 44, 45, 53). These studies suggest that cholinergic excitation of LC neurons following AChE inhibition could lead to a sustained release of NE from LC terminals.

Recent experiments in this laboratory confirm this inference. In anesthetized rats, systemic administration of soman causes a sustained, five-fold increase in mean LC neuron firing rate (El-Etri et al., 1990, 1991, Chapter 6, this report). Microinjections of soman directly into LC cause a similar increase in the firing rate of LC neurons. This increased firing rate continues for several hours. Systemic injection of scopolamine rapidly reverses the soman-induced activation of LC neurons (^{46, 48}, Chapter 6, this report). Thus, there is direct evidence that soman causes a sustained, probably muscarinic, excitation of LC neurons.

We suggest, therefore, that one effect of systemic soman injection is rapid, sustained firing of LC neurons, causing increased release of NE. In convulsive rats, this period of rapid release may be followed by depressed NE release because the pool of stored neurotransmitter is exhausted. The consequence of rapid, sustained NE release, or of NE depletion, for seizures depends on the effect of NE on seizure thresholds. There is, however, conflicting evidence on the effect of NE on cortical excitability and susceptibility to seizures.

Effect of Excess NE on Seizure Susceptibility.

Evidence for an Anti-Seizurogenic Role for NE. Manipulations which increase NE levels in cortical structures by transplantation of NE neurons (¹⁶) or by electrical stimulation of LC (¹⁰⁸) increase seizure thresholds. Forebrain NE depletion by 6-hydroxydopamine (6-OHDA) reduces seizure threshold (¹¹⁹). However, such studies are equivocal. Interpretation of the effects of electrical stimulation of LC is problematical because current spread from LC may unavoidably stimulate neurons in the adjacent parabrachial and lateral dorsal tegmental (LDT) nuclei. Both of these structures contain neurons which project to the thalamus and cortex (^{167, 179}). LDT, in particular, may play a critical role in regulating cortical activity, as these neurons project heavily to the thalamic reticular nucleus which potently modulates thalamocortical excitability (^{99, 104, 186}). Since electrical stimulation of LC may activate other, non-NE neurons, which may regulate the excitability of cortical neurons, inferences about the role of LC-NE neurons on seizures are equivocal. Interpretation of LC lesions or 6-OHDA-induced NE fiber lesions (¹⁰⁹) is complicated by compensatory mechanisms (receptor up-regulation, sprouting) which may obscure the functional consequences of NE-specific lesions (^{19, 39, 196}).

Evidence for a Seizurogenic Role for NE. There is also evidence that NE *increases* susceptibility to seizures. In the single-gene, mutant mouse tottering (*tg/tg*), which is extremely susceptible to seizures, there is a 50% increase in the number of LC fibers and NE in the forebrain (¹⁰⁵). Recent *in vitro* cellular studies have identified a potent, β -receptor-mediated postsynaptic action of NE which may lower the threshold for seizures. NE increases the excitability of cortical neurons by a disinhibitory mechanism similar to that of ACh (^{38, 61, 73, 75, 85, 114, 144}). This disinhibition should increase

susceptibility to seizures. Consistent with this, systemic administration of the β -receptor *antagonist* propranolol reduces the duration of pentylenetetrazol-induced convulsions in rats (¹¹¹). In the hippocampal slice, β -adrenergic *agonists* are proconvulsive (¹⁴⁰).

Based on the present results, it is reasonable to conclude that a convulsive dose of soman may cause an excess of both ACh and NE in the forebrain. Excessive levels of *both* ACh and NE is probably a unique circumstance which could have potent seizurogenic effects. Intracellular recording studies have demonstrated that the postsynaptic actions of NE and ACh are frequently mediated by the same second messenger systems and ionic channels (¹⁴⁴). Therefore, sustained excessive levels of NE and ACh might produce disinhibitory actions greater than those produced by either neurotransmitter alone. Thus, it is reasonable to speculate that the rapid accumulation of both NE *and* ACh following soman intoxication has potent seizurogenic actions.

NE Pharmacology in the Treatment of OP Intoxication. The α_2 -receptor agonist clonidine protects against OP-induced behavioral convulsions (but not lethality) as effectively as atropine. Furthermore, the protective effect of clonidine is synergistic with the protective effect of atropine (^{10, 28-30}). These studies suggested that presynaptic depression of ACh release by clonidine accounted for the protective action of this drug. However, the strong correlation between NE depletion and convulsions shown in the present study, taken with the observation that soman directly applied to LC causes a dramatic, sustained increase in LC neuronal discharge rate, (^{46, 48}; Chapter 6, this volume) suggests an alternative and more direct mechanism for the anticonvulsant action of clonidine. It is well known that clonidine acts at α_2 -adrenergic receptors on LC neurons to reduce their firing rate (^{2, 15, 118, 188}). Recently, clonidine was shown to block the excitatory action of ACh on LC neurons (²). Thus the protective action of clonidine in soman-intoxicated rats may result from its ability to inhibit cholinergic activation of LC neurons as well as its presynaptic inhibition of ACh release from cholinergic terminals.

Numerous agonists and antagonists specific to different classes of adrenergic receptors are in clinical use. If NE release plays an important role in the response of the brain to OP intoxication, as suggested by the present and other studies, then adrenergic pharmacological intervention may prove useful in the treatment of OP poisoning.

6. TONIC ACTIVATION OF LOCUS COERULEUS NEURONS BY SYSTEMIC OR INTRACOERULEAR MICROINJECTION OF AN IRREVERSIBLE ACETYLCHOLINESTERASE INHIBITOR: INCREASED DISCHARGE RATE AND INDUCTION OF C-FOS

INTRODUCTION

Recent experiments in this laboratory have demonstrated that systemic administration of the irreversible acetylcholinesterase (AChE) inhibitor, soman (pinacolyl methyphosphonofluoridate), produces a rapid (1-2 hrs) and profound depletion (60-70% of control) of olfactory bulb and forebrain norepinephrine (NE) (⁴⁷). This depletion of NE occurs only in animals that develop convulsions; animals receiving the same dose of soman and exhibiting other signs of intoxication but not convulsions had no change in NE (^{46, 48, 178}; Chapter 5, this report). The pontine nucleus locus coeruleus (LC) is the sole source of noradrenergic innervation of the olfactory bulb and neocortex, and is the major source of NE input to the rest of the forebrain (⁶⁵). Thus, it is reasonable to hypothesize that the anti-AChE action of soman produces tonic elevation of LC neuronal activity, thus causing depletion of NE in the olfactory bulb and forebrain.

There are several mechanisms by which soman might activate LC neurons. AChE staining, receptor binding and pharmacological studies indicate that LC neurons may receive a cholinergic input (^{2-4, 9, 44, 45, 101, 164}). Thus, the anti-AChE actions of soman could activate LC neurons by increased postsynaptic excitation due to tonically released ACh onto LC neurons. Alternatively, soman could activate other, non-cholinergic excitatory afferent inputs to LC. This latter alternative is possible because systemic soman administration produces a variety of peripheral sensory/motor effects that might directly or indirectly influence systems afferent to LC. It is also possible that the brain seizures produced by systemic soman administration might secondarily activate LC neurons. Finally, soman may deplete NE by a mode of action that does not involve excitation of LC neurons, for example, by presynaptic effects on LC axonal terminals causing the release of NE.

In order to investigate these possibilities, the present experiments assessed the effects of systemic and direct application of soman on the spontaneous activity of LC neurons *in vivo*. Both systemic and intracoerulear application of soman rapidly and potently increased the spontaneous discharge rate of LC neurons by 3-7 fold; this activation occurred in the absence of seizures. The discharge rates of LC neurons remained elevated at all post-soman intervals examined (up to 2 hr). The maintained excitation caused by soman was completely reversed by systemic administration of the muscarinic

receptor antagonist scopolamine, but not by the nicotinic receptor antagonist mecamylamine.

In addition, we examined the effects of systemic and intracerebral administration of soman on AChE staining and the expression of the immediate early gene protein product, *c-fos* (*FOS*), in LC. Both routes of soman administration caused nearly complete inhibition of AChE staining in LC and rapidly induced the expression of *FOS* in LC neurons.

METHODS

General Surgical Procedures. Male Sprague-Dawley rats (Harlan Laboratories, Indianapolis, IN) weighing 250 to 375 g were anesthetized with chloral hydrate (400 mg/kg, ip). Anesthesia was maintained throughout all procedures with additional injections of 30-40 mg/kg chloral hydrate administered approximately every 30 min. Core body temperature was maintained at 36-38⁰ C with a feedback controlled heating pad.

LC Recordings. Animals were anesthetized with chloral hydrate and placed in a stereotaxic instrument with the incisor bar lowered to place the skull 12 degrees below the horizontal plane (bregma 2 mm below lambda). A hole was drilled in the skull at the coordinates for LC (3.7 mm posterior to lambda, 1.2 mm lateral to midline), and the underlying dura was reflected. A glass recording micropipette (2-4 um tip diameter) filled with 2% pontamine sky blue in 0.5 M sodium acetate was advanced into LC with a hydraulic microdrive. Extracellular recordings from individual neurons were amplified and displayed as filtered (300 Hz - 10 KHz bandpass) electrode signals. Impulse activity was also monitored with a loudspeaker. Action potentials were isolated from background activity with a waveform discriminator which generated logic pulses for signals that crossed a lower voltage gate and peaked below an upper voltage gate. Discriminator logic pulses were led to a computer and chart recorder for on-line data collection. LC neurons were tentatively identified at the time of recording by characteristic impulse waveforms, and spontaneous and sensory-evoked discharge patterns as previously described (55, 57).

In most experiments micropipette penetrations were marked by iontophoretic ejection of dye with current pulses (-7 μ A, 50% duty cycle for 10 min). Animals were then deeply anesthetized and perfused with 10% formalin. Brains were removed and stored in a similar solution containing 20% sucrose. Select brain regions were cut into 50 um-thick frozen sections, mounted on subbed slides and stained with neutral red. All recording sites were histologically localized from such tissue sections. Alternatively, when brains were to be used in *FOS* immunohistochemistry experiments, inhibition of AChE staining (see below) was used to localize recording and soman microinjection sites.

EEG Recordings. Two jewelers screws were threaded into the skull over the parietal and occipital cortices to monitor electroencephalograph (EEG) signals. The EEG was amplified by conventional

methods and displayed on a chart recorder.

Pharmacology. Soman (pinacolyl methyphosphonofluoridate) was prepared as a 40 μ M solution (73.6 μ g/ml, in 0.0333% saline; pH 4.5-5.0). Soman was injected intramuscularly at a dose of 78 μ g/kg. Microinjections of soman into LC were made with a double barrel electrode assembly consisting of a calibrated glass micropipette (Fisher Scientific; 40-50 μ m tip diameter), cemented to a recording micropipette (similar to that described above) to position the microinjection pipette tip 80 to 200 μ m beyond the tip of the recording electrode). The microinjection pipette was connected to a Picospritzer II (General Valve Corporation) for pressure ejection. Visual inspection of the movement of a small bubble relative to a calibration grid on the injection pipette allowed injections as small as 5 nl. For the purposes of establishing dose-response relationships, boluses of 5-120 nl (2-48 pmol) were injected.

A 26g needle was inserted into a lateral tail vein for intravenous (iv) injection of scopolamine hydrochloride (0.5 mg/ml in distilled water), methylscopolamine bromide (0.5 mg/ml in distilled water) or mecamlamine hydrochloride (1.0 mg/ml in distilled water). In some experiments, aqueous solutions of scopolamine hydrochloride (5 mg/ml) or methylscopolamine bromide (5 mg/ml) were injected intraperitoneally.

C-FOS Immunohistochemistry. Animals were deeply anesthetized and perfused transcardially with 100-200 ml of 0.9% saline (4^o C) for 1 min, followed by 1 liter of 4% paraformaldehyde in 0.1 M phosphate buffer (PB) (pH 7.4, 4^o C). Brains were postfixed in this same solution (4^o C) for 1.5 hr, and then placed in 20% sucrose in 0.1 M PB overnight. Serial, 30 μ m-thick frozen sections were cut in the coronal plane and alternately placed into two trays containing 0.1 M PB for immunocytochemical visualization of *FOS* or for histochemical visualization of AChE (see below). For *FOS* immunohistochemistry, free floating sections were (1) rinsed (30 min) in 0.1 M phosphate buffered saline (PBS); (2) placed in 2% normal serum (normal goat -NGS- for rabbit primary or normal rabbit -NRS- for sheep primary) in PBS containing 0.2-2.0% Triton X-100 overnight; (3) incubated in primary antibody (Dr. M. Greenberg, Harvard Univ., rabbit; Cambridge Biochemicals, sheep) at a 1:5,000 dilution in 0.3% Triton X-100 and 2% NGS/NRS for 24-48 hr at 4^o C with constant agitation; (4) rinsed in PBS (30 min) and then incubated in biotinylated IgG directed against the species producing the primary antibody, in PBS (1 hr, room temp.); (5) rinsed in PBS (30 min) and incubated for 1 hr in avidin-biotin-peroxidase complex in 0.1 M PBS and then rinsed in PBS (20 min); and (6) incubated in 0.05% diaminobenzidine (DAB) with 0.1% hydrogen peroxide in PB for 10 min, then rinsed in PB.

Acetylcholinesterase Histochemistry. In experiments where alternate tissue sections were processed for AChE histochemistry and *FOS* immunohistochemistry, animals were perfused with 4% paraformaldehyde in 0.1 M PB (pH 7.4, 4^o C) for maximal preservation of *FOS* antigenicity. In some

experiments only AChE histochemistry was performed. These animals were perfused with 0.9% saline with 0.2% dimethyl sulfoxide (room temperature) until venous return was clear. This was followed by one liter of 1% paraformaldehyde - 2.5% glutaraldehyde fixative containing 2% sucrose in 0.1 M PB (pH 7.4, room temperature), followed by one liter of 10% sucrose in 0.1 M PB (pH 7.4, 4° C). Brains were removed and stored at 4° C in 20% sucrose in 0.1 M PB overnight (pH = 7.4). Serial 30- or 40-um thick frozen sections were cut and placed in 0.1 M PB. Sections were processed for AChE according to a modification (Van Ooteghem and Shipley, 1984; Shipley et al, 1989) of the Koelle-Friedenwald (1949) histochemical reaction. Sections were rinsed (7 x 1 min) in distilled water to remove residual phosphates, then incubated with gentle agitation for 2 hrs (37° C) in the following solution: 2 mM copper (II) sulfate, 10 mM glycine, 50 mM sodium acetate, 4.2 mM acetylthiocholine iodide, and 0.21 mM ethopropazine; this solution was freshly prepared and adjusted to a final pH of 5.25 with glacial acetic acid. Following incubation, sections were again rinsed (7 x 1 min) with distilled water and then reacted (1 min, constant agitation) in a freshly prepared solution of 1% sodium sulfide, carefully adjusted to pH 7.8 with concentrated hydrochloric acid; this was terminated by water rinses (7 x 1 min). The sections were then agitated for one min in a freshly prepared solution of 1% silver nitrate, followed by water rinses (3 x 1 min). The sections were stored 3-18 hrs in 0.1 M PB, and rinsed (3 x 1 min) in distilled water prior to mounting from an alcohol-gelatin solution onto subbed slides. Sections were dehydrated through graded alcohols (70%, 95%, 100%, 100%) and xylene before coverslipping with Permount.

RESULTS

Systemic Soman Administration

LC NEURONAL ACTIVITY. Our recent studies demonstrated that systemic injection of soman in unanesthetized rats produces rapid, profound reduction of forebrain NE in convulsing rats (46, 48; Chapter 5 this report). The soman-induced NE depletion may be due to a tonic excitatory effect of AChE inhibition on LC neurons. To investigate this possibility, the effect of systemically administered soman on the discharge of LC neurons was examined.

Injection of soman (78 ug/kg, im) substantially increased the activity of 2 LC neurons recorded before and after soman injection; the increase in discharge occurred approximately 7 to 11 min after injection. However, only 1 or 2 min of post-soman data were collected before the cell was lost due to labored breathing movements or death of the animal, probably due to bronchoconstriction and bronchial secretion produced by the anti-AChE action of soman on peripheral autonomic neurons. To circumvent these peripheral effects of soman, rats were pretreated 60-90 min prior to soman injection with the peripherally acting scopolamine analog, methylscopolamine bromide (0.5 mg/kg, iv; n = 2; 1.5

mg/kg, n = 3). Methylscopolamine bromide had no effect on the baseline discharge rate of LC neurons as there was no difference ($p > 0.9$) between the mean spontaneous discharge rate of LC neurons in intact animals (1.6 ± 0.2 spikes/sec, n = 15) and that in methylscopolamine-pretreated rats (1.6 ± 0.2 , n = 6). Data from these two groups were pooled for statistical comparisons. With this peripheral muscarinic blockade, soman elicited a 5 to 10 min period of labored breathing; however, this effect gradually decreased and LC neurons were recorded as long as 45 min after soman injection.

The spontaneous discharge rates of LC neurons before soman injection ranged from 0.4 to 3.5 spikes/sec, with a mean spontaneous rate of 1.6 ± 0.1 spikes/sec (n = 21, pooled data from above). Systemic soman injection (78 μ g/kg im; n=4 animals) elicited a pronounced increase in the spontaneous discharge rates of LC neurons, ranging from 5.6 to 9.9 spikes/sec (Figs. 10 and 11). The mean discharge rate of LC neurons after soman injection, 7.9 ± 0.4 spikes/sec (n = 11), was substantially greater ($p < 0.004$) than the mean baseline discharge rate of LC neurons (Fig. 11).

Soman-induced activation of LC neurons was maintained throughout the period of recordings; there was no difference ($p > 0.9$) between the mean discharge rate of LC neurons examined 8-20 min after soman (7.9 ± 0.5 spikes/sec, n = 5) and that of LC neurons sampled 25-45 min after soman (7.9 ± 0.6 spikes/sec, n = 6). EEG records showed that while soman administration produced a desynchronization of cortical EEG, there was no evidence of seizures (spike activity) at any time following the administration of soman.

In one animal tested, administration of the centrally active muscarinic receptor antagonist, scopolamine hydrochloride (10 mg/kg, ip), rapidly and completely reversed the soman-induced excitation of LC neurons, reducing LC firing rates to presoman control values. There was no difference ($p > 0.4$) between the mean LC discharge prior to soman administration (1.6 ± 0.1) and that of LC neurons recorded after combined soman and scopolamine hydrochloride administration (1.8 ± 0.3 , n = 9).

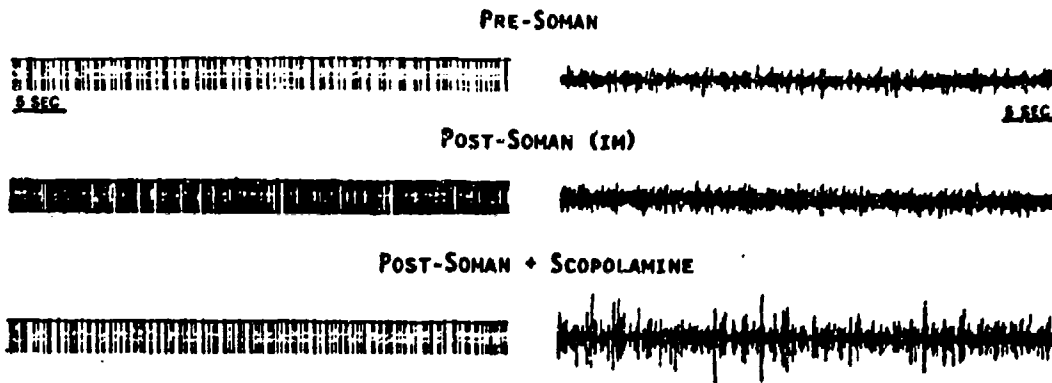


FIG. 10 Systemic soman increases LC discharge and desynchronizes cortical EEG. Left: (Top) Strip chart record showing the spontaneous discharge of an LC neuron; the mean discharge rate of this neuron was 2.2 spikes/s. (Middle) LC neurons were robustly and tonically activated by systemically administered soman (78 $\mu\text{g}/\text{kg}$, im), as shown for a typical cell 42 min after soman injection. The postsoman mean discharge rate of this neuron was 9.9 spikes/s. (Bottom) Injection of scopolamine (12 mg/kg, ip) decreased the discharge rate of the same cell from 9.9 to 2.9 spikes/s, as shown 15 min after scopolamine. Right: Strip chart EEG records show that soman administration produced a desynchronization of the EEG (middle), an effect reversed by scopolamine (bottom).

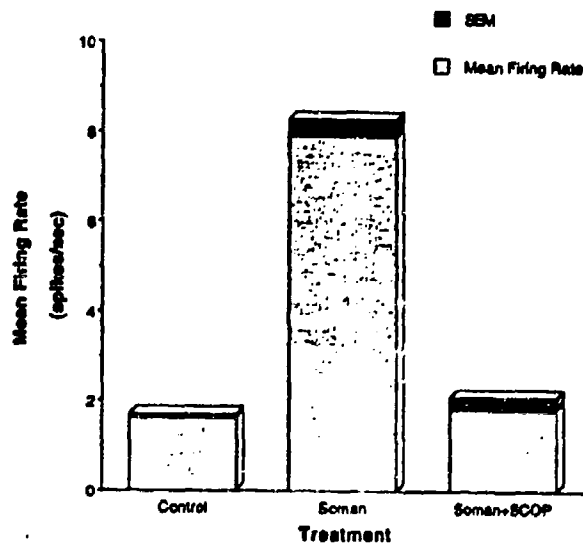


FIG. 11. Effect of systemic soman on LC discharge rate. Bar graph summarizing the mean spontaneous discharge rate of LC neurons before and after a systemic injection of soman and after administration of both soman and scopolamine. The mean spontaneous discharge rate of LC neurons sampled 8-45 min after soman injection ($n = 11$) was greater than that in control animals ($n = 21$); $P < 0.004$. There was no difference between the mean spontaneous discharge rate of LC neurons in control animals and in animals receiving soman and posttreated with scopolamine ($n = 9$).

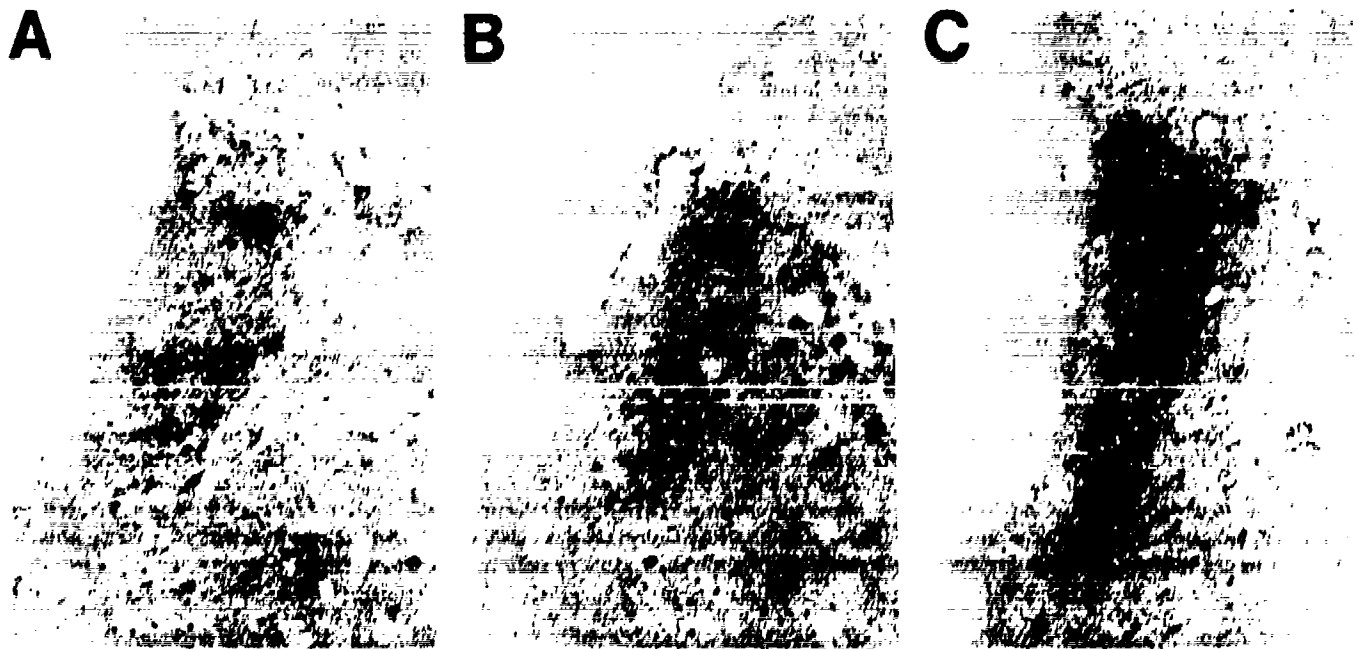


FIG. 12. Systemic injection of soman induces *c-fos* expression in LC neurons. A group of animals received a systemic single dose of soman ($78 \mu\text{g}/\text{kg}$). The animals were sacrificed and processed for immunohistochemical detection of *c-fos* at various time intervals. Sections from all animals were processed simultaneously in the same reaction solutions to control for variation in processing. In control animals (A) there is no detectable *c-fos* staining in LC neurons. At 45 (B) and 120 (C) min postsoman, there is a progressive increase in the number of LC neurons expressing *c-fos* and the intensity of *c-fos* staining. Note that there is no *c-fos* staining in neurons adjacent to LC.

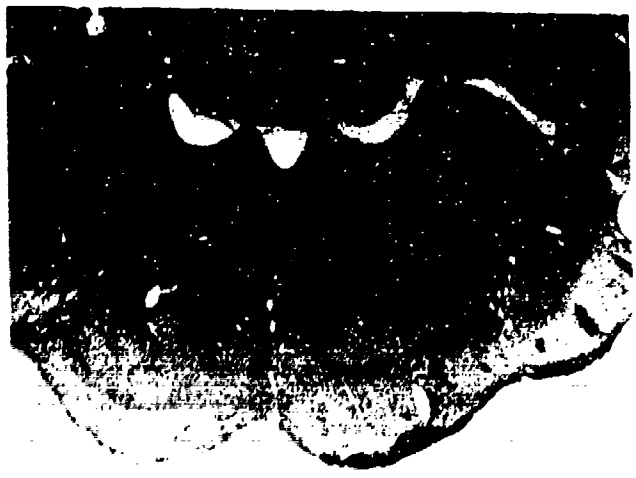


Figure 13. Systemic soman inhibits AChE in LC. A: Low power micrograph of a coronal section through LC processed for histochemical visualization of AChE. After the same systemic dose of soman used in the electrophysiological and c-fos experiments, there is a nearly complete inhibition of AChE staining in the pons except for neuronal staining in LC (at arrows) and the motor nucleus of the Vth nerve. B: Higher power micrograph showing the right LC from the same section.

FOS STAINING. Systemic injection of soman (78 $\mu\text{g}/\text{kg}$, im) in unanesthetized animals induced rapid and selective expression of *FOS* in only two areas: LC and PC (^{46, 48}); soman-induced *FOS* expression in PC will be the subject of a forthcoming report. As shown in Figure 12, systemic soman administration caused *FOS* expression in LC neurons by 30-45 min after injection; this expression was restricted to LC neurons as *FOS* was not expressed in neurons in nuclei surrounding LC, including the medial parabrachial nucleus, mesencephalic trigeminal nucleus, and lateral dorsal tegmental nucleus. With longer post-injection survival times, the number and intensity of *FOS*-stained LC neurons progressively increases, and *FOS* expression occurs in other brain regions.

ACHE STAINING. As shown in Figure 18A, AChE staining in LC of normal animals is so intense (^{34, 59}) that individual neurons cannot be distinguished. In contrast, AChE was nearly completely inhibited in LC and other parts of the brain after systemic soman administration (Fig. 13). Some residual AChE staining remained in LC neurons and in some basal forebrain neurons after peripheral soman injection, similar to the pharmacohistochemical methods previously used to limit AChE staining to cell bodies (³⁴).

Intracoeular Soman Administration. The finding that systemic soman administration increased LC spontaneous discharge rates and induced *FOS* expression is consistent with the hypothesis that LC neurons may be subject to tonic cholinergic afferent regulation. However, it is also possible that systemically injected soman increases LC activity by nonspecific peripheral sensory/motor effects, or by tonic activation of excitatory afferent inputs to LC neurons. In order to circumvent these possible indirect sites of soman action, we recorded the spontaneous activity LC neurons before, during and after focal microinjection of soman directly into LC.

LC NEURONAL ACTIVITY. The mean spontaneous discharge rate of LC neurons recorded with a double barrel recording/microinfusion assembly containing soman (2.2 ± 0.2 spikes/sec, $n = 22$) was slightly, but significantly, greater than the mean spontaneous rate of LC neurons recorded with single barrel pipettes (1.6 ± 0.1 , $n = 21$). This slightly higher spontaneous discharge rate was probably due to diffusion of soman from the soman injection pipette.

As shown for a typical neuron in Figure 14A, microinjection of small doses of soman into LC resulted in rapid, pronounced, tonic elevation of the spontaneous rate of LC neurons. Increases in LC discharge elicited by one of the smallest doses of soman tested, 6 pmol, ranged from 373.3% to 733.3% of control discharge rate, with a mean of 517.7% of control discharge rate ($n = 8$). Soman-induced-elevation of LC discharge was typically observed within 5 to 20 sec after microinjection, and was not associated with any discernible change of either the amplitude or the waveform of LC action potentials.

Larger doses of soman elicited even more pronounced increases in LC neuron spontaneous firing rates. As shown in Figure 16 the mean discharge rates of LC neurons increased progressively with cumulative doses of soman ranging from 2 to 48 pmol (in 5 to 120 nl). Thus, there was a strong dose-response relationship.

Consistent with a recent study, soman-induced activation of LC neurons was associated with desynchronization of the cortical EEG (²⁰). However, in no case was there evidence of seizure activity in the EEG records at any time during LC recordings after soman administration in the anesthetized preparation.

A significant observation with both the systemic and local administration of soman was that the discharge rate of LC neurons remained elevated as long as examined in these experiments (approximately 2 hr). For example, there was no significant difference between the mean spontaneous discharge rate of LC neurons sampled 5-14 min (7.2 ± 0.6 , $n = 16$), 15-30 min (5.7 ± 1.0 , $n = 5$) and 90-120 min after soman (5.4 ± 0.8 spikes/sec, $n = 5$); data represent firing rates for cells sampled after cumulative doses in excess of 12 pmol. Thus, there appeared to be little or no desensitization to or recovery from the excitatory effect of soman within the time periods examined in the present experiments.

Previous studies in anesthetized rats demonstrated that LC neurons exhibit a biphasic response to noxious somatosensory stimuli, such as paw- or tail-pinch or electrical stimulation of the sciatic nerve (13, 36, 54-56). This biphasic response consists of a brief burst of 2-5 spikes followed by a postburst inhibition of impulse activity lasting 500 to 1000 msec. Since microinjections of soman markedly increased spontaneous discharge rates, it was of interest to determine if the elevated level of tonic activity altered the responses of LC neurons to such excitatory stimuli. All LC neurons tested ($n=20$) exhibited the characteristic biphasic response to a paw or tail pinch throughout the prolonged period of soman-induced hyperactivity. Although possible changes in the magnitude of the excitatory or inhibitory components of this response were not quantified, it appeared that a similar burst of tail- or paw-pinch-evoked activity was superimposed upon the soman-evoked increase in spontaneous discharge.

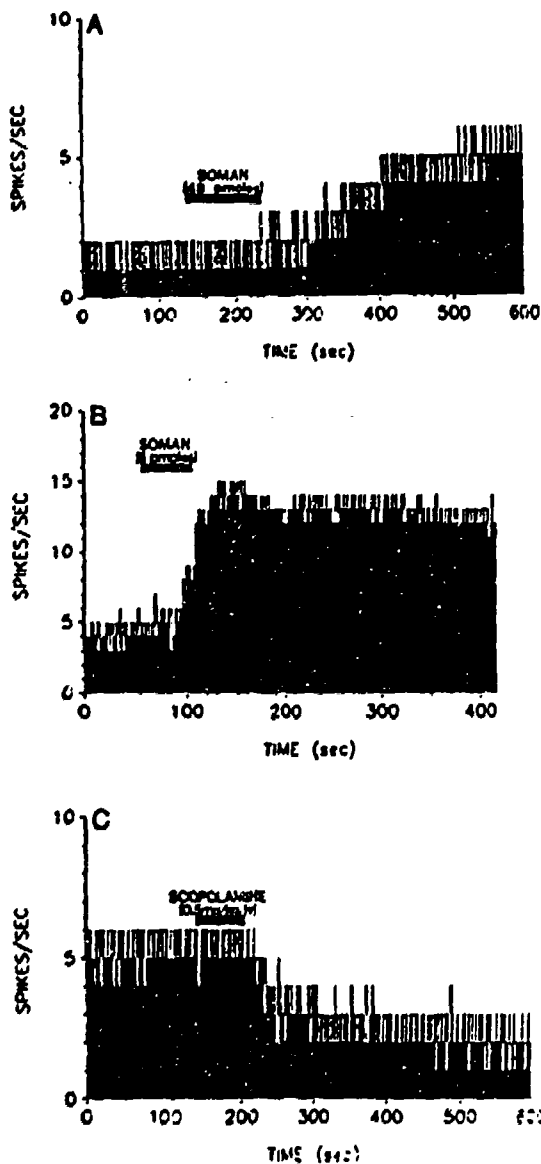


Figure 14. Microinjection of soman directly into LC tonically activates LC neurons via muscarinic cholinergic receptor activation. A: Computer ratemeter record showing spontaneous activity of a single LC neuron before and after microinjection of a single dose of soman into LC. Before application of soman, this typical LC neuron had a slow and regular spontaneous discharge rate of 1.5 spikes/sec. Microinjection of 48 picomoles of soman (n 120 nl, shown at upper bar) from a micropipette positioned 150 μ m above the tip of the recording microelectrode (see text for details) rapidly increased the spontaneous discharge of this neuron to approximately 5.5 spikes/sec. The spontaneous rate of this neuron continued to increase to a final rate of 7 spikes/sec (not shown). B: Computer ratemeter showing the spontaneous discharge of an LC neuron; recordings from this LC neuron were initiated 7 minutes after microinjection of soman (12 picomoles) - the firing rate of this neuron after this initial dose of soman was 4.0 spikes/sec. Microinjection of a second dose of soman (8 picomoles in 15 nanoliters, shown at upper bar) from an adjacent micropipette positioned 100 μ m above the recording electrode rapidly and potently increased the spontaneous rate of this cell to 12.3 spikes/sec. C: Computer ratemeter showing tonic elevation of spontaneous discharge of an LC neuron 30 minutes after microinjection of soman (96 picomoles) into LC. Intravenous administration of the muscarinic cholinergic antagonist scopolamine (0.5 mg/kg) rapidly and completely reversed the soman-induced tonic excitation of this neuron from 5.5 spikes/sec to 2.0 spikes/sec.

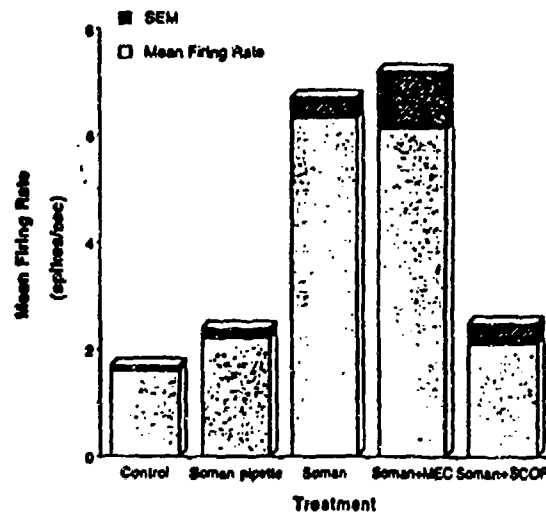


FIG. 15. Analysis of the effects of intracerebral soman on LC neuronal activity. Bar graph showing the mean (\pm SEM) spontaneous discharge rate of LC neurons after the following experimental treatments. Control, recordings in control animals ($n = 21$, 1.6 ± 0.1 spikes/s) with single-barrel recording micropipettes. Soman pipette, the discharge rate of LC neurons ($n = 20$) recorded with a double-barrel recording pipette/soman injection pipette assembly (2.2 ± 0.2 spikes/s) was significantly greater ($P = 0.05$) than the mean of control animals. Soman, the discharge rate of LC neurons ($n = 30$) recorded after intracerebral microinjections of 2-121 pmol (6.4 ± 0.4 spikes/s) was significantly greater ($P < 0.0001$) than that of control animals. Soman + MEC, the mean discharge rate of LC neurons (6.1 ± 1.1 spikes/s) after soman and mecamylamine (MEC, 1.0-2.0 mg/kg, iv) did not differ from the postsoman mean. Soman + SCOP, the mean discharge rate of LC neurons after soman and scopolamine (SCOP, 1.0-2.0 mg/kg, iv) was not significantly different from that of the control animals.

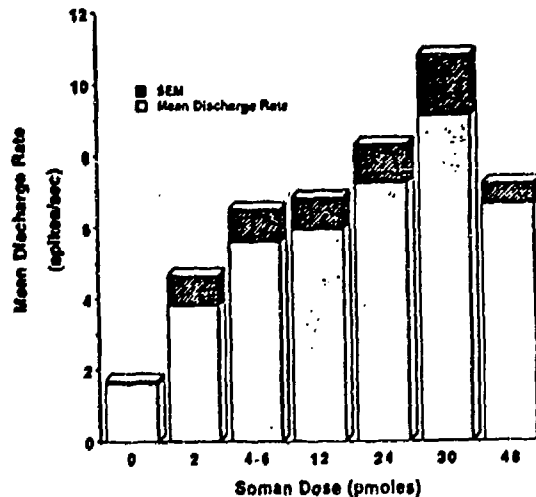


FIG. 16. Dose-dependent activation LC neurons by intracerebral soman. Bar graph shows the mean discharge rate of LC neurons sampled after cumulative doses of 2 ($n = 2$), 4-6 ($n = 8$), 12 ($n = 5$), 24 ($n = 4$), 30 ($n = 4$), and 45 ($n = 7$) pmol soman.

Injection of vehicle alone sometimes elicited a phasic (1-3 min) increase in LC discharge rate, perhaps due to the low ionic concentration or low pH of the vehicle solution. However, microinjections of 15 (n = 3) or 30 nl (n = 3) of vehicle, equivalent to volumes of soman that potently and tonically activated LC neurons, elicited only a small, insignificant elevation of LC discharge rate (mean discharge rate before and after vehicle injection, 2.1 ± 0.3 and 2.8 ± 0.4 spikes/sec, respectively). In contrast to the strong tonic excitation of LC neurons produced by soman, the modest increase in LC activity elicited by vehicle microinjection never lasted longer than 2 to 3 min.

A parsimonious explanation for the pronounced, tonic elevation of LC discharge caused by directly applied soman is that this agent inhibited AChE in LC, causing LC neurons to be exposed to tonically elevated levels of unhydrolyzed ACh. If this were true, then cholinergic receptor antagonists should reverse the elevated discharge rates of LC neurons induced by soman. As illustrated in Figure 14C, intravenous injection of the centrally active muscarinic receptor antagonist scopolamine at a dose (0.5 mg/kg, iv) previously shown to block excitation of LC neurons to directly applied ACh (Engberg and Svensson, 1980), rapidly and potently reversed soman-induced elevation of LC discharge. The mean spontaneous discharge rate of LC neurons sampled after relatively high doses of soman (48-97 pmol in 120-240 nl) followed by scopolamine (2.1 ± 0.4) did not differ ($p > 0.18$) from the mean baseline discharge rate of LC neurons (Fig. 15). In marked contrast, intravenous injection of the nicotinic receptor antagonist mecamlamine (1.0 - 2.0 mg/kg) did not reduce ($p > 0.8$) the tonic elevation of LC discharge rate induced by 75 nl soman (mean rate after mecamlamine = 6.1 ± 1.1 spike/sec). It is important to note however, that previous studies have demonstrated that nicotinic responses in LC are transient and rapidly desensitize (Egan and North, 1986). As the experiments with mecamlamine were conducted at times longer than 3 min after soman microinjection, nicotinic responses subsequent to soman injection may have desensitized by this time.

FOS STAINING. Intracocerulear injections of soman at doses that potently activated LC neurons (24-36 pmoles in 60-90 nl) caused the rapid induction of *FOS* expression in LC neurons. As shown in Figure 17, LC neurons ipsilateral, but not contralateral, to the injection site exhibited *FOS* expression within 2 hrs after soman microinjection into LC. In contrast, there was little or no *FOS* expression in neurons in nuclei adjacent to LC (i.e., medial parabrachial nucleus, mesencephalic trigeminal nucleus, and lateral dorsal tegmental nucleus). By contrast, when saline rather than soman was injected into LC, only occasional cells near the tip of the pipette were positive for *FOS*.

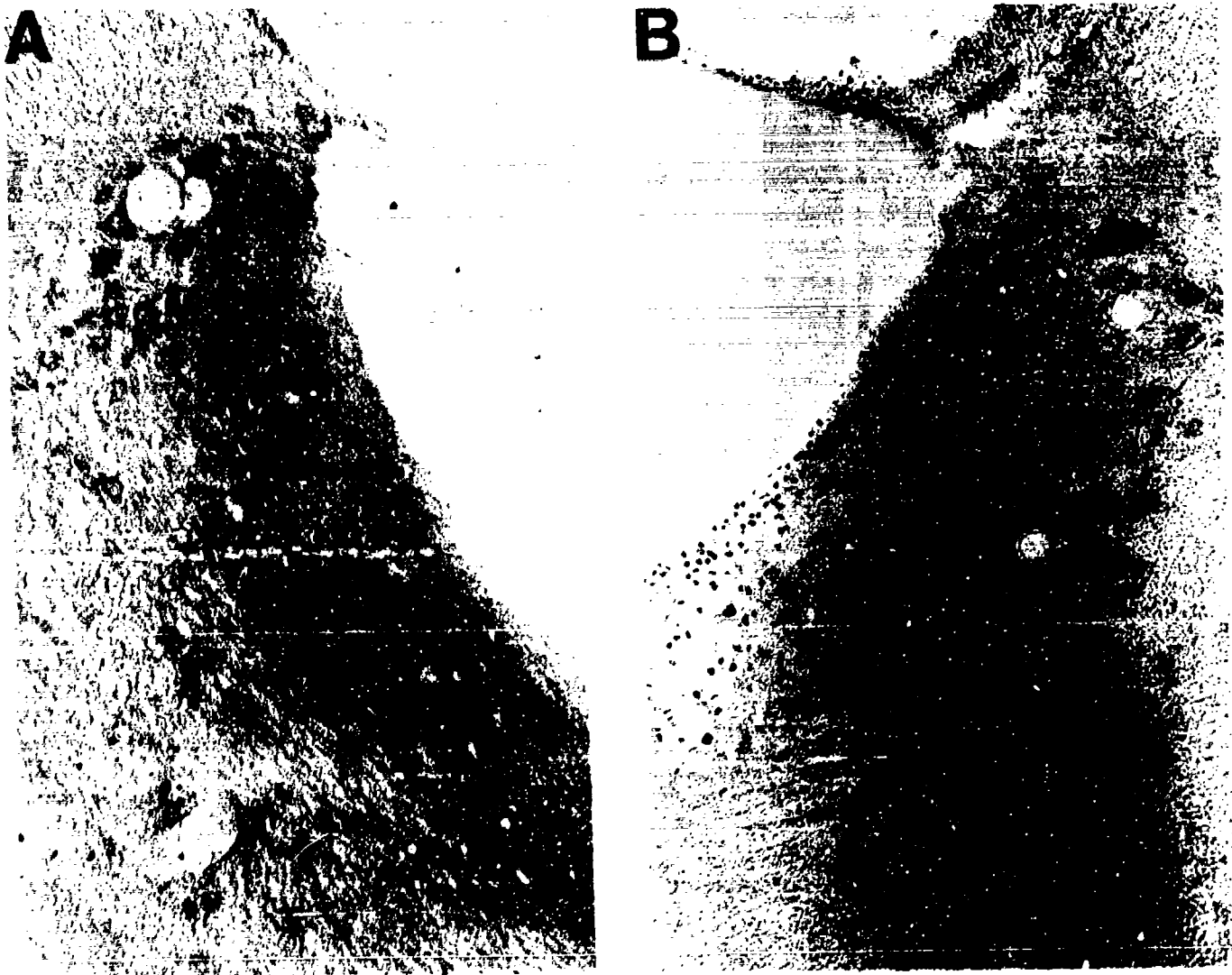


Figure 17. Induction of *FOS* expression in LC neurons by intracereular microinjection of soman. Soman was microinjected into LC and single LC neurons were recorded for two hours. The animal was sacrificed and adjacent sections were stained for *FOS* (A and B) and AChE. **A:** Photomicrograph of a coronal section through LC contralateral to the soman microinjection site. Immunocytochemical processing for *FOS* shows that there very little *FOS*s expression in LC neurons contralateral to the injection site. **B:** Photomicrograph of LC which received a microinjection of soman. Note that 2 hours of local, restricted AChE inhibition induced *FOS* expression in the majority of LC neurons but not in adjacent neurons.

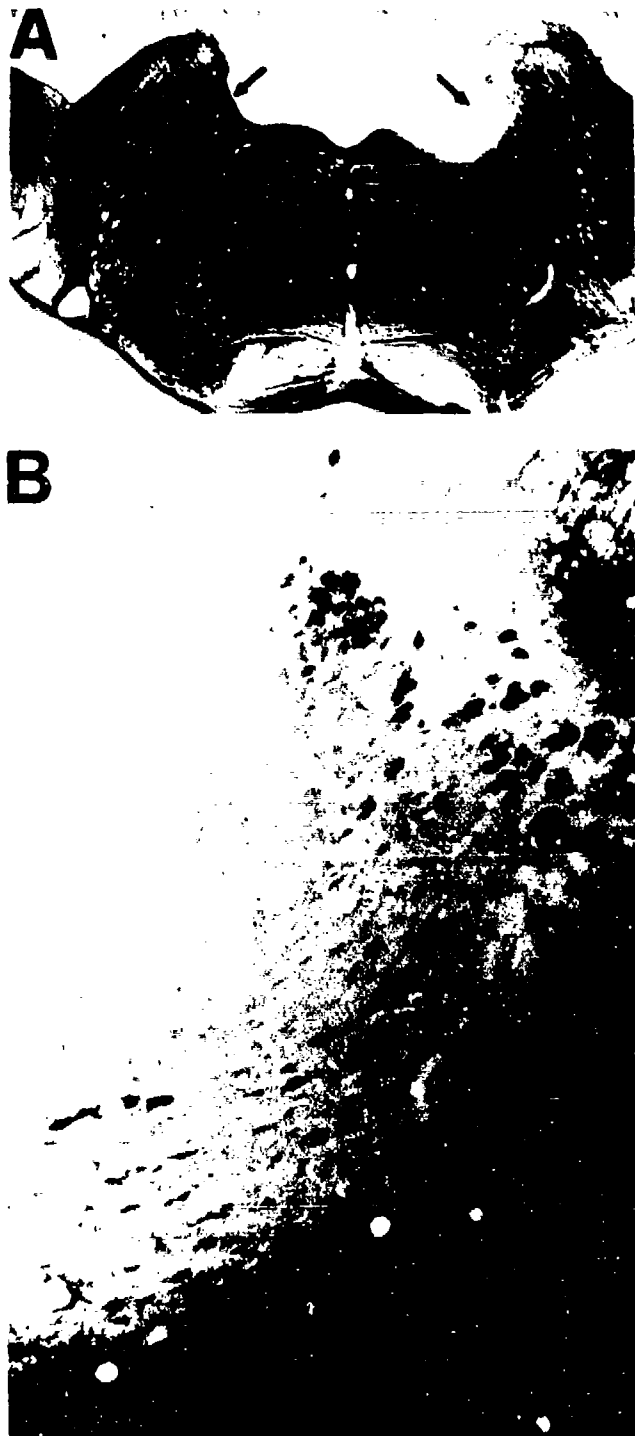


Figure 18. Intracereular microinjection of soman focally inhibits AChE in LC. **A:** AChE stained section through LC from an same experiment in which soman was microinjected into LC. AChE staining in the left, non-injected side (at arrow) is normal. Soman was microinjected into LC on the right side (at arrow). **B:** Higher magnification of section shown in panel A. AChE is completely inhibited in the vast majority of LC neurons.

ACHE STAINING. As shown in Figure 18, AChE histochemistry demonstrated that microinjections of soman into LC nearly completely inhibited AChE staining in LC and the adjacent pericoerulear area (n = 4). With microinjections of soman (less than cumulative doses of 36 pmol), AChE inhibition was limited to LC proper, the rostromedial pericoerulear region, including the lateral dorsal tegmental nucleus and Barrington's nucleus, the mesencephalic trigeminal nucleus, and the medial border of the parabrachial complex. With larger microinjections of soman (48 to 97 pmol in 120 - 240 nl), inhibition of AChE staining extended further laterally into the parabrachial complex, rostromedially into the dorsal tegmental nucleus, and caudally into the medial vestibular nucleus.

DISCUSSION

The present findings demonstrate that both systemic and focal, intracoerulear microinjection of small doses of the irreversible AChE inhibitor soman causes a dramatic, sustained increase in the spontaneous discharge rates of LC neurons. Following either route of soman administration, the spontaneous rates of LC neurons remained elevated at the longest postsoman time interval examined (2 hr), consistent with the irreversible actions of this AChE inhibitor. The maintained activation of LC neurons evoked by soman was rapidly and completely reversed by the centrally active muscarinic receptor antagonist scopolamine hydrochloride, but not by the nicotinic receptor antagonist mecamylamine. A molecular correlate of this tonically elevated physiologic activity was the induction of *FOS* expression in LC neurons. These overall results indicate that LC neurons *in vivo* may receive tonic cholinergic input.

Various lines of anatomic evidence, although largely indirect, suggest that LC neurons receive a cholinergic input. LC neurons stain intensely for the degradative enzyme AChE; indeed, AChE staining in LC is one of the densest in the brain (3, 4, 34). Receptor binding studies show that LC contains both muscarinic and nicotinic receptor subtypes (101, 164). Biochemical measurements indicate that the biosynthetic enzyme for ACh, choline acetyltransferase (ChAT), is present, presumably in fibers, in the LC area. However, such measurements may have been contaminated by ChAT contained in cholinergic neurons or fibers located adjacent to LC (165).

Even stronger evidence for cholinergic modulation of LC neurons comes from a wealth of neurophysiological studies. *In vivo* neuropharmacologic studies have shown that LC neurons are potently excited by direct application of ACh and muscarinic analogs (2, 21, 77). This excitation was completely blocked by direct application of the muscarinic receptor antagonist scopolamine. In contrast, the actions of nicotinic agonists are less clear. Systemic, but not iontophoretic, administration of nicotine activates LC neurons *in vivo* (53). In slices, ACh excites LC neurons through both nicotinic and muscarinic receptors (44, 45); in the presence of muscarinic antagonists, nicotine produces a fast,

brief depolarization of LC neurons that exhibits rapid desensitization. Nicotine-evoked responses were blocked by hexamethonium, but not by alpha-bungarotoxin. By contrast, muscarinic responses have a longer time course than nicotinic responses, and muscarinic responses do not appear to desensitize (⁴⁵). Thus, neuropharmacologic experiments indicate that ACh can excite LC neurons via activation of either muscarinic or nicotinic receptors.

LC neurons were robustly activated after peripheral injection of the irreversible AChE inhibitor, soman. Soman produces a host of peripheral cholinomimetic side effects e.g., labored breathing, hypoxia, gastrointestinal activation, hypotension, bradycardia. It is conceivable that such side effects could indirectly influence LC activity. However, in the present experiments, soman was able to activate LC neurons despite pretreatment with the peripherally acting muscarinic receptor antagonist methylscopolamine bromide, which significantly reduced these side effects. The increased discharge rate of LC neurons produced by soman in methylscopolamine bromide-pretreated animals was identical to that in animals that did not receive this pretreatment, thus indicating that the peripheral cholinomimetic side effects of soman probably did not contribute significantly to the observed activation of LC neurons. By contrast, soman-induced activation of LC neurons was completely reversed by the centrally active muscarinic receptor antagonist scopolamine hydrochloride. In addition, the increase in LC neuronal discharge rates following *systemic* soman administration was essentially the same as that following *intracoerulear* microinjection of soman. Finally, preliminary experiments in this laboratory indicate that increases in LC neuronal activity comparable to those seen with soman are produced by intracoerulear microinjection of the muscarinic agonist pilocarpine (in preparation). Thus, we conclude that the increase in LC neuron firing rates produced by systemically administered soman is mediated primarily, if not entirely, by central cholinergic stimulation of LC neurons.

In further support of this conclusion, we found that focal microinjection of picomolar concentrations of soman directly into LC robustly activated every LC neuron tested. The finding that LC neurons were activated after injections of soman as small as 2-6 pmol (in 5-15 nl) indicates that this activation was probably mediated by facilitation of cholinergic transmission at synapses on LC neurons. This is supported by the histochemical finding that intracoerulear microinjection of volumes of soman as large as 36 pmol (in 90 nl) produced a focal zone of AChE inhibition restricted almost entirely to the LC nucleus and the adjacent rostromedial zone that contains a dense plexus of extranuclear dendrites (^{70, 175}). The progressive increases in LC firing rates with incremental doses of soman thus may be due to additional facilitation of transmission at cholinergic synapses on the more distal dendrites of LC neurons, or to a more complete inhibition of AChE. Despite the diffusion of soman into adjacent structures with larger injections, *FOS* staining revealed that LC neurons were the only cells in the dorsolateral pons to exhibit elevated expression of this transcriptional regulatory protein.

Similar to results with systemic injections, intracoerulear infusion of soman tonically activated LC neurons. LC discharge rates were significantly elevated at all times sampled in these experiments (up to 2 hr), with only a small decrease in firing rate after the first 15 min of soman injection. This maintained activation of LC neurons was completely reversed by intravenous injection of scopolamine hydrochloride at a dose previously shown⁽⁵³⁾ to antagonize LC responses to directly applied ACh. This result indicates that the maintained activation of LC neurons by soman is mediated by muscarinic receptors and further argues that increased firing of LC cells was not due to some as yet unknown direct neurotoxic action of soman. In agreement with this hypothesis, tonic activation of LC neurons produced by soman was not significantly affected by the nicotinic receptor antagonist mecamylamine. However, as noted above, studies *in vitro* indicate that nicotinic excitation of LC neurons undergoes rapid desensitization⁽⁴⁵⁾. Thus, it is possible that the initial phase of soman-induced activation of LC has a nicotinic component. The present studies did not address this possibility because, as noted earlier, vehicle injection alone sometimes caused a brief increase in LC discharge rate. Thus, it would be difficult to assess any brief lasting nicotinic activation under these conditions.

The most parsimonious explanation for increased LC firing rates after soman administration is that soman's inhibition of AChE facilitates the excitation of LC neurons to a tonically active cholinergic input. However, there are several alternative possibilities. 1) Systemic soman could activate LC neurons as a consequence of the seizurogenic actions of this agent. However, EEG recordings showed that systemic soman did not produce seizures in anesthetized animals, but did cause a potent, sustained increase in LC neuronal discharge rates. 2) Soman could activate local neurons in the pericoerulear area that, in turn, have excitatory connections with LC neurons. This possibility seems unlikely because increases in LC discharge were obtained with intracoerulear injections of soman as small as 5 nl (2 pmol). In addition, AChE staining revealed that microinjections of soman as large as 90 nl (36 pmol) produced a focal zone of AChE inhibition largely restricted to LC. 3) AChE inhibition could inhibit intracoerulear NE release from LC axonal and dendritic terminals or inhibit the G protein associated with the intracoerulear α -2 autoreceptor, thereby decreasing inhibitory collateral interactions among LC neurons (disinhibition). These possible actions of soman are unlikely to solely mediate the increased spontaneous rate of LC neurons as these cells still exhibit a pronounced postactivation inhibition in response to a tail- or hindpaw-pinch following soman administration. Furthermore, direct blockade of inhibitory α -2 autoreceptors by microinjection of idazoxan into LC elicits only very small (less than 0.5 spike/sec) increases in the spontaneous discharge rate of LC neurons⁽¹¹⁾. 4) Soman could activate excitatory afferent inputs to LC. For example, AChE inhibition could lead to accumulated ACh which in turn could cause the release of excitatory amino acids⁽⁵⁵⁾ from the terminals of afferents to LC. Future experiments will address this possibility.

The present observation that direct injection of an AChE inhibitor potently increases the spontaneous discharge of LC neurons thus suggests that LC neurons receive a tonically active cholinergic input. If this is true, then direct or systemic administration of the muscarinic antagonist scopolamine might be expected to decrease the spontaneous rate of LC neurons, but this has not been observed (53, 55), except with near-lethal doses of this agent. The reason for this discrepancy is unclear, but it is possible that high levels of AChE expressed by LC neurons normally functions to rapidly degrade ACh spontaneously released by cholinergic afferent synapses, thus minimizing tonic postsynaptic drive of LC neurons.

The source(s) of possible cholinergic input to LC neurons have not been directly identified with double labeling techniques. It is noteworthy that the two major afferent inputs to LC, nucleus prepositus hypoglossi and nucleus paragigantocellularis located in the medulla (12), contain ChAT-positive cell bodies (165). Both of these medullary regions project heavily to the central core of LC proper and also to the pontine tegmentum rostral and medial (rostromedial pericoerulear zone) to LC proper (12). A recent study of immunocytochemical localization of ChAT indicated that the LC nucleus proper is nearly devoid of ChAT-positive fibers. However, the pericoerulear region rostromedially adjacent to LC contains a considerable plexus of ChAT-positive fibers (165), indicating that this region receives strong cholinergic innervation. We have recently demonstrated that this same rostromedial pericoerulear region contains a dense, focal plexus of LC dendrites (70, 175). These extranuclear dendrites receive dense synaptic input. Thus, there is extensive spatial overlap between these extranuclear dendrites of LC neurons and ChAT-positive fibers in the rostromedial pericoerulear region. Taken together, the evidence to date suggests that LC neurons receive cholinergic innervation, possibly on these extranuclear dendrites, but the sources of these cholinergic inputs have not been identified. Anatomical studies are under way to determine which of these possible systems provide cholinergic inputs to LC.

Recent experiments in this laboratory demonstrated that systemic injections of soman that induce convulsions cause a rapid and profound reduction of NE in the olfactory bulb and forebrain (Chapter 5, this report). Within 1 hr after peripheral soman administration, NE levels were reduced by 50% from control values; by 2 hrs post-soman, NE levels were reduced by 70%. NE levels were not altered in animals receiving the same dose of soman but not exhibiting convulsive activity. As NE is depleted only in convulsing animals it is conceivable that generalized brain seizures, and not cholinergic stimulation, causes activation of LC neurons. The present studies demonstrate, however, that seizures are not the cause of the increased firing rates of LC neurons in anesthetized animals, as both systemic and intracoerulear microinjection of soman robustly and tonically activate LC neurons *in the absence of seizures* (Figure 10). Moreover, as both systemic and intracoerulear soman-induced activation of LC

could be completely blocked by scopolamine, we conclude that soman causes activation of LC by direct cholinergic stimulation.

Thus, it is reasonable to argue that the reduction of olfactory bulb and forebrain NE caused by systemic soman administration is due to a tonic cholinergic stimulation of LC neurons which in turn leads to depletion of NE in LC terminals. However, as soman inhibits acetylcholinesterase, thus causing increased ACh, it is possible that NE release is also influenced by activation of cholinergic receptors located on LC terminals. Presynaptic muscarinic receptors reduce and nicotinic receptors increase, terminal NE release (204-206). Soman, by increasing ACh should stimulate both muscarinic and nicotinic receptors, but it is unclear how combined stimulation of both receptor subtypes would influence NE release. If muscarinic *reduction* of NE release predominates, then a muscarinic agonist should increase LC discharge rate but cause less NE release than seen with soman. Recent studies in this laboratory (in preparation) demonstrate that administration of the muscarinic agonist, pilocarpine, causes increases in LC neuronal discharge activity that are identical to those caused by soman. However, pilocarpine also caused forebrain NE reductions of the same magnitude and time course as those produced by soman. This argues that any reduction in NE release attributable to presynaptic muscarinic stimulation is insufficient to offset the increase in release of NE due to the sustained increase of LC neuronal activity. As any nicotinic action would presumably further *increase* NE release, we conclude that soman increases NE release primarily because it increases the activity of LC neurons.

As soman directly activates LC neurons and since NE levels are only reduced in convulsing animals, it is therefore reasonable to suggest that soman-induced activation of LC, producing a sustained release of NE throughout the forebrain, plays a role in the generation and/or maintenance of seizures. When given systemically to unanesthetized animals, soman caused convulsions and dramatic NE depletion in two thirds of the rats. By contrast, when soman was microinjected directly into LC it caused 3-7-fold increases in firing rates in all cells tested. At face value, this might imply that increased firing of LC neurons, *per se* is not sufficient to trigger seizure activity. Consistent with this, seizures were never observed in our acute experiments where soman, at a systemic dose sufficient to induce convulsions in two-thirds of unanesthetized animals, increased LC neuronal activity 3-7-fold. Recordings from LC following systemic administration of soman were obtained in only four animals pretreated with the peripheral muscarinic antagonist methylscopolamine, as animals without this pretreatment died within 5-10 min of soman administration. Even with this pretreatment, the animals' labored breathing made it difficult to record the activity of isolated units for long periods of time. Thus, had we been able to record from a larger population of animals with systemic administration of soman we might have observed some animals in which the same dose of soman caused no increase of LC activity corresponding to the third of the unanesthetized animals that do not convulse. The reason a

third of the animals do not convulse is not clear, although it may reflect variability in the amount of soman that reaches the brain following intramuscular administration. Consistent with this, other observations from this laboratory show that the same dose of soman can cause different degrees of AChE inhibition in the brain. We have also observed that the same dose of soman can cause differential inhibition of AChE in different neurons in LC (unpublished observations); it is possible, therefore that inhibition of AChE in a critical proportion of LC neurons may be necessary to cause sufficient forebrain release of NE to contribute to the generation and/or maintenance of seizures. It is further possible that anesthesia prevents the expression of soman-induced seizures through either a generalized reduction of neural excitability or a selective reduction of LC neuronal excitability. Thus soman might cause even greater increases in LC neuronal firing rates in unanesthetized animals. Recordings of LC in soman-treated, unanesthetized animals might shed light on these alternatives. Thus, while it is difficult to directly compare the actions of soman on LC neuronal activity with the occurrence of seizures in the unanesthetized rat, it is nonetheless intriguing that the results of our companion study clearly demonstrated that convulsions only occurred when NE levels were dramatically reduced. Thus we hypothesize that soman-induced activation of LC causing sustained release of NE in the forebrain is a necessary condition for the expression of seizures.

While the role of NE in seizures is equivocal, there is strong evidence that NE, acting via *B*-receptors, is proconvulsive (111, 140). Exposure to soman leads to generalized hypercholinergic stimulation of brain neurons. The present results, taken with the neurochemical findings in Chapter 5, show that soman also leads to the generalized release of NE. The consequences of *combined* cholinergic and noradrenergic stimulation has not been investigated but, as both of these transmitters are known to block spike accommodation mechanisms in cortical and thalamic neurons (38, 81, 85, 113-115, 120), it is conceivable that *sustained* release of these two transmitters conspires to *initiate* soman-induced seizures. Should this hypothesis prove correct, it might be possible to prevent the seizurogenic actions of soman and other cholinolytic agents by conventional pharmacological manipulation of these two neurotransmitter systems.

7. PILOCARPINE-INDUCED CONVULSIONS IN RATS: EVIDENCE FOR MUSCARINIC RECEPTOR MEDIATED ACTIVATION OF LOCUS COERULEUS AND NOREPINEPHRINE RELEASE IN CHOLINOLYTIC SEIZURE DEVELOPMENT

INTRODUCTION

There is an increasing interest in the role of acetylcholine (ACh) in seizures, including human epilepsy (194). Additional interest stems from the fact that organophosphate (OP) nerve agents such as the irreversible acetylcholinesterase (AChE), soman, cause severe convulsions associated with irreversible brain damage. Soman significantly increases brain ACh in the course of seizures (173). However, several lines of evidence suggest that soman-induced convulsions may not be due solely to an excess of ACh. For example, centrally acting muscarinic antagonists such as atropine, alleviate but do not block the convulsive actions of OP nerve agents (121). Moreover, there is little systematic relation between the incidence or severity of soman-induced convulsions and the elevation in ACh or γ -aminobutyrate (GABA) levels in the rat striatum and cerebellum (110). Likewise, we showed that there is only a moderate correlation between forebrain AChE reductions and the incidence of convulsions in rats following soman intoxication (Chapter 5, this report).

There is evidence that effects of ACh on other modulatory neurotransmitters, such as norepinephrine (NE), dopamine (DA), and serotonin (5-HT) may be involved in cholinolytic convulsions (89). Soman administration was found to increase release of all three of these neurotransmitters (66). We recently demonstrated that soman causes a rapid, profound depletion of forebrain NE and that there is a strong correlation between NE depletion and the incidence of convulsions (Chapter 5, this report). Based on the findings, we hypothesized that NE depletion might be caused by sustained activation of neurons in the locus coeruleus (LC).

Noradrenergic neurons in LC send fibers to all parts of the forebrain and are the sole source of NE in the cortex, hippocampus and the olfactory bulb. Therefore, LC exerts a global influence on neuronal excitability. Several lines of evidence suggest that excess ACh caused by soman's irreversible inhibition of AChE might excite LC neurons causing increased NE release from LC terminals: (i) LC neurons contain high levels of AChE (3); (ii) cholinergic agonists strongly increase the firing rates of LC neurons (2) and (iii) activation of LC causes increased release of NE in the forebrain (102). Sustained release of NE in the forebrain could contribute to the generation of seizures; NE increases the excitability of cortical neurons by a disinhibitory mechanism similar to that of ACh (38, 144). Moreover, there is evidence that NE has pro-convulsant actions. Therefore, NE release caused by AChE inhibitors

may play an important role in the initiation and/or maintenance of cholinolytic seizures, as inhibition of AChE should lead to a rapid accumulation of ACh in LC and accumulated ACh might tonically activate LC neurons.

Thus, we recently investigated the actions of systemic and intracoerulear injections of soman on the discharge characteristics of LC neurons. Systemic injection (im) of soman increased the mean firing rate of LC neurons to five times the control rate (Chapter 6, this report). This increased firing rate was sustained for several hours. Likewise, microinjection of soman confined to LC caused a comparable sustained increase in the firing rate of LC neurons. These findings demonstrated that soman causes a rapid, sustained increase in the discharge of LC neurons. Further consistent with the idea that soman causes sustained excitation of LC neurons, we also found that either systemic or intracoerulear soman selectively induced the expression of the immediate early gene, *FOS*, in LC neurons.

The most parsimonious explanation for these actions is that soman blocks AChE, leading to an excess of ACh in LC. If true, then muscarinic and/or nicotinic antagonists should block increased LC firing caused by soman. Indeed, our previous experiments showed that muscarinic, but not nicotinic, receptor antagonists completely reversed the excitatory action of either systemic or intracoerulear injection of soman on LC neurons (Chapter 6, this report). This suggests that soman-induced ACh accumulation leads to increased LC firing by activation of muscarinic receptors. If this hypothesis is correct, then administration of a muscarinic agonist should, like soman, also cause *both a sustained increase in LC firing rates and depletion of NE in the forebrain*. Pilocarpine is a potent muscarinic receptor agonist. Systemic administration of pilocarpine causes seizures (¹⁹⁵). Pilocarpine induced seizures are attenuated by the muscarinic antagonists atropine and scopolamine (^{96, 152}). The goal of the present experiments, therefore, was to test the prediction that a selective muscarinic agonist, pilocarpine, would produce effects on NE release and LC neuronal activity similar to those caused by the anticholinesterase soman.

METHODS

Chemicals. Pilocarpine hydrochloride, monochloroacetic acid, octyl sodium sulfate, brain monoamines and the internal standard 3,4-dihydroxybenzylamine hydrobromide (DHBA) were obtained from Sigma Chemical Co. Fisher Scientific was the source of L-cysteine, Na₂EDTA, perchloric acid and HPLC grade acetonitrile.

Pilocarpine Administration. Adult male Sprague-Dawley rats (290-340 g) were obtained from Harlan Laboratories, (Indianapolis, IN). Rats were housed in pairs with free access to food and water at least

one week before use. A single dose of 300 mg/kg pilocarpine in saline was injected (ip). This dose was selected because it causes convulsive seizures in 60% of the animals compared to 90-100% induced by the larger dose of 380 mg/kg used in previous studies (129, 156). Thus, by using this "perithreshold" convulsive dose, it was possible to determine if any changes in monoamines and/or changes in LC discharge were a consequence of pilocarpine *per se*, or were *dependent* on the development of convulsions. For each survival period a control group of rats was injected with a proportional volume of saline.

Scoring of Convulsive versus Nonconvulsive Rats. Pilocarpine injected rats were observed every 5 min during the first 30 min after injection, every 30 min for the next 8 hr, and once daily during the remainder of the 24-96 hr survival period. For each injected rat, the presence or absence of convulsions was noted during this observation period. Pilocarpine-intoxicated rats fell into clearly distinguishable convulsive and nonconvulsive groups. Those rats which developed convulsions did so within 40 min after pilocarpine administration and continued to be convulsive for at least 4 hr.

Neurochemical Measures.

Animals. Rats were sacrificed by decapitation at 1, 2, 4, 8, 24 and 96 hr following pilocarpine administration. The brains were rapidly removed and the olfactory bulbs were separated from the remainder of the brain by cutting the olfactory peduncle. The cerebellum and underlying brainstem were removed and the forebrain was divided at the midline, followed by the removal of the remaining brainstem including the thalamus and hypothalamus. Forebrain samples and two olfactory bulbs were immediately frozen on dry ice, and stored at -70° C until assay.

Individual forebrain tissues were homogenized at 0° C for 2 min in 1.0 ml of 0.10 M perchloric acid containing 0.1% cysteine as antioxidant and 10 ng of the internal standard (DHBA). About 200 µl of individual homogenates was transferred to an Eppendorf polypropylene tube and centrifuged at 1360 g for 7 min at 4° C. One hundred microliters of the supernatant was diluted with 200 µl of the homogenization solvent. The olfactory bulbs were treated identically except that these were homogenized for 1 min in 200 µl of solvent. For either tissue, 10 µl of the final solution was injected into the HPLC.

Chromatographic Methods and Assay of Brain Monoamines. Monoamine levels were determined using a Bioanalytical Systems (West Lafayette, IN) Model 200 Liquid Chromatograph, equipped with a Model LC-4B Electrochemical Detector. The glassy carbon working electrode was kept at 0.70 V against an Ag/AgCl reference electrode and the sensitivity of detection was kept at 10 nA (full scale). Chromatographic separations were effected with a 10 cm x 3.2 mm ODS 3-µm column (Bioanalytical

Systems, Inc.). The mobile phase consisted of 0.06 M monochloroacetic acid Buffer (pH 3.0) containing 1.30 mM octyl sodium sulfate, 0.2 mM Na₂EDTA, and 3.5% acetonitrile. The flow rate of the mobile phase through the column was kept at 1.0 ml/min. The column and the electrochemical cell were held at 40 and 41° C, respectively. For forebrain monoamine assays, five standard solutions (10 µl each) were injected daily between the runs containing 0.2-1.0 ng of NE, HVA, DOPAC, 5-HT; 0.10-0.50 ng of 5-HIAA; 0.5-2.50 ng of DA and a constant amount (0.2 ng) of the internal standard DHBA. For olfactory bulb monoamine assays, five standard solutions (10 µl) were similarly injected into HPLC but containing 0.2-1.0 ng of NE and 5-HT; 0.10-0.50 ng of DA, HVA, DOPAC, 5-HIAA and a constant amount (0.2 ng) of DHBA.

Statistical Analysis. Statistical analysis of the data was performed using unpaired, two-tailed Student's t-tests

Neurophysiological Measures:

General Surgical Procedures. Male Sprague-Dawley rats (Harlan Laboratories, Indianapolis, IN) weighing 250 to 375 g were anesthetized with chloral hydrate (400 mg/kg, ip). Anesthesia was maintained throughout all procedures with additional injections of 30-40 mg/kg chloral hydrate administered approximately every 30 min. Core body temperature was maintained at 36-38° C with a feedback-controlled heating pad.

LC Recordings. Animals were anesthetized with chloral hydrate and placed in a stereotaxic instrument with the incisor bar lowered to place the skull 12 degrees below the horizontal plane (bregma 2 mm below lambda). A hole was drilled in the skull at the coordinates for LC (3.7 mm posterior to lambda, 1.2 mm lateral to midline), and the underlying dura was reflected. A glass recording micropipette (2-4 µm tip diameter) filled with 2% Pontamine Sky Blue in 0.5 M sodium acetate was advanced into LC with a hydraulic microdrive. Extracellular recordings from individual neurons were amplified and displayed as filtered (300 Hz - 10 KHz bandpass) and unfiltered electrode signals. Impulse activity was also monitored with a loudspeaker. Action potentials were isolated from background activity with a waveform discriminator which generated logic pulses for signals that crossed a lower voltage gate and peaked below an upper voltage gate. Discriminator logic pulses were led to a computer and chart recorder for on-line data collection. LC neurons were tentatively identified at the time of recording by characteristic impulse waveforms, and spontaneous and sensory-evoked discharge patterns as previously described (⁵⁴). Micropipette penetrations were marked by iontophoretic ejection of dye with current pulses (-7 µA, 50% duty cycle for 10 min). At the end of recording sessions, animals were deeply anesthetized and perfused with 10% formalin. Brains were removed and stored in a similar solution containing 20% sucrose. Select brain regions were cut into 50 µm-thick

frozen sections, mounted on subbed slides and stained with neutral red. All recording sites were histologically localized from such tissue sections.

EEG Recordings. A pair of stainless steel microwires (250 μm diameter), factory insulated except for bluntly cut tips, were used to monitor cortical EEG. The tips of the wires were separated dorsoventrally by 1.5 mm and the electrode was implanted into the cortex (1-3 mm caudal to bregma, 1 mm lateral to midline) so that the tip of the superficial electrode extended 160 μm below the cortical surface. The electrode was secured to adjacent skull screws with dental cement. The EEG was amplified by conventional methods and displayed on a chart recorder.

Pharmacology. In the first set of experiments, pilocarpine was injected intraperitoneally at the same dose used in the neurochemical studies (300 mg/kg). In the second set of experiments, microinjections of pilocarpine were made directly into LC while simultaneously recording LC neurons. Intracoeular injections were made with a double barrel electrode assembly consisting of a calibrated glass micropipette (Fisher Scientific; 40-50 μm tip diameter), cemented to a recording micropipette (similar to that described above) to position the recording pipette tip 80 to 250 μm beyond the tip of the microinjection electrode. The microinjection pipette was filled with a 40 μM solution of pilocarpine in 0.9% sodium chloride (pH 7.0) and was connected to a Picospritzer II (General Valve Corporation) for pressure ejection. Visual inspection of the movement of a small bubble relative to a calibration grid on the injection pipette allowed injections as small as 15 nl. A 26 g needle was inserted into a lateral tail vein for intravenous (iv) injection of scopolamine hydrochloride (0.5 mg/ml in distilled water) or mecamlamine hydrochloride (1.0 mg/ml in distilled water). In some experiments, aqueous solutions of scopolamine hydrochloride (5 mg/ml) or methylscopolamine bromide (2 mg/ml) were injected intraperitoneally.

C-fos Immunohistochemistry. Animals were deeply anesthetized and perfused transcardially with 100-200 ml of 0.9% saline (4°C) for 1 min, followed by 1 liter of 4% paraformaldehyde in 0.1 M phosphate buffer (PB) (pH 7.4, 4°C). Brains were postfixed in this same solution (4°C) for 1.5 hr, and then placed in 20% sucrose in 0.1 M PB overnight. Serial, 40 μm -thick frozen sections were cut in the coronal plane and alternately placed into two trays containing 0.1 M PB for immunocytochemical visualization of *FOS* or for histochemical visualization of AChE (see below). For *FOS* immunohistochemistry, free-floating sections were (1) rinsed (30 min) in 0.1 M phosphate buffered saline (PBS); (2) placed in 2% normal serum (normal goat -NGS- for rabbit primary or normal rabbit -NRS- for sheep primary) in PBS containing 0.2 - 2.0% Triton X-100 overnight; (3) incubated in primary antibody (Dr. M. Greenberg, Harvard Univ., rabbit; Cambridge Biochemicals, sheep) at a 1:5,000 or 1:10,000 dilution in 0.2% Triton X-100 and 2% NGS/NRS for 24 hr (4°C) with constant agitation; (4) rinsed in PBS (30 min) and then incubated in biotinylated IgG directed against the

species producing the primary antibody, in PBS (1 hr, room temp); (5) rinsed in PBS (30 min, room temp) and incubated for 1 hr in avidin-biotin-peroxidase complex in 0.1 M PBS and then rinsed in PBS (20 min, room temp); and (6) incubated in 0.05% diaminobenzidine (DAB) with 0.1% hydrogen peroxide in PB for 10 min, then rinsed in PB.

RESULTS

Neurochemical Findings

Characteristics of Pilocarpine-Induced Convulsions. All rats injected with pilocarpine (300 mg/kg, ip) exhibited both physical and behavioral signs of intoxication. Both convulsive and nonconvulsive rats exhibited "red lacrimation" and defecation beginning about 5 min after drug administration. Convulsions were observed in 60% of the rats. Behavioral signs of convulsive rats included tonic shaking movements of the head and body. Rats developed convulsions at times ranging from 10 to 40 min after pilocarpine injection; the mean latency for onset of convulsions was 18.8 ± 0.9 min. Convulsions gradually increased and intense, sustained convulsive activity was typically expressed for 1-4 hr; convulsive activity gradually declined in intensity thereafter. By 8 hr, half of the rats in the convulsive group (5/10) had completely recovered, while convulsive activity in the remaining five rats had nearly subsided. By 96 hr, surviving convulsive rats had lost on the average 32% of body weight. Despite the weight loss, the rats had fully regained normal activity by this time. Nonconvulsive rats maintained their pre-drug body weight. The spectrum of behavioral manifestations of convulsions produced by pilocarpine, and the onset, severity and duration of these convulsions were similar to those produced by the anticholinesterase soman (Chapter 5, this report). In contrast to convulsive animals, nonconvulsive animals exhibited a decrease in motor activity and reduced responsiveness to external stimuli during the first few hours of intoxication. The mortality rate for all pilocarpine-treated rats was only 3%. All the rats that died prior to sacrifice had exhibited intense, tonic convulsions.

Time-Course of Changes in NE. NE levels in the rat forebrain and olfactory bulbs of convulsive rats declined rapidly and dramatically following pilocarpine intoxication (Figure 19, Tables 4 and 5). By one hr following pilocarpine administration, forebrain or olfactory bulb NE levels in convulsive rats decreased to 49.5 and 47.6% ($p = 0.0001$) of control level, respectively. The decrease in NE levels was maximal at 2 hr in the forebrain (37% of control, $p = 0.0001$) and in the olfactory bulb (24.8% of control, $p = 0.0001$). The reduction in forebrain and olfactory bulb NE levels was sustained between 2-4 hr of pilocarpine intoxication. By 8 hr, NE levels in both cortical structures recovered to 49% of control levels ($p = 0.0001$) and continued to increase slowly over the next 4 days. By 96 hr after

intoxication, NE levels in forebrain or olfactory bulb of convulsive rats were not significantly different from control levels.

In marked contrast, forebrain NE levels decreased to only about 78.0% of control levels in nonconvulsive rats at 1 hr following intoxication. This decrease, although significant ($p = 0.004$), was not as profound as the 49.5% reduction in convulsive rats ($p = 0.0001$). A similar decrease to 80.0% of control level ($p = 0.035$) in olfactory bulbs NE of nonconvulsive rats was found at the same time interval. This decrease was also significantly less than that in convulsive rats (47.6%, $p = 0.0001$). At 2 hr, forebrain NE levels in nonconvulsive rats were 83.0 % of control levels ($p = 0.002$); olfactory bulb NE levels in nonconvulsive rats was not significantly different from control levels. NE levels in forebrain or olfactory bulbs of nonconvulsive rats at 4, 8, 24 or 96 hr were not significantly different from control levels.

Time-Course of Changes in DA. Mean values of DA and metabolites DOPAC and HVA in the forebrain and olfactory bulb of pilocarpine-intoxicated rats as compared to those of control rats are given in Tables 1 and 2. The time-courses of changes of these monoamines and their metabolites are plotted in Figure 20. The mean levels of DA in convulsive and nonconvulsive rats were not significantly different from those of control. However, the levels of the metabolites DOPAC and HVA were significantly increased. In the forebrains of convulsive and nonconvulsive rats, there was a progressive, comparable increase in DOPAC and HVA, reaching levels 200-250% of control ($p = 0.0001$) by 4 hr, of intoxication. Forebrain DOPAC and HVA levels in nonconvulsive rats returned to control levels by 4 hr while those in convulsive rats remained high for 8 hr after pilocarpine intoxication. These findings demonstrate that there is a gradual, similar increase in DA release in forebrain that is of similar magnitude in both convulsive and nonconvulsive rats in the first 4 hr following intoxication.

Olfactory bulb DA, DOPAC and HVA levels increased in convulsive rats at 1 hr following pilocarpine administration; DOPAC levels at 1 hr were increased to 229% of control ($p = 0.0001$) and HVA levels were increased to 190% of control ($p = 0.0001$). Olfactory bulb DA and metabolite levels in convulsive rats, unlike those in the forebrain, returned to near control level by 8 hr of intoxication. In nonconvulsive rats, there were delayed (2 hr), smaller increases in DOPAC (127% of control, $p = 0.004$) and HVA (158% of control, $p = 0.0001$). At 4 hr, DOPAC reached maximum levels (136% of control, $p = 0.008$) while HVA returned to control levels. By 8 hr, DOPAC levels in nonconvulsive rats returned to control levels.

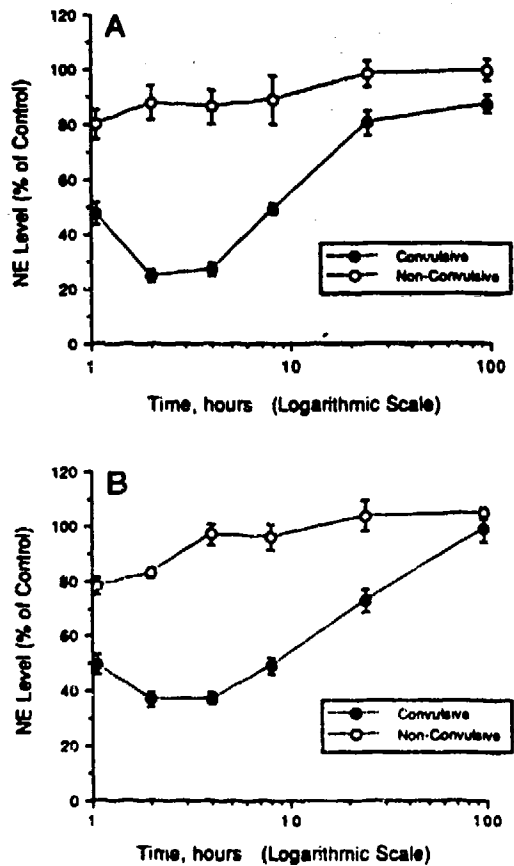


FIG. 19. Effect of pilocarpine on NE levels in olfactory bulb and forebrain of convulsive and nonconvulsive animals. NE levels in convulsive and nonconvulsive rats following a single dose of 300 mg/kg pilocarpine in (A) olfactory bulb and (B) forebrain.

TABLE 4

Time Course of Changes in Forebrain Level of NE, DA, 5-HT, and Metabolites Following a Single Dose of Pilocarpine (300 mg/kg, ip)

Amine	Group	1 h	2 h	4 h	8 h	24 h	96 h
NE	C	386.1 ± 16.8	386.6 ± 15.0	365.9 ± 12.3	433.0 ± 14.2	391.4 ± 9.2	386.2 ± 18.9
	CV	191.2 ± 13.8*	143.0 ± 11.2*	137.0 ± 7.5*	212.5 ± 12.3*	284.5 ± 17.6*	382.5 ± 19.3
	NCV	301.3 ± 11.5**	320.6 ± 7.4	354.3 ± 13.7	415.0 ± 19.9	405.5 ± 22.5	403.3 ± 7.6
DA	C	966.6 ± 25.2	1101.1 ± 35.5	925.1 ± 25.6	982.6 ± 3.2	979.3 ± 13.3	982.8 ± 36.5
	CV	956.4 ± 28.0	1047.5 ± 61.0	840.0 ± 23.9**	1072.3 ± 42.6	1145.7 ± 48.4**	1104.1 ± 44.5
	NCV	966.6 ± 43.7	1201.8 ± 67.2	1044.4 ± 34.2**	969.4 ± 57.2	985.5 ± 49.7	1010.6 ± 48.7
DOPAC	C	85.9 ± 6.2	90.8 ± 4.7	76.5 ± 3.8	63.6 ± 3.2	90.0 ± 5.3	54.2 ± 2.8
	CV	143.2 ± 7.5*	158.7 ± 7.2*	140.1 ± 7.9*	141.9 ± 11.2*	113.1 ± 5.9**	65.5 ± 3.7**
	NCV	144.7 ± 9.0*	163.7 ± 13.7*	134.3 ± 8.3*	59.4 ± 6.2	78.6 ± 9.6	58.2 ± 6.0
HVA	C	101.4 ± 4.5	84.4 ± 4.0	81.7 ± 4.1	81.8 ± 3.9	85.9 ± 6.3	94.6 ± 1.5
	CV	141.3 ± 6.6*	202.0 ± 15.9*	177.9 ± 11.9*	216.6 ± 15.3*	116.9 ± 8.5**	91.1 ± 6.7
	NCV	169.5 ± 13.6*	198.1 ± 19.7*	173.7 ± 6.3*	86.3 ± 6.2	80.7 ± 6.5	83.2 ± 7.3
5-HT	C	344.0 ± 13.3	311.6 ± 14.7	308.8 ± 6.3	252.0 ± 6.8	274.2 ± 6.0	294.0 ± 12.6
	CV	367.9 ± 16.2	332.3 ± 14.0	309.5 ± 10.5	281.2 ± 14.9	391.0 ± 24.6**	383.0 ± 21.0**
	NCV	358.8 ± 10.0	359.3 ± 16.9	343.7 ± 14.1**	309.4 ± 29.2**	335.5 ± 30.0	317.9 ± 13.8
5-HIAA	C	109.0 ± 5.5	123.8 ± 7.7	127.6 ± 6.0	108.5 ± 4.1	136.1 ± 8.3	124.1 ± 5.1
	CV	159.7 ± 8.3*	364.2 ± 25.5*	386.5 ± 41.4*	377.7 ± 17.2**	453.4 ± 11.0*	238.0 ± 8.0*
	NCV	134.9 ± 9.0**	191.3 ± 13.5**	232.5 ± 17.1*	158.0 ± 15.5**	139.0 ± 10.4	157.6 ± 27.9
	C	n = 8	n = 8	n = 8	n = 6	n = 6	n = 6
	CV	n = 8	n = 8	n = 9	n = 10	n = 8	n = 6
	NCV	n = 5	n = 7	n = 5	n = 4	n = 5	n = 9

Note. Data are expressed in means (ng/g tissue) ± SE. Abbreviations: C, control; CV, convulsive; NCV, nonconvulsive rats, and n, number of rats sacrificed in each group at the indicated time interval. Statistics: * $P < 0.0005$; ** $P < 0.05$, significant difference from the control mean as determined using an unpaired, two-tailed Student t test.

TABLE 5

Time Course of Changes in Olfactory Bulb Level of NE, DA, 5-HT, and Metabolites Following a Single Dose of Pilocarpine (300 mg/kg, ip)

Amine	Group	1 h	2 h	4 h	8 h	24 h	96 h
NE	C	229.3 ± 13.1	244.4 ± 9.1	215.5 ± 7.0	258.6 ± 19.3	238.7 ± 8.6	220.7 ± 6.7
	CV	109.2 ± 9.6*	60.6 ± 5.4*	58.7 ± 5.0*	126.6 ± 5.3*	191.8 ± 10.8**	192.5 ± 6.9**
	NCV	183.4 ± 11.8**	214.5 ± 15.4	188.0 ± 13.1	229.4 ± 23.0	234.2 ± 11.3	219.6 ± 8.7
DA	C	64.6 ± 6.4	78.0 ± 3.5	56.5 ± 4.1	93.3 ± 7.5	54.9 ± 4.3	78.9 ± 8.2
	CV	91.4 ± 4.9**	92.3 ± 3.7**	68.4 ± 3.4**	93.5 ± 7.8	51.5 ± 3.6	95.8 ± 6.9
	NCV	72.9 ± 4.8	83.9 ± 6.4	58.0 ± 4.0	79.5 ± 8.6	54.9 ± 6.9	95.0 ± 5.2
DOPAC	C	27.0 ± 2.5	31.8 ± 1.9	27.7 ± 1.9	36.4 ± 1.5	21.7 ± 1.5	25.8 ± 2.3
	CV	61.8 ± 4.2*	54.8 ± 3.1*	44.8 ± 3.3**	32.9 ± 2.2	16.7 ± 0.9**	29.1 ± 2.2
	NCV	33.3 ± 1.0	40.4 ± 1.5**	37.8 ± 2.5**	29.8 ± 1.6	20.5 ± 3.6	24.3 ± 1.3
HVA	C	80.2 ± 4.5	72.3 ± 2.6	81.7 ± 4.9	97.0 ± 4.1	76.6 ± 2.0	77.4 ± 4.8
	CV	152.0 ± 11.7*	168.7 ± 5.8*	129.6 ± 7.9*	115.6 ± 7.9	74.7 ± 5.6	75.4 ± 5.0
	NCV	97.3 ± 7.2	114.4 ± 6.2*	82.7 ± 5.2	74.0 ± 5.4	70.2 ± 5.7	68.5 ± 4.1
5-HT	C	164.8 ± 6.7	163.9 ± 4.1	127.4 ± 8.4	172.4 ± 7.9	162.9 ± 8.2	177.2 ± 9.1
	CV	187.9 ± 6.4**	162.7 ± 15.0	134.1 ± 5.6	174.6 ± 6.4	152.7 ± 8.2	209.9 ± 7.5**
	NCV	177.5 ± 11.1**	173.9 ± 7.5	152.7 ± 11.4	180.3 ± 25.2	158.0 ± 4.5	200.3 ± 11.1
5-HIAA	C	112.0 ± 5.3	93.1 ± 4.7	74.3 ± 4.1	99.4 ± 6.3	99.3 ± 6.6	86.6 ± 6.9
	CV	108.3 ± 6.2	132.1 ± 14.3**	143.8 ± 12.0*	175.7 ± 12.9**	110.5 ± 9.1	119.6 ± 5.5**
	NCV	88.6 ± 6.3**	110.7 ± 10.6	98.3 ± 6.5**	102.1 ± 5.3	106.0 ± 7.7	102.6 ± 10.9
	C	n = 8	n = 8	n = 8	n = 6	n = 6	n = 6
	CV	n = 8	n = 8	n = 9	n = 10	n = 8	n = 6
	NCV	n = 5	n = 7	n = 5	n = 4	n = 5	n = 9

Note. Data are expressed as means (ng/g tissue) ± SE. Abbreviations: C, control; CV, convulsive; NCV, nonconvulsive rats, and n, number of rats sacrificed in each group at the indicated time interval. Statistics: * $P < 0.0005$; ** $P < 0.05$, significant difference from the control mean as determined using an unpaired, two-tailed Student t test.

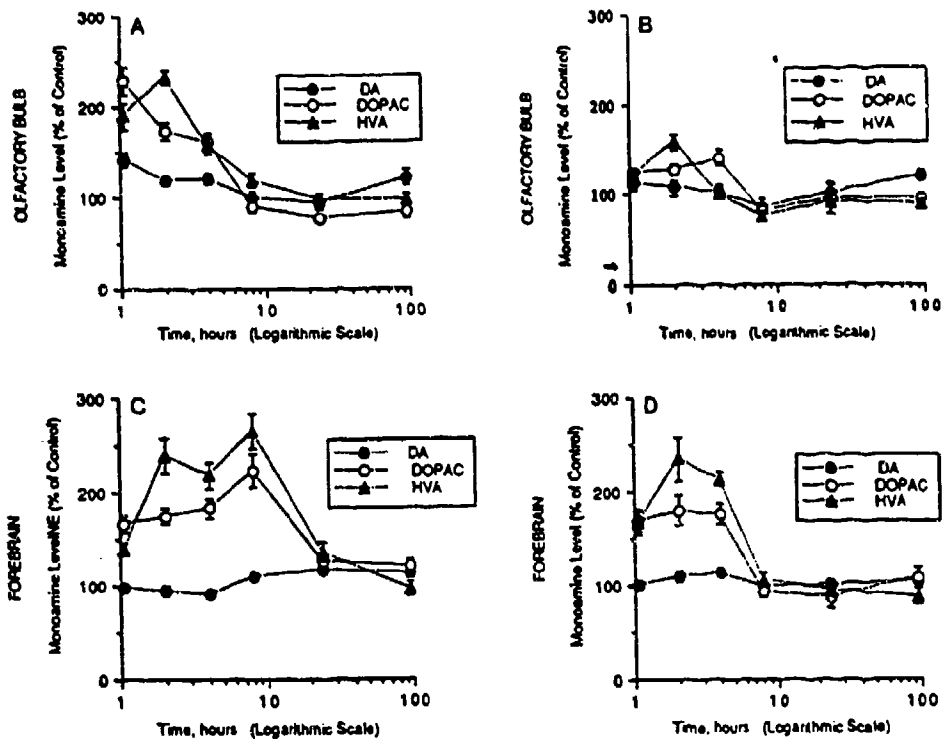


FIG. 20. Effect of pilocarpine on DA and metabolite (DOPAC and HVA) levels. Time-course changes in the levels of DA, DOPAC, and HVA following a single dose of 300 mg/kg pilocarpine in (A) olfactory bulbs of convulsive rats, (B) olfactory bulbs of nonconvulsive rats, (C) forebrains of convulsive rats, and (D) forebrains of nonconvulsive rats.

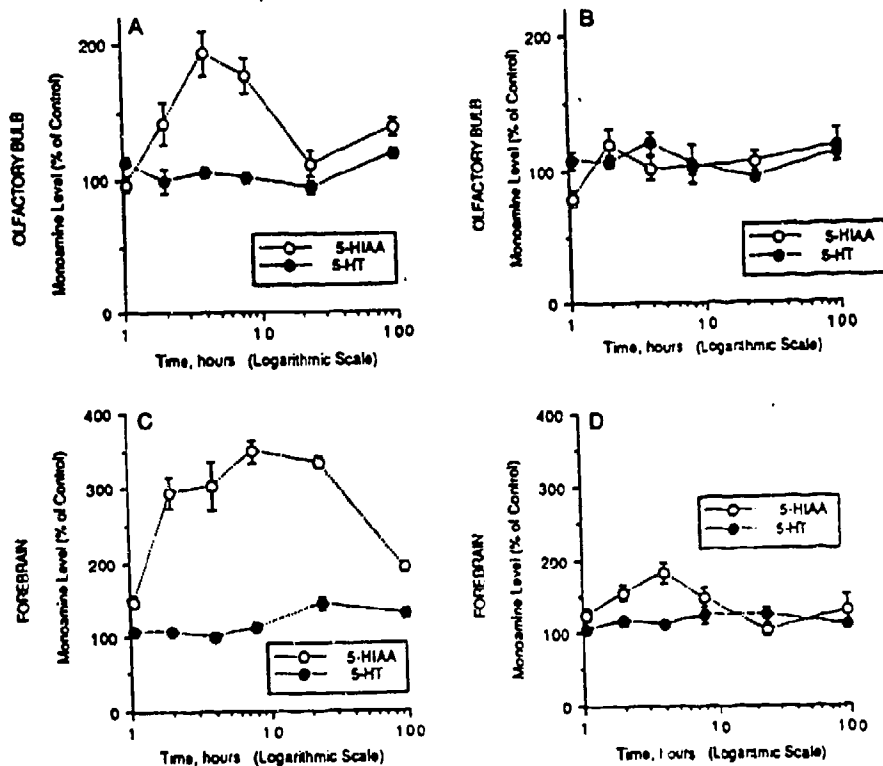


FIG. 21. Effect of pilocarpine on 5-HT and metabolite (5-HIAA) levels. Time-course changes in the levels of 5-HT and major metabolite 5-HIAA following a single dose of 300 mg/kg pilocarpine in (A) olfactory bulbs of convulsive rats, (B) olfactory bulbs of nonconvulsive rats, (C) forebrains of convulsive rats, and (D) forebrains of nonconvulsive rats.

Time-course of Changes of 5-HT. Mean values of 5-HT and the metabolite 5-HIAA in the forebrain and olfactory bulb of pilocarpine-intoxicated rats as compared to those of control rats are listed in Tables 1 and 2; the time-courses of these changes in convulsive versus nonconvulsive rats are plotted in Fig. 21. Pilocarpine did not significantly change forebrain 5-HT levels in the first 8 hr. There was however, a delayed increase in the 5-HT metabolite, 5-HIAA, in the forebrain of convulsive rats; 5-HIAA reached a maximum level of 300-350% of control ($p = 0.0001$) between 2 and 24 hr of intoxication, and declined afterward to 192% by 96 hr. In the olfactory bulb, there was a delayed increase in 5-HIAA levels in convulsive rats, although the increase was much smaller than that in the forebrain. In convulsive rats, the increase in olfactory bulb 5-HIAA levels was maximal at 4 hr (193% of control, $p = 0.0001$) and declined slowly afterward to reach near control levels by 24 hr of intoxication.

NEUROPHYSIOLOGICAL FINDINGS

Systemic Pilocarpine Administration

LC NEURONAL ACTIVITY. The preceding studies demonstrated that systemic injection of pilocarpine in unanesthetized rats produces rapid, profound reduction of forebrain NE in convulsing rats. As we hypothesize that this NE depletion may be due to an excitatory effect of pilocarpine on LC neurons, we next examined the effects of systemically administered pilocarpine on the discharge of LC neurons.

In anesthetized rats, systemic injection of pilocarpine () rapidly (3-7 min) produced excessive salivation and labored breathing; these effects, along with peripheral vasoconstriction and bronchial secretion produced by the muscarinic stimulation of autonomic neurons and the depressant action of anesthetics, led to rapid death of the animal. To circumvent the peripheral autonomic effects of pilocarpine, rats were pretreated 60-90 min prior to pilocarpine injection with the peripherally-acting scopolamine analog methylscopolamine bromide (2 mg/kg, ip). Peripheral muscarinic receptor blockade substantially reduced the side effects of pilocarpine, and under these conditions, LC neurons were recorded for as long as 6 hr after a systemic injection of pilocarpine. We recently demonstrated there was no difference between the mean spontaneous discharge rates of LC neurons of methylscopolamine-pretreated versus control animals (after 6, this report).

The spontaneous discharge rates of LC neurons before pilocarpine injection ranged from 1.4 to 2.4 spikes/sec, with a mean spontaneous rate of 1.9 ± 0.1 spikes/sec ($n = 12$). As shown in Figure 22, systemic pilocarpine injection (300 mg/kg, ip, $n=8$ animals) caused a pronounced increase in the spontaneous discharge rates of LC neurons beginning 3-5 min after injection. This sustained increase in LC neuronal discharge was maintained for the first 2 hr after injection. The spontaneous rates of LC neurons during this period ranged from 4.8-11.1 spikes/sec, the mean discharge rate of neurons

recorded in the first two hr following systemic pilocarpine administration was 8.6 ± 0.4 spikes/sec ($n = 13$). This was substantially greater ($p < 0.001$) than the mean discharge rate of LC neurons in the same animals before pilocarpine.

The excitatory action of pilocarpine was extremely long lasting. As summarized in Figure 23, the mean discharge rate of LC neurons was significantly elevated at 2-3 hr (8.2 ± 1.2 spikes/sec, $n = 3$; $p < 0.001$), 3-4 hr (6.4 ± 0.4 spikes/sec, $n = 3$; $p < 0.001$) and 4-5 hr (4.3 ± 0.1 spikes/sec, $n = 4$; $p < 0.001$) after pilocarpine injection. By 5-6 hr after pilocarpine administration, the mean discharge rate of LC neurons (2.4 ± 0.1 spikes/sec, $n = 4$) had returned to near that of the mean control rate. Thus, systemic pilocarpine caused a robust activation of LC neurons that was sustained at peak levels for 3 hr; LC discharge rates then progressively declined but remained significantly elevated until 5-6 hr. Analysis of EEG records showed that although pilocarpine administration produced a desynchronization of cortical EEG, there was no evidence of seizure activity at any time following the administration of pilocarpine (not shown).

In all four animals tested, administration of the centrally active muscarinic receptor antagonist scopolamine hydrochloride (5 mg/kg, ip, $n = 1$; 0.5 mg/kg, iv, $n = 3$), rapidly (30-120 sec) and completely reversed the pilocarpine-induced excitation of LC neurons to pre-pilocarpine control values (Fig. 22A). There was no significant difference ($p > 0.05$) between the mean LC discharge rate prior to pilocarpine administration (1.9 ± 0.1) and that following combined pilocarpine and scopolamine administration (2.4 ± 0.2 , $n = 5$).

FOS STAINING. Systemic injection of pilocarpine (300 mg/kg, ip) in unanesthetized animals induced rapid and selective expression of *FOS* in two areas: IC and PC. Systemic pilocarpine administration caused *FOS* expression in LC neurons beginning 30-45 min after injection; by contrast, there were only occasional, scattered *FOS*-positive LC neurons in saline injection control cases. As shown in figure 24, by 2.7 hr after injection, the majority of LC neurons show robust expression of *FOS*. This expression was restricted to LC neurons as *FOS* was not expressed in neurons in nuclei surrounding LC, including the medial parabrachial nucleus, mesencephalic trigeminal nucleus, and lateral dorsal tegmental nucleus. With longer postinjection survival times, the number and intensity of *FOS*-stained LC neurons progressively increased, and *FOS* expression was present in other brain regions.

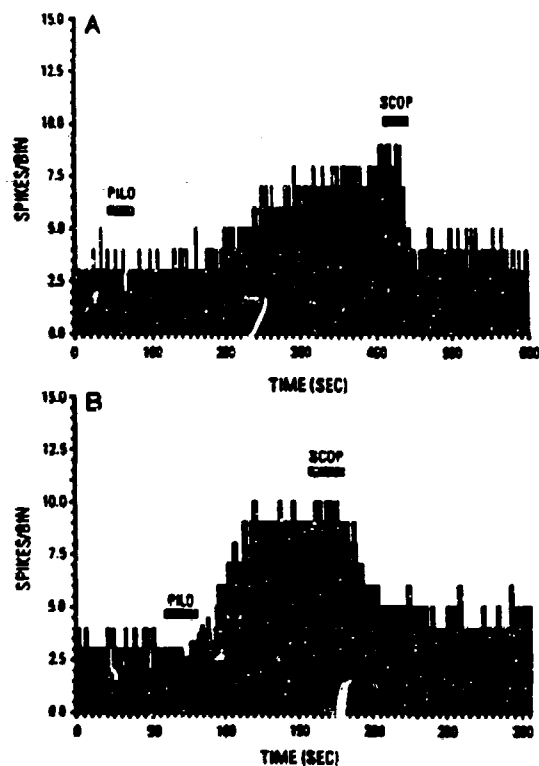


FIG. 22. Robust activation of LC neurons by systemic or intracoeular microinjection of pilocarpine. (A) Computer ratemeter record showing the spontaneous discharge of an LC neuron. Systemic administration of 300 mg/kg pilocarpine (ip), shown at lower bar, activates this LC neuron 3 min after injection. Intravenous injection of scopolamine (0.5 mg/kg, iv) rapidly reversed the pilocarpine-induced activation of this LC neuron. (B) Ratemeter record showing spontaneous activity of a single LC neuron before and after microinjection of pilocarpine into LC. Intracoeular microinjection of 1.2 nmol of pilocarpine (in 30 nl, shown at lower bar) rapidly increased the spontaneous discharge of this neuron. Intravenous administration of scopolamine (0.5 mg/kg) rapidly and completely reversed the pilocarpine-induced tonic excitation of this neuron

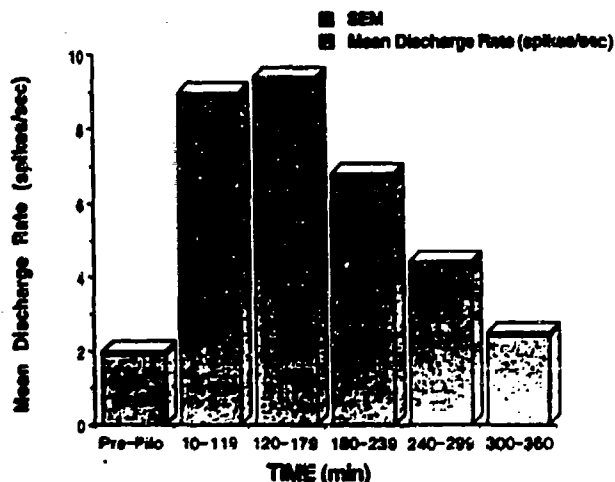


FIG. 23. Systemic administration of pilocarpine causes a long-lasting activation of LC neurons. Bar graph summarizing the mean spontaneous discharge rate of LC neurons before (Pre-Pilo), and at various time intervals after systemic injection of pilocarpine (300 mg/kg, ip). The mean discharge rate of LC neurons was significantly elevated at 10 min-2 h (8.6 ± 0.4 spikes/s, $n = 13$, $P < 0.001$), 2-3 h (8.2 ± 1.2 spikes/s, $n = 3$, $P < 0.001$), 3-4 h (6.4 ± 0.4 spikes/s, $n = 3$, $P < 0.001$), and 4-5 h (4.3 ± 0.1 spikes/s, $n = 4$, $P < 0.001$) after pilocarpine injection. By 5-6 h after pilocarpine administration, the mean discharge rate of LC neurons (2.4 ± 0.1 spikes/s, $n = 4$) had returned to near the mean control rate, although still slightly elevated at this time ($P < 0.03$).

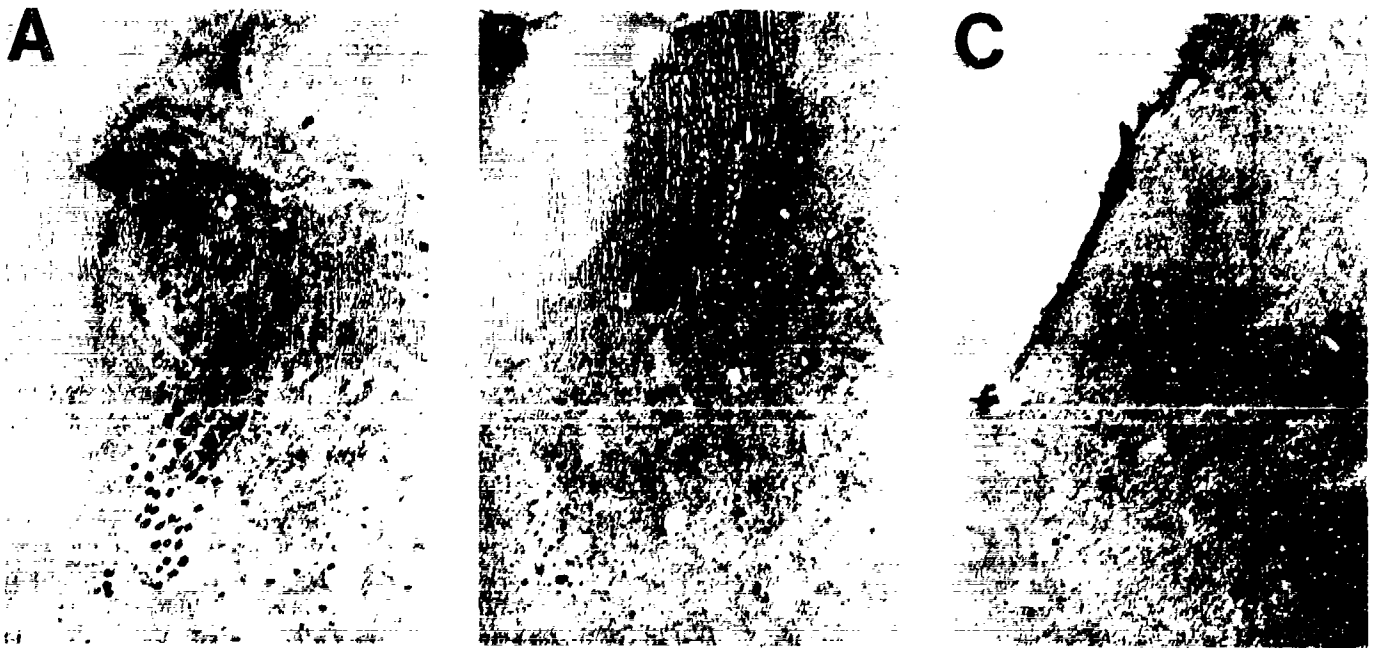


FIG. 24. Activation of LC neurons by systemic or intracereular microinjection of pilocarpine induces expression of *c-fos* in LC neurons. Photomicrographs of coronal sections through LC showing *c-fos* immunostaining after systemic injection of pilocarpine (A), and intracereular microinjection of pilocarpine (B) or vehicle (C). In the first study, animals received a single systemic dose of pilocarpine (300 mg/kg, ip) and were sacrificed and processed for immunohistochemical detection of *c-fos* at various time intervals. Sections from all animals were processed simultaneously in the same reaction solutions to control for variation in processing. In control animals (not shown) there is no detectable *c-fos* staining in LC neurons. From 30 (not shown) to 150 min (A), there is a progressive increase in the number of LC neurons expressing *c-fos* and in the intensity of *c-fos* staining. In a second study, pilocarpine was microinjected into LC and single LC neurons were recorded for 2 h. Injections (60-nl) of pilocarpine were made at 15 min intervals to maintain elevated LC discharge during the 2-h period. Animals were then sacrificed and sections stained for *c-fos*. As shown in B, there is robust, selective expression of *c-fos* in LC neurons after pilocarpine microinjection. By contrast, microinjection of identical volumes of saline over a 2-h period did not induce *c-fos* expression in LC neurons (C).

Intracoerulear Pilocarpine Administration

The finding that systemically administered pilocarpine increased LC spontaneous discharge rates and induced *FOS* expression is consistent with the hypothesis that this agent produces NE depletion as a result of tonic muscarinic receptor activation of LC neurons. However, it is also possible that systemically injected pilocarpine increased LC activity by nonspecific peripheral sensory/motor actions, or by tonic activation of excitatory afferent inputs to LC neurons. In order to circumvent these possible indirect actions of pilocarpine, we recorded the spontaneous activity LC neurons before, during and after focal microinjection of pilocarpine directly into LC.

LC NEURONAL ACTIVITY. The mean spontaneous discharge rate of LC neurons recorded with a double-barrel recording/microinfusion assembly containing pilocarpine (2.5 ± 0.2 spikes/sec, $n = 11$) was slightly but significantly ($p < 0.02$) greater than the mean spontaneous rate of LC neurons recorded with single-barrel pipettes (1.9 ± 0.1). This slightly higher spontaneous discharge rate was probably due to low level diffusion of pilocarpine from the injection pipette.

As shown for a typical neuron in Figure 22, microinjection of pilocarpine into LC caused a rapid and pronounced elevation of the spontaneous rate of LC neurons. The discharge rates of LC neurons after microinjection of 1.2 nmol of pilocarpine (in 30 nl) ranged from 5.7 to 10.8 spikes/sec with a mean rate of 7.9 ± 0.9 spikes/sec ($n = 6$). The elevation of LC discharge was typically observed within 5 to 20 sec after microinjection, and was not associated with any discernible change of either the amplitude or the waveform of LC action potentials. Larger doses of pilocarpine elicited even more pronounced increases in LC neuron spontaneous firing rates. The mean spontaneous discharge rate of LC neurons after microinjection of 2.4 nmol (in 60 nl) of pilocarpine was 9.7 ± 0.8 spikes/sec ($n = 5$). The spontaneous discharge rates of 2 two cells examined after microinjection of 9.8 nmol (in 240 nl) pilocarpine were 11.5 and 14.4 spikes/sec. In contrast to the tonic excitation of LC neurons produced by systemically injected pilocarpine, a single intracoerulear microinjection of pilocarpine activated LC neurons for only 10-15 min. In no case was there seizure activity in the EEG records at any time following intracoerulear pilocarpine administration in the anesthetized preparation. Injection of vehicle at volumes equal to those used for pilocarpine elicited only a small, insignificant elevation of LC discharge rate (mean discharge rate before and after vehicle injection, 2.1 ± 0.2 and 2.6 ± 0.2 spikes/sec, $n = 10$). Changes in LC discharge rate produced by vehicle injection never lasted longer than 60-180 sec.

LC neurons in anesthetized rats exhibit a characteristic biphasic response to noxious somatosensory stimuli, such as paw- or tail-pinch or electrical stimulation of the sciatic nerve (³⁶). This biphasic response consists of a brief burst of 2-3 spikes followed by a post-burst inhibition of impulse

activity lasting 500 to 1000 msec (12,20). Previous studies have demonstrated that the cholinergic agonist carbachol increases LC discharge, but reduces excitatory responses of these cells to sciatic nerve stimulation (¹⁴). Thus, it was of interest to determine if responses to such excitatory stimuli were altered during the elevated level of LC discharge produced by pilocarpine. In agreement with previous findings (¹⁴), we found that LC excitatory responses to sciatic nerve stimulation (n = 3) were substantially reduced during the period of increased spontaneous activity produced by intracoerulear microinjection of pilocarpine (1.2 - 2.4 nmol in 30 to 60 nl).

As illustrated in Figure 22, intravenous injection of the centrally active muscarinic receptor antagonist scopolamine hydrochloride, at a dose (0.5 mg/kg, iv) previously shown to block excitation of LC neurons to directly applied ACh (⁵³), rapidly and potently reversed the pilocarpine-induced elevation of LC discharge. The mean spontaneous discharge rate of LC neurons (n = 5) sampled after microinjection of pilocarpine (1.2-3.6 pmoles in 30-90 nl) followed by scopolamine (2.2 ± 0.5) did not differ ($p > 0.5$) from the mean baseline discharge rate of LC neurons. In marked contrast, intravenous injection of the nicotinic receptor antagonist mecamylamine (1.0 mg/kg) had no measurable effect on the elevated LC discharge rate caused by pilocarpine in two cells tested.

FOS STAINING. Intracoerulear injections of pilocarpine at doses that potently activated LC neurons (1.2 to 2.4 nmol in 60-90 nl) caused the rapid induction of *FOS* expression in LC neurons. As shown in Figure 24, LC neurons exhibited robust *FOS* expression within 2 hr after pilocarpine microinjection into LC. There was little or no *FOS* expression in neurons in nuclei adjacent to LC (i.e., medial parabrachial nucleus, mesencephalic trigeminal nucleus, and lateral dorsal tegmental nucleus). By contrast, when saline rather than soman was injected into LC, only occasional cells near the tip of the pipette were positive for *FOS* (Fig. 24).

DISCUSSION

The major results of this study are: (1) Pilocarpine induces convulsions whose onset, severity and duration are remarkably similar to those caused by soman (Chapter 5, this report). (2) Pilocarpine causes a rapid and dramatic reduction of forebrain NE only in convulsing animals. The time course and magnitude of NE reductions in convulsing animals are remarkably similar to those found for soman (Chapter 5, this report). (3) Both systemic and restricted intracoerulear injection of pilocarpine increased the spontaneous discharge rate of LC neurons in anesthetized rats and caused the expression of *FOS* in LC neurons. The magnitude of pilocarpine-induced increases in LC firing were essentially identical to those caused by soman (Chapter 6, this report). Taken together, these results strongly

support the hypothesis that sustained muscarinic activation of LC neurons causes a rapid and profound release of NE from LC terminals. Based on these findings, it is reasonable to hypothesize that sustained activation of both noradrenergic and muscarinic receptors on forebrain neurons may play a key role in the generation of cholinolytic seizures.

Pilocarpine-Induced Release of NE, DA and 5-HT

Norepinephrine. Despite the presence of frank signs of pilocarpine intoxication, NE levels in nonconvulsive rats remained near control levels at all intervals tested, except for modest decreases at 1 and 2 hr. By contrast, the decrease in forebrain NE levels in convulsive rats was profound, falling to 50% of control at 1 hr after pilocarpine treatment and to 37% at 2 and 4 hr. The time-course and magnitude of these decreases in forebrain NE level are essentially identical (32% at 2 and 4 hr) to those induced by a peri-convulsive dose of the irreversible AChE inhibitor, soman (Chapter 5, this report). NE levels in convulsive rats began to recover slowly at around 8 hr, the beginning of this recovery coincided roughly with the termination of convulsions. By 96 hr, NE levels were not significantly different from controls, indicating a complete recovery. The slow recovery of NE levels in convulsive rats is almost identical to that found in convulsive rats following soman intoxication. This observation initially was somewhat surprising as soman is an irreversible inhibitor of AChE and full recovery of this enzyme takes several days. Pilocarpine, on the other hand, is a muscarinic agonist which competes with endogenous ACh for receptor occupancy and is probably competed and/or diffused away relatively quickly. This later inference is supported by our neurophysiological finding that LC activity remains elevated only 10-15 min following direct intracoerulear injection of pilocarpine. The long-lasting neurochemical changes caused by systemic pilocarpine thus were difficult to attribute to primary action on LC neurons given the relatively short duration of the drug's effect on LC neurons following intracoerulear injection. However, additional subsequent experiments showed that *systemically* administered pilocarpine produced a long-lasting (4 hr) activation of LC neuronal discharge. Possible reasons for this prolonged action of pilocarpine on LC neurons following systemic administration versus its relatively brief duration of action following intracoerulear injection are discussed below. In any event, however, the present findings demonstrate that there is an excellent temporal correlation between the prolonged, progressive decrease of forebrain NE and the prolonged activation of LC neuronal activity in the first 4 hr following systemic administration of pilocarpine.

In those animals in which systemic pilocarpine caused convulsions and NE reductions, NE levels did not recover until 96 hr. Systemic pilocarpine caused increased LC firing rates for only 4 hr, however. Taken together, these two findings suggest that 3-4 hr of sustained 5-7-fold increases in LC firing may lead to a depletion of releasable NE from LC terminals. This further suggests that the factor limiting NE recovery may be the time required to synthesize and, possibly, transport new NE to LC

terminals. In this regard, it is interesting to note that systemically administered cholinergic agonists have been found to alter the activity of brain tyrosine hydroxylase (TH), the enzyme catalyzing the rate limiting step in the biosynthesis of catecholamines. Subcutaneous injection of the muscarinic receptor agonists oxytremorine or pilocarpine, or the AChE inhibitor physostigmine, produces a delayed, progressive activation of TH in LC neurons (^{106, 107}). TH activity begins to increase in LC after 24-48 hr and peaks at 72 hr after oxytremorine injection; TH activity was also significantly increased in LC 72 hr after injection of pilocarpine (¹⁰⁶). It is important to note that this TH activation occurred selectively in LC as there were no changes in TH activity in other brainstem catecholaminergic cell groups or in noradrenergic terminals in the cerebral cortex (¹⁰⁶). Convulsive activity was not assessed in these studies; thus, it is not known if there were any selective changes in TH activity in convulsive *vs* nonconvulsive animals. Taken together, these findings suggest that NE reserves in LC terminals may be relatively low. Tonic activation of LC for even relatively short periods may result in significant reductions of terminal NE that takes a long time to replenish. It would be of interest, in this regard, to continuously monitor NE release by *in vivo* dialysis following sustained activation of LC to determine if this suggestion is true. Such studies are in progress.

Finally, it is conceivable that pilocarpine influences forebrain NE levels by direct actions on NE terminals, although to date, there is no evidence for muscarinic receptor-mediated release of NE. Indeed, *in vitro* slice experiments indicate that while nicotinic agonists increase NE release, muscarinic agonists *decrease* terminal release of NE (²⁰⁴⁻²⁰⁶). Since the present findings demonstrate that pilocarpine *depletes* forebrain NE as a result of sustained NE release, the most parsimonious explanation is that pilocarpine's activation of LC neurons overrides any possible inhibitory action of this agent on NE terminal release.

Dopamine. In the forebrain of both convulsive and nonconvulsive rats, DA levels were unchanged at all times sampled. However, there was a progressive increase in the DA metabolites, DOPAC and HVA. This increase was essentially identical in both convulsive and nonconvulsive animals, reaching maximum levels of 200-250% of controls at 2 and 4 hr. However, in nonconvulsive rats, the levels of DOPAC and HVA returned to control levels at 8 hr, whereas they remained significantly elevated at 24 hr (200% of control) and at 96 hr (125% of control) in convulsive animals. Insofar as increased levels of metabolites with no change in DA levels may be taken as an indication of increased DA release, the finding that DA release was essentially identical in convulsive and nonconvulsive rats throughout the period of time when convulsions were initiated strongly suggests that DA release does not play a significant role in pilocarpine-induced convulsions.

It is interesting to compare these results with those of soman (Chapter 5, this report). As soman causes an accumulation of ACh, this should lead to activation of both nicotinic and muscarinic

receptors; pilocarpine, a muscarinic agonist, should only activate muscarinic receptors. With soman, DOPAC and HVA levels in the forebrains of convulsive animals were increased by 300-350% compared to 200-250% increases for pilocarpine in the present study. The larger increase in DOPAC and HVA caused by soman, therefore may indicate that forebrain DA release is augmented by both nicotinic and muscarinic activation.

In the olfactory bulb of convulsive rats, DA, DOPAC and HVA levels were significantly increased at 1-4 hr following pilocarpine administration. In nonconvulsive rats, there was much smaller increase in DOPAC and HVA only at the 2 hr time point. In contrast to the forebrain, levels of olfactory bulb DA and its metabolites returned to control levels in both convulsive and nonconvulsive rats by 8 hr after pilocarpine. A further difference with the forebrain was a significant increase in the levels of DA in nonconvulsive rats throughout the first 4 hr.

These differences in DA and its metabolites in olfactory bulb versus forebrain may be related to differences in the anatomical organization of the DA systems supplying these two structures. Forebrain DA innervation is supplied largely by DA projections from the substantia nigra and ventral tegmental area; DA in the olfactory bulb derives entirely from a large population of intrinsic DAergic interneurons in the glomerular layer of the bulb. The olfactory bulb receives a heavy cholinergic innervation from the basal forebrain while midbrain DA neurons projecting to the forebrain receive their cholinergic input from the brainstem.

Serotonin. There were no consistent changes in forebrain 5-HT in either convulsive or nonconvulsive rats in the first 8 hr after pilocarpine (Fig. 21). There was, however, a significant increase in 5-HIAA levels of both convulsive and nonconvulsive animals in the first 8 hr. At 1 hr, the period during which convulsions develop, the increase in 5-HIAA was comparable in both groups. At later time points, 5-HIAA was elevated in both groups but to a greater extent in convulsive animals. Indeed, this metabolite was still 333% of control at 24 hr and 192% at 96 hr. These increases in 5-HIAA levels are interpreted to reflect increases in 5-HT turnover. We found (Chapter 5, this report) that the anticholinesterase soman stimulates similar maximal increases in 5-HIAA levels (300-400%) which remain elevated at 96 hr (226%). In the olfactory bulb, there was an increase in 5-HIAA levels in convulsive rats, although the increase was smaller (200%) than that in the forebrain. 5-HIAA levels in the olfactory bulb of convulsive rats returned to approximately control levels by 24 hr.

Possible Roles of Forebrain Monoamines in Cholinolytic Seizures

The present findings clearly demonstrate that there is a similar increase in DOPAC and HVA in the forebrains of *both* convulsive and nonconvulsive rats during the first 4 hr after pilocarpine

administration. This is interpreted to reflect an increase in DA release, although these increases could also be due, in part, to increased NE release. However, this seems unlikely as these metabolites increased significantly in nonconvulsive animals whereas there were only very small changes in NE in nonconvulsive animals. The fact that DA metabolites changed equally in convulsive and nonconvulsive animals suggests that DA release does not play a determinant role in the generation of pilocarpine-induced seizures. Similarly, 5-HIAA increases were essentially the same in convulsive and nonconvulsive animals in the first hour. This suggests that 5-HT release likewise does not play a determinant role in the generation of pilocarpine-induced seizures, as convulsions were typically fully developed by 30 min. Only for NE was there a strong dichotomy between convulsive and nonconvulsive animals in the time frame when convulsions develop. This rapid, dramatic reduction in NE is taken to reflect a selective, sustained release of NE in convulsive animals. This is further supported by the electrophysiological findings of the present study showing that either systemic or intracoerulear administration of pilocarpine causes a dramatic, sustained increase in the firing rate of LC neurons.

Pilocarpine Potently Activates Locus Coeruleus Neurons

Systemically administered pilocarpine caused a sustained (4 hr), robust increase in LC neuron discharge rate in anesthetized rats. Microinjections of pilocarpine directly into LC caused a similar increase in the firing rate of LC neurons; however, this increased firing rate lasted for only 10-15 min. Systemic injection of scopolamine rapidly reversed both systemic and intracoerulear pilocarpine-induced activation of LC neurons. Thus, pilocarpine causes a sustained, muscarinic activation of LC neurons which is nearly identical to that caused by accumulated ACh resulting from the anticholinesterase actions of soman (21). In addition, systemic and intracoerulear microinjection of pilocarpine caused a rapid and selective induction of *FOS* in LC neurons. These results are consistent with both *in vivo* extracellular and *in vitro* intracellular recording studies showing that LC neurons are strongly excited by muscarinic agonists (2, 44, 45).

The reason for the relatively long duration of increased LC discharge after systemic administration of pilocarpine is unclear. There are several possibilities: (1) The long duration of action could be due simply to the large dose of pilocarpine used (300 mg/kg, ip), which may be available at central muscarinic synapses for a relatively longer period of time. (2) It may be due to prolonged exposure to the drug in circulation due to binding and subsequent release by peripheral tissue compartments. (3) In light of the convulsions produced by this same dose of pilocarpine in unanesthetized rats, it is possible that seizures could produce a sustained increase in LC activity. However, our neurophysiological experiments demonstrated that pilocarpine-induced activation of LC neurons occurred in the complete absence of cortical seizures. (4) Finally, it is also possible that systemically administered pilocarpine tonically activates an excitatory afferent input to LC. The present experiments

cannot rule out this later possibility.

Role of NE in Cholinolytic Seizures

Taken together with the essentially identical neurochemical and electrophysiological findings for soman in our previous studies (Chapters 5 and 6, this report), the present results suggest that sustained release of NE may play a determinant role in the generation of cholinolytic seizures.

There is relatively little information on the role of forebrain NE in the development and spread of pilocarpine-induced seizures. A recent study reported that pilocarpine-induced seizures were potentiated 14 days following the administration of the NE neurotoxin, DSP-4 (¹⁵³). This was taken as an evidence for an anticonvulsant activity of NE. However, in that study, there were no reported measures of forebrain NE levels following DSP-4 treatment; thus, the effectiveness of the so-called NE lesion was not evaluated. Moreover, as previously noted (Chapter 5, this report), the results of chronic NE lesions are extremely difficult to interpret because lesions of NE fiber systems provoke rapid and potent compensatory mechanisms, including receptor up-regulation and sprouting, which obscure the functional consequences of NE-lesions (^{19, 39, 196}). Indeed, a recent study (Zahnisher et al., 1986) demonstrated that when DSP-4 is used to destroy NE fibers, there is a dramatic and selective up-regulation of β -receptors and an increase in β -receptor-mediated electrophysiological responses in hippocampal slices. This same group of investigators had previously shown that β -receptor activation has proconvulsant effects (¹⁴⁰). Thus, destruction of some proportion of NE fibers leads to a compensatory up-regulation of the very adrenergic receptor demonstrated to have proconvulsive activity. In the single gene mutant mouse tottering (*tg/tg*), which is extremely susceptible to seizures, there is a 50% increase in the number of LC fibers and NE in the forebrain (¹⁰⁵), although in another rodent model GEPR (genetically epilepsy-prone rats), there is evidence that NE is anticonvulsive (^{92, 93, 100}). At the cellular level, recent *in vitro* studies have identified a potent, β -receptor-mediated postsynaptic action of NE which may lower the threshold for seizures (^{114, 140, 144}). Taken together, these findings indicate that there is evidence for both pro- and anticonvulsive roles for NE and underscore the need for additional studies to assess the role of this transmitter in different seizure models, in particular when other transmitters, such as ACh in the present case, are known to be involved.

The Jope group (¹⁵³) also suggested that NE is anticonvulsive based on their finding that the α -2 receptor agonist clonidine *suppressed*, and the α -2 receptor antagonist idazoxan *enhanced* pilocarpine seizures. These investigators apparently felt that these results were due to post-synaptic actions of these agents on neurons targeted by LC-NE terminals. However, this interpretation is rather odd, as it fails to take into account a wealth of evidence demonstrating that α -2 receptors inhibit LC neurons: Clonidine potently *inhibits* LC neurons (^{2, 188}) and directly *decreases* release of NE from LC terminals (²⁰⁶). Both

of these effects lead to a *decrease* in forebrain NE release, consistent with recent *in vivo* dialysis studies demonstrating that clonidine reduces forebrain NE release (24, 102). Taken together, these results are entirely consistent with a *proconvulsant* action for NE. Furthermore, clonidine has been shown to *block* the excitatory effect of cholinergic agonists on LC discharge (2). Indeed, several studies have shown that clonidine in fact significantly *attenuates* the convulsant actions of soman (10, 28-30). Idazoxan, on the other hand, robustly *increases* LC discharge causing *increased* NE release. Thus, the finding by (153) that clonidine *suppresses* and idazoxan *enhances* seizures, in fact, better supports a *proconvulsant* than an anticonvulsant action of NE in cholinolytic seizures, an interpretation entirely consistent with the results of our present and previous studies.

We reviewed (Chapters 5 and 6, this report) additional experimental evidence favoring a proconvulsant action for forebrain NE. Such a role is entirely consistent with our recent finding that when rats were given the same peri-threshold convulsive dose of soman, only those animals that had rapid, profound reductions of NE developed seizures, and with the present results showing that pilocarpine only induced seizures in animals that had similar rapid, profound depletion of forebrain NE. The strong correlation between forebrain NE depletion and the development of convulsions in both pilocarpine- and soman-treated animals could imply either that NE release is proconvulsive or that NE release is *caused by* the convulsions. Several observations argue against the latter alternative: (1) Both the present study of pilocarpine and our previous study of soman (Chapter 6, this report) showed that both agents delivered either systemically or directly into LC in anesthetized rats caused a robust increase in LC discharge rate in anesthetized animals in the complete *absence of seizures*. Thus, sustained LC activation, the presumed cause of forebrain NE release and depletion, can occur in the complete absence of seizures. (2) Moreover, in the present study, systemically administered pilocarpine caused an increase in LC firing rate with a latency of 2-5 min, whereas the behavioral observations in the neurochemical studies showed that convulsions developed with a latency of 15-30 min. This latency of convulsion onset was nearly identical to that observed with soman. (3) Finally, in a previous study by (66), forebrain reductions of NE were observed as early as 15 min following systemic injection of a convulsive dose of soman. These findings demonstrate that LC activation and forebrain NE release and depletion both *precede* the onset of convulsions. It could be argued that it is the depletion of NE that is in fact pro-convulsive and that NE release per se is anticonvulsive. However, the time course data discussed above (points 1 and 2) suggest that the *release* of NE precedes the seizures; the *depletion* of NE has a slower and longer time course. Nonetheless, it is conceivable that sustained release of NE rapidly leads to a "functional depletion" of this transmitter. Thus it is prudent to leave the door open to the alternative possibility that *depletion* rather than *release* could be the causal event in seizurogenesis. Future experiments using *in vitro* methods to measure NE levels are needed to distinguish among these alternatives. Taken together, however, the weight of the available evidence suggests that sustained

activation of LC neurons leading to sustained release of forebrain NE has a pro-convulsant role in the generation of cholinolytic seizures.

In conclusion, the present study demonstrates that stimulation of muscarinic receptors leads to high, sustained increase in the firing rate of LC neurons and rapid, profound and sustained depletion of forebrain NE. Only animals with NE reductions developed convulsions. The similarity of these findings to those previously reported for the anticholinesterase inhibitor soman further supports the hypothesis that cholinolytic seizures may be triggered by the combined, sustained activation of muscarinic and adrenergic receptors on forebrain neurons. Sustained activation of both muscarinic and β -adrenergic receptors could significantly attenuate the afterhyperpolarization demonstrated to limit the excitability of cortical neurons (81, 85, 113, 120, 144). This, increased excitability of cortical neurons could cause the potentiation of NMDA receptors further increasing the excitability of cortical cells resulting in seizures. In this speculative scenario, excessive cholinergic and noradrenergic stimulation would thus comprise a "dual-trigger" for the initiation of cholinolytic seizures. Once established, however, the seizures might become progressively more dependent on the potentiation of EAA synaptic mechanisms. Thus, it is conceivable that early intervention with some combination of cholinergic and adrenergic antagonists might prevent the onset or continued expression of seizures, but that at some point, EAA antagonists might be necessary to block the seizures. Consistent with this, sparenborg et al. have found that soman-induced cholinolytic seizures are blocked by systemic administration of the NMDA antagonist MK-801⁽¹⁸⁴⁾.

8. DETERMINATION OF THE EXTRACELLULAR NOREPINEPHRINE LEVELS IN THE OLFACTORY BULB USING *IN VIVO* MICRODIALYSIS

INTRODUCTION

Our recent findings indicate that soman- and pilocarpine-induced depletion of forebrain norepinephrine (NE) results from sustained hypercholinergic activation locus coeruleus (LC) neurons leading to sustained release of NE in the forebrain. We have suggested elsewhere; that a combined excess of ACh and NE could be profoundly seizurogenic. Thus, a major goal of our research is to confirm that soman- and pilocarpine-induced activation of LC results in a sustained release of NE using *in vivo* microdialysis. In addition, there is evidence in the autonomic nervous system and in brain slice preparations that presynaptic cholinergic receptors located on NE terminals influence NE release. These findings raise the possibility that soman administration may also alter forebrain NE release by presynaptic actions of unhydrolyzed ACh on NE terminals. The goal of the present study was to determine: (1) the time-course and magnitude of forebrain NE release following, selective, confirmed activation of LC, and (2) the influence of presynaptic cholinergic receptors on terminal NE release.

We have conducted our first series of microdialysis experiments in the olfactory bulb. The olfactory bulb was selected because: (1) This structure receives a dense, highly organized NE projection from LC. (2) LC inputs provide the sole source of NE inputs to the bulb, thus, NE recovered by dialysis probes derives entirely from LC terminals. (3) LC-NE inputs to the olfactory bulb terminate almost exclusively in the granule cell layer. The granule cell layer comprises a relatively large, central portion of the olfactory bulb that is readily accessible to implantation of microdialysis probes.

METHODS

Chemicals. Acetylcholine hydrochloride, pilocarpine hydrochloride, nicotine, monochloroacetic acid, octyl sodium sulfate, NE bitartrate, desipramine (DMI) hydrochloride, and ascorbate oxidase (EC 1.10.3.3) were obtained from Sigma Chemical Co. Fisher Scientific was the source of L-cysteine, Na₂EDTA, perchloric acid and HPLC grade acetonitrile.

Chronic Probe Implantation. Adult male Sprague-Dawley rats (280-350 g) were obtained from Harlan Laboratories (Indianapolis, IN). The rats were housed in pairs with free access to food and water at least 1 week before use. Concentric microdialysis CMA/12 probes (Carnegie Medicine), 2 mm active

tip, 0.5 mm O.D.) were stereotaxically implanted in the olfactory bulb glomerular layer (7.5 mm rostral to bregma, 0.5 mm lateral to midline, 4.0 mm ventral to brain surface) in chloral hydrate-anesthetized rats (400 mg/kg, ip). The probe in each case was surrounded with a protective plastic cap and secured to skull screws with dental acrylic. At the end of each experiment, the dialysis probe implantation in the olfactory bulb was verified by cutting selected regions into 40 μ m-thick frozen sections on a freezing microtome, mounted on sbbbed slides and stained with Cresyl Violet staining.

Relative Probe Recoveries and Microdialysis Procedures. Dialysis probes are calibrated for relative recovery before implantation and when possible after the completion of dialysis experiments using an osmotically balanced artificial cerebrospinal fluid (ACSF; composition 147 mM NaCl, 2.71 mM KCl, 1.22 mM CaCl₂, pH 7.4) to which NE standards are added. Relative recoveries are determined by comparing the peak heights of NE in the dialysate to those in the standard (20 pg/10 μ l of ACSF, pH 7.4). The mean relative recoveries of the probes was $11.8 \pm 0.5\%$ (n = 27).

The perfusate (filtered, degassed) was placed in a 2.5 ml microdialysis syringe (CMA/105) and continuously perfused through the probe at a flow rate of 2 μ l/min using a microinfusion pump (CMA/100) equipped with an electronic syringe selector (CMA/111) which holds a maximum of three 2.5 ml microdialysis syringes. Dialysate samples (20 μ l) are collected at 10 min intervals in 250 μ l microdialysis vials using a microfraction collector (CMA/140). To examine possible presynaptic cholinergic control of terminal NE release, cholinergic agents were perfused through the dialysis probe.

Chromatographic Methods and Norepinephrine Assay. The catecholamine norepinephrine (NE) level was determined using a Bioanalytical Systems (BAS) Model 200 Liquid Chromatograph, equipped with a LC-4B electrochemical detector. The glassy carbon working electrode is held at 0.65 V against an Ag/AgCl reference electrode and the sensitivity of detection is held at 0.2 nA (full scale). Chromatographic separations are effected with a 100 x 3.2 mm Biophase ODS 3- μ m (C18) column (BAS) in a 10 min run. The mobile phase consists of 0.06 M monochloroacetic acid, 1.30 mM octyl sodium sulfate and 0.2 mM Na₂EDTA in the aqueous phase (pH 3.0) and 3% acetonitrile at a flow rate of 1.0 ml/min. The column and mobile phase are held at 40 and 35 °C, respectively. For calibration, standard solutions (10 or 15 μ l) containing NE were injected. The concentrations of monoamines in the brain dialysate were determined by comparing peak heights of dialysate to those of standards. Positive identification of the neurotransmitter NE in brain dialysates are conducted in each experiment by spiking methods. At the above chromatographic conditions, the brain dialysate samples have a large solvent front which interferes with the early eluting peaks. To circumvent this chromatographic problem, each collected dialysate sample (20 μ l) was treated with 0.5 μ l of ascorbate oxidase (activity, 250 units/0.5 ml of water). Aqueous solutions containing this enzyme can be stored at about +5 °C for 3-4 weeks.

Neurophysiological Techniques

General Surgical Techniques. Approximately 24-48 hr after microdialysis probe implantation, rats were intubated with a tracheal cannula under methoxyflurane (metofane) anesthesia (0.3-1.0% in moist air). A second ascending cannula was inserted into the distal (nasal) part of the trachea and attached to a small animal respirator to produce moist airflow through the nasal cavity. Animals were mounted in a stereotaxic instrument with the incisor bar lowered to angle the skull 12 degrees from the flat skull position. Core body temperature was maintained at 36-37°C with a feedback-controlled heating pad.

EEG Recording. A transcortical EEG electrode was made from a pair of 250 μm stainless steel wires, totally insulated except for bluntly cut tips. The tips were separated dorsoventrally by 500-1000 μm . The electrode was implanted in the cortex so that the superficial tip was approximately 200 μm ventral to the brain surface and glued in place with dental acrylic. In every experiment EEG activity was monitored continuously to assess the plane of anesthesia. Following anesthetic induction and equilibration, the animals were stabilized at an anesthetic plane at which a vigorous pinch of the hindlimb elicited a brief desynchronization of the cortical EEG without causing a withdrawal reflex.

Locus Coeruleus (LC) Recording and Activation. A hole was drilled in the skull at coordinates for LC (4.0 mm posterior to lambda, 1.2 mm lateral to midline) through which an electrode assembly was inserted. A composite recording/microinjection electrode was used to record extracellular action potentials from single LC neurons during microinjection of acetylcholine (ACh) into LC. The electrode consisted of a conventional glass recording pipette (4-6 μm tip diameter, 5-10 $\text{M}\Omega$ impedance) filled with 2% Pontamine Sky Blue in 0.5 M sodium acetate glued to a calibrated injection pipette (60-80 μm tip diameter). The tip of the recording pipette extended 100-200 μm beyond the tip of the injection pipette.

The electrode was positioned so that the tip of the injection pipette was in the center of LC. This was accomplished by monitoring LC activity at several rostrocaudal locations and identifying a position where LC activity could be recorded for at least 500 μm in the dorsal-ventral axis. LC units were identified by the following criteria: a characteristic waveform; low and regular spontaneous discharge (less than 5 Hz); and a rapid and transient increase in firing rate evoked by a moderate pinch of the contralateral paw. To activate LC for at least a period of 10 min, four 90 nl injections of ACh hydrochloride in water (36 mg/ml, 0.2 M) were made at 2.5 min intervals. Direct visual inspection of meniscus movement relative to grid lines applied to the calibrated injection pipette assured that known drug volumes were injected.

Electrode signals were amplified and displayed continuously using conventional

electrophysiological methods as described in our previous publications (54, 55). Ratemeter recordings of LC neurons were used to determine the degree and time-course of LC activation. At the end of the experiment, iontophoretic ejection of Pontamine Sky Blue with current pulses (-10 μ A, 7 sec on/3 sec off duty cycle for 10 min) marked the position of the recording electrode. At the end of each experiment, the position of the electrode in LC was determined using neural red staining.

Statistical Analysis. Data were expressed as mean \pm S.E.M. of the results obtained from a group of rats (n). The level of NE in each sample was expressed as a percentage of the average NE concentration of six baseline 10 min-samples. The significance of differences (P) between the mean of baseline NE level and that after each experimental manipulation was assessed using unpaired, two-tailed Student's test.

RESULTS

Extracellular NE levels in the Olfactory Bulb: Basal Levels and Depolarization-Evoked Release.

The mean basal NE level in the olfactory bulb of anesthetized rats was estimated to be 0.55 ± 0.11 pg/10 μ l-dialysate (n = 21); this value is nearly identical to rat hippocampal NE levels obtained with other implanted concentric probes (1). In order to confirm that NE levels in our samples could be increased by stimuli known to evoke synaptic release, a brief infusion of ACSF containing high potassium (30 mM) through the dialysis probe was used to depolarize synaptic terminals. As shown in Figure 25, infusion of potassium chloride (30 mM in an osmotically balanced ACSF, pH 7.4) for 10 min increased NE levels to $166.3 \pm 24.3\%$ of baseline (n = 6; P = 0.0001) during this period. The NE levels decreased to 138.8 ± 20.0 (P = 0.0001) in the second 10 min-sample and returned to baseline levels by 30 min.

Influence of the NE-Uptake Blocker, Desipramine (DMI), on NE Release. DMI is a tricyclic antidepressant that is a selective blocker of NE-uptake into the noradrenergic terminal. Administration of DMI produces an increase of NE at the synaptic cleft. We predicted that if NE present in our samples was due to spontaneous synaptic release of NE, then local infusion of DMI should increase NE recovery. Infusion of DMI (1 μ M) in ACSF was found to increase the NE levels to a maximum level of $239.7 \pm 16.4\%$ of baseline (n = 5) at 1 hr following continuous infusion of the drug (Fig. 26). The increase in NE level is gradual in the first 30 min. then essentially plateaus afterward.

In another set of experiments, the NE uptake blocker desipramine (DMI, 1 μ M) was perfused for at least 1 hr before infusion of 30 mM of potassium in ACSF (pH 7.4) containing DMI (1 μ M). This manipulation increased NE to $156.4 \pm 13.9\%$ (n = 5, P = 0.0001) of basal levels. This increase was comparable to the 166.3% increase caused by high potassium in the absence of DMI. Thus, DMI increases the baseline NE recovery, but does not enhance depolarization-evoked release of NE.

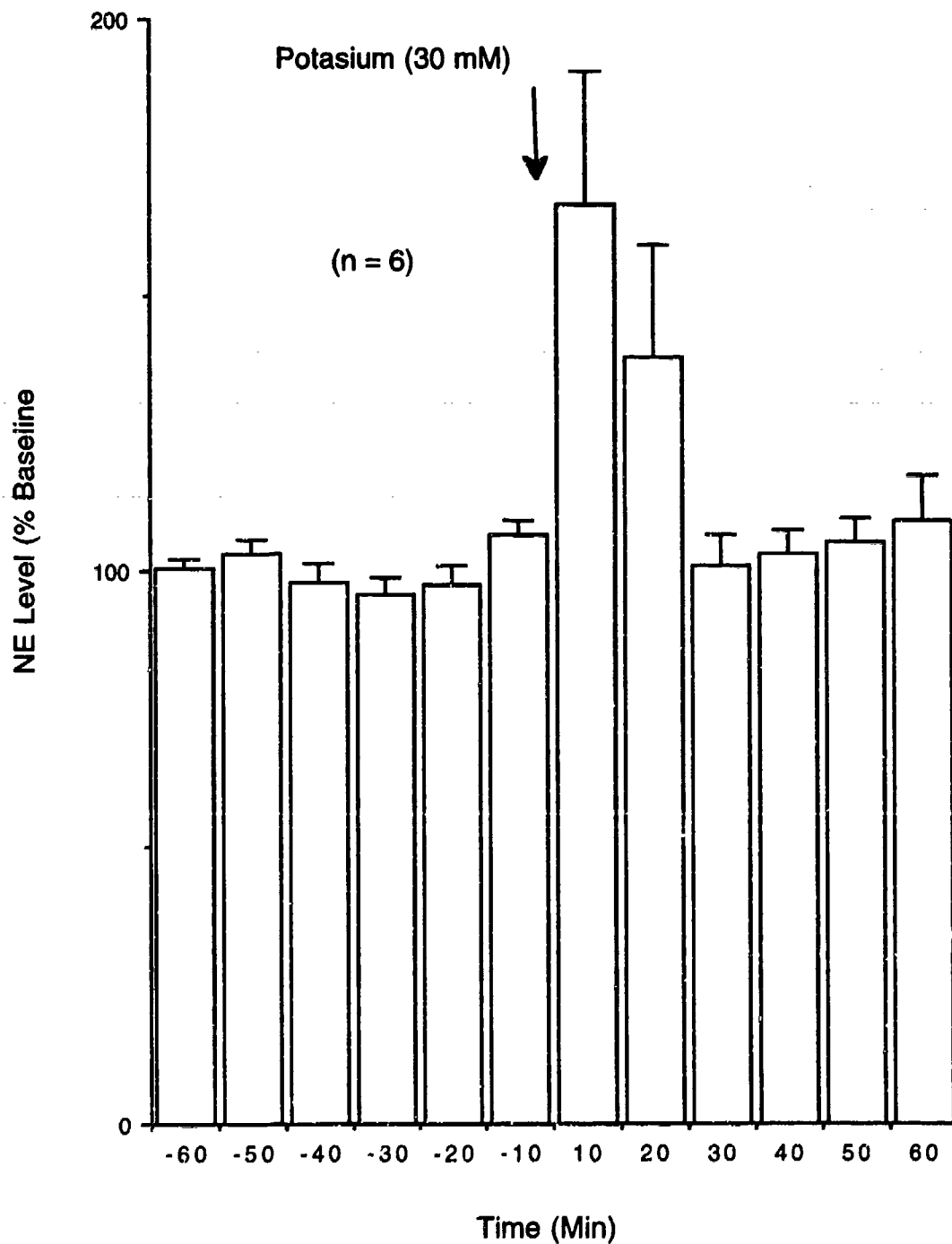


Fig. 25. Elevated extracellular potassium increases synaptic release of NE. Evoked release of olfactory bulb NE by a 10 min perfusion of an osmotically balanced artificial CSF containing 30 mM of potassium (n = 6). Data are expressed in mean \pm SEM.

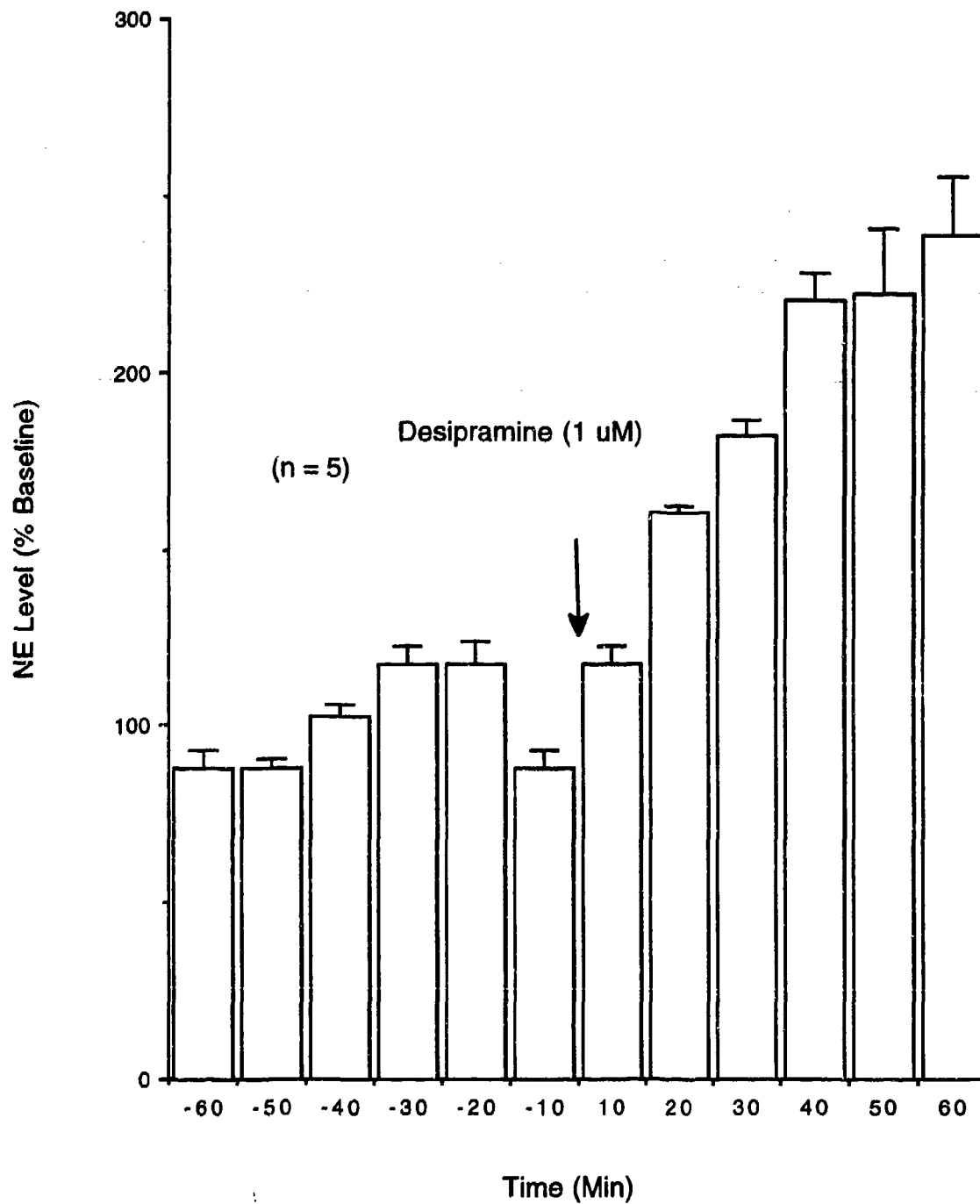


Fig. 26. Local infusion of the NE uptake blocker desipramine (DMI) increases NE recovery. Effect of a 1 hr perfusion of artificial CSF containing DMI(1 μ M) on olfactory bulb NE levels (n = 5).

Presynaptic Cholinergic Regulation of NE Release

Local Infusion of Acetylcholine (ACh). Local infusion (10 min) of ACh in ACSF (40 mM, pH = 7.4) increased the release of NE to a maximum level of 317.0 ± 30.4 % of baseline ($n = 4$; $P = 0.0001$) in the second 10 min-sample as shown in Figure 27. Local infusion of ACh in ACSF containing the uptake blocker DMI (1 μ M) increased the baseline NE level to 470.8 ± 179.2 % of baseline ($n = 2$) in the first 10 min-dialysate fraction. NE levels remained elevated, but progressively declined, with prolonged infusion of DMI; NE levels in 2nd, 3rd and 9th 10 min-fractions were 389.4 ± 39.4 %, 227.9 ± 22.1 % and 152.2 ± 2.2 % of baseline, respectively.

Local Infusion of Pilocarpine. Pilocarpine is a selective muscarinic agonist. As illustrated in Figure 28, local infusion of pilocarpine (40 mM in ACSF, pH 7.4) induced a maximal decrease in NE levels to 53.6 ± 4.6 % of baseline ($n = 6$, $P = 0.0001$) in the second 10 min-dialysate fraction.

Local Infusion of Soman. Infusion of soman in ACSF (0.4 mM, pH 7.4) increased NE levels by 163.1 ± 5.1 % of baseline in 57% ($n = 4$ out of 7; $P = 0.0001$) of the animals tested in the first 10 min-sample, as shown in Figure 29. However, soman infusion did not substantially affect NE levels in the remaining three cases. AChE histochemical analysis after soman infusion in the olfactory bulb was confirmed at the end of each experiment as described elsewhere (⁵⁸).

Local Infusion of Nicotine. Infusion of nicotine in ACSF (40 mM, pH 7.4) increased NE levels by 178.1 ± 8.7 % of baseline ($n = 4$, $P = 0.0001$) in the second 10-min-sample. The NE levels in the third 10 min-sample remained high (168.0 ± 22.8 , $P = 0.0001$) in the third 10 min-sample and then rapidly returned to basal level afterward (Figure not shown).

Selective Activation of Locus Coeruleus (LC) Neurons Increases Extracellular NE Levels in the Olfactory Bulb. The preceding findings indicate that presynaptic cholinergic receptors significantly modify terminal release of NE. The next series of experiments determined the relationship between the neuronal firing rate of LC cell bodies and extracellular NE levels. While several previous studies have demonstrated that electrical stimulation of LC axons increases NE release, the relationship between the degree of LC neuronal activity and synaptic NE release has not been examined.

Four local microinjection (90 nl) of ACh in ACSF (0.2M, pH 7.4) in LC produced a robust increase in LC discharge rate beginning 5-7 sec after injection. Simultaneous recordings from LC neurons demonstrated that the spontaneous discharge rate of LC neurons increased from a mean of 3 spikes/sec to 10-15 spikes/sec during the 10 min period of activation. As illustrated in Figure 30, microdialysis samples collected during this period demonstrated that LC activation increased olfactory bulb NE levels by 250% above baseline values (mean = 247.4 ± 9.3 %; $n = 6$; $P = 0.0001$) in the first

10 min after injection.

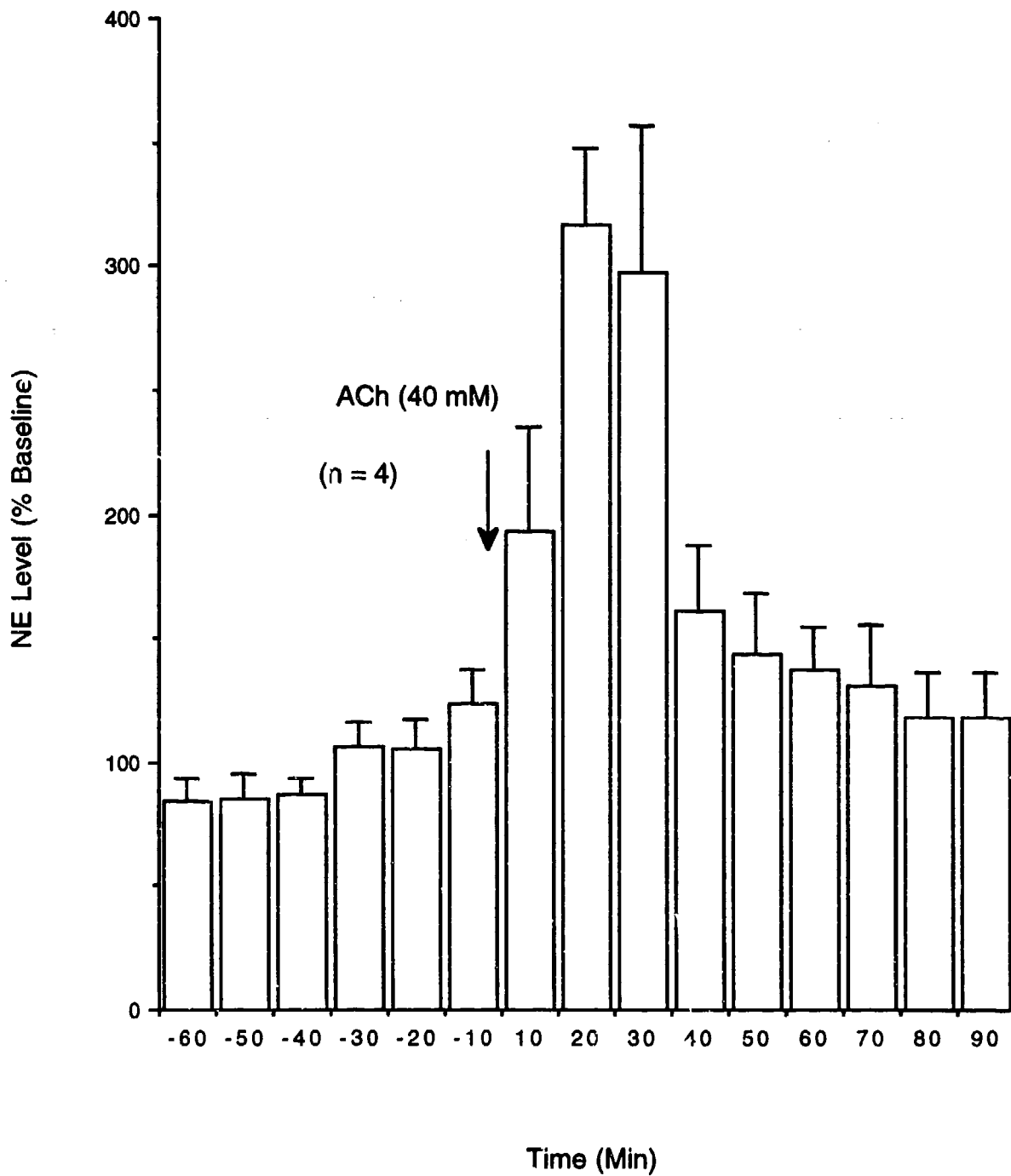


Fig. 27. Local infusion of acetylcholine (ACh) potently increases extracellular NE levels. Increased release of NE in the olfactory bulb by a 10 min perfusion of artificial CSF containing acetylcholine hydrochloride (40 mM, pH 7.4) (n = 4).

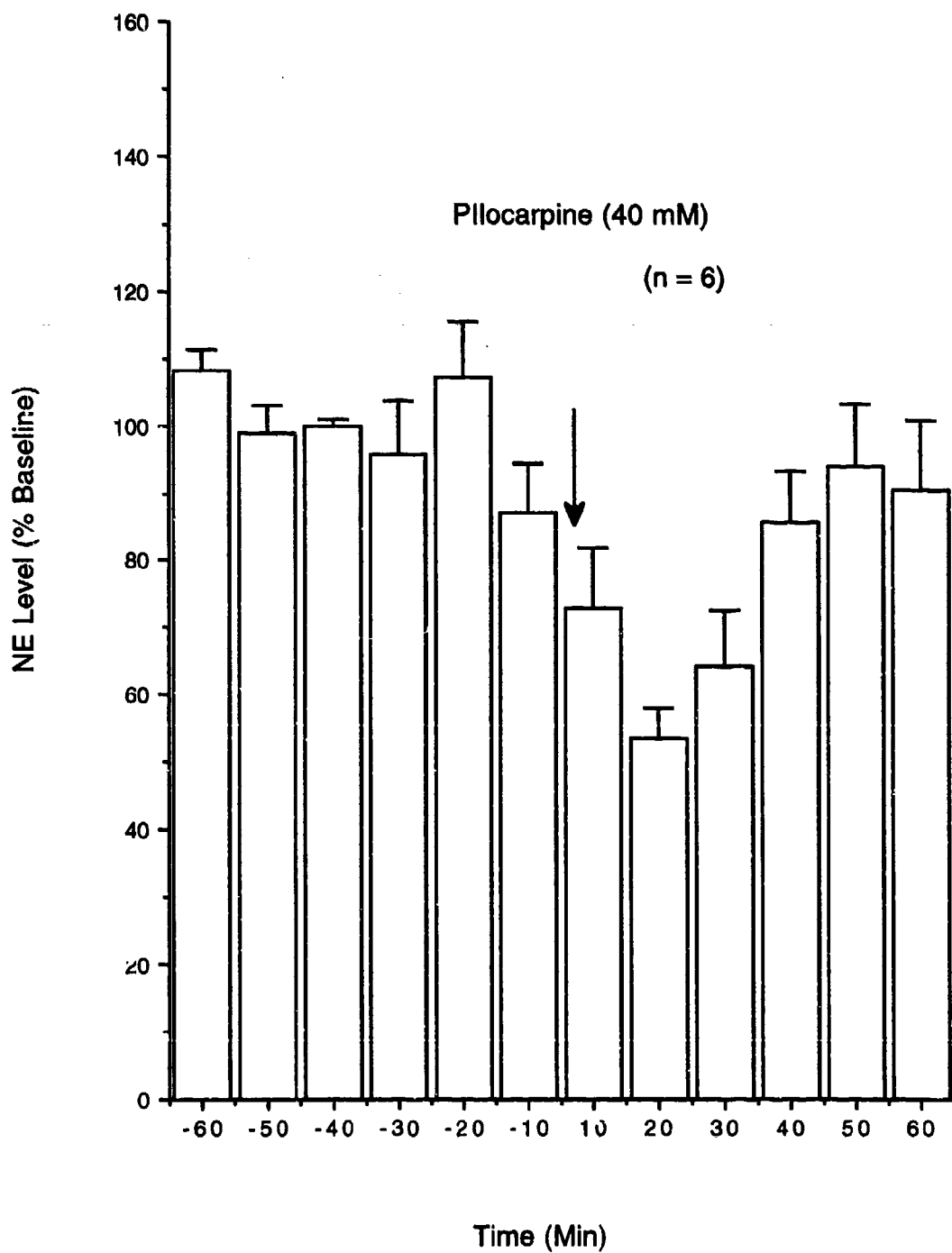


Fig. 28. Local infusion of the muscarinic agonist pilocarpine reduces NE levels. A 10 min perfusion of artificial CSF containing pilocarpine hydrochloride (40 mM, pH 7.4) reduced NE levels in the olfactory bulb (n = 6).

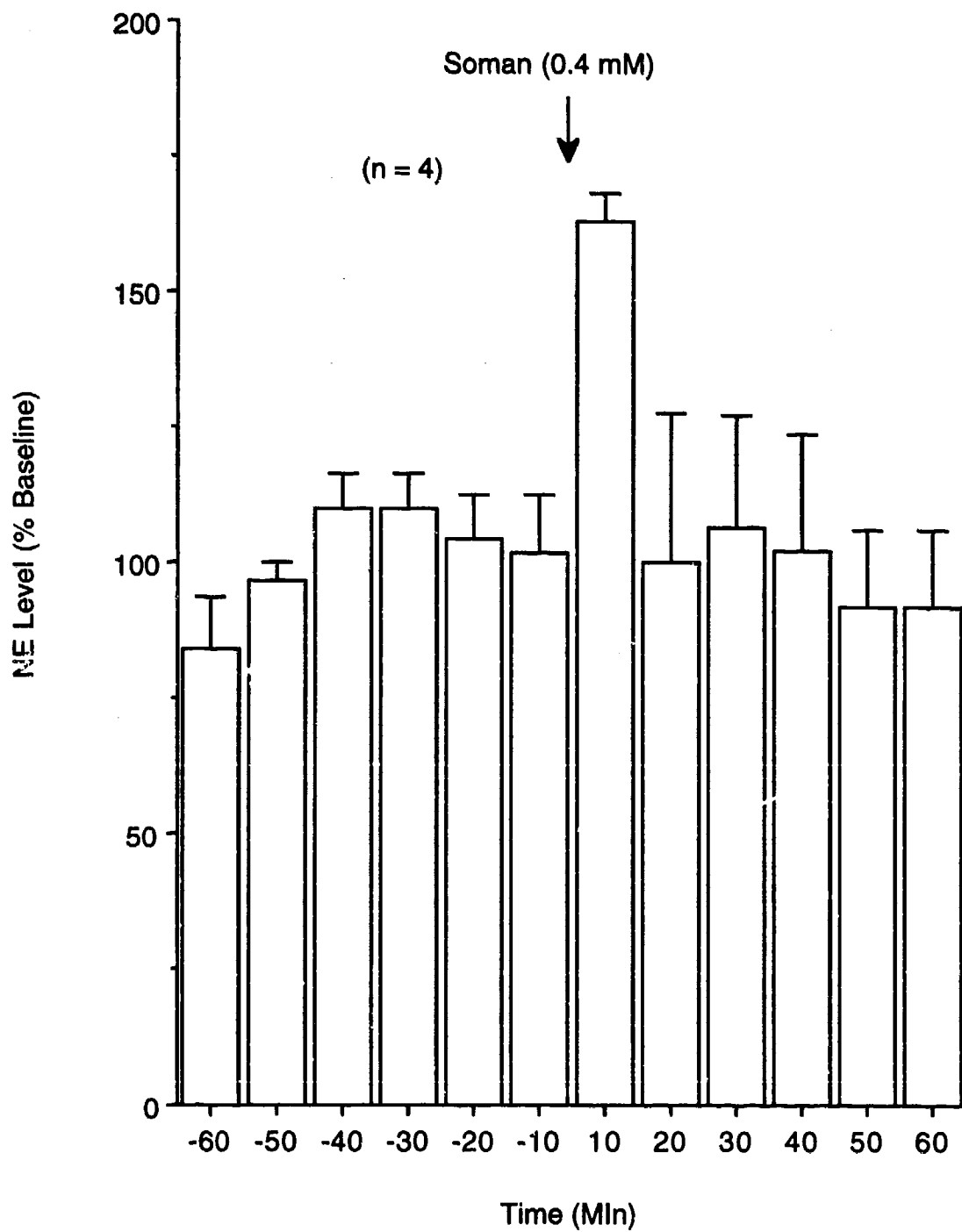


Fig. 29. Local infusion of soman increases NE recovery. Increased release of NE in the olfactory bulb by a 10 min perfusion of artificial CSF containing soman (0.074 mg/ml, 0.4 mM) (n =4).

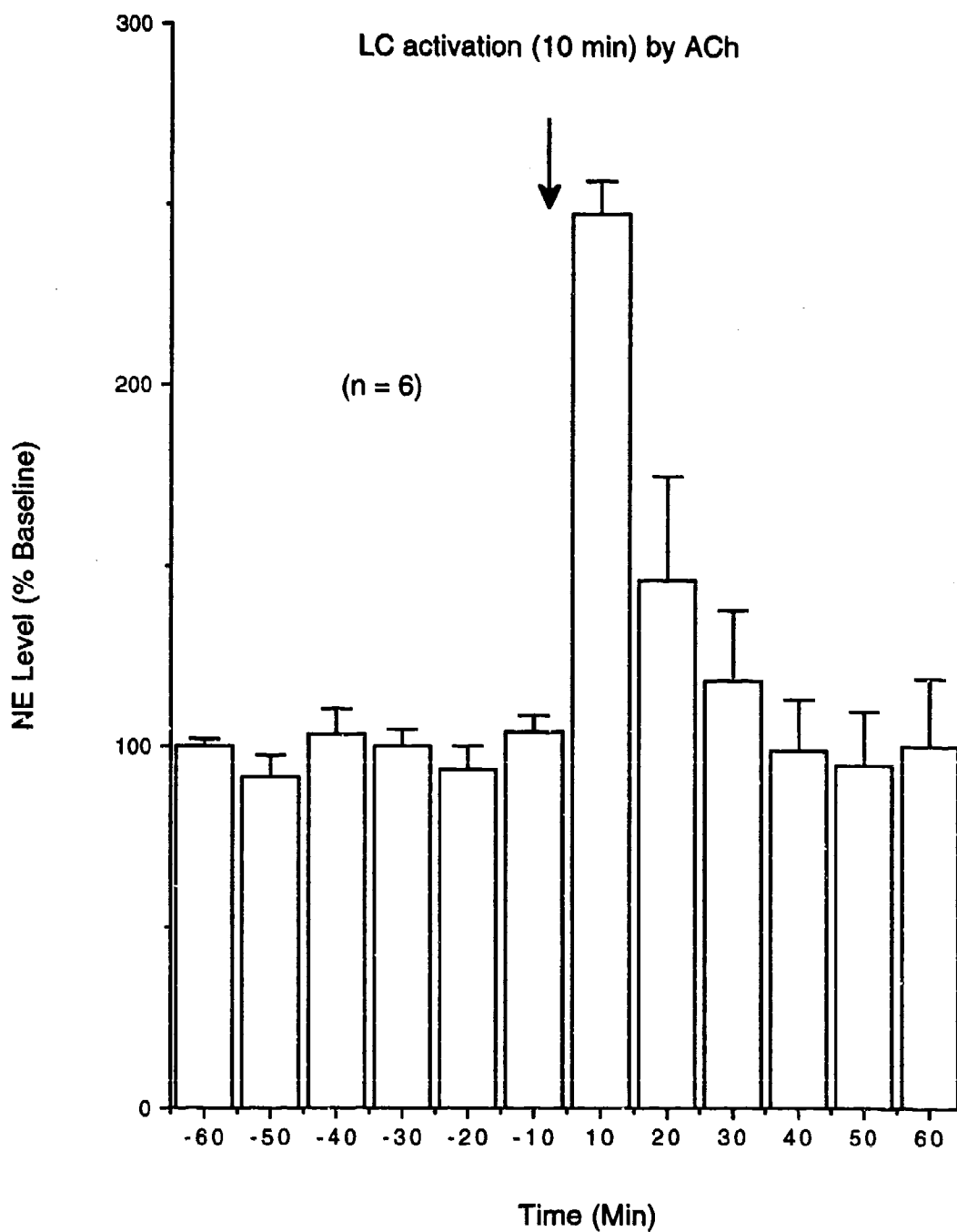


Fig. 30. Selective, confirmed activation of locus coeruleus (LC) increases release of olfactory bulb NE. LC activation for 10 min by 4 intracoerulear injections (90 nl) of acetylcholine (see method) increased NE levels to 250% of baseline (n = 6).

DISCUSSION

The major findings of this study are: (1) Robust, tonic activation of LC neurons via intracoerulear ACh microinfusion produces a substantial increase in NE levels in the olfactory bulb. This is the first direct demonstration that confirmed, selective stimulation of LC neuronal discharge produces a rapid increase in extracellular NE levels *in vivo*. (2) Stimulation of presynaptic cholinergic receptors on LC terminals substantially influences NE release. Presynaptic muscarinic and nicotinic receptors appear to exert opposing actions on terminal NE release; specifically, stimulation of muscarinic receptors inhibits, and stimulation of nicotinic receptors augments NE release.

To date, there have been very few studies of synaptic release of NE in the central nervous system with *in vivo* microdialysis because the levels of NE present in dialysis samples are extremely low and at the limit of quantitative HPLC measurement. In addition, several previous NE-microdialysis studies were performed within 2-12 hr after probe implantation, times at which studies by others indicate that synaptic release of neurotransmitters is substantially impaired by the damage associated with probe implantation (¹). We circumvented this problem by conducting our experiments 3-7 days after surgery in chronically implanted animals. Although the present studies were performed in anesthetized animals, the olfactory bulb NE level in our dialysis samples (0.55 ± 0.11 pg/10 μ l) is identical to that of the rat hippocampus obtained with similar probes in awake animals (0.55 ± 0.1 pg/10 μ l) (¹). This is not surprising since both brain regions receive a dense projection of LC noradrenergic neurons. The potassium-evoked increase in NE levels observed here (166.3%) is compatible with a 196% increase reported by others using a similar concentration of potassium (¹). In addition, our DMI infusion results which are illustrated in Figure 26 are remarkably similar to those obtained from *in vivo* electrochemical studies in which DMI was systemically administered (10 mg/kg, ip) (^{26, 127}).

LC neurons in anesthetized rats typically exhibit relatively low spontaneous discharge rates ranging from 1-5 spikes/sec. The mean firing rate of LC neurons recorded in the present studies was approximately 3 spikes/sec. This low level of spontaneous activity, and consequently the low rate of spontaneous NE release, may partially account for the low levels of extracellular NE. We found that increasing the mean spontaneous discharge of LC neurons five-fold (3 spikes/sec to 15 spikes/sec) by intracoerulear NE infusion caused a rapid and pronounced increase in NE levels in the olfactory bulb. NE levels were increased by nearly 1.5-fold (250% of baseline levels). While the increase in NE levels determined by microdialysis was not proportional to the increase in LC discharge, there are several factors that limit the accuracy of this comparison. ACh injections were made into the center of LC and neurons distant from the injection site may not have been as robustly activated as those near the infusion site. The spread of ACh through LC was not instantaneous; therefore, there was some delay before LC neurons were firing at peak rates.

The present finding that LC activation produces rapid increases in forebrain NE levels, taken together with findings described earlier in this report, is consistent with our hypothesis that depletion of forebrain NE following systemic soman administration is due to prolonged activation of LC neurons that causes sustained release, leading rapidly to depletion of terminal pools of NE. Systemic injections of soman that induce convulsions cause a rapid and profound reduction of NE in the olfactory bulb and forebrain within 1 hr (Chapter 5 this report). As NE was depleted only in convulsing animals, it is conceivable that generalized brain seizures, and not cholinergic stimulation, cause activation of LC neurons. However, we found that seizures are not the cause of the increased firing rates of LC neurons in anesthetized animals, as both systemic and intracerebrular microinjections of soman robustly and tonically activate LC neurons in the absence of seizures. Thus, it is reasonable to argue that the reduction of olfactory bulb and forebrain NE caused by systemic soman administration is due to a tonic cholinergic stimulation of LC neurons and sustained release of NE which in turn leads to depletion of NE in LC terminals. In support of this hypothesis, we found that ACh-induced activation of LC neurons causing increased firing rates comparable with those caused by systemic soman produced a large (250%), rapid (10 min) increase in NE release in the olfactory bulb. We predict that longer periods of LC stimulation will lead to a progressive, but rapid decline, and ultimately to exhaustion of synaptic release of NE. Experiments to test this prediction using soman to tonically activate LC neurons are in progress.

The present experiments suggest that presynaptic cholinergic receptors also exert significant regulatory actions on terminal NE release. We found that local infusion of cholinergic receptor agonists substantially modified extracellular NE levels in the olfactory bulb. Local infusion of ACh, soman, and in preliminary experiments, nicotine, increased NE levels. In contrast, the selective muscarinic agonist pilocarpine reduced NE levels. These overall findings are in excellent agreement with studies conducted in the peripheral nervous system and in brain slices demonstrating that nicotinic receptors facilitate, and muscarinic receptors reduce, terminal NE release (204-206).

Soman, by increasing ACh levels, should cause dual stimulation of both muscarinic and nicotinic receptors present on LC terminals. Given the opposing actions of these cholinergic receptor subtypes on NE release, it is reasonable to speculate that combined stimulation of both nicotinic and muscarinic presynaptic receptors produced by soman may have had no net influence on NE levels. However, the present microdialysis results obtained with local infusion of soman indicate that nicotinic receptor-mediated facilitation of NE release predominates in 57% of the cases over the inhibitory influence of muscarinic receptors. The present microdialysis results, taken together with findings presented earlier in this report, indicate that increased forebrain NE levels after systemic soman are mediated by two distinct sites of action: (1) a direct excitatory action on LC cell bodies mediated by muscarinic receptor

stimulation, and (2) a presynaptic, nicotinic receptor-mediated facilitation of NE release.

While presynaptic cholinergic receptors may presynaptically modulate LC terminals, additional findings reported herein indicate that caution must be exercised in estimating the relative influence of these receptors. We found that systemic administration of the muscarinic agonist, pilocarpine, causes increases in LC neuronal discharge activity that are identical to those caused by soman. Based on the preceding observations, it is reasonable to speculate that presynaptic muscarinic *reduction* of NE release caused by pilocarpine would cause less NE release than seen with soman. However, pilocarpine also caused forebrain NE reductions of the same magnitude and time course as those produced by soman. This indicates that any reduction in NE release attributable to presynaptic muscarinic stimulation is insufficient to offset the increase in release of NE due to the sustained increase of LC neuronal activity. Finally, it should be noted that locally infused substances may modify NE release by actions that do not involve presynaptic receptors on LC terminals. For example, infusion of nicotine may increase the activity of local neurons in the vicinity of the probe. Release of EAAs or increased extracellular potassium levels following such activity may cause depolarization of LC terminals, and hence, increased NE release.

9. *IN VITRO* WHOLE-CELL PATCH CLAMP RECORDING OF RAT OLFACTORY BULB MITRAL CELLS: BIOPHYSICAL AND SYNAPTIC PROPERTIES

INTRODUCTION

The responses of primary olfactory neurons to odors are conveyed to the central nervous system by thin unmyelinated primary olfactory axons that terminate in the glomerular layer of the olfactory bulb. The major synaptic targets of these axons are the apical dendrites of the mitral and tufted cells, the output neurons of the olfactory bulb. Axons of mitral and tufted cells project to the primary olfactory cortex. The activation of mitral and tufted cells by primary olfactory nerves is the first stage of synaptic integration in the olfactory pathway.

Although both mitral and tufted cells provide important outputs of the olfactory bulb, the mitral cell has received most attention in studies of olfactory bulb physiology. The mitral cells are unusual neurons. Their cell bodies lie in a narrow band in the interior of the olfactory bulb. Five or six secondary or lateral dendrites extend from each mitral cell soma; these dendrites travel as far as 2 mm through the external plexiform layer (^{132, 154}). These secondary dendrites make reciprocal contacts with dendrites of inhibitory interneurons, the granule cells. The connections between mitral and granule cells comprise a feedback system in which increased activity of mitral cells results in self- and lateral inhibition of mitral cell activity. Each mitral cell also extends a single unbranched primary dendrite through the external plexiform layer to the glomerular layer. The olfactory nerve synapses onto the distal ends of this apical dendrite which are located 300-400 μm from the cell body. These apical dendritic tufts also have extensive synaptic interactions with interneurons of the glomerular layer.

The long distance between the synaptic input to the apical dendrite in the glomerular layer and the presumed spike generation site at the mitral soma leads to the suggestion that there are two distinct levels of synaptic integration in the mitral cell (^{124, 171, 172}): (i) Several classes of juxtglomerular interneurons modulate transmission from the terminals of the olfactory nerve to the mitral cell apical dendrite; (ii) these synaptic interactions are distinct from those between the secondary dendrites of the mitral cells and the apical dendrites of the granule cells located in the external plexiform layer. However, the degree of coupling between these two levels of synaptic regulation of mitral cell excitability is not clear. Depending upon the membrane properties of the apical and the secondary dendrites, membrane currents in the apical tuft might be closely or weakly coupled to the soma. Thus, improved understanding of synaptic integration in the mitral cell requires more detailed information about the biophysical properties of these neurons than is presently available.

Previous *in vivo* intracellular studies of mammalian olfactory bulb neurons have been limited by the technical difficulties of recording from relatively small cells in intact animals (133, 138, 139, 201-203). Detailed *in vitro* studies of olfactory bulb physiology and pharmacology have been mainly limited to amphibian and reptilian preparations, most notably the isolated turtle olfactory bulb (91, 131, 134, 136, 137, 146-149, 198) and salamander (83, 84). However, there may be substantial differences between the olfactory bulbs of mammals and non-mammalian vertebrates. Thus, there is a need for high-quality intracellular recordings from mammalian mitral cells during their synaptic activation by the olfactory nerve.

Although the mammalian brain slice has been a standard preparation for more than 20 years, there have been few reports of *in vitro* recordings from mammalian olfactory bulbs. Several workers have used culture systems to study the pharmacology of olfactory bulb neurons (69, 190-193) and whole-cell patch clamp recordings from mitral and periglomerular cells in thin (150 - 200 μm) slices of neonatal rabbit olfactory bulbs (31, 32, 42) and from mitral and granule cells in thin slices of rat olfactory bulb have been reported. None of these studies, however, have reported synaptic activation of mitral cells by stimulation of the olfactory nerve. Activation of mitral cells in thin slice preparations may not have been possible either because the plane of section was not optimized to preserve olfactory nerve-to-mitral dendrite synapses, or because few mitral cells retained their long apical dendrite in such thin slices (31). The present experiments were designed to overcome these limitations.

In order to study synaptic integration in the mitral cell in more detail, we wished to obtain whole cell patch recordings of the synaptic responses of mitral cells to stimulation of the olfactory nerve layer in mature rat olfactory bulb slices of conventional (400 μm) thickness. Several considerations shaped these objectives. First, the effect of synaptic activity in the glomerular layer upon the firing of action potentials by mitral cells may depend critically upon membrane properties of mitral cells. For this reason, we chose to use whole cell patch techniques, which provide superior recordings to those obtained with conventional sharp electrodes. Second, conventional 400 μm thick sections were deemed optimal in order to preserve the mitral cell body, its 300-400 μm long apical dendrite and the olfactory nerve axons synapsing on the dendrite in the slice. Thus, although whole-cell patch recordings are more easily obtained in thin slices, thick slices would significantly enhance the chances of synaptically activating mitral cells. Finally, functionally mature olfactory bulbs were used so that results could be compared with the extensive *in vivo* literature and because there may be significant differences in the synaptic and membrane properties of cells in mature and immature olfactory bulbs. Here we report: (1) the development of the olfactory bulb slice preparation, (2) the membrane properties of mitral cells in the slice, and (3) the first whole-cell patch recordings of the synaptic responses of mitral cells to olfactory nerve stimulation.

A preliminary account of these studies has appeared (¹⁴¹).

METHODS

Slice Preparation. Juvenile and young adult Sprague-Dawley rats weighing 65 to 250 grams were used. This weight range corresponds to ages of 4 to 7 weeks postnatal. The olfactory bulb continues to develop postnatally, but is substantially mature by 4 weeks (^{5-7, 116, 117, 122, 123, 181, 183}).

Rats were deeply anesthetized with chloral hydrate and both olfactory bulbs were exposed by removing the dorsal and lateral portions of the skull between the lambda suture and the cribriform plate while the brain was still perfused by normal circulation. The dura was removed with forceps. Next, the bulbs were washed with ice-cold Krebs's solution (composition, mM: NaCl = 124; KCl = 5; CaCl₂ = 2.5; MgSO₄ = 1.3; KH₂PO₄ = 1.24; NaHCO₃ = 26). The olfactory bulbs were repeatedly washed with cold oxygenated Krebs's solution while remaining bone was dissected from the lateral sides of the olfactory bulbs. The olfactory nerves were then severed by carefully passing a thin probe, cut from a sheet of mylar drawing film, between the rostral-ventral olfactory bulb surface and the cribriform plate. A cut was then made through the caudal forebrain and most of the forebrain, including the two olfactory bulbs, was removed from the skull by lifting the forebrain from the rear. The forebrain and olfactory bulbs were left in cold oxygenated Krebs's solution for 1 to 3 min. At the end of this period, the brain was placed, ventral side down, on moistened filter paper and a cut was made with a razor blade through the forebrain at an angle approximately parallel to the rostral-ventral surface of the olfactory bulbs. The cut surface of the forebrain was then mounted on the stage of a Vibratome using cyanoacrylate adhesive. A small piece of "gelfoam" was also placed on the Vibratome stage beneath the two olfactory bulbs. The gelfoam absorbed Krebs's solution, swelled, and supported the two olfactory bulbs during sectioning. The forebrain and olfactory bulbs were covered with cold oxygenated Krebs's solution, and the olfactory bulbs were cut in 400 μ m sections. As a result of the angle of the blocking cut through the forebrain, the plane of the sections of the olfactory bulb was approximately horizontal, corresponding to the trajectory of the olfactory nerve fibers (²⁰²).

The olfactory bulb slices were incubated at room temperature in oxygenated Krebs's solution for at least 1 hr. After this incubation period individual slices were transferred to a submerged-slice recording chamber as needed. In the recording chamber, slices were supported upon a nylon mesh and held in place by nylon strings attached to a platinum frame. The temperature of the solution continuously perfusing the slice chamber (1 ml/min) was maintained at 32 °C.

Stimulation and Recording. We used the technique of Blanton et al. (²²) to obtain whole cell patch

recordings from mitral cells in the 400 μm olfactory bulb slices. Patch pipettes of approximately 1 μm tip diameter and resistance of 5-10 $\text{M}\Omega$ were pulled using a Brown and Flaming type electrode puller. In all recordings described here, pipettes were filled with low-chloride medium (composition: potassium gluconate, 140 mM; EGTA, 10 mM; HEPES, 10 mM; MgCl_2 , 1 mM; CaCl_2 , 1 mM; MgATP, 2 mM). With a small positive pressure applied to the pipette to maintain a slow outward flow, the electrode tip was guided into the mitral cell layer. Pipette resistance was monitored by passage of a 100 pA current pulse. With the amplifier bridge (Axoclamp 2A, Axon Instruments, Inc.) balanced, approach of the pipette tip to a cell membrane was indicated by voltage deflections proportional to the increase in resistance and by an increase in background noise. After contact with a cell membrane, the pipette was carefully advanced until there was no further increase in resistance. The positive pressure was then released and suction was applied to aid the formation of a gigaohm seal. If a gigaohm seal formed, we attempted to break the membrane patch separating the cell interior from the pipette by additional suction or by current pulses to permit whole-cell recording.

The continuous bridge mode of the amplifier was used for both voltage and current clamp of the cell membrane. Current-voltage curves were determined under voltage clamp using a commercial software package (pClamp, Axon Instruments, Inc.). Passive membrane currents were subtracted using the leak subtraction procedure provided in the pClamp software. In some cells, fast sodium currents were blocked by addition of 2 μM tetrodotoxin (TTX) to the bathing solution.

Voltage and current signals were recorded digitally on a modified video tape recorder at 16 bit resolution. Selected segments of these signals were later played back and digitized at 12 bit resolution using an MS-DOS compatible computer and the pClamp software package. These data were stored on floppy disks as MS-DOS files. These files were later analyzed using a second commercial program (Axograph, Axon Instruments, Inc.) running on an Apple Macintosh computer.

The geometry of the mitral cell is poorly suited to voltage clamp analysis. Although the high membrane resistances measured with whole-cell patch recording (Results) suggest that the length constants of the primary and secondary dendrites are less than previously supposed, it cannot be assumed that the apical dendrite in the glomerular layer and the distal parts of the secondary dendrites are under voltage control from the soma, particularly for fast events. For this reason, "current clamp" recording was primarily used in the present experiments.

Patch electrodes proved effective for obtaining high quality extracellular recordings. Pipette seals of 100 $\text{M}\Omega$ or greater were often obtained; with these seals, high-amplitude extracellular spikes could be recorded for several hours. These extracellular recordings were used to characterize the spontaneous activity and response to ONL stimulation of a substantial number of mitral cells in the slice.

The olfactory nerve layer (ONL) of the slice was stimulated using a bipolar electrode constructed by gluing together a pair of 50 μm diameter stainless steel wires. The wires were insulated except at the tips, which were separated by 400 μm . Stimulus currents of 200 μA and 50 μsec duration were delivered by a photo-isolated constant current source. After isolation of a mitral cell by the recording electrode, the forward tip of the stimulating electrode was placed against the nerve layer slightly rostral to the estimated location of the apical dendrite of the patched mitral cell. In those cases in which the mitral cell responded weakly or not at all to stimulation at the initial placement, the stimulating electrode was repositioned in an attempt to obtain a larger response.

Biocytin fills of mitral cells. In some experiments, 1% biocytin was added to the contents of the recording electrode. Cells were filled after prolonged extracellular contact with the biocytin-containing pipette. Slices were fixed overnight in formalin and filled cells were made visible using the avidin biotin reaction (Vectastain Elite ABC kit, Vector Laboratories, Burlingame, California). Selected filled mitral cells were traced at 20X magnification using an image analysis system.

RESULTS

Identification of Mitral Cells. The mitral cell layer (Mi) was visible under the dissecting microscope as a narrow translucent band. The tip of the recording electrode was visually guided into this layer. Because of the predominance of mitral cell soma in the Mi, it was probable that most neurons isolated in this layer would be mitral cells. To confirm that recorded neurons were mitral cells and to assess the morphology of mitral cells in the slice, a small number of neurons were filled with biocytin. Cells that responded to ONL stimulation were filled by 1 hr of recording through the biocytin-containing electrode.

Five neurons at the Mi were filled in this manner. Although the degree of filling varied, all were clearly identifiable as mitral cells. Camera lucida drawings of three well-filled mitral cells are presented in Figure 31. These mitral cells retained their primary dendrite and its arborization in the glomerular layer. The extent of the secondary dendrites is probably reduced in all three cells, although in two of the three, secondary dendrites extend for more than 500 μm from the soma.

Mitral cell Membrane Properties. Whole-cell patch recordings were obtained from 53 neurons. Membrane potentials measured immediately after break of the membrane patch ranged from -40 to -77 mV. Cells with resting potentials more positive than -50 mV were stabilized by injection of current. Cells that required more than 10 pA to block spontaneous action potentials were not tested further. Successfully patched mitral cells were held for periods ranging from 10 min to 2 hr.

Membrane resistances, measured by injection of a 0.1 nA hyperpolarizing current of 100 to 500 msec duration, ranged from 100 to 600 M Ω (mean 272 ± 123 SD) (Figure 32A). These membrane resistances are 10 to 20 times higher than those (10-20 M Ω) previously measured in rats *in vivo* using sharp electrodes (^{133, 138, 139, 202, 203}). Mitral cell membrane resistances in isolated turtle olfactory bulb (30-100 M Ω ; ¹⁹⁸) were higher than those measured in mammals *in vivo*, but still much lower than those measured in the present experiments. Very high (1008 ± 566 [SD] M Ω) membrane resistances were recently reported in mitral cells of salamander olfactory bulb using whole cell patch recording (²⁰⁰, in press).

In all but two cells in the present study, the response to a hyperpolarizing current injection decayed to half amplitude in less than 10 msec (Figure 32A). These membrane time constants were shorter than those measured in isolated turtle bulb (24 to 93, mean 52 msec; ¹³⁵). A probable cause for the shorter membrane time constant in the slice preparation is partial transection of secondary dendrites during preparation of the slice.

Spontaneous action potentials were seen in some mitral cells. As shown in Figure 32C, spontaneous spikes were usually followed by a brief hyperpolarization, but never by a long-duration afterhyperpolarization (AHP). Moreover, there was no apparent accommodation of spike discharge during a prolonged depolarization produced by current injection (Figure 32B). Thus, it appears that, unlike many other large-projection neurons, mitral cells do not have calcium-activated conductances that limit their excitability.

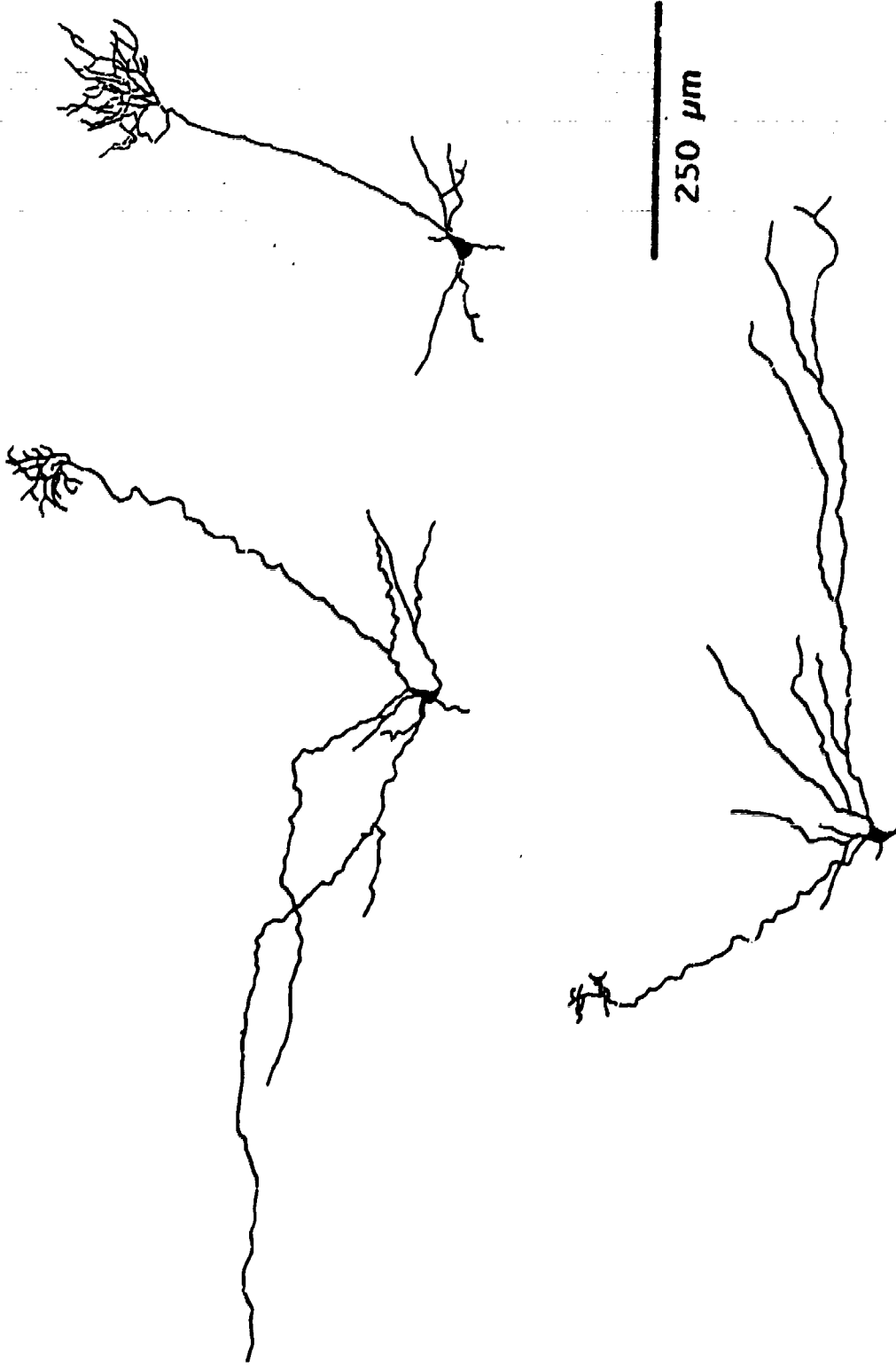


Figure 31. Biocytin-filled mitral cells in olfactory bulb slices. Cells were filled by contact with a recording pipette filled with 1% biocytin and traced at 20X magnification. The morphologies of these neurons are similar to mitral cells stained by classical methods.

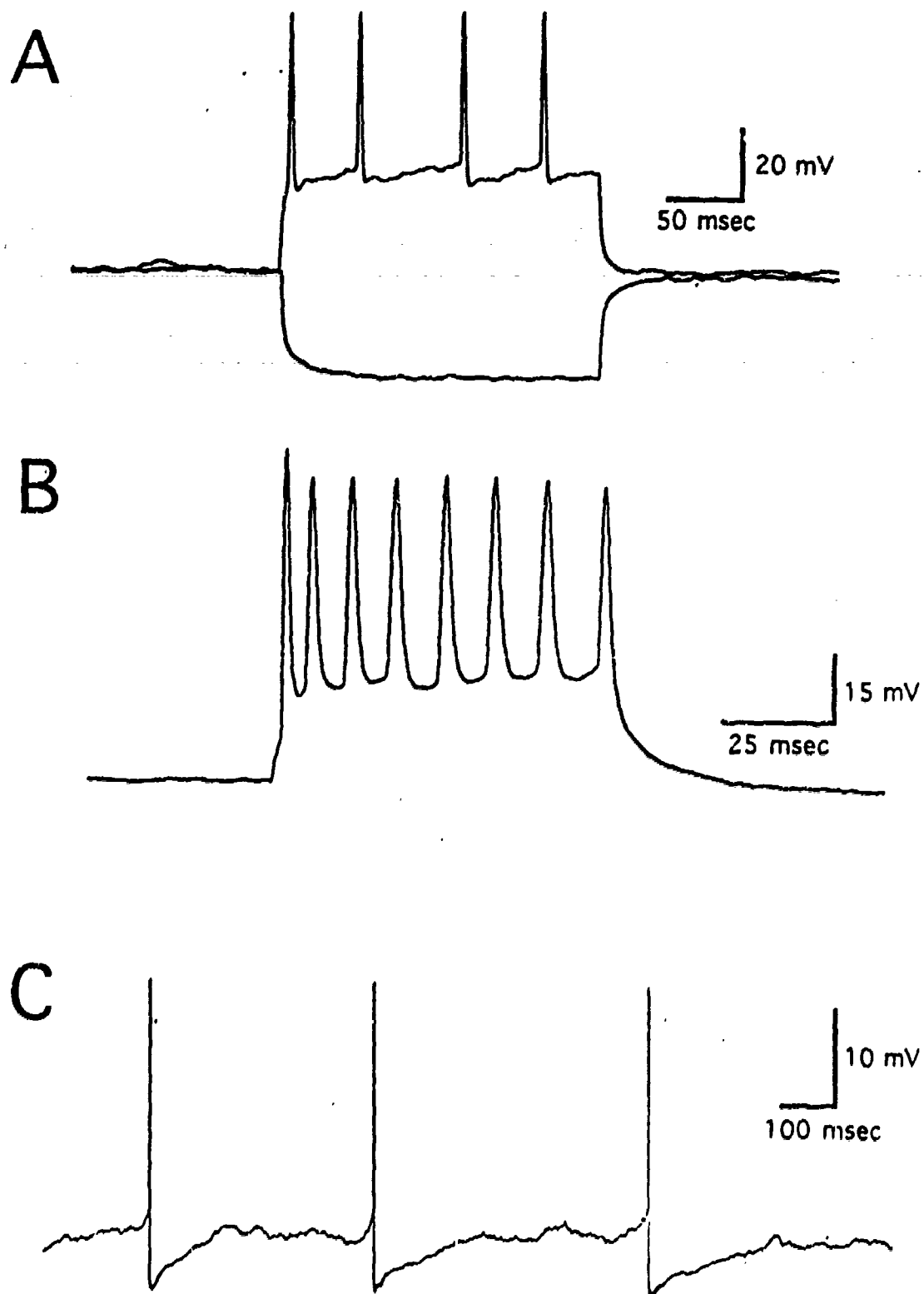


Figure 32. Mitral cell membrane properties. A. Membrane voltage response to 200 msec, 100 pA, hyperpolarizing and depolarizing currents. B. Multiple spikes in response to a 75 msec, 100 pA, depolarizing current. Spike frequency is constant during the depolarizing current. C. Spontaneously occurring action potentials.

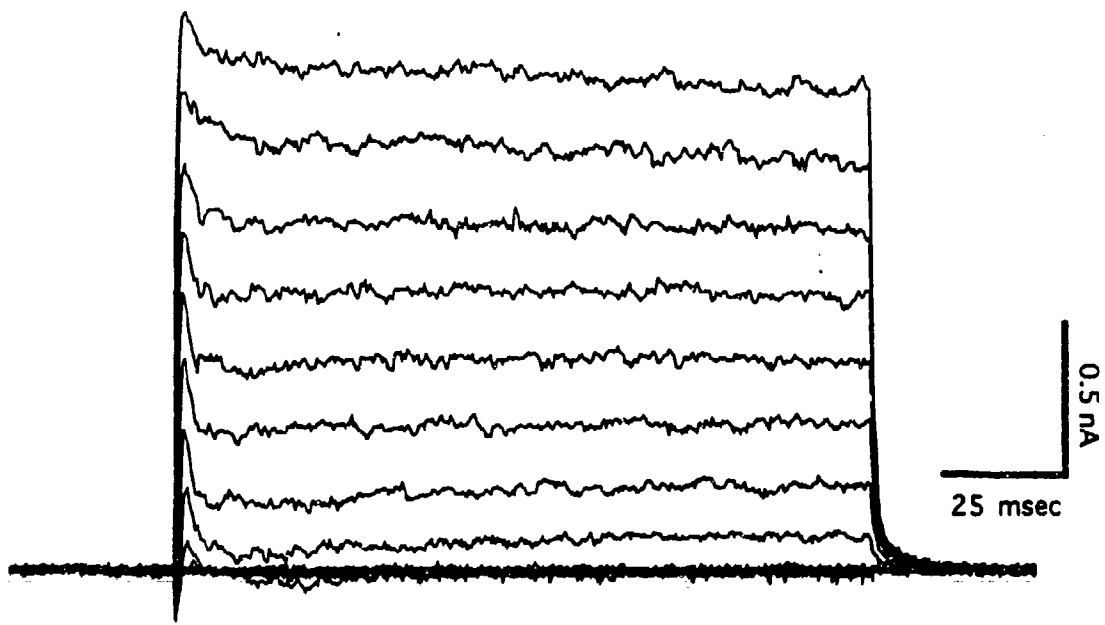
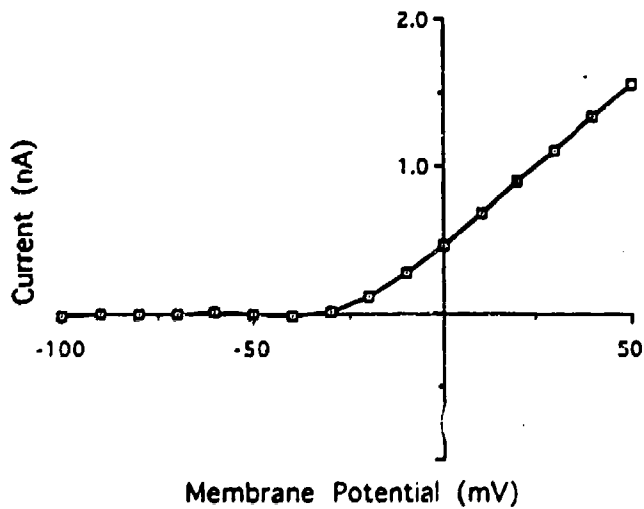
A**B**

Figure 33. Mitral cell membrane currents measured under voltage clamp. Fast Na^+ currents were blocked by $5 \mu\text{M}$ TTX. Leak currents are subtracted. A. Current responses to voltage steps between -100 and $+50$ mV. B. Current-voltage curve derived from data in A. The current values are means of current over the final $1/3$ of the voltage step.

Current-voltage (I-V) curves for voltage-clamped mitral cells were generated by stepping the command potential from -100 to +50 mV from a holding potential of -60 mV. I-V curves were determined for 10 mitral cells. In four additional cells, the slice was treated with 2 μ M TTX to block fast sodium currents. In neither normal nor TTX-treated mitral cells were there any detectable active currents for voltage jumps between -100 and -60 mV (Fig. 33). In the non-TTX-treated cells, voltage steps to membrane potentials below -50 mV resulted in repetitive spikes. In the TTX-treated cells, voltage steps to membrane potentials less negative than -40 mV resulted in large outward currents (Fig. 33).

Spontaneous Depolarizing Potentials. In about a third of the mitral cells studied, small spontaneous depolarizing potentials were present. The polarity of these potentials did not reverse at any potential between -50 and -100 mV, confirming their excitatory nature. Figure 34 illustrates several characteristics of these potentials in a cell for which the spontaneous depolarizations were especially distinct. A raster scan showing a typical epoch from this recording is shown in Figure 34A. The amplitude and duration of a 10 second sample from this record were measured using a commercial program (AxoGraph, Axon Instruments, Inc.). The mean amplitude of 44 spontaneous potentials in this interval was 2.95 ± 0.91 mV (mean \pm SD). The largest depolarization was 5.8 mV. The membrane resistance of this cell was 300 M Ω ; therefore, a 1 mV depolarization corresponds to a synaptic current of approximately 3 pA. Thus, the mean synaptic current was approximately 8.9 ± 2.7 pA, and the largest deflection corresponds to a synaptic current of 17.4 pA. Spontaneous currents of similar amplitude were measured under voltage clamp. The amplitude of these spontaneous potentials is within the range of currents expected of miniature excitatory postsynaptic potentials (⁶³).

The half-amplitude duration of these depolarizing potentials was 10 ± 2.2 msec (mean \pm SD). The frequency distribution of the durations of these potentials is shown in Figure 34C; a histogram plotting the frequency of spontaneous potentials as a function of their amplitude is shown in Figure 34B. The number of potentials is greatest for the range 2.0 to 2.5 mV; the number of events decreases for larger amplitudes. Events smaller than 2 mV could not be reliably distinguished from the background noise and were not included in the statistics; thus, below 2 mV the frequency of potentials may continue to increase. The observed distribution of amplitudes could arise if quantal currents of similar amplitude are distributed over the entire apical dendrite. Synaptic conductances in distal parts of the dendrite presumably produce smaller depolarization at the soma than synaptic events in more proximal parts of the apical dendrite.

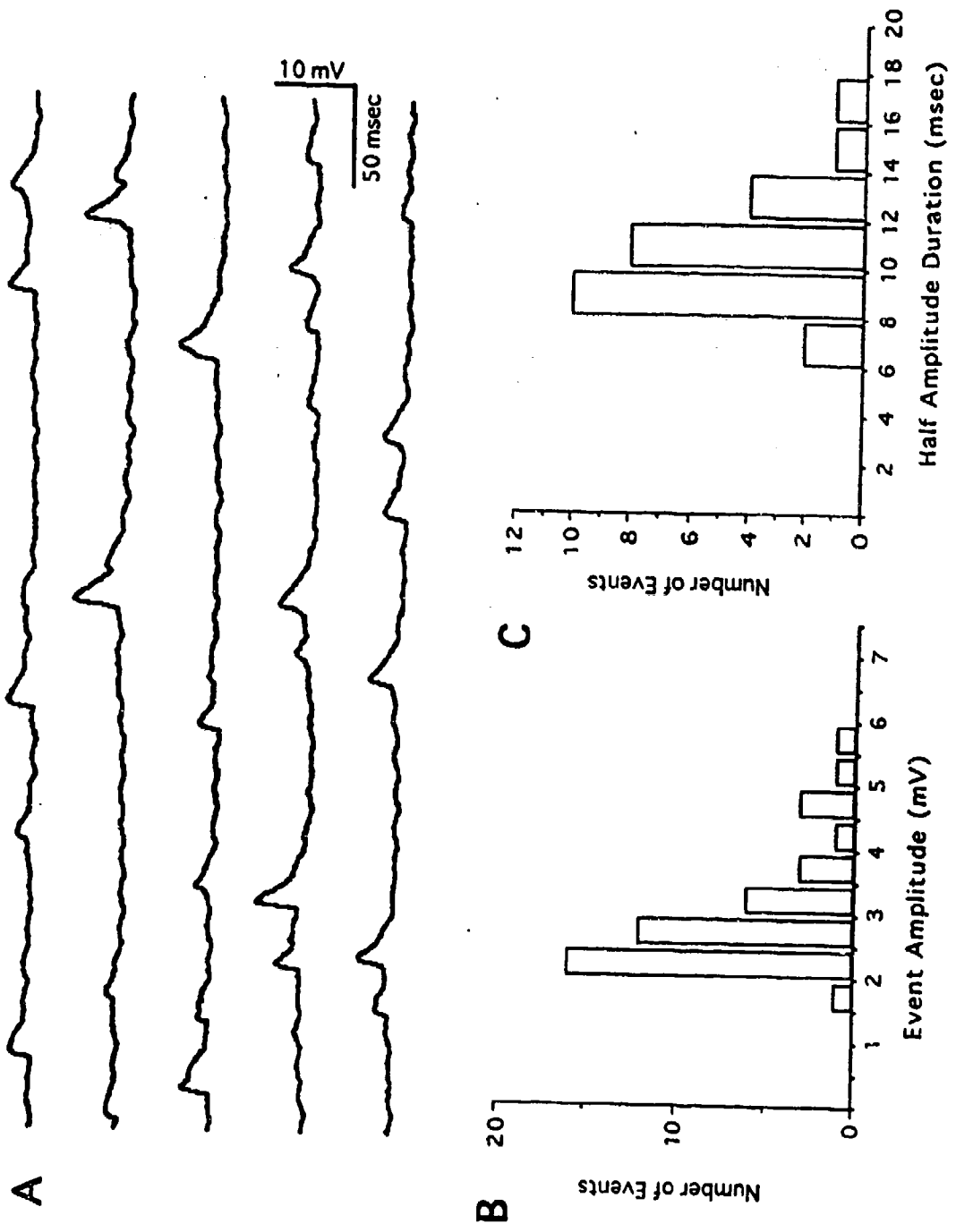


Figure 34. Spontaneous excitatory potentials in mitral cells. A. Raster scan of spontaneous excitatory potentials. B. Histogram of spontaneous potential amplitudes. C. Histogram of spontaneous potential half-amplitude durations.

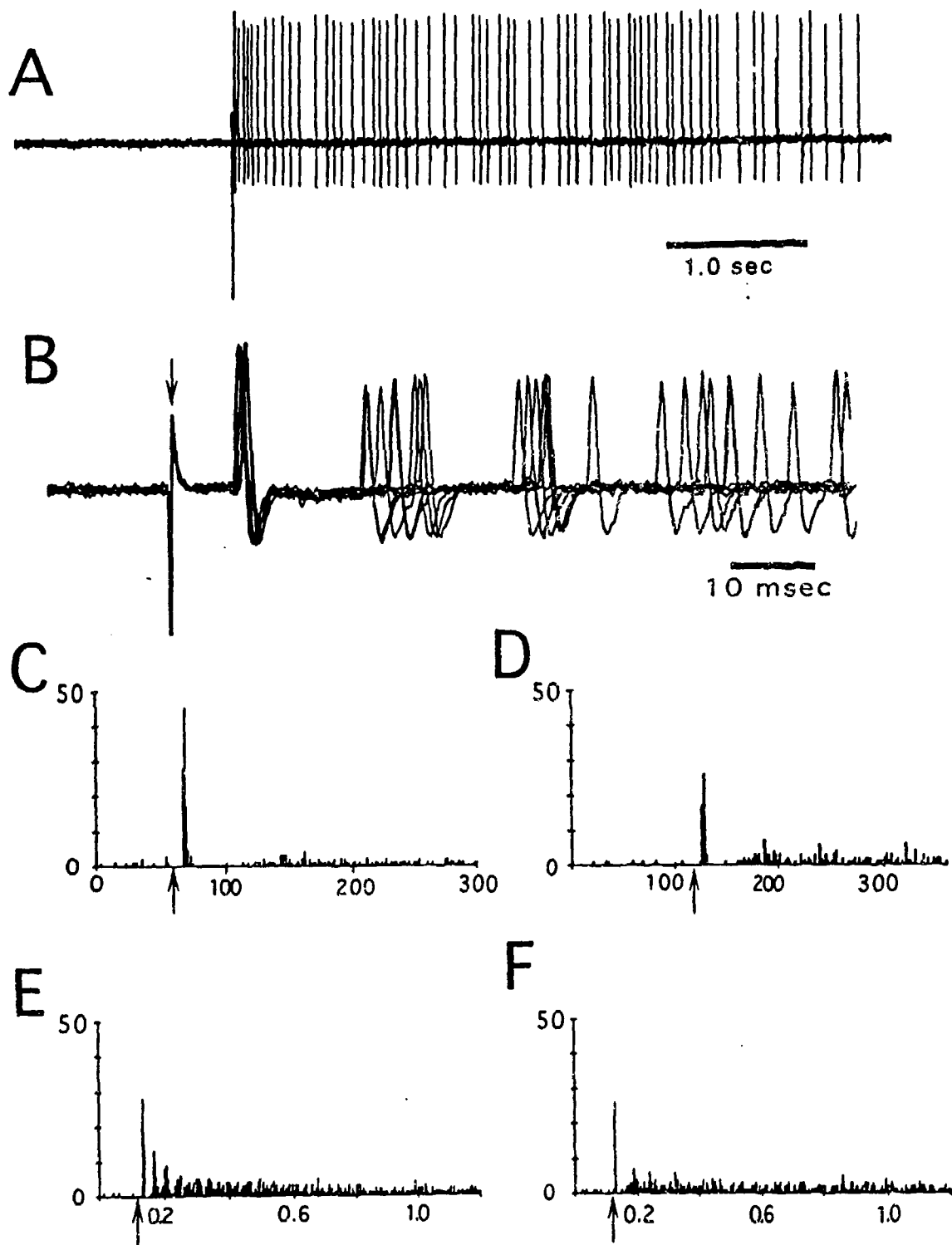


Figure 35. Extracellularly recorded responses of cells in the mitral cell layer to stimulation of the olfactory nerve layer. (ONL). A. Extracellularly recorded response to stimulation of olfactory nerve layer. B. Superposition of 8 responses to ONL stimulation. Note nearly constant latency of first spike. C.-E. Peristimulus time histogram (PSTH) records of typical extracellularly recorded mitral cell activity following single ONL shocks. In each PSTH record the stimulus occurs at the upward arrow. Time axis scales in C and D are in msec; in E and F the time scale is in seconds. PSTH are the accumulated responses to 50 shocks given every 4 sec.

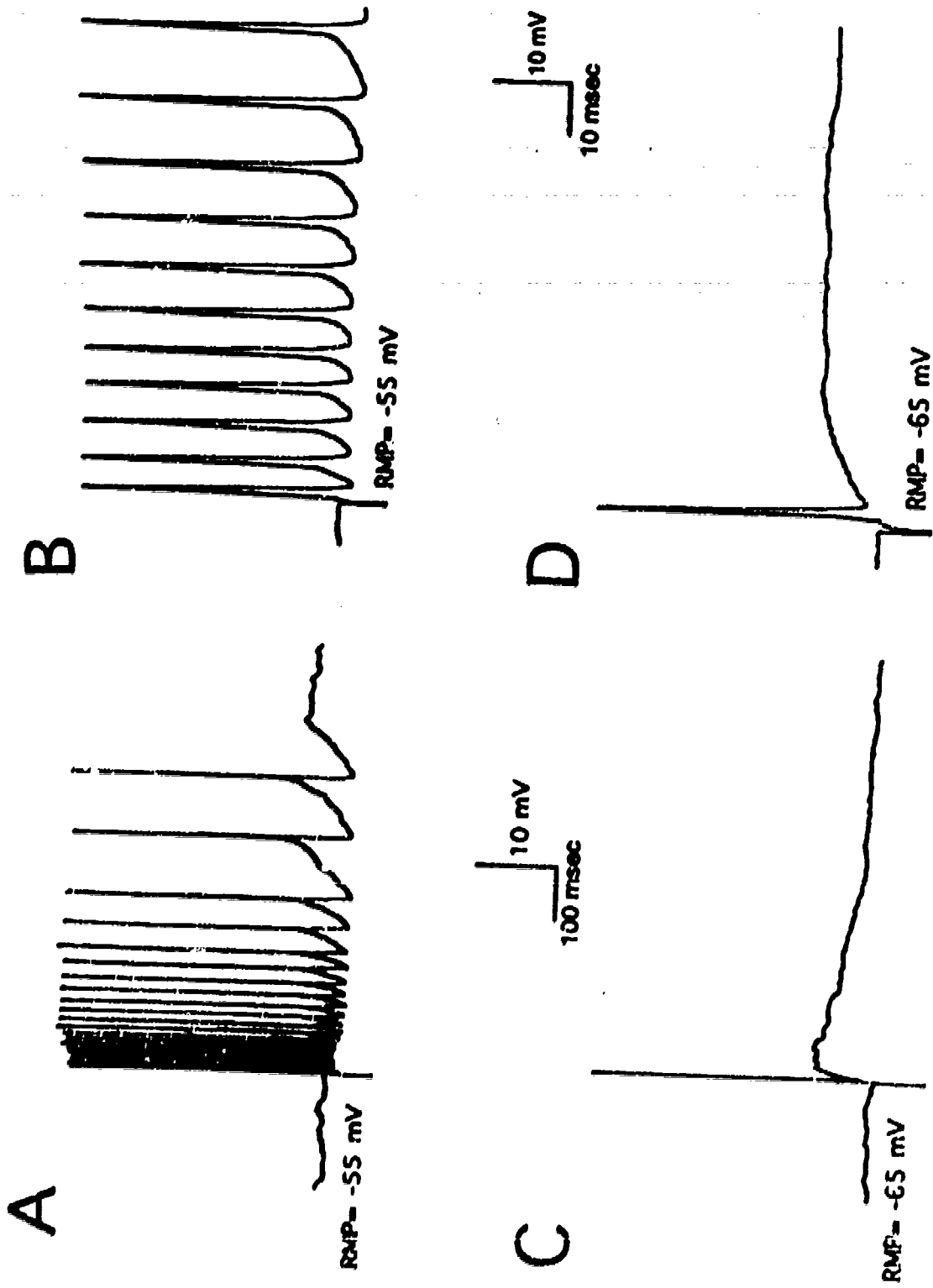


Figure 36. EPSP responses to olfactory nerve layer stimulation. A and B. Membrane potential at -55 mV. C and D. Membrane potential increased to -65 mV by injection of current. All spikes except the first are blocked. The sweep rate in B and D is 10 times that in A and C.

Synaptic Response to ONL Stimulation.

Extracellular Recordings. The approach of the electrode tip to a cell membrane was signified by increased electrode resistance. At this point positive pressure was terminated and negative pressure was applied in order to form a gigaseal. As the seal resistance increased, about 20% of the neurons began to fire spontaneous action potentials. Frequently, the seal resistance could not be increased beyond a few hundred M Ω ; thus, whole-cell recording was not possible. However, these low-resistance seals did allow stable high-amplitude extracellular recordings of spike activity. The extracellular activity of 85 cells thus recorded was analyzed.

Most mitral cells could be recorded for long periods of time (> 20 min). These cells fired at low spontaneous rates, between 1 and 4 Hz. The firing of some mitral cells (~20%) oscillated with a period of several minutes from near silence to a spike discharge rate of several 1-5Hz. Similar patterns are observed in extracellular recordings from mitral cells *in vivo* in this laboratory (Jiang et al., unpublished observations). Persistence of similar spontaneous patterns of oscillation in the slice suggests that they are generated within the olfactory bulb.

We attempted to obtain synaptic responses to stimulation of the ONL in 75 extracellularly recorded neurons. Excitatory responses were obtained in 39 (52%) of these cells. Mitral cells in the slice typically responded to the ONL shock with a single constant-latency spike followed by a 20-30 msec period of inhibition. Most (85%) of these cells also exhibited a prolonged (0.5 to 2 sec) period of weaker excitation following the period of inhibition. The range of latencies of the initial spike was 3-10 msec. Perfusion of the slice with high-magnesium (10 mM), low-calcium solution to block synaptic activity, eliminated both the synaptic response and the spontaneous activity (n=5). This suggests that in the absence of synaptic input, mitral cells have little or no intrinsic spontaneous activity.

Extracellular responses of several mitral cells to ONL stimulation are illustrated in Figure 35. The mitral cell illustrated in Figure 35A responded to a single ONL shock with a period of excitation lasting several seconds. In Figure 35B eight responses of another cell to ONL stimulation are superimposed at a higher sweep rate. The initial spike has a nearly constant latency of approximately 8 msec. The second and third spikes follow at 15 msec intervals.

Figures 35C-F show peristimulus time histogram (PSTH) records of the responses of other mitral cells to ONL stimulation. In each PSTH record, a single ONL shock was applied at the upward arrow. In Figure 35C the ONL shock is followed by a single, nearly constant latency spike, and a period of inhibition. In this cell, there was little additional activity following the period of inhibition. Figures 35D and 35E illustrate the responses of another mitral cell at two different time scales. In this cell, 43

of 46 initial responses to 50 ONL shocks fall into one of two 2 msec bins, thus indicating constant latency (6 msec) of the initial spike. The duration of the post-excitatory inhibition is 28 msec. Following this period of inhibition the cell fired at a discharge rate higher than its spontaneous rate for a period longer than the 1.2 sec duration of the PSTH record (Figure 35F). Figure 35E illustrates the response of another cell; this cell responded to ONL stimulation with an oscillatory response similar to that seen in Figure 35B. The first spike occurs at a short constant latency; the second and third spikes following ONL stimulation occur at relatively constant intervals, resulting in secondary peaks. These repetitive peaks are similar to the oscillatory responses that follow weak stimulation of the olfactory nerve *in vivo* (67, 68).

The patterns of spikes that follow ONL stimulation provide some information concerning the underlying excitatory synaptic conductance. The initial short-latency spike requires a rapid depolarization; the long-duration excitation may require a long duration excitatory process. These conclusions were confirmed with intracellular recordings.

Whole-Cell Patch Recordings of Synaptic Responses. Whole-cell patch clamp recordings of synaptic responses to ONL stimulation were obtained from 15 neurons. One cell responded to an ONL shock with a single spike followed by an apparent IPSP, three cells responded with a slow EPSP that lacked an initial rapid rise, and four responded with short duration (30 msec) EPSPs. The synaptic responses of the remaining seven neurons were consistent with the predominant pattern of extracellular responses. These responses are illustrated in Figures 36 and 37. In Figure 36A, ONL stimulation produces a train of action potentials lasting 600 msec. Figure 36B shows the same response with the time scale expanded 10 times. Hyperpolarization of the membrane to -65 mV blocked all spikes except the first and revealed the underlying EPSP (Figure 36C and 36D). The EPSP reaches its peak in about 20 msec; the depolarization persists for more than 800 msec.

The response of another cell to ONL stimulation is shown in Figure 37. With the membrane potential at -55 mV, a single shock to the ONL produces a longduration depolarization and a train of spikes (Figure 37A). As with the cell in Figure 36, a 10 mV hyperpolarization of the membrane potential to -65 mV blocked all but the initial spike (Figure 37B). Hyperpolarization of the mitral cell soma to -120 mV caused only occasional failure of this initial spike (Figures 37C and 37D). This difficulty in blocking the initial spike was characteristic of all mitral cells tested. Blockade of this spike always required hyperpolarization to a potential significantly more negative than that required to block all subsequent spikes. The least hyperpolarization required to blocked the initial spike was -80 mV in one cell; for all other cells greater hyperpolarization was needed.

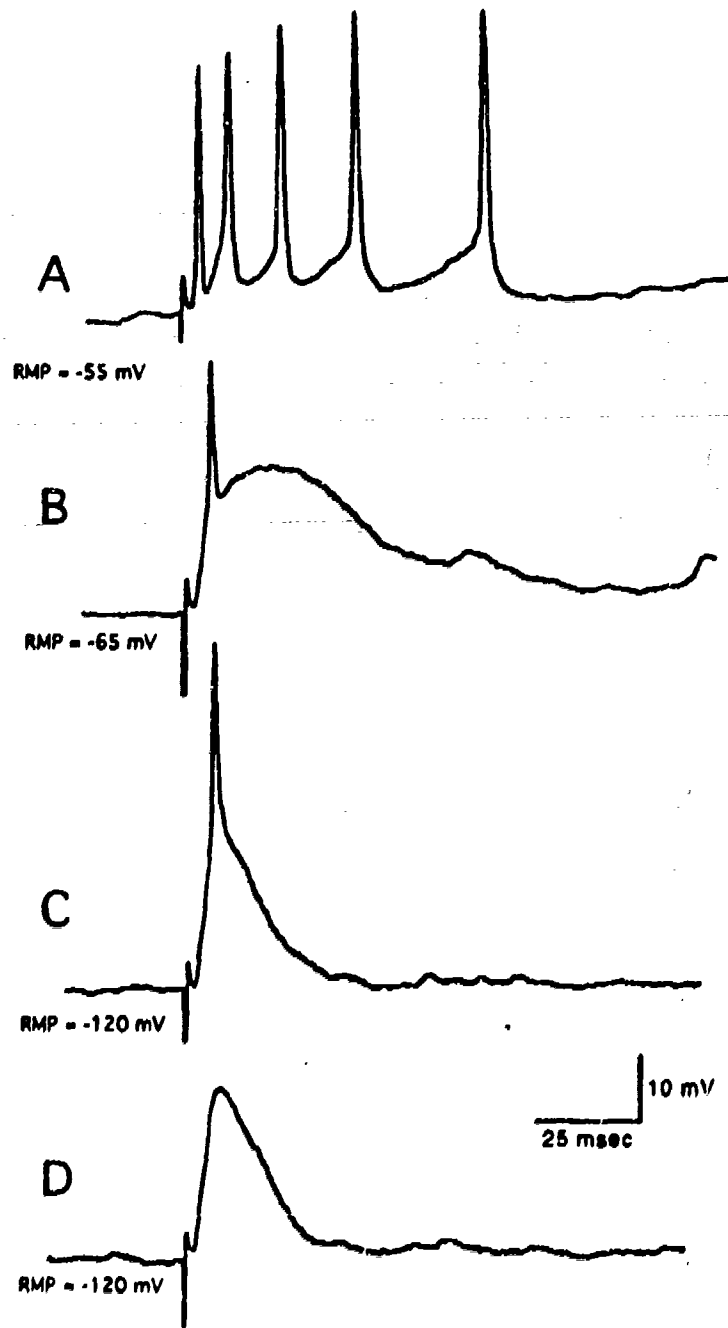


Figure 37. Spike generation in the mitral cell apical dendrite. A. At the resting membrane potential, olfactory nerve stimulation causes a burst of action potentials and a long duration depolarization. B. Hyperpolarization to -55 mV blocks all but the first spike. C. and D. Hyperpolarization of the soma to -120 mV causes occasional failures of the initial spike.

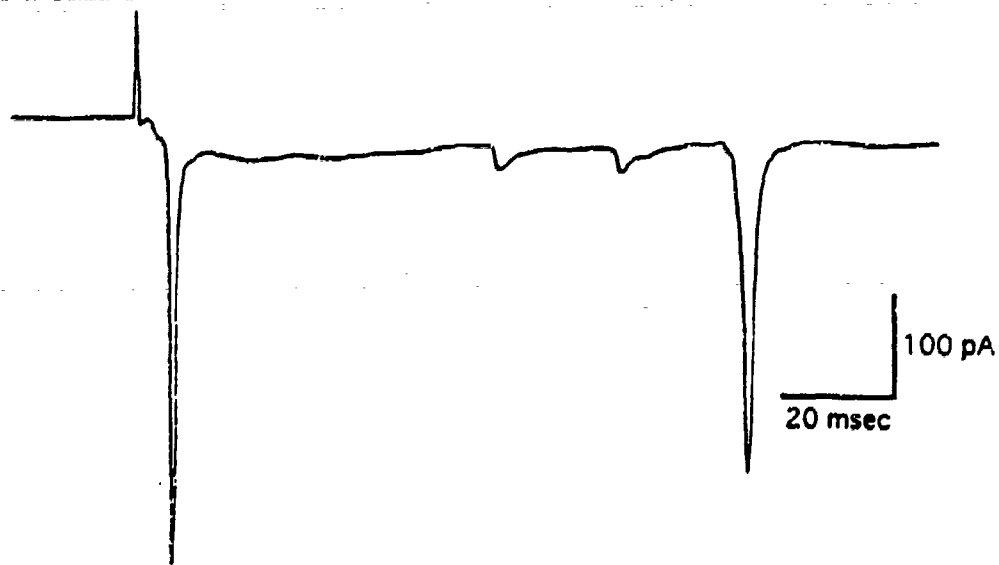


Figure 38. Voltage clamp record of mitral cell response to olfactory nerve layer stimulation. Olfactory nerve layer stimulation results in fast inward currents even though the soma membrane is clamped at -70 mV.

Blank page for Tables 4 and 5

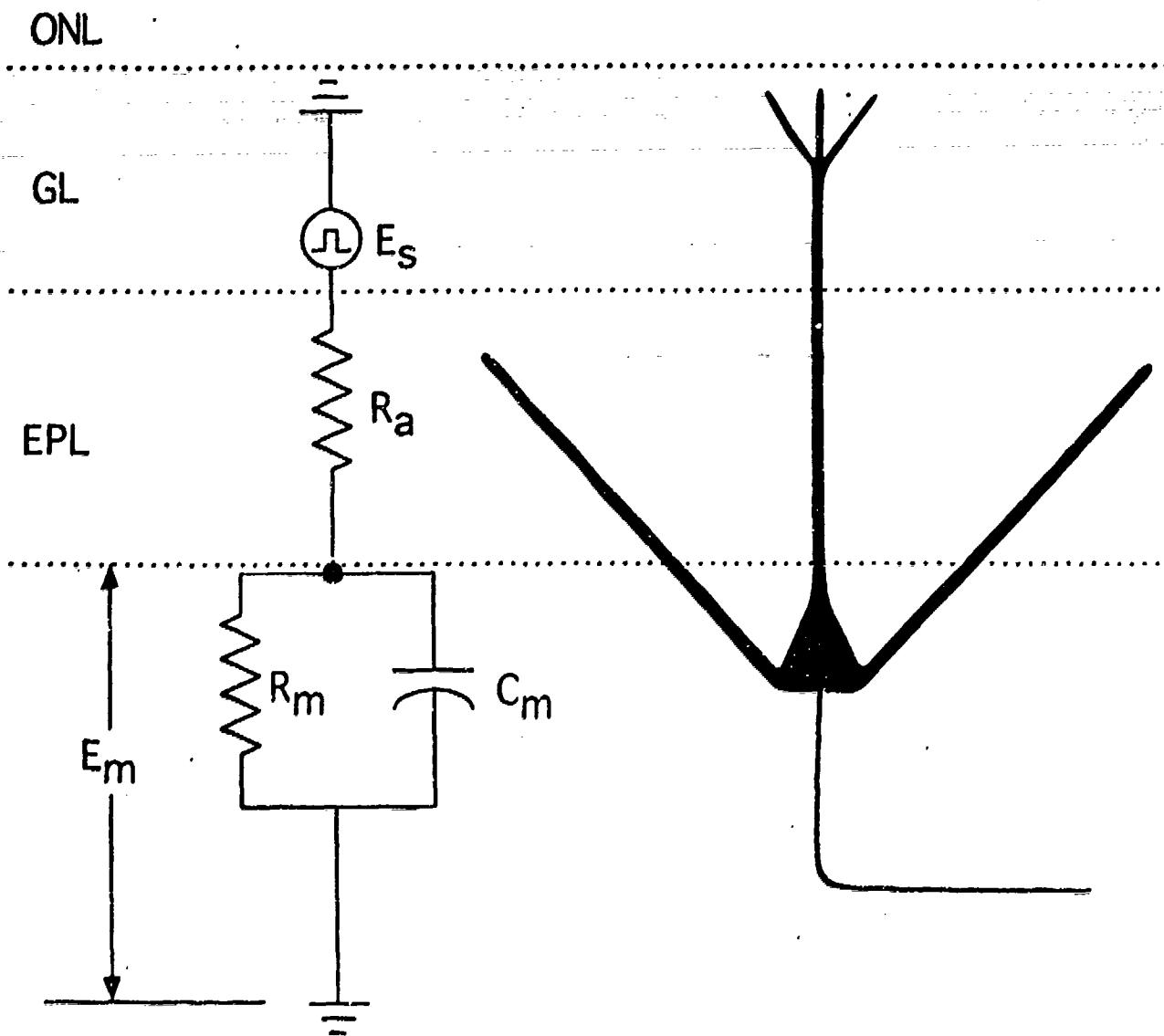


Figure 39. Voltage division between axial resistance of the apical dendrite and the membrane resistance of the mitral cell. Voltage changes E_s in the apical dendrite generated by synaptic currents or regenerative spikes are coupled to the soma through the axial resistance of the primary dendrite, R_a . R_a is estimated at about $25\text{ M}\Omega$. The impedance of the soma, Z_m , is represented by the parallel combination of the membrane resistance, R_m , and the membrane capacitance, C_m . The fraction of a depolarization in the apical tuft that appears at the soma is determined by voltage division between R_a and Z_m .

The amplitude of the ONL-evoked EPSPs did not increase linearly with membrane potential, as would be expected if the EPSP is caused by the opening of a single ohmic conductance in the apical dendrite. This is illustrated in Figure 37, where the amplitude of the EPSP is increased only 20% when the membrane potential of the soma is increased from -65 to -120 mV. Also in Figure 37, the time-to-peak amplitude and the duration of the EPSP are markedly shortened by hyperpolarization. Similar effects of membrane potential on the time course of the EPSP were seen in other cells. These observations might be explained by a single voltage-sensitive ionic channel or by multiple channels having different time courses and ionic selectivities, but further experiments are required to determine the kinds of ionic channels activated by olfactory nerve stimulation.

The excitatory postsynaptic current (EPSC) produced by ONL stimulation was recorded during voltage clamp of the soma in two cells. The current record for one of these cells is illustrated in Figure 38 (holding potential, -70 mV). The time course of this current was similar to the time course of the depolarization recorded under current clamp conditions. In this record, small spontaneous inward currents are superimposed on the evoked EPSC. Two spikes (fast inward currents) occur after ONL stimulation. The occurrence of these spikes during voltage clamp of the soma is further evidence that the membrane potential in parts of the apical dendrite receiving synaptic input from the olfactory nerve is not controlled by voltage clamp of the soma.

DISCUSSION

As the length of the primary dendrite is comparable to thickness of the 400 μm slice, a large fraction of mitral cells might have been disconnected from the glomerular layer during preparation of the slice. Thus, the relatively high percentage (50%) of mitral cells that responded to ONL stimulation in the present experiments is somewhat surprising. This indicates that use of conventional (400 μm) thickness slices and an approximately horizontal plane of section that corresponds to the trajectory of axons in the ONL are probably optimal for obtaining synaptic responses of mitral cells to ONL stimulation in the slice. In thin (150 - 200 μm) olfactory bulb slices, many more primary dendrites would be severed (³¹). Primary dendrites tilt in a rostral direction (³³). A coronal section through the bulb might, therefore, sever substantially more primary dendrites than a horizontal section of equal thickness. Activation of olfactory nerve to mitral cell synapses also requires continuity of the nerve fibers from the ONL to the terminals in the glomeruli. Since these fibers run with an approximately horizontal trajectory in the ONL (²⁰²), their continuity in the slice is also optimized when the slice is cut in the horizontal plane.

There are a number of important similarities between the characteristics of mitral cells in the slice and in the intact olfactory bulb. Although many mitral cells in the slice were not spontaneously active, others fired action potentials at rates comparable to those observed *in vivo*. Mitral cells in the slice responded robustly to stimulation of the ONL. The initial portion of the *in vitro* response (a single spike followed by a period of inhibition) is similar to that observed *in vivo*. The long period of weak excitation following the excitatory-inhibitory response to ONL stimulation seen in many cells in the slice was not reported in most earlier *in vivo* studies. However, a similar long duration excitation was seen in the isolated turtle olfactory bulb following block of GABA_A-mediated inhibition (¹⁴⁷). The alternating periods of inhibition and excitation seen in some mitral cells in the slice following ONL stimulation (Figures 35B and 35E) are similar to the damped oscillations following peri-threshold olfactory nerve stimulation *in vivo* (^{67, 68}).

ONL stimulation in the rat olfactory bulb slice did not produce the large IPSPs that follow activation of the entire turtle olfactory nerve or the lateral olfactory tract (LOT) in the intact bulb. Electrical stimulation of the turtle olfactory nerve or of the rat LOT probably activates nearly all mitral cells, resulting in nearly maximal activation of the mitral/granule inhibitory system. In contrast, the focal electrical stimulation of the ONL in the present experiments activated only a small number of olfactory nerve axons. Thus, the responses of mitral cells in the slice may resemble the response to restricted orthodromic or antidromic stimulation of the intact bulb. Near-threshold stimulation of LOT or of the olfactory nerve generates only weak inhibition (or even facilitation) of the responses to succeeding shocks (^{91, 169, 187}). Thus, the responses of mitral cells in the slice to olfactory nerve activation are similar to those seen *in vivo* under comparable conditions of stimulation.

Electrical Properties of Mitral Cell Membranes.

Membrane Resistance. Membrane resistances of mitral cells (100-600 M Ω) in the present investigation were substantially higher than those measured in previous studies with sharp electrodes. The membrane resistance of rat mitral cells *in vivo* was 10 to 20 M Ω (^{138, 139, 203}). The membrane resistance of mitral cells in isolated turtle bulb (mean 60 M Ω) was higher than in the rat, but still substantially lower than was measured in the present experiments (¹³⁵). Thus, the 270 M Ω mean resistance of rat mitral cells in the present experiments is about 4 times the mean resistance of mitral cells in the isolated turtle olfactory bulb and at least 10 times the resistance of previous *in vivo* measurements of rat mitral cell membrane resistance. The high membrane resistances measured in the present study are, however, comparable to values recently obtained in salamander olfactory bulb mitral cells using the whole-cell patch technique (²⁰⁰).

One factor that contributes to higher mitral cell membrane resistances *in vitro* is transection of

some mitral cell secondary dendrites during preparation of the slice. Since the conductance of these secondary dendrites is in parallel with the soma, truncation of the secondary dendrites will increase membrane resistance measured at the soma.

A larger proportion of increased resistance, however, is probably due to the use of whole-cell patch rather than sharp electrode recording techniques. Previous whole cell patch clamp studies in other preparations have generally reported higher membrane resistances than were measured in similar experiments that used sharp-electrodes. This difference was investigated systematically for granule cells of the dentate gyrus (¹⁸⁵). For these neurons, the average membrane resistance measured with the whole cell patch technique was 4.2 times higher than the average resistance of similar cells measured with sharp electrodes. Thus, it is reasonable to suggest that the major reason for the higher membrane resistance measured in the present study is the use of whole-cell patch recording techniques and not to trimming of the secondary dendrites. This would imply that the resting membrane resistance of mitral cells in the intact bulb is several times higher than previously supposed. It follows that the length constant of mitral cell processes is much less than previously estimated (¹⁶⁰).

Active Currents. Mitral cells may be considered analogous to the pyramidal cells of the hippocampus, piriform cortex, and neocortex: Mitral cells are highly integrative neurons that have extensive synaptic contacts with interneurons. Some pyramidal cells exhibit a Ca^{++} -activated K^{+} conductance that causes the slow afterhyperpolarization (AHP) following action potentials. These slow potentials cause accommodation of spike discharge to a sustained depolarization. Spikes in mitral cells were not followed by a slow AHP, and there was no apparent accommodation of spike discharge during prolonged depolarization. Further, there was no evidence of outward currents following depolarization under voltage clamp. These observations are consistent with previous reports in isolated turtle bulb (¹⁹⁸) and in thin olfactory bulb slices (^{31, 32}). It appears, therefore, that the mitral cell lacks some of the modulatory currents present in some hippocampal, piriform cortex, and neocortical pyramidal cells.

Long-Duration Synaptic Excitation.

ONL stimulation produced a long-duration excitation of mitral cells. This prolonged excitation in the slice is similar to the long-duration excitation produced by olfactory nerve stimulation in isolated turtle bulb after blockade of Cl^{-} mediated inhibition by bicuculline or low Cl^{-} solution (¹⁴⁸). In the intact bulb, $GABA_A$ -mediated inhibitory conductances may be large enough to prevent detection of the long-duration excitation. It appears that the inhibitory conductances are more weakly activated by ONL stimulation in the slice than by olfactory nerve stimulation in the intact olfactory bulb, allowing the long duration excitation to be observed without blockade of $GABA_A$ -mediated inhibition. However, as noted earlier, the present experiments involved only restricted stimulation of the nerve layer. With similarly

restricted stimulation *in vivo*, intrabulbar inhibitory mechanisms are not activated to the same degree as with stimulation of larger numbers of olfactory nerve axons. Other factors may also be involved in the relatively reduced inhibition seen in the slice. Truncation of secondary dendrites would reduce excitatory inputs to granule cell dendrites thus reducing granule cell inhibitory feedback. In addition, the lack of anesthetic in the slice may also account for lower inhibition. Most of the *in vivo* studies of the mammalian olfactory bulb have used anesthetics that considerably enhance GABA-mediated inhibition (¹⁴³). Thus, the relative lack of ONL-activated post-excitatory inhibition seen in the present studies may be closer to the situation of odor-evoked activation of mitral cells in unanesthetized animals than that seen in anesthetized preparations in response to strong shocks applied to the ONL.

A consistent feature of mitral cell responses to ONL stimulation was the long duration of the EPSP. At least two mechanisms may be involved in generation of the prolonged EPSP. The *long duration* (1 sec or greater) of the depolarization suggests that it involves a second-messenger coupled mechanism. On the other hand, the *rapid risetime* (10 - 20 msec) of the EPSP, suggests that the potential is mediated by a ligand gated ion channel. One system that exhibits somewhat similar characteristics is the sympathetic ganglion, where one transmitter (ACh) activates both fast (nicotinic) and slow (muscarinic) responses (¹⁴⁸). Alternatively, there may be two different olfactory nerve transmitters acting upon two different receptors. There are now numerous examples of synapses that release both a conventional transmitter and a neuropeptide.

Although the long duration of the EPSP could be explained exclusively by transmitters(s) released from olfactory nerve terminals, at least three other plausible explanations have been suggested (¹⁴⁸): (1) Olfactory nerve terminals might release transmitter for an extended period, or the transmitter might be slowly removed or inactivated. (2) Peri- or juxtglomerular neurons activated by ONL stimulation might form excitatory synapses with mitral cell apical dendrites. This synapse might release a second, slowly acting, excitatory transmitter. (3) Peri- or juxtglomerular neurons might participate in reverberating circuits that maintain activity for an extended period after an ONL shock.

At present, the transmitter(s) released by primary olfactory nerve terminals are not known. The dipeptide carnosine is present in olfactory nerve terminals and meets some of the classical criteria for a transmitter (^{87, 88, 163}), but carnosine does not have clear excitatory effects on mitral cells (^{74, 112}). Thus, at the present time there are several hypotheses that could account for the rapid onset and long duration of the ONL-evoked EPSP in mitral cells. To distinguish among these possibilities, additional information is needed, in particular the identity of the transmitter(s) used at this synapse.

Spike Generation in Mitral Cell Apical Dendrites.

The initial spike response to ONL stimulation appears to arise in distal parts of the apical dendrite of the mitral cell. Hyperpolarization of the soma had no effect on this initial spike, but blocked all subsequent spikes. Therefore, these later spikes appear to be generated at the soma. The apical dendrite branches extensively in the glomerulus; distal parts of this dendrite are thus electrotonically distant from the soma. These distal processes would be less affected by hyperpolarization of the soma, and thus they might be brought to spike threshold by a strong local synaptic current even when the soma is hyperpolarized. The initial spike, therefore, appears to arise in the apical dendrite. Several previous studies also concluded that the mitral cell apical dendrite supports spikes. In *in vivo* rabbit olfactory bulb (¹³⁸), isolated turtle olfactory bulb (¹³³), and salamander olfactory bulb (⁸³), stimulation of the olfactory nerve produced both a full-amplitude spike and a small "fast pre-potential." Hyperpolarization of the soma by injection of current (100 - 500 pA) blocked the full-amplitude spike, leaving only the "fast pre-potential." The "fast pre-potential" was interpreted as evidence of regenerative spikes in the apical dendrite.

There are important differences between the present results and earlier descriptions of the "fast pre-potential." In the earlier studies, the amplitude of the "fast pre-potential" was only a small fraction of the amplitude of the action potential in the soma and did not propagate through the soma to the mitral cell axon. In contrast, in the present whole-cell patch recordings, the action potential in the apical dendrite almost always produced a full-amplitude all-or-nothing spike in the soma even when the soma was hyperpolarized to very high potentials. Thus, the apical dendrite appears to be electrically more tightly coupled to the soma than was the case in earlier studies that used sharp electrode recordings in intact olfactory bulb.

This tighter coupling is most easily explained by the higher membrane resistances measured with whole-cell patch recordings in the slice. A reasonable estimate of the axial resistance, R_a , of the mitral cell primary dendrite is about 25 M Ω (assuming a diameter of 6 μm , a length of 500 μm , and a specific resistance of 100 $\Omega\text{-cm}$ for the internal medium). If, as was the case in the present experiments, the mitral cell membrane resistance, R_m , is 200 M Ω , the axial resistance of the primary dendrite is negligible and the apical tuft is effectively short-circuited to the soma. However, in previous recordings with sharp electrodes, the measured cell membrane resistance R_m was similar to the estimated 25 M Ω axial resistance of the primary dendrite (R_a). In that case, the axial resistance of the primary dendrite and the membrane resistance of the mitral cell form a voltage divider that would reduce the voltage change in the soma caused by a depolarization in the apical dendrite (Figure 39).

The present findings reveal new mechanisms that contribute to the regulation of mitral cell excitation. First, the magnitude of the currents generated by the initial spike indicates that the entire apical dendrite, not just the distal portions, is invaded by the spike. Second, unlike the "fast pre-

potential" the initial spike invades the soma even when the soma is hyperpolarized by external current. A spike in the soma almost certainly propagates to the axon and, thus, to piriform cortex and other central olfactory structures. K^+ conductances evidently would have little efficacy in controlling propagation of these spikes through the soma, since hyperpolarization past the K^+ equilibrium potential is unable to block spike invasion of the soma. Shunting conductances in the secondary dendrites, however, might block propagation of the spike. When the peripheral and centrifugal afferent inputs to the olfactory bulb are present and active, GABA-activated Cl^- conductances in the secondary dendrites might reach the same magnitude as the axial resistance of the primary dendrite. In that situation, the voltage-division between the combined conductance of the soma and secondary dendrites and the axial resistance of the primary dendrite could reduce the amplitude of the apical dendritic spike sufficiently to block its propagation through the soma (Figure 39). Thus, one function of the mitral-granule inhibitory system located on the secondary dendrites may be to regulate the propagation of spikes originating in the apical dendrite through the soma to the piriform cortex.

These considerations emphasize the pivotal role of the apical dendrite in the function of the mitral cell. The anatomy of this dendrite suggests its specialization for conduction of current from the dendritic arborization in the glomerular layer to the soma. The apical dendrite is of unusually large diameter. In the rat the primary dendrite is unbranched and appears to be surrounded by a loose glial sheath (^{157, 158}); in the monkey olfactory bulb the apical dendrite of some mitral cells is myelinated (¹⁵⁸). Using the Golgi EM technique, Shipley and Zahm reported the presence of a unique glial sheath over virtually the entire length of the dendrite and found only rare synaptic specializations onto the primary dendrite (¹⁸⁰). These features of the primary dendrite are similar to the morphological specializations of axons that reduce their membrane capacitance and increase their electrotonic length. These morphological specializations, taken with the presently observed biophysical characteristics, suggest that the apical dendrite of the mitral cell is ideally suited for effective conduction of currents from the apical dendrite to the soma. In view of the relatively long distance between the olfactory nerve synapses onto the distal branches of the apical dendrite and the cell body located 300 - 400 μ m away, these characteristics of the mitral cell are probably required for efficient transmission of sensory information.

Conclusions

These experiments demonstrate that conventional slices of mature rat olfactory bulb are viable and retain response characteristics typical of mitral cells in the intact olfactory bulb. Mitral cells in the slice are spontaneously active and exhibit firing characteristics similar to those seen in mitral cells *in vivo*. The membrane resistance of mitral cells recorded with the whole cell patch technique is higher than in previous experiments that used conventional sharp-electrode recording methods. This higher measured impedance indicates that the length constant of mitral cell dendritic processes is significantly longer than previously estimated. Stimulation of the ONL in the slice produces a long-duration excitation of mitral cells. The apical dendrite sustains regenerative spikes during synaptic activation. These spikes can propagate through the mitral cell soma to the axon even when the soma is significantly hyperpolarized by injected current. Thus, spikes arising in the glomerular layer may propagate to the piriform cortex.

10. CONCLUSION: A TWO-STAGE MECHANISM FOR SOMAN-INDUCED SEIZURES

The results presented above provide a new picture of the events leading to induction of seizures by organophosphates. The sensitive probe for cellular stress, *FOS*, is generated in two structures very soon after soman intoxication. The first of these, PC, receives a very heavy cholinergic innervation from the basal forebrain and is the structure most susceptible to gross damage after soman exposure. Stimulation of the known source of the cholinergic input to the PC, the horizontal limb of the diagonal band, resulted in the same pattern of *FOS* expression in the ipsilateral PC as that caused by systemic soman. Thus, it appears that *FOS* may be an early marker for seizure-induced injury and that cholinergic hyperstimulation is causal to seizures.

The second structure expressing *FOS* soon after soman intoxication is the LC, the source of noradrenergic innervation of the forebrain. Studies from other laboratories had demonstrated that cholinergic agonists stimulate LC neurons. Thus, it was probable that the *FOS* in LC following soman intoxication reflected excessive activity of LC neurons caused by build up of ACh after destruction of the degradative enzyme AChE by soman. We tested this hypothesis directly by microinjecting soman into LC while recording from single-locus cells. As predicted, injection of soman caused LC neurons to increase their firing rate far above their normal physiological range. This increased activity was sustained for as long as 2 hr, the longest period examined. This increased firing probably accounts for the earlier observation that NE levels in forebrain are decreased by soman intoxication.

Taken together, these findings support a new hypothesis for the generation and maintenance of seizures by soman (¹⁷⁷). This hypothesis postulates that there are two stages in the generation of seizures by soman intoxication. In the first stage, cortical neurons, most important in the PC, are subjected to excess ACh as a result of AChE blockade. But, this direct effect of soman intoxication is accompanied by an excess of NE, which is secondary to accumulation of ACh in LC. Studies in other central neurons, primarily the hippocampal pyramidal cell, have shown that both NE and ACh can act through similar mechanisms to reduce the effectiveness of inhibitory conductances which would otherwise prevent the neuron from sustaining long trains of discharges. These conductances are activated by membrane depolarization or by the calcium ions which enter the cell after an action potential and block further depolarization and spiking. Both NE and ACh modulate the strength of these inhibitory currents through similar second-messenger systems (¹⁴⁴). The coupling of the two transmitters to the same effector systems suggests the possibility that there could be a synergistic (more than additive) interaction when both transmitters are present (¹⁷⁷). Even without this postulated synergism, however, it is clear that simultaneous excess of NE and ACh could lead to greater excitation than is possible with either transmitter alone, and that this simultaneous excess of NE and ACh could be a necessary condition for generation of seizures in the target cortex.

NE levels drop rapidly in seizing but not in nonseizing, soman-intoxicated rats. This observation is compatible with at least two scenarios for the involvement of NE in the generation of convulsions:

1. Depletion of NE depends on the degree of AChE inhibition in LC. In those animals in which AChE inhibition exceeds some threshold, LC neurons may fire at a rate which results in release of NE beyond the ability of the cell to synthesize the transmitter. The rapid release of NE might be the trigger necessary for generation of convulsions in these animals. In animals with slightly more residual AChE activity, regulatory processes within LC might maintain LC neuron firing rates at a physiologically sustainable level; this lower rate of NE release might be insufficient to drive target neurons into convulsive activity. The difference between convulsing and nonconvulsing rats might then reflect the amount of AChE in one critical region of the brain.

2. NE might be decreased in seizing but not nonseizing rats because of secondary effects of the convulsions such as anoxia or buildup of toxic substances (⁶⁴). In this case, NE might be rapidly released in both convulsive and nonconvulsive rats. NE might be essential to the generation of seizures, but differences in NE release would not be the trigger.

Two observations suggest that NE decreases are not the result of general effects of seizures. First, NE levels in guinea pig cortex and hippocampus are decreased at 15 and 30 min after soman intoxication, before the beginning of convulsions (⁶⁶). Second, other monoamines are not changed or have increased turnover following OP intoxication, suggesting that monoamine synthetic pathways are not impaired (^{66, 72}).

The present data provide no direct measure of the rate of release of NE. However, the rapid decline of NE levels in convulsing animals strongly suggests rapid release of the transmitter. The decrease in total NE presumably reflects exhaustion of stored NE by rapid release. After exhaustion of stored transmitter, release would be limited by the maximum rate of neosynthesis. Thus, it is probable that soman intoxication results in an initial surge in NE release. There is no available evidence on the rate of release after this initial surge.

Once seizures are triggered, however, both NE and ACh might become unnecessary for their maintenance. It has long been known that prolonged electrical or chemical stimulation of cortical inputs can cause permanent convulsive activity. One possible explanation for these observations is the phenomenon of long-term potentiation (LTP), in which tetanic stimulation of excitatory amino acid (EAA) inputs to a cortical structure results in permanent strengthening of synaptic connections. A particular class of EAA receptor (NMDA receptors) is required for generation of LTP, and pharmacological blockade of this receptor can block both LTP and seizures (^{25, 128, 129, 151, 174, 189}).

Thus, there may be two stages in the generation of soman-induced seizures (¹⁷⁸).

1. Initial induction. In the first stage, excess ACh and (as argued here) NE result in removal of normal regulatory processes from neurons in PC. As a result, cortical neurons increase their firing rate, therefore increasing the amount of EAA they themselves release onto other cortical neurons. Mutually excitatory reciprocal interactions between cortical neurons then lead to positive feedback of stimulation, activation of NMDA receptors, and seizures.

2. Maintained expression. Once initiated, the rapid firing of these neurons associated with convulsions might cause strengthening of synaptic connections; eventually, relatively little excess ACh and NE might be needed to sustain the convulsions. Thus, in the second stage, seizures might become independent of cholinergic or adrenergic mechanisms.

These hypotheses have important therapeutic implications:

1. Involvement of NE in generation of seizures. If excess NE is necessary for soman-induced seizures, then the well-developed pharmacology of adrenergic receptors may provide promising therapeutic approaches. It has already been shown that the α_2 -agonist clonidine provides significant protection against soman-induced convulsions (²⁸⁻³⁰). Adams and Foote have shown that clonidine blocks the excitatory action of carbachol on LC neurons (²). A likely basis of this effect is the ability of this agonist to inhibit firing of LC neurons by stimulation of autoreceptors on LC neurons (^{43, 118}). It is probable that by combining clonidine with antagonists of postsynaptic adrenergic receptors and cholinergic antagonists, soman-generated seizures could be prevented without the use of barbiturates or excitatory amino acid antagonists.

The use of adrenergic agents which have been in clinical use for many years to prevent seizures and resulting brain damage might have significant advantages over the use of NMDA antagonists to suppress seizures. The NMDA antagonists are relatively untested clinically, may increase brain injury (¹⁵⁰), and, at doses necessary to prevent seizures, may cause psychological disturbances. Thus, if effective, adrenergic agents such as clonidine offer an attractive alternative therapy.

2. Independence of seizures and ACh after induction of convulsions. The possibility that, after some threshold is passed, convulsions may become independent of cholinergic or adrenergic mechanisms, suggests that timing of treatment is critical. During induction of seizures, treatment with cholinergic blockers and adrenergic drugs may block seizures; however, once these seizures have been maintained for some undetermined time, these agents may be ineffective, and sedatives or EAA antagonists may be necessary.

3. Importance of early treatment. Our finding of *FOS* expression at very short times after soman administration may suggest that some damage is occurring to brain structures even before the onset of behavioral convulsions and long before gross brain damage would be visible in histological sections. Thus, immediate treatment of exposed personnel is imperative.

REFERENCES

- 1 Abercrombie, E. D. and Finlay, J. M., Monitoring extracellular norepinephrine in brain using in vivo microdialysis and HPLC-EC. In Robinson, T. E. and Justice, J. B., Jr(Eds.), *Microdialysis in the Neurosciences*, Vol. 7, Elsevier, Amsterdam, 1991, pp.253-274.
- 2 Adams, L. M. and Foote, S. L., Effects of locally infused pharmacological agents on spontaneous and sensory-evoked activity of locus coeruleus neurons, *Brain Research Bulletin*, 21(1988) 395-400.
- 3 Albanese, A. and Butcher, L. L., Locus Ceruleus somata contain both acetylcholinesterase and norepinephrine: direct histochemical demonstration on the same tissue section, *Neuroscience Letter*, 14(1979) 101-104.
- 4 Albanese, A. and Butcher, L. L., Acetylcholinesterase and catecholamine distribution in the locus coeruleus of the rat, *Brain Research Bulletin*, 5(1980) 127-134.
- 5 Altman, J., Autoradiographic and histological studies of postnatal neurogenesis -- II. A longitudinal investigation of the kinetics, migration, and transformation of cells incorporating tritiated thymidine in infant rats, with special reference to postnatal neurogenesis in some brain areas, *Journal of Comparative Neurology*, 128(1966) 431-474.
- 6 Altman, J., Autoradiographic and histological studies of postnatal neurogenesis -- IV. Cell proliferation and migration in the anterior forebrain, with special reference to persisting neurogenesis in the olfactory bulb, *Journal of Comparative Neurology*, 137(1969) 433-458.
- 7 Altman, J. and Das, G. D., Autoradiographic and histological studies of postnatal neurogenesis -- I. A longitudinal investigation of the kinetics, migration, and transformation of cells incorporating tritiated thymidine in neonate rats, with special reference to postnatal neurogenesis in some brain regions, *Journal of Comparative Neurology*, 137(1966) 433-458.
- 8 Amaducci, L., Forno, K. I. and Eng, L., Glial fibrillary acidic protein in cryogenic lesions of the rat brain, *Neuroscience letter*, 21(1981) 27-32.
- 9 Arimatsu, Y., Seto, A. and Amano, T., An atlas of alpha-bungarotoxin binding sites and structures containing acetylcholinesterase in the mouse central nervous system, *Journal of Comparative Neurology*, 198(1981) 603-631.
- 10 Aronstam, R. S., Smith, M. D. and Buccafusco, J. J., Clonidine protection from soman and ecothiophate toxicity in mice, *Life Sciences*, 39(1986) 2097-2102.
- 11 Aston-Jones, G., Astier, B. and Ennis, M., Inhibition of noradrenergic locus coeruleus neurons by C1 adrenergic cells in the rostral ventral medulla, *Neuroscience*, 48(1992) 371-381.
- 12 Aston-Jones, G., Ennis, M., Pieribone, V. A., Nickell, W. T. and Shipley, M. T., The brain nucleus locus

- coeruleus: restricted afferent control of a broad efferent network, *Science*, 234(1986) 734-737.
- 13 Aston-Jones, G., Foote, S. L. and Bloom, F. E., Low doses of ethanol disrupt sensory responses of brain noradrenergic neurones, *Nature*, 296(1982) 857-860.
- 14 Aulisi, E. F. and Valentino, R. J., Carbachol-induced increases in locus coeruleus spontaneous activity are associated with an altered pattern of response to sensory stimuli, *Neuroscience Letters*, 74(1987) 297-303.
- 15 Bannon, M. J., Bunney, E. B. and Roth, R. H., Mesocortical dopamine neurons: rapid transmitter turnover compared to other brain catecholamine systems, *Brain Research*, 218(1981) 376-382.
- 16 Barry, D. I., Kikvadze, I., Brundin, P., Bolwig, T. G., Bjorklund, A. and Lindvall, O., Transplanted noradrenergic neurons suppress seizure development in kindling-induced epilepsy, *Proceeding of National Academy of Science USA*, 84(1987) 8712-8715.
- 17 Bartel, D. P., Sheng, M., Lau, L. F. and Greenberg, M. E., Growth factors and membrane depolarization activate distinct programs of early response gene expression: Dissociation of fos and jun induction, *Genes. Dev.*, 3(1989) 304-313.
- 18 Benardo, L. S. and Prince, D. A., Ionic mechanisms of cholinergic excitation in mammalian hippocampal pyramidal cells, *Brain Research*, 249(1982) 333-344.
- 19 Berridge, C. W. and Dunn, A. J., DSP-4-induced depletion of brain norepinephrine produces opposite effects on exploratory behavior 3 and 14 days after treatment, *Psychopharmacology*, 100(1990) 504-508.
- 20 Berridge, C. W. and Foote, S. L., Effects of locus coeruleus activation on electroencephalographic activity in neocortex and hippocampus, *Journal of Neuroscience*, 11(1991) 3135-3145.
- 21 Bird, S. J. and Kuhar, M. J., Iontophoretic application of opiates to the locus coeruleus, *Brain Research*, 122(1977) 523-533.
- 22 Blanton, M. G., LoTurco, J. J. and Kriegstein, A. R., Whole cell recording from neurons in slices of reptilian and mammalian cerebral cortex, *Journal of Neuroscience Methods*, 30(1989) 203-210.
- 23 Booze, R. M., Crisotomo, E. A. and Davis, J. N., Species differences in the localization and number of CNS Beta adrenergic receptors: Rat versus guinea pig, *J. Pharmacol. Exper. Ther.*, 249(1989) 911-920.
- 24 Boulat, O., Waldmeier, P. and Maitre, L., 3,4-Dihydroxyphenylacetic acid (DOPAC) as an index of noradrenaline turnover: effects of hydergine and vincamine, *Journal of Neural Transmission*, 82(1990) 181-195.
- 25 Braitman, D. J. and Sparenborg, S., MK-801 protects against seizures induced by the cholinesterase inhibitor soman, *Brain Research Bullitin*, 23(1989) 145-148.
- 26 Braun, In vivo noradrenaline release evoked in the anteroventral thalamic nucleus by locus coeruleus activation: An electrochemical study., *Neuroscience*, 52(1993) 961-972.

- 27 Brown, D. A. and Adams, P. R., Muscarinic suppression of a novel voltage-sensitive K current in a vertebrate neurone, *Nature*, 283(1980) 673-676.
- 28 Buccafusco, J. J., Clonidine inhibits the turnover of ACh in rat brain, *Brain Research Bulletin*, 13(1984) 257-262.
- 29 Buccafusco, J. J. and Aronstam, R. S., Clonidine protection from the toxicity of soman, an organophosphate acetylcholinesterase inhibitor, in the mouse, *J. Pharmacol. Exper. Ther.*, 239(1986) 43-47.
- 30 Buccafusco, J. J., Graham, J. H. and Aronstam, R. S., Behavioral effects of toxic doses of soman, an organophosphate cholinesterase inhibitor, in the rat: Protection afforded by clonidine, *Pharmacol. Biochem. Behav.*, 29(1988) 309-313.
- 31 Bufler, J., Zufall, F., Franke, C. and Hatt, H., Patch-clamp recordings of spiking and non-spiking interneurons from rabbit olfactory bulb slices: membrane properties and ionic currents, *Journal of Comparative Physiology*, 170(1992a) 153-159.
- 32 Bufler, J., Zufall, F., Franke, C. and Hatt, H., Patch-clamp recordings of spiking and non-spiking interneurons from rabbit olfactory bulb slices: GABA- and other transmitter receptors, *Journal of Comparative Physiology*, 170(1992b) 153-159.
- 33 Buonoviso, N., Chaput, M. A. and Scott, J. W., Mitral cell-to-glomerulus connectivity: An HRP study of the orientation of mitral cell apical dendrites, *Journal of Comparative Neurology*, 307(1991) 57-64.
- 34 Butcher, L. L., Recent advances in histochemical techniques for the study of central cholinergic mechanisms. In Jenden, D. J.(Eds.), *Cholinergic Mechanisms and Psychopharmacology*, Vol. Plenum Press, New York, 1978, pp.93-124.
- 35 Ceccatelli, S., Villar, M. J., Goldstein, M. and Hokfelt, T., Expression of c-Fos immunoreactivity in transmitter-characterized neurons after stress, *Proceeding of National Academy of Science USA*, 86(1989) 9569-9573.
- 36 Cederbaum, J. M. and Aghajanian, G. K., Activation of the locus coeruleus by peripheral stimuli: Modulation by a collateral inhibitory mechanism, *Life Sciences*, 23(1978) 1383-1392.
- 37 Cole, A. E. and Nicoll, R. A., Characterization of a slow cholinergic post-synaptic potential recorded in vitro from rat hippocampal pyramidal cells, *J. Physiol.*, 352(1984) 173-188.
- 38 Collins, G. G. S., Probett, G. A., Anson, J. and McLaughlin, N. J., Excitatory and inhibitory effects of noradrenaline on synaptic transmission in rat olfactory cortex slice, *Brain Research*, 294(1984) 211-223.
- 39 Diaz, J., Ellison, G. and Masouka, D., Stages of recovery from central norepinephrine lesions in enriched and impoverished environments: a behavioral and biochemical study, *Experimental Brain Research*, 31(1978) 117-130.

- 40 Dodd, J., Dingleline, R. and Kelly, S. J., The excitatory action of acetylcholine on hippocampal neurones of the guinea pig and rat maintained in vitro, *Brain Research*, 207(1981) 109-127.
- 41 Dutar, P. and Nicoll, R. A., Stimulation of phosphatidylinositol (PI) turnover may mediate the muscarinic suppression of the M-current in hippocampal pyramidal cells, *Neuroscience Letters*, 85(1988) 89-94.
- 42 Egan, T. M., Dagan, D., Kupper, J. and Levitan, I. B., Properties and rundown of sodium-activated potassium channels in rat olfactory bulb neurons, *Journal of Neuroscience*, 12(1992) 1964-1976.
- 43 Egan, T. M., Henderson, G., North, R. A. and Williams, J. T., Noradrenaline mediated synaptic inhibition in rat locus coeruleus neurones, *J. Physiol.*, 345(1983) 477-488.
- 44 Egan, T. M. and North, R. A., Acetylcholine acts on m2-muscarinic receptors to excite rat locus coeruleus neurones, *Br. J. Pharmacol.*, 85(1985) 733-735.
- 45 Egan, T. M. and North, R. A., Actions of acetylcholine and nicotine on rat locus coeruleus neurons in vitro, *Neuroscience*, 19(1986) 565-571.
- 46 El-Etri, M., Ennis, M., Shipley, M. T. and Nickell, W. T., Cholinolytic seizures: possible role of nucleus locus coeruleus (LC), *Neuroscience Abstract*, 17(1991) 529.
- 47 El-Etri, M., Nickell, W. T., Ennis, M., Skau, K. A. and Shipley, M. T., Brain norepinephrine reductions in soman-intoxicated rats: Association with convulsions and AChE inhibition, time course, and relation to other monoamines, *Experimental Neurology*, 118(1992) 153-163.
- 48 El-Etri, M., Shipley, M. T., Ennis, M. and Nickell, W. T., Cholinergic modulation of locus coeruleus: Possible role in cholinolytic seizures, *Neuroscience Abstract*, 16(1990) 1177.
- 49 El-Etri, M. M., Ennis, M., Jiang, M. and Shipley, M. T., Pilocarpine-induced convulsions in Rats: Evidence for muscarinic receptor-mediated activation of locus coeruleus and norepinephrine release in cholinolytic seizure development, *Experimental Neurology*, 121(1993) 24-39.
- 50 Ellman, G. L., Courtney, D., Andres, V., jr and Featherstone, R. M., A new and rapid colorimetric determination of acetylcholinesterase activity, *Biochemical Pharmacology*, 7(1961) 88-95.
- 51 Eng, L. and Shiurba, R. A., Glial fibrillary acidic protein: A review of structure, function, and clinical application, 1988) 339-359.
- 52 Eng, L. F. and Shiurba, R. A., Glial fibrillary acidic protein. In Marangos, P. J., Cambell, I. and Cohen, R. M.(Eds.), *Functional and Clinical Aspects of Neuronal and Glial Proteins*, Vol. 2, Academic Press, New York, 1987,
- 53 Engberg, G. and Svensson, T. H., Pharmacological analysis of a cholinergic receptor mediated regulation of brain norepinephrine neurons, *Journal of Neural Transmission*, 49(1980) 137-140.
- 54 Ennis, M. and Aston-Jones, G., Evidence for self- and neighbor- mediated postactivation inhibition of locus coeruleus neurons, *Brain Research*, 374(1986) 299-305.

- 55 Ennis, M. and Aston-Jones, G., Activation of locus coeruleus from nucleus paragigantocellularis: a new excitatory amino acid pathway in brain, *Journal of Neuroscience*, 8(1988) 3644-3657.
- 56 Ennis, M. and Aston-Jones, G., GABA-mediated inhibition of locus coeruleus from the dorsomedial rostral medulla, *Journal of Neuroscience*, 9(1989) 2973-2981.
- 57 Ennis, M. and Aston-Jones, G., Potent inhibitory input to locus coeruleus from the nucleus prepositus hypoglossi, *Brain Research Bulletin*, 22(1989) 793-803.
- 58 Ennis, M. and Shipley, M. T., Tonic activation of locus coeruleus neurons by Systemic or intracoerulear microinjection of an irreversible acetylcholinesterase inhibitor: Increased discharge rate and induction of C-fos, *Experimental Neurology*, 118(1992) 164-177.
- 59 Ennis, M., Shipley, M. T. and Behbehani, M. M., A double-labeling method for AChE and fluorescent retrograde tracers, *Brain Research Bulletin*, 24(1990) 113-118.
- 60 Eriksson-Nilsson, M., Bjorklund, H., Dahl, D., Olson, L. and Ingvar, M., Sustained seizures cause circumscribed cerebral changes in glial fibrillary acidic protein, neurofilament and laminin immunofluorescence, *Experimental Brain Research*, 69(1987) 155-166.
- 61 Fain, J. N. and Garcia-Sainz, J. A., Role of phosphatidylinositol turnover in alpha-1, and of adenylate cyclase inhibition in alpha-2 effects of catecholamines, *Life Sciences*, 26(1980) 1183-1194.
- 62 Fallon, J. H. and Moore, R. Y., Catecholamine innervation of the basal forebrain. III. Olfactory bulb, anterior olfactory nuclei, olfactory tubercle and piriform cortex, *Journal of Comparative Neurology*, 180(1978) 533-544.
- 63 Finch, D. M., Fisher, R. S. and Jackson, M. B., Miniature excitatory synaptic currents in cultured hippocampal neurons, *Brain Research*, 518(1990) 257-268.
- 64 Flynn, C. J. and Wecker, L., Elevated choline levels in the brain. A non-cholinergic component of organophosphate toxicity, *Biochemical Pharmacology*, 35(1986) 3115-3121.
- 65 Foote, S. L., Bloom, F. E. and Aston-Jones, G., Nucleus locus coeruleus: New evidence of anatomical and physiological specificity, *Physiological Rev.*, 63(1983) 844-914.
- 66 Fosbraey, P., Wetherell, J. R. and French, M. C., Neurotransmitter changes in guinea-pig brain regions following soman intoxication, *Journal of Neurochemistry*, 54(1990) 72-92.
- 67 Freeman, W. J., Depth recording of averaged evoked potential of olfactory bulb, *Journal of Neurophysiology*, 35(1972a) 780-796.
- 68 Freeman, W. J., Measurement of oscillatory responses to electrical stimulation in olfactory bulb of cat, *Journal of Neurophysiology*, 35(1972b) 762-769.
- 69 Frosch, M. P. and Dichter, M. A., Physiology and pharmacology of olfactory bulb neurons in dissociated cell culture, *Brain Research*, 290(1984) 321-332.

- 70 Fu, L., Shipley, M. T. and Aston-Jones, G., Dendrites of rat locus coeruleus neurons are asymmetrically distributed: Immunocytochemical LM and EM studies, *Society of Neuroscience Abstract*, 15(1989) 1013.
- 71 Gage, F. H., Olejniczak, P. and Armstrong, D. M., Astrocytes are important in sprouting in the septohippocampal circuit, *Exp. Neurol.*, 102(1988) 2-13.
- 72 Glisson, S. N., Karczmar, A. G. and Barnes, L., Effects of diisopropylfluorophosphate on acetylcholine, cholinesterase and catecholamines of several brain parts of rabbit brain, *Neuropharmacology*, 13(1974) 623-631.
- 73 Gonzales, R. A. and Crews, F. T., Cholinergic- and adrenergic-stimulated inositide hydrolysis in brain: Interaction, regional distribution, and coupling mechanisms, *Journal of Neurochemistry*, 45(1985) 1076-1084.
- 74 Gonzales-Estrada, M. T. and Freeman, W. J., Effects of carnosine of olfactory bulb EEG, evoked potentials and DC potentials, *Brain Research*, 202(1980) 373-386.
- 75 Gray, R. and Johnston, D., Noradrenaline and B-adrenoceptor agonists increase activity of voltage-dependent calcium channels in hippocampal neurons, *Nature*, 327(1987) 620-622.
- 76 Greenberg, E. M., Ziff, E. B. and Greene, L. A., Stimulation of neuronal acetylcholine receptors induces rapid gene transcription, *Science*, 3(1986) 80-83.
- 77 Guyenet, P. G. and Aghajanian, G. K., Acetylcholine, substance P, and met-enkephalin in the locus coeruleus: Pharmacological evidence for independent sites of action, *European Journal of Pharmacology*, 53(1979) 319-328.
- 78 Haas, H. L. and Konnerth, A., Histamine and noradrenaline decrease calcium-activated potassium conductance in hippocampal pyramidal cells, *Nature*, 302(1983) 432-434.
- 79 Haberly, L. B., Neuronal circuitry in olfactory cortex: anatomy and functional implications, *Chemical Senses*, 10 No. 2(1985) 219-238.
- 80 Halasz, N., Ljungdahl, A. and Hokfelt, T., Transmitter histochemistry of the rat olfactory bulb. II. Fluorescence histochemical, autoradiographic and electron microscopic localization of monoamines, *Brain Research*, 154(1978) 253-271.
- 81 Halliwell, J. V. and Adams, P. R., Voltage-clamp analysis of muscarinic excitation in hippocampal neurons, *Brain Research*, 250(1982) 71-92.
- 82 Hallman, H. and Jonsson, G., Neurochemical studies on central dopamine neurons -- regional characterization of dopamine turnover, *Med. Biol.*, 62(1984) 198-209.
- 83 Hamilton, K. A. and Kauer, J. S., Responses of mitral/tufted cells to orthodromic and antidromic electrical stimulation in the olfactory bulb of the tiger salamander, *Journal of Neurophysiology*, 59(1988) 1736-1755.

- 84 Hamilton, K. A. and Kauer, J. S., Patterns of intracellular potentials in salamander mitral/tufted cells in response to odor stimulation, *Journal of Neurophysiology*, 62(1989) 609-625.
- 85 Hass, H. L. and Konnerth, A., Histamine and noradrenaline decreases calcium-activated potassium conductance in hippocampal pyramidal cells, *Nature*, 302(1983) 432-434.
- 86 Herrera, D. G. and Robertson, H. A., N-methyl-D-aspartate receptors mediate activation of the c-fos proto-oncogene in a model of brain injury, *Neuroscience*, 35(1990) 273-281.
- 87 Hirsch, J. D., Grillo, M. and Margolis, F. L., Ligand binding studies in the mouse olfactory bulb: Identification and characterization of a L-[³H]carnosine binding site, *Brain Research*, 158(1978) 407-422.
- 88 Hirsch, J. D. and Margolis, F. L., L-[³H]carnosine binding in the olfactory bulb. II. Biochemical and biological studies, *Brain Research*, 174(1979) 81-94.
- 89 Hoskins, B., Fernando, J. C. R., Dulaney, M. D., Lim, D. K., Liu, D. D., Watanabe, H. K. and Ho, I. K., Relationship between the neurotoxicities of soman, sarin, and Tabun, and acetylcholinesterase inhibition, *Toxicol. Lett.*, 30(1986) 121-129.
- 90 Hunt, S. P., Pini, A. and Evan, G., Induction of c-fos-like protein in spinal cord neurons following sensory stimulation, *Nature*, 328(1987) 632-634.
- 91 Jahr, C. E. and Nicoll, R. A., An intracellular analysis of dendrodendritic inhibition in the turtle *in vitro* olfactory bulb, *J. Physiol.*, 326(1982) 213-234.
- 92 Jobe, P. C., Dailey, J. W. and Reigel, C. E., Noradrenergic and serotonergic determinants of seizure susceptibility and severity in genetically epilepsy-prone rats, *Life Sciences*, 39(1986) 775-782.
- 93 Jobe, P. C., Ko, K. H. and Dailey, J. W., Abnormalities in norepinephrine turnover rate in the central nervous system of the genetically epilepsy-prone rat, *Brain Research*, 290(1984) 357-360.
- 94 Jones, L. S., Gauger, L. L. and Davis, J. N., Anatomy of brain alpha-adrenergic receptors: In vitro autoradiography with [¹²⁵I]-heat, *Journal of Comparative Neurology*, 231(1985a) 190-208.
- 95 Jones, L. S., Miller, G., Gauger, L. L. and Davis, J. N., Regional distribution of rat brain alpha-1 adrenergic receptors: Correlation between [¹²⁵I]HEAT membrane binding and *in vitro* autoradiography, *Life Sciences*, 36(1985b) 45-51.
- 96 Jope, R. S., Morrisette, R. A. and Snead, O. C., Characterization of lithium potentiation of pilocarpine induced status epilepticus in rats, *Experimental Neurology*, 91(1986) 471-480.
- 97 Jordan, F. L. and Thomas, W. E., Brain macrophages: Questions of origin and interrelationship, *Brain Research Review*, 13(1988) 165-178.
- 98 Jovic, R. C., Correlation between signs of toxicity and some biochemical changes in rats poisoned by soman, *European Journal of Pharmacology*, 25(1973) 159-164.

- 99 Kayama, Y., Sumitomo, I. and Ogawa, T., Does the ascending cholinergic projection inhibit or excite neurons in the rat thalamic reticular nucleus, *Journal of Neurophysiology*, 56 No. 5(1986) 1310-1320.
- 100 Ko, K. H., Dailey, J. W. and Jobe, P. C., Effects of increments in norepinephrine concentrations on seizure intensity in the genetically epilepsy-prone rats, *Journal of Pharmacology and Experimental Therapeutics*, 222(1982) 662-669.
- 101 Kobayashi, R. M., Palkovits, M., Hruska, R. E., Rothchild, R. and Yamamura, H. I., Regional distribution of muscarinic cholinergic receptors in rat brain, *Brain Research*, 154(1978) 13-23.
- 102 L'Heureux, R., Dennis, T., Curet, O. and Scatton, B., Measurement of noradrenaline release in the rat cerebral cortex in vivo by transcortical dialysis: Effects of drugs affecting noradrenergic transmission., *J. Neurochem.*, 46(1986) 1794-1801.
- 103 Lemercier, G., Carpentier, P., Sentenae-Roumanou, H. and Morelis, P., Histological and histochemical changes in the central nervous system of the rat poisoned by an irreversible anticholinesterase organophosphorous compound, *Acta. Neuropathol.*, 61(1983) 123-129.
- 104 Levey, A. I., Hallanger, A. E. and Wainer, B. H., Cholinergic nucleus basalis neurons may influence the cortex via the thalamus, *Neuroscience Letters*, 74(1987) 1-13.
- 105 Levitt, P. and Noebels, J. L., Mutant mouse tottering: Selective increase of locus coeruleus axons in a defined single-locus mutation, *Proceeding of National Academy of Science USA*, 78(1981) 4630-4634.
- 106 Lewander, T., Joh, T. H. and Reis, D. J., Prolonged activation of tyrosine hydroxylase in noradrenergic neurones of rat brain by cholinergic stimulation, *Nature*, 258(1975) 440-441.
- 107 Lewander, T., Joh, T. H. and Reis, D. J., Tyrosine hydroxylase: delayed activation in central noradrenergic neurons and induction in adrenal medulla elicited by stimulation of central cholinergic receptors, *The Journal of Pharmacology and Experimental Therapeutics*, 200 No. 3(1977) 523-534.
- 108 Libet, B., Gleason, C. A., Wright Jr., E. W. and Feinstein, B., Suppression of an epileptiform type of electrocortical activity in the rat by stimulation in the vicinity of locus coeruleus, *Epilepsia*, 8(1977) 451-462.
- 109 Lidbrink, P., The effects of lesions of the ascending noradrenaline pathways on sleep and waking in the rat, *Brain Research*, 74(1974) 19-40.
- 110 Liu, D. D., Ueno, E., Ho, I. K. and Hoskins, B., Evidence that alterations in gamma-aminobutyric acid and acetylcholine in rat striata and cerebella are not related to soman-induced convulsions, *Journal of Neurochemistry*, 51(1988) 181-187.
- 111 Louis, W., J., Papanicolaou, J., Summers, R. J. and Vajda, F. J. E., Role of central b-adrenoceptors in the control of pentylentetrazole-induced convulsions in rats, *British Journal of Pharmacology*, 75(1982) 441-446.

- 112 MacLeod, N. K. and Straughan, D. W., Responses of olfactory bulb neurones to the dipeptide carnosine, *Experimental Brain Research*, 34(1979) 183-188.
- 113 Madison, D. V., Lancaster, B. and Nicoll, R. A., Voltage clamp analysis of cholinergic action in the hippocampus, *Journal of Neuroscience*, 7(1987) 733-741.
- 114 Madison, D. V. and Nicoll, R. A., Noradrenaline blocks accommodation of pyramidal cell discharge in the hippocampus, *Nature*, 299(1982) 636-638.
- 115 Madison, D. V. and Nicoll, R. A., Actions of noradrenaline recorded intracellularly in rat hippocampal CA1 pyramidal neurons, in vitro, *J. Physiol. (Lond)*, 372(1986) 221-244.
- 116 Mair, R. G., Gellman, R. L. and Gesteland, R. C., Postnatal proliferation and maturation of olfactory bulb neurons in the rat, *Neuroscience*, 7(1982) 3105-3116.
- 117 Mair, R. G. and Gesteland, R. C., Response properties of mitral cells in the olfactory bulb of the neonatal rat, *Neuroscience*, 7(1982) 3117-3125.
- 118 Marwaha, J. and Aghajanian, G. K., Related potencies of alpha-1 and alpha-2 antagonists in the locus coeruleus, dorsal raphe and dorsal lateral geniculate nuclei: an electrophysiological study, *J. Pharmacol. Exp. Ther.*, 222(1982) 287-293.
- 119 Mason, S. T. and Corcoran, M. E., Catecholamines and convulsions, *Brain Research Review*, 170(1979) 497-507.
- 120 McCormick, D. A. and Prince, D. A., Two types of muscarinic response to acetylcholine in mammalian cortical neurons, *Proc. Natl. Acad. Sci. USA*, 82(1985) 6344-6348.
- 121 McDonough, J. H., Jaax, N. K., Crowley, R. A., Mays, M. Z. and Modrow, H. E., Atropine and/or diazepam therapy protects against soman-induced neural and cardiac pathology, *Fundam. Appl. Toxicol.*, 13(1989) 256-276.
- 122 McLean, J. H. and Shipley, M. T., Serotonergic afferents to the rat olfactory bulb: II. Changes in fiber distribution during development, *Journal of Neuroscience*, 7(1987) 3029-3039.
- 123 McLean, J. H. and Shipley, M. T., Postmitotic, postmigrational expression of tyrosine hydroxylase in olfactory bulb dopaminergic neurons, *Journal of Neuroscience*, 8(1988) 3658-3669.
- 124 McLean, J. H. and Shipley, M. T., Neuroanatomical substrates of olfaction. In Serby, M. and Chobor, K. (Eds.), *The Science of Olfaction*, Vol. Springer-Verlag, New York, 1992, pp.126-171.
- 125 McLean, J. H., Shipley, M. T., Nickell, W. T., Aston-Jones, G. and Reyher, C. K., Chemoanatomical organization of the noradrenergic input from locus coeruleus to the olfactory bulb of the adult rat, *Journal of Comparative Neurology*, 285(1989) 339-349.
- 126 MacLeod, N. K., Leod, C. J., jr, Singer, A. W. and Harrington, D. G., Acute neuropathology in soman poisoned rats, *Environmental Applied Toxicology*, 5(1984) 53-58.

- 127 Mermet, Electrically evoked noradrenaline release in the rat hypothalamic paraventricular nucleus studied by *in vivo* electrochemistry: Autoregulation by alpha-2 receptors., *Neuroscience*, 34(1990) 423-432.
- 128 Millan, M. H., Patel, S. and Meldrum, B. S., The involvement of excitatory amino acid receptors within the prepiriform cortex in pilocarpine-induced seizures in rats, *Experimental Brain Research*, 72(1988) 517-522.
- 129 Millan, M. H., Patel, S., Mello, L. M. and Meldrum, B. S., Focal injection of 2-amino-7-phosphonoheptanoic acid into prepiriform cortex protects against pilocarpine-induced limbic seizures in rats, *Neuroscience Letters*, 70(1986) 69-74.
- 130 Morgan, J. I., Cohen, D. R., Hempstead, J. L. and Curran, T., Mapping patterns of c-fos expression in the central nervous system after seizure, *Science*, 237(1987) 192-197.
- 131 Mori, K. and Kishi, K., The morphology and physiology of the granule cells in the rabbit olfactory bulb revealed by intracellular recording and HRP injection, *Brain Research*, 247(1982) 129-133.
- 132 Mori, K., Kishi, K. and Ojima, H., Distribution of dendrites of mitral, displaced mitral, tufted, and granule cells in the rabbit olfactory bulb, *Journal of Comparative Neurology*, 219(1983) 339-355.
- 133 Mori, K., Nowycky, C. and Shepherd, G. M., Impulse activity in presynaptic dendrites: analysis of mitral cells in the isolated turtle olfactory bulb, *Journal of Neuroscience*, 2(1982) 497-502.
- 134 Mori, K., Nowycky, M. C. and Shepherd, G. M., Analysis of synaptic potentials in mitral cells in the isolated turtle olfactory bulb, *Journal of Physiology*, 314(1981) 295-309.
- 135 Mori, K., Nowycky, M. C. and Shepherd, G. M., Electrophysiological analysis of mitral cells in the isolated turtle olfactory bulb, *Journal of Physiology*, 314(1981) 281-294.
- 136 Mori, K., Nowycky, M. C. and Shepherd, G. M., Synaptic excitatory and inhibitory interactions at distal dendritic sites on mitral cells in the isolated turtle olfactory bulb, *Journal of Neuroscience*, 4 No. 9(1984) 2291-2296.
- 137 Mori, K. and Shepherd, G. M., Synaptic excitation and long-lasting inhibition of mitral cells in the *in vitro* turtle olfactory bulb, *Brain Research*, 173(1979) 155-159.
- 138 Mori, K. and Takagi, S. F., Spike generation in the mitral cell dendrite of the rabbit olfactory bulb, *Brain Research*, 100(1975) 685-689.
- 139 Mori, K. and Takagi, S. F., An intracellular study of dendrodendritic inhibitory synapses on mitral cells in the rabbit olfactory bulb, *J. Physiol.*, 279(1978) 569-588.
- 140 Mueller, A. L. and Dunwiddie, T. V., Anticonvulsant and proconvulsant actions of alpha and beta-noradrenergic agonists on epileptiform activity in rat hippocampus, *Epilepsia*, 24(1983) 57-64.
- 141 Nickell, W. T., Behbehani, M. M. and Shipley, M. T., *In vitro* synaptic activation of adult rat olfactory

bulb mitral cells recorded by conventional and whole cell patch techniques, Society of Neuroscience Abstract, 18(1992) 1200.

142 Nickell, W. T. and Shipley, M. T., Neurophysiology of magnocellular forebrain inputs to the olfactory bulb in the rat: frequency potentiation of field potentials and inhibition of output neurons, *Journal of Neuroscience*, 8(1988) 4492-4502.

143 Nicoll, R. A., The effects of anaesthetics on synaptic excitation and inhibition in the olfactory bulb, *J. Physiol.*, 223(1972) 803-814.

144 Nicoll, R. A., The coupling of neurotransmitter receptors to ion channels in the brain, *Science*, 241(1988) 545-551.

145 Norgren, R. B., jr. and Lehman, M. N., A double-label pre-embedding immunoperoxidase technique for electron microscopy using diaminobenzidine and tetramethylbenzidine as markers, *Journal of Histochemistry and Cytochemistry*, 37(1989) 1283-1289.

146 Nowycky, M. C., Halasz, N. and Shepherd, G. M., Evoked field potential analysis of dopaminergic mechanisms in the isolated turtle olfactory bulb, *Neuroscience*, 8 No. 4(1983) 717-722.

147 Nowycky, M. C., Mori, K. and Shepherd, G. M., GABAergic mechanisms of dendrodendritic synapses in isolated turtle olfactory bulb, *Journal of Neurophysiology*, 46(1981a) 639-648.

148 Nowycky, M. C., Mori, K. and Shepherd, G. M., Analysis of a long-duration inhibitory potential in mitral cells in the isolated turtle olfactory bulb, *J. Physiol.*, 314(1981b) 311-320.

149 Nowycky, M. C., Mori, K. and Shepherd, G. M., Blockade of synaptic inhibition reveals long-lasting synaptic excitation in isolated turtle olfactory bulb, *Journal of Neurophysiology*, 46 No. 3(1981c) 649-658.

150 Olney, J. W., Labruyere, J. and Price, M. T., Pathological changes induced in cerebrocortical neurons by phencyclidine and related drugs, *Science*, 244(1989) 1360-1362.

151 Olney, J. W., Price, M. T., Zorumski, C. F. and Clifford, D. B., Cholinotoxic syndromes: Mechanisms and protection. In Moore, D. H.(Eds.), *Proceedings of the Workshop on Convulsions and Related Brain Damage Induced by Organophosphorus Agents*, Vol. U.S. Army Medical Research Institute of Chemical Defense, Aberdeen Proving Grounds, Maryland, 1990, pp.147-161.

152 Ormandy, G. C., Jope, R. S. and Snead, O. C., Anticonvulsant actions of MK-801 on the lithium-pilocarpine model of status epilepticus in rats, *Experimental Neurology*, 106(1989) 172-180.

153 Ormandy, G. C., Jope, R. S. and Snead, O. C., Analysis of the convulsant-potentiating effects of lithium in rats, *Experimental Neurology*, 111(1991) 356-361.

154 Orono, E., Rainer, E. C. and Scott, J. W., Dendritic and axonal organization of mitral and tufted cells in the rat olfactory bulb, *Journal of Comparative Neurology*, 226(1984) 346-356.

155 Palacios, J. M. and Kuhar, M. J., Beta-adrenergic-receptor localization by light microscopic

autoradiography, *Science*, 208(1980) 1378-1380.

156 Patel, S., Millan, M. H. and Meldrum, B. S., Neurotransmission in the pedunculopontine nucleus and pilocarpine-induced motor limbic seizures in rats, *Neuroscience Letters*, 74(1987) 243-249.

157 Pinching, A. J., Synaptic connexions in the glomerular layer of the olfactory bulb, *J. Physiol.*, 210(1970) 14P-15P.

158 Pinching, A. J., Myelinated dendritic segments in the monkey olfactory bulb, *Brain Research*, 29(1971) 133-138.

159 Piredda, S. and Gale, K., A crucial epileptogenic site in the deep piriform cortex, *Nature*, 317(1985) 623-625.

160 Rall, W., Dendritic neuron theory and dendrodendritic synapses in a cortical system. In Schmitt, F. O.(Eds.), *The Neurosciences: Second Study Program*, Vol. Rockefeller University Press, New York, 1972, pp.552-565.

161 Reier, P. J. and Houle, J. D., The glial scar: Its bearing on axonal elongation and transplantation approaches to CNS repair. In Waxman, S. G. (Ed.), *Functional Recovery in Neurological Disease*, Vol. 47, Raven Press, New York, 1988, pp.87-138.

162 Robinson, A. P., White, T. M. and Wilson, D. W., Macrophage heterogeneity in the rat as delineated by two monoclonal antibodies to MRC OX-41 and MRC OX-42, the latter recognizing complement receptor type 3, *Immunology*, 57(1986) 239-247.

163 Rochel, S. and Margolis, F. L., Carnosine release from olfactory bulb synaptosomes is calcium-dependent and depolarization-stimulated, *Brain Research*, 202(1980) 373-386.

164 Rotter, A., Birdsall, N. J. M., Field, P. M. and Raisman, G., Muscarinic receptors in the central nervous system of the rat: II. Distribution of binding of [³] propylbenzilycholine mustard in the midbrain and hindbrain, *Brain Research Review*, 1(1979) 167-183.

165 Ruggiero, D. A., Giuliano, R., Awwar, M., Stornetta, R. and Reis, D. J., Anatomical substrates of cholinergic-autonomic regulation in the rat, *Journal of Comparative Neurology*, 292(1990) 1-53.

166 Sagar, S. M., Sharp, F. R. and Curran, S. T., Expression of c-fos protein in brain: Metabolic mapping at the cellular level, *Science*, 240(1988) 1328-1331.

167 Scott, K. and Fibiger, H. C., Cholinergic neurons of the laterodorsal tegmental nucleus: Efferent and afferent connections, *Journal of Comparative Neurology*, 253(1986) 277-302.

168 Schwarcz, R., Speciale, C. and Turski, W. A., Kynurenines, glia, and pathogenesis of neurodegenerative disorders. In Calne, D. B.(Eds.), *Parkinsonism and Aging*, Vol. Raven Press, New York, 1989, pp.97-105.

169 Scott, J. W. and Stewart, W. B., Mechanisms of augmented field potential responses in the rat olfactory bulb, *Brain Research*, 163(1979) 21-32.

- 170 Sheng, M. and Greenberg, M. E., The regulation and function of c-fos and other immediate early genes in the nervous system, *Neuron*, 4(1990) 477-485
- 171 Shepherd, G. M., Synaptic organization of the mammalian olfactory bulb, *Physiology Review*, 52(1972a) 864-917.
- 172 Shepherd, G. M., The olfactory bulb as a simple cortical system: Experimental analysis and functional implications. In Schmitt, F. O.(Eds.), *The Neurosciences: Second Study Program*, Vol. Rockefeller University Press, New York, 1972b, pp.539-552.
- 173 Shih, T.-M., Time course effects of soman on acetylcholine and choline levels in six discrete areas of rat brain, *Psychopharmacology*, 78(1982) 170-175.
- 174 Shih, T.-M., Koviak, T., Capacio, B. and Hayward, I. J., Studies of potential anticonvulsants in soman poisoning. In Moore, D. H.(Eds.), *Proceedings of the Workshop on Convulsions and Related Brain Damage Induced by Organophosphorus Agents*, Vol. U.S. Army Medical Research Institute of Chemical Defense, Aberdeen Proving Grounds, Maryland, 1990, pp.197-220.
- 175 Shipley, M. T., Harris, G., Williams, J., van Bockstaele, E., Aston-Jones, G. and Ennis, M., Asymmetric orientation of locus coeruleus (LC) dendrites in the pericoerulear region: Biocytin-filled LC neurons in vitro, *Society of Neuroscience Abstract*, 16(1990) 1177.
- 176 Shipley, M. T., Holloran, F. J. and de la Torre, J., Surprisingly rich projection from locus coeruleus to the olfactory bulb in the rat, *Brain Research*, 329(1985) 294-299.
- 177 Shipley, M. T., McLean, J. H. and Nickell, W. T., *Neurobiology of soman*, U.S. Army Medical Research and Development Command, 1988,
- 178 Shipley, M. T., Nickell, W. T., Ennis, M. and El-Etri, M., Mechanisms of soman-induced seizures and neuropathology. In Moore, D. H.(Eds.), *Proceedings of the Workshop on Convulsions and Related Brain Damage Induced by Organophosphorus Agents*, Vol. U.S. Army Medical Research Institute of Chemical Defense, Aberdeen Proving Grounds, Maryland, 1990, pp.131-143.
- 179 Shipley, M. T. and Sanders, M. S., Special senses are really special: Evidence for a reciprocal bilateral pathway between insular cortex and the nucleus parabrachialis, *Brain Research Bulletin*, 8(1982) 493-508.
- 180 Shipley, M. T. and Zahm, S., Differential synaptic processing on apical versus lateral mitral/tufted cell dendrites, *Chemical Senses*, 15(1990) 638.
- 181 Singh, D. N. and Nathaniel, E. J. H., Postnatal development of mitral cell perikaryon in the olfactory bulb of the rat. A light and ultrastructural study, *Anatomical Record*, 189(1977) 413-432.
- 182 Skau, K. A., Distribution and solubilization of the molecular forms of acetylcholinesterase in rat urinary bladder and sphincter, *Biochimica et Biophysica Acta*, 995(1989) 195-200.
- 183 Smith, C. G., The change in the volume of the olfactory and accessory olfactory bulb of the albino rat

during postnatal life, *Journal of Comparative Neurology*, 61(1935) 477-508.

184 Sparenborg, S., Brennecke, L. H. and Braitman, D. J., Soman-induced seizures and brain damage prevented by novel anticonvulsant drugs. In Moore, D. H.(Eds.), *Proceedings of the Workshop on Convulsions and Related Brain Damage Induced by Organophosphorus Agents*, Vol. U.S. Army Medical Research Institute of Chemical Defense, Aberdeen Proving Grounds, Maryland, 1990, pp.191-194.

185 Staley, K. J., Otis, T. S. and Mody, I., Membrane properties of dentate gyrus granule cells: Comparison of sharp microelectrode and whole-cell recordings, *Journal of Neurophysiology*, 67(1992) 1346-1358.

186 Steriade, M., Parent, A., Pare, D. and Smith, Y., Cholinergic and non-cholinergic neurons of cat basal forebrain project to reticular and mediodorsal thalamic nuclei, *Brain Research*, 408(1987) 372-376.

187 Stewart, W. B. and Scott, J. W., Anesthetic-dependent field potential interactions in the olfactory bulb, *Brain Research*, 103(1976) 487-499.

188 Svensson, T. H., Bunney, B. S. and Aghajanian, G. K., Inhibition of both noradrenergic and serotonergic neurons in brain by the alpha-adrenergic agonist clonidine, *Brain Research*, 92(1975) 291-306.

189 Switzer, R. C. I., Cambell, S. K., Murphy, M. R., Kerényi, S. Z., Miller, S. A. and Hartgraves, S. K., Soman-induced convulsions and brain damage as a function of chronic and acute exposure in rats and diazepam therapy in Rhesus monkeys. In Moore, D. H.(Eds.), *Proceedings of the Workshop on Convulsions and Related Brain Damage Induced by Organophosphorus Agents*, Vol. U.S. Army Medical Research Institute of Chemical Defense, Aberdeen Proving Grounds, Maryland, 1990, pp.33-67.

190 Trombley, P. Q., Norapinephrine inhibits calcium currents and EPSPs via a G-protein-coupled mechanism, *Journal of Neuroscience*, 12(1992) 3992-3998.

191 Trombley, P. Q. and Shepherd, G. M., Noradrenergic inhibition of synaptic transmission between mitral and granule cells in mammalian olfactory bulb cultures, *Journal of Neuroscience*, 12(1992) 3895-3991.

192 Trombley, P. Q. and Westbrook, G. L., Excitatory synaptic transmission in cultures of rat olfactory bulb, *Journal of Neurophysiology*, 64(1990) 598-606.

193 Trombley, P. Q. and Westbrook, G. L., L-AP₄ inhibits calcium currents and synaptic transmission via a G-protein-coupled glutamate receptor, *Journal of Neuroscience*, 12(1992) 2043-2050.

194 Turski, L., Ikonomidou, C., Turski, W. A., Bortolotto, Z. A. and Cavalheiro, E. A., Review: Cholinergic mechanisms and Epileptogenesis. The seizures induced by pilocarpine: A novel experimental model of intractable epilepsy, *Synapse*, 3(1989) 154-171.

195 Turski, W. A., Cavalheiro, E. A., Schwarz, M., Czuczwar, S. J., Kleinrok, A. and Turski, L., Limbic seizures produced by pilocarpine in rats: Behavioral electroencephalographic and neuropathological study, *Behavioural Brain Research*, 9(1983) 315-336.

- 196 U'Pritchard, D. C., Reisine, T. D., Mason, S. T., Fibiger, H. C. and Yamamura, H. I., Modulation of rat brain α - and β -adrenergic receptor populations by lesion of the dorsal noradrenergic bundle, *Brain Research*, 187(1980) 143-154.
- 197 Wade, V., Samson, F. E., Nelson, S. R. and Pazdernik, T. L., Changes in extracellular amino acids during soman- and kainic acid-induced seizures, *Journal of Neurochemistry*, 49(1987) 645-650.
- 198 Waldo, U., Nowycky, M. C. and Shepherd, G. M., Evoked potential and single unit responses to olfactory nerve volleys in the isolated turtle olfactory bulb, *Brain Research*, 211(1981) 267-283.
- 199 Wall, H. G., Jaax, N. K. and Hayward, I. J., Motor activity and brain lesions in soman intoxicated Rhesus monkeys. In Moore, D. H.(Eds.), *Proceedings of the Workshop on Convulsions and other Related Brain Damage Induced by Organophosphorus Agents*, Vol. U.S. Army Medical Research Institute of Chemical Defense, Aberdeen Proving Grounds, Maryland, 1990, pp.21-29.
- 200 Wellis, D. P. and Kauer, J. S., GABAA and glutamate receptor involvement in dendrodendritic synaptic interactions from salamander olfactory bulb, *J. Physiol.*, in press(1993)
- 201 Wellis, D. P. and Scott, J. W., Intracellular responses of identified rat olfactory bulb interneurons to electrical and odor stimulation, *Journal of Neurophysiology*, 64 No. 3(1990) 932-947.
- 202 Wellis, D. P. and Scott, J. W., Localized denervation demonstrates the innervation pattern of olfactory bulb glomeruli and second order cells, *Journal of Comparative Neurology*, 304(1991) 544-554.
- 203 Wellis, D. P., Scott, J. W. and Harrison, T. A., Discrimination among odorants by single neurons of the rat olfactory bulb, *Journal of Neurophysiology*, 61(1989) 1161-1177.
- 204 Westfall, T. C., Effect of nicotine and other drugs on the release of ^3H -norepinephrine and ^3H -dopamine from rat brain slices, *Neuropharmacology*, 13(1974a) 693-700.
- 205 Westfall, T. C., Effect of muscarinic agonists on the release of ^3H -norepinephrine and ^3H -dopamine by potassium and electrical stimulation from rat brain slices, *Life Sciences*, 14(1974b) 1641-1652.
- 206 Westfall, T. C., Evidence that noradrenergic transmitter release is regulated by presynaptic receptors, *Fed. Proc.*, 43(1984) 1352-1357.
- 207 Worley, P. F., Baraban, J. M., McCarren, M., Snyder, S. H. and Alger, B. E., Cholinergic phosphatidylinositol modulation of inhibitory, G protein-linked, neurotransmitter actions: Electrophysiological studies in rat hippocampus, *Proceeding of National Academy of Science USA*, 84(1987) 3467-3471.